AN INVESTIGATION OF TUMOUR SUSCEPTIBILITY IN A MODIFIED ATM-/- MOUSE WITH NO THYMOMA RISK

By

TEGAN ADELINE FRANCIS

A thesis submitted to the University of Birmingham for the degree of
DOCTOR OF PHILOSOPHY

School of Cancer Sciences

School of Medical and Dental Sciences

University of Birmingham

September 2014

UNIVERSITY^{OF} BIRMINGHAM

Abstract

Ataxia telangiectasia (A-T) is characterised by a predisposition to the development of a range of lymphoid tumours of both T and B cell origin. Currently, Atm-/- mice develop an aggressive thymic lymphoma and die by 13 weeks of age. In order to overcome this barrier to long lived mice and expand the range of lymphoid tumours driven by Atm loss, I crossed the Atm-/- mouse with the nude mouse (nu-/-).

The resulting Atm-/-nu-/- mice had a greater lifespan compared to the Atm-/- mice (median survival of 175 days versus 91 days). Of 17/69 Atm-/-nu-/- mice that developed a tumour sixteen were of B cell origin occurring in the spleen, liver, gut and axillary nodes. Histological examination of the B cell-derived tumours revealed that they were phenotypically heterogeneous. No tumours were observed in the control mice (Atm+/+nu-/- or Atm+/+nu+/-).

Fluorescence in situ hybridisation (FISH) revealed the presence of IgH translocations in 1/6 B cell lymphomas and 2/6 tumours had an additional copy of Myc. M-FISH revealed clonal abnormalities involving chromosomes 17 and/or 18 in 5/6 tumours analysed.

We conclude that in contrast to T cell lymphoma development in Atm-/- mice, which is associated with immune gene translocations and Myc amplification, the Atm-/-nu-/- model of A-T gives B cell lymphomas arising at different stages of B cell development and may be more representative of the types of B cell lymphoma in patients with A-T.

'Science is a way of thinking much more than it is a body of knowledge'

Acknowledgements

I would like to thank my supervisors Professor Malcolm Taylor and Professor Tanja Stankovic for giving me the opportunity to carry out this study and to CRUK for funding the study. I would like to thank Malcolm for reviewing all my work, helping me to develop my scientific thinking and persevering through many meetings and Tanja for her valuable input.

I would like to thank members of the Taylor and Stankovic labs, past and present, for their help and support. Especially Angelo for his technical guidance, Tracey for her assistance with the mice, Jim for teaching me how to do a Western blot, Phil for knowing everything related to molecular biology, and Nick for sharing his unique but effective methods. I would like to acknowledge the members of the Frampton lab; Paloma and Mary for teaching me FACS, letting me use the Cyan and all their advice over the years. Thank you to Eszter for teaching me IHC, when all hope of phenotyping the tumours was nearly lost. Thank you to the WMRGL for their collaboration and to Emma and Gaz for teaching me about FISH.

Thank you to all my friends who have made this experience so enjoyable, especially Casper, Ellis and Laura for their counsel and the social outings, all of which have maintained my sanity.

I would like to acknowledge my family for their support and understanding of my absence over these busy few years. Thank you to Mum, Dad and Nanny for their unrelenting interest despite not understanding anything about my project and to Lovemore for listening and providing perspective.

Finally, thank you to Lewin for letting me move into his study, putting up with me being present but not 'present', his constant encouragement and never failing to make me laugh.

Table of Contents

List of Figures

List of Tables

Abbreviations

A-EJ	Alternative end-joining
AID	Activation-induced (Cytidine) deaaminase
ALCL	Anaplastic large cell lymphoma
BCR	B cell receptor
CSR	Class switch recombination
DDR	DNA damage response
DLBCL	Diffuse large B cell lymphoma
DP	Double positive
DSB	Double strand break
FACS	Fluorescence activated cell sorting
FDC	Follicular dendritic cell
FISH	Fluorescence in situ hybridisation
FL	Follicular lymphoma
GC	Germinal centre
hpf	High power field

HR	Homologous recombination
HSC	Haematopoietic stem cell
IgH	Immunoglobulin heavy chain
IgL	Immunoglobulin light chain
IHC	Immunohistochemical
IR	Ionising radiation
M-FISH	Multicolour fluorescence in situ hybridisation
MCL	Mantle cell lymphoma
MZ	Marginal zone
MZL	Marginal zone lymphoma
NHEJ	Non-homologous end-joining
NHL	Non-Hodgkin's lymphoma
RSS	Recombination signal sequence
SP	Single positive
SSB	Single strand break
TCR	T cell receptor

CHAPTER 1

INTRODUCTION

1 INTRODUCTION

1.1 An introduction to ataxia telangiectasia (A-T)

1.1.1 The clinical phenotypes associated with ataxia telangiectasia

Ataxia Telangiectasia (A-T) is an autosomal recessive disorder with multiple associated phenotypes. Primarily a neurodegenerative disease, A-T patients develop progressive cerebellar ataxia, which results in them becoming wheelchair bound by approximately 10 years of age (Sedgwick and Boder, 1991, Swerdlow, 2008, Mavrou et al., 2008). In addition, patients also show both ocular and cutaneous telangiectasia (dilated blood vessels), immunodeficiency (Nowak-Wegrzyn et al., 2004), chromosome instability, particularly translocations involving chromosomes 7 and 14 in T lymphocytes (Meyn, 1999) (Chun and Gatti, 2004), unusual clinical (Cunliffe et al., 1975) and cellular radiosensitivity (Taylor et al., 1975) and an increased incidence of cancer (Hecht et al., 1966) (Sedgwick and Boder, 1991). Patients have a median survival of 19-25 years (Crawford et al., 2006) and most patients die from respiratory tract infections but a significant proportion (22%) develop cancer, mostly of lymphoid origin (Reiman et al., 2011, Micol et al., 2011). The incidence of A-T in the UK is about 1 in 330,000 (Taylor et al., 1996).

1.1.2 The *ATM* gene; loss of which causes ataxia telangiectasia

 A-T is caused by biallelic mutation of the ataxia telangiectasia mutated (*ATM*) gene (Savitsky et al., 1995) located at 11q22-23 (Gatti et al., 1988). There are 62 coding exons and no evidence of splice variants (Uziel et al., 1996). Mutations in *ATM* that are found in A-T patients are evenly spread throughout the gene and are mostly truncating resulting in instability and loss of the ATM protein. These include nonsense mutations, small in frame deletions or insertions and splice site mutations resulting in exon skipping. Some splice site

mutations are 'leaky' and can result in expression of a low level of normal ATM protein. In addition, some small in-frame deletions or missense mutations can result in expression of some mutant ATM protein (Reiman et al., 2011). The *ATM* gene encodes a large 350kDa protein with kinase activity (Savitsky et al., 1995).

1.1.3 The cellular phenotypes associated with A-T

The most important cellular feature is that cells from patients with A-T are hypersensitive to ionising radiation as shown by reduced colony survival and also increased chromosomal damage after exposure to IR compared to normal cells. This was discovered following the realisation that patients were clinically radiosensitive (Morgan et al., 1968, Cunliffe et al., 1975). The increased radiosensitivity is caused by a defect affecting both classical non-homologous end joining (C-NHEJ) and homologous recombination (HR) repair resulting in unrepaired DNA DSB, as a consequence of loss of ATM in these cells. ATM loss also causes cell cycle defects. In cells from A-T patients there is a defect in the activation of the G1-S, intra-S and G2-M checkpoints in response to DNA damage. A defect in activation of the S phase checkpoint results in radioresistant DNA replication and cell cycle progression in the presence of unrepaired DSB, which are both damaging to the cell (Chun and Gatti, 2004, Lavin and Kozlov, 2007).

In addition to defects in the DNA damage response (DDR) A-T cells have accelerated shortening of telomeres, suggesting that ATM plays a role in the maintenance of telomeres (Metcalfe et al., 1996). Similarly, studies of the yeast ortholog of ATM, Tel1, show that Tel1 is required for maintenance of yeast telomeres (Ma and Greider, 2009). On the other hand, the chromosomes of bone marrow cells from A-T mice that lack Atm protein have normal length telomeres (Feldser et al., 2006). This suggests that the role of ATM in the maintenance of telomeres could vary between species.

In human primary fibroblasts, ATM is recruited to damaged telomeres and subsequently activates the DNA damage response. Normally, the shelterin complex protects telomeres. Disruption of this complex by depletion of one of its components, TRF2, results in ATM activation. Overexpression of TRF2 also inhibits the ability of ATM to signal DDR. The inhibitory action of TFR2 on ATM is likely to prevent ATM from recognising telomeres as sites of DNA damage (Karlseder et al., 2004). Overall ATM plays an important role in detecting abnormal telomeres.

Studying the cellular defects in A-T cells has provided some basis, although incomplete, for the clinical phenotype of the disease. Gross genomic instability leads to the development of malignancies and impaired development of the immune system in A-T (see below). On the other hand, it is still not clear what is the cause of neurodegeneration in these patients but increased oxidative stress combined with neuronal sensitivity to genotoxic stresses are all possible contributors.

1.1.4 Genotype- phenotype relationships in A-T

As mentioned previously, A-T is a both genetically and phenotypically heterogeneous. The relationship between the type of *ATM* mutation and clinical symptoms is beginning to be understood. *ATM* mutations can be divided into those that result in loss of all ATM kinase activity and those that result in retention of some kinase activity (Reiman et al., 2011). Total loss of ATM activity is associated with the cellular and clinical features of classical A-T including early onset (<2 years of age), and is most commonly caused by biallelic loss of ATM protein. Patients with *ATM* mutations in whose cells residual ATM kinase activity is detected, either through expression of a measurable level of normal ATM protein or the expression of mutant ATM protein, are associated with a milder clinical phenotype (Reiman et al., 2011, Taylor et al., 2014). This includes a slower progression of neurological features,

longer survival and protection against tumours in childhood. An example of the first type of mutation is the leaky splice site mutation c.5763-1050A>G (p.Pro1922fs) which allows a low level expression of normal ATM protein that, of course, has the ability to phosphorylate ATM targets (Reiman et al., 2011). This mutation is found in one allele in a significant proportion of A-T patients in the British Isles and these patients usually have a second mutation that is truncating.

An example of the second type of mutation, a missense mutation giving rise to mutant protein with activity, is the c.7271T>G (p.Val2424Gly) *ATM* mutation, which is usually found in individuals that are diagnosed as adults but had some A-T symptoms from childhood (Reiman et al., 2011). Generally patients homozygous for these 'milder' mutations have an even milder phenotype than those with just one such allele. This genotype phenotype correlation is helpful in providing some indication to families of prognosis although this needs to be done with caution.

1.2   The ATM protein kinase

ATM is a phospho-inositide- 3 kinase (PI3K) related protein kinase (PIKK family). Other members of the family include Ataxia Telangiectasia and Rad 3 related protein (ATR), mammalian target of rapamycin (mTOR) and DNA protein kinase catalytic sub-unit (DNA-PKcs). ATM phosphorylates target proteins on serine or threonine residues that are followed by a glutamine (SQ or TQ) (Shiloh, 2003). In addition to the kinase domain the ATM protein has a FAT domain and FATC domain. ATM binds many substrates including NBS1, BRCA1 and p53 via an N-terminal substrate-binding site (SBS) (Difilippantonio et al., 2005, Lavin, 2008) (Figure 1.1). Most ATM protein is located in the nucleus but some ATM expression has been detected in the cytoplasm of neuronal cells (Lakin et al., 1996, Ambrose and Gatti,

2013). A proportion of cytoplasmic ATM is localised to the peroxisomes possibly via its FATC domain (Guo et al., 2010).

1.2.1 Activation of ATM

ATM has to be activated and this occurs by autophosphorylation or transphosphorylation at Ser367, Ser1893, Ser1981 and Ser2996 (Lavin and Kozlov, 2007, Kozlov et al., 2011) in human cells. In addition to phosphorylation, ATM is acetylated on a lysine residue (K3016) by the acetyl-transferase TIP60 (Sun et al., 2005) (Figure 1.1). ATM exists as an inactive homodimer that becomes monomerised on activation (Bakkenist and Kastan, 2003). Activation can occur following exposure of cells in vitro to agents that cause DNA DSB, including IR, various drugs such as neocarcinostatin and bleomycin as well as oxidative stress (Ambrose and Gatti, 2013, Taylor et al., 1983, Shiloh et al., 1982). Complete activation of ATM requires the MRN complex (Lee and Paull, 2005).

Figure 1.1 Schematic representation of ATM
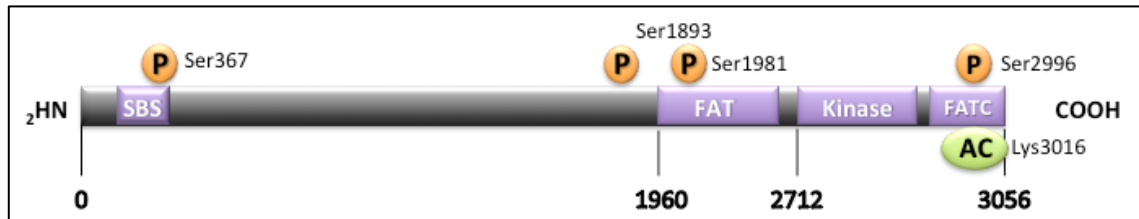
Schematic representation of ATM, a 3056 amino acid protein, showing the SBS, FAT, FATC and the important kinase domain. The four major autophosphorylation (P) and acetylation (AC) sites are indicated. (Modified from (Lavin, 2008), and (Stracker et al., 2013).

SBS= substrate binding site

FAT= focal adhesion kinase target

FATC = FAT C-terminal

1.3 Role of ATM in the DNA damage response

1.3.1 The DNA damage response

DNA is constantly the target of damage caused by endogenous and exogenous factors. Types of damage include single strand breaks (SSB), double strand breaks (DSB), DNA cross-links and bulky adducts (Jeggo and Löbrich, 2007) To maintain the integrity of the genome, cells have highly conserved DNA repair machinery that responds to genotoxic stress. This is important because compromised genomic integrity can lead to potentially harmful mutations and apoptosis (Lavin, 2008). In addition, unrepaired DSB can lead to translocations that have potential to cause malignancy e.g. IgH-MYC that is frequently found in B cell malignancies (Jackson, 2002).

ATM is part of the DNA repair machinery. *ATM* is not an essential gene unlike *NBN*, *MRE11* and *RAD50* (in the same repair pathway). In the absence of ATM, the efficiency of DSB repair is reduced and a subset of breaks remain unrepaired (Kühne et al., 2004).

The first step in the DNA damage response (DDR), following DSB induction, is activation of the MRE11/NBS1/RAD50 complex, which in turn activates the ATM kinase. This results in phosphorylation of ϒ-H2AX by ATM, which facilitates the recruitment of other proteins involved in the sensing and maintenance of signalling to the break. Following this, MDC1 binds to the break and is phosphorylated by ATM, which leads to the recruitment of the MR11, Rad50 and NBS1 (MRN) complex to the site (Stewart et al., 2003, Jungmichel et al., 2012). NBS1, part of the MRN complex acts as an adapter protein tethering ATM to the site, stabilising it at the site of the DSB and allowing phosphorylation of its target proteins (Lee and Paull, 2005). In addition to its role as an adapter, the MRN complex acts like a scaffold to tether the two broken ends of DNA together via RAD50 protein (He et al., 2012, Moreno-

Herrero et al., 2005). MDC1 also recruits RNF8 which ubiquitilates H2AX and this allows the binding of p53 and BRCA1 to the site and further amplification of the signal (Kolas et al., 2007, Lavin, 2008).

1.3.2 Down stream signaling of ATM

If damaged DNA persists in a cell it can lead to mutagenic events that could harm the organism and, therefore, following recognition of DNA damage, the cell cycle pauses to allow time for the damaged DNA to be repaired. If the damage to the DNA is too great then the cell undergoes apoptosis. ATM is a key regulator of this process. On sensing DNA damage, ATM initiates a signalling cascade that results in activation of different cell cycle checkpoints, DNA repair or apoptosis (Abraham, 2001, Shiloh, 2003).

ATM co-ordinates the G1-S checkpoint by phosphorylating p53 at Ser53, the G2/M checkpoint by phosphorylating Chk2 at Thr68, and the intra-S phase checkpoint by phosphorylating SMC1 at Ser957 and Ser966 (Ambrose and Gatti, 2013).

1.3.3 ATM and DNA DSB repair

DNA DSBs are repaired through one of two distinct pathways; homologous recombination (HR) and classical non-homologous end joining (C-NHEJ). HR is less error prone and only occurs immediately following S/G2 phase as it requires the presence of a homologous sister chromatid to be used as a template (Jackson, 2002). C-NHEJ occurs throughout the cell cycle, but unlike HR predominates in the G1 phase and is the main type of repair that takes place in non-dividing cells.

1.3.4 Non-homologous end joining

Classical Non-homologous end joining (C-NHEJ) repairs externally induced DNA DSB, mainly, in the G1 phase of the cell cycle and also in the repair of physiological breaks

generated in immune gene rearrangement during lymphocyte development. Repair is initiated by binding of the Ku hetero-dimer, which consists of Ku70 and Ku80, at the DSB. The Ku complex acts as a scaffold for the binding of the serine/threonine protein kinase DNA-dependent protein kinase catalytic subunit (DNA- PKcs). On binding, DNA-PKcs undergoes autophosphorylation and phosphorylation by ATM (Chen et al., 2007, Weterings and Chen, 2007). These phosphorylation events are important for the activity of DNA-PKcs and the efficient completion of C-NHEJ. Targets of DNA-PKcs include other C-NHEJ proteins and proteins involved in the DDR response including XRCC4, KU70/80, Artemis and p53 (Burma et al., 2006, Burma and Chen, 2004). Depending on where the two strand breaks occurred the DNA ends may contain a 3' or 5' overhang which are not compatible for ligation and require shortening or filling to produce two blunt ends. DNA processing is done by DNA polymerase-μ and DNA polymerase-λ, as well as the nuclease Artemis, which are recruited by the Ku-DNA-PKcs complex (Ma et al., 2002, Lieber, 2010). Finally, repair is completed by ligation of the two DNA ends by Ligase IV and XRCC4 (Grawunder et al., 1997).

1.3.5 V(D)J recombination and NHEJ

V(D)J recombination is a process that is only undertaken in lymphocytes. It creates genetic diversity in the immune antigen receptors. V(D)J recombination occurs before antigen exposure. It is a process of recombination to generate a unique coding sequence composed of variable (V), diversity (D), and joining (J) segments. These gene segments are flanked by recombination signal sequences (RSS) that are separated by either 12-bp or 23-bp sequence. Recombination will only take place between two segments flanked by 12-bp and 23-bp spacers. This 12/23 rule prevents the joining of two similar gene segments. V(D)J recombination is divided into two stages; (1) cleavage and (2) repair. Cleavage is undertaken by the recombinase activating genes 1 and 2 (RAG1 and RAG2). These proteins, signalled by

the RSSs, introduce DSB between the V, D and J genes that are sensed by ATM, which initiates the DDR (Bredemeyer et al., 2006, Gapud et al., 2011). The RAG complex along with ATM are temporarily involved in stabilising the post cleavage complex before it is repaired by the proteins involved in NHEJ (Deriano et al., 2011). ATM also plays role in safeguarding against RAG mediated breaks being generated at multiple loci at the same time (Chaumeil et al., 2013). RAG proteins generate a coding end, that has a covalently sealed hairpin intermediate which requires processing before repair and contributes to the diversification of this gene, and a signal end that can be fused directly (Mcblane et al., 1995). The processing step of NHEJ adds additional diversity to the immune gene in the following ways. The Artemis protein undoes the covalently sealed hairpin at the coding end of the break by making a cut at or near the apex of the loop, which causes nucleotide deletions or insertions at this position (Lieber, 2010). Once the hairpin is open, the lymphocyte specific polymerase, terminal deoxynucleotidyltransferase (TdT), adds further diversity to the immune gene by inserting non-templated nucleotides (Bollum, 1979, Gilfillan et al., 1993). Finally, V(D)J recombination is completed by the ligation of the two coding ends and the two signal ends by the XRCC4- Ligase IV complex (Malu et al., 2012, Rooney et al., 2004, Alt et al., 2013).

1.3.6 Homologous recombination

Homologous recombination (HR) will repair DSB, inter –strand cross links (ICL) and in the recovery of stalled replication forks. In the late S/ G2 phase of the cell cycle both HR and C-NHEJ can be used to repair DSB (Geuting et al., 2013). Although ATM is not essential for HR it must play a role because ATM phosphorylates the HR protein Rad51 and cells from A-T patients have a higher frequency of recombination events (Chen et al., 1999, Morrison et al.,

2000, Bryant and Helleday, 2006). More recently it has been shown that RPA phosphorylation during HRR is also ATM dependent.

HR is a multistep process that can be broken down into three main phases: pre-synapsis, synapsis and post synapsis. In pre synapsis the DSB are recognised and processed. In the synapsis phase, Rad51 binds the single stranded overhang. The Rad51 coated filament performs a homology search and the invading strand generates a displacement –loop (D-loop). In the final phase, post-synapsis, DNA synthesis begins and second strand invasion forms a holiday junction. Resolution of this complex can occur with or without chromatid crossover (Li and Heyer, 2008, Heyer et al., 2010).

1.4 The role of ATM in T and B lymphocyte development

1.4.1 Lymphocyte development

Haematopoietic stem cells (HSC) in the bone marrow are responsible for the production of all blood cell lineages throughout life including T and B lymphocytes. From HSC, progenitor cells are produced, which in turn differentiate into more specialised cells losing pluripotency at each stage of differentiation. The common lymphoid progenitor (CLP) has the potential to produce both T and B cells. The fate of each cell is determined by cytokine signalling in the bone marrow (Kondo et al., 1997, Kondo et al., 2001). Lymphocytes have specialised immune genes that encode specific antigen receptors. Lymphocyte development is centred around producing and selecting a high affinity T cell receptor (TCR) or B cell receptor (BCR) in order to recognise and respond to pathogen invaders (Cooper and Alder, 2006).

1.4.2 The development of T cells

The thymus does not contain any self-renewing progenitors, instead it relies on the migration of T cell progenitors from the bone marrow. Haematopoietic stem cells (HSCs) in the bone

marrow produce multipotent progenitors (MPPs), that give rise to lymphoid primed multipotent progenitors (LMPPs), that differentiate into common lymphoid progenitors (CLPs). LMPPs and CLPs leave the bone marrow and enter the circulation before settling in the thymus. The majority of T cell development takes place in the thymus (Zlotoff and Bhandoola, 2011). T cell progenitors in the thymus can give rise to cells expressing an $\alpha\beta$ TCR, or less commonly a $\Upsilon\delta$ TCR. On entering the cortex of the thymus, double negative (CD4-CD8-) progenitor T cells first undergo V(D)J recombination of their β/δ chain and form pre T cells that express a pre-TCR complex. Signalling through the pre-TCR complex promotes survival and further development. Double positive (CD4+CD8+) T cells then recombine the second receptor chain (α/γ) and express a TCR complex. In some cases, further rounds of receptor editing occur to reduce autoreactivity or increase affinity of the receptor to antigen that is expressed on the surface of cortical thymic epithelial cells. Ultimately strong signalling through the TCR in response to antigen leads to positive selection and prevents further rearrangements After positive selection, T cells move to the thymic medulla and those that exhibit auto reactivity are eliminated by negative selection (Sprent and Surh, 2002, Sprent and Kishimoto, 2002). The double positive (DP) T cells then lose expression of CD4 or CD8 and become single positive (SP) T cells (Nemazee, 2006).

1.4.3 The development of B cells

B cells are part of the adaptive immune system and can be simply described a set of cells that express clonally diverse surface immunoglobulin that recognise specific antigens (Cooper and Alder, 2006). B cell development begins in the bone marrow then the cells travel to secondary lymphoid tissue, including the spleen, where maturation is completed. B cell development can be characterised by an ordered stepwise progression of gene and surface marker expression

(Alt et al., 1986). In the mouse, the most commonly used surface antigens used for the identification of B cells are C-Kit, B220, CD43 IgM, IgD (Miosge and Goodnow, 2005).

Part of the B cell development is rearrangement and editing of the BCR through three processes that occur at different stages of maturation; V(D)J recombination, class witch recombination (CSR) and somatic hypermutation (SHM). Rearrangement at each stage is strictly regulated by a series of checkpoints. Cells that generate receptors that lack antigen affinity or are autoreactive are dismissed. Selection occurs through signalling of BCR. A high affinity to antigen produces BCR signalling which promotes cells survival and clonal selection of these cells. In addition, in the mechanism of receptor selection, BCR signalling switches off RAG proteins and thus stops further recombination. Those cells with a low affinity rearrangement will undergo further rounds of editing until a high affinity antibody is produced or a non productive rearrangement occurs that leads to cells death (Nemazee, 2006, Ehlich et al., 1994).

1.4.4   The role V(D)J recombination in B cell development

The recognition of specific antigens is conferred by a specific antigen receptor on the B cell surface. This antigen receptor, the B cell receptor (BCR), is made up of two chains, the immunoglobulin heavy chain (IgH) and an immunoglobulin light chain (IgL) (Nemazee, 2006). The heavy chain of the BCR is made up of a constant region and a variable region. The variable region is encoded by three gene groups; variable (V), diversity, (D) and joining (J). In humans the V genes, J genes and D genes are randomly joined by a process of V(D)J recombination (See section above) (Tonegawa, 1983). The light chain has a variable region and a joining region only. The quasi-random nature of recombination events ensures a high possibility of unique receptors being produced (Nemazee, 2006). Additional diversity is

created at the joining of the junctions between these genes, which adds to the variability and specificity of the receptor.

The first immune gene rearrangement to take place is D-J of the IgH gene and it occurs in progenitor (Pro) B cells. At the next developmental stage the V-DJ recombination takes place. and leads to expression of an IgH with a μ (M) constant region and a surrogate light chain that make the pre-BCR complex. (Ehlich et al., 1994, Allman et al., 1999). This is the first check point in B cell development and 75% of B cells fail to pass this checkpoint and undergo apoptosis (Osmond, 1991).

After rearrangement of IgH the B cell goes on to rearrange immunoglobulin light chain (IgL). This gene locus lacks a D segments and therefore has much less diversity potential. V-J recombination along with further rounds of editing takes place and finally a BCR receptor with an IgH and IgL chain is expressed on the surface of the cells (IgM). These immature B cells then leave the bone marrow and travel to the secondary lymphoid tissues (Nemazee, 2006).

1.4.5   Antigen dependent B cell development

Antigen stimulation in the secondary lymphoid tissues gives rise to further differentiation in a process known as the germinal centre (GC) reaction, which is characterised by clonal expansion and is summarised in Figure 1.2. In the germinal centre the immunoglobulin genes under go class switch recombination (CSR) and somatic hyper mutation (SHM) with the aim of increasing the affinity of the BCR to antigen (Rajewsky, 1996, Kocks and Rajewsky, 1988, Lebien and Tedder, 2008).

The process of isotype switching of the constant region of the BCR is called class switch recombination (CSR). CSR is initiated by the protein AID (Activation-Induced (cytidine)

Deaminase). The constant region of the antibody determines the effector function of BCR signalling. The BCR constant region is switched from IgM to either IgG, IgD, IgE or IgA through intra-chromosomal deletion. The broken ends of DNA are repaired by C-NHEJ (see section 1.3.4) (Stavnezer et al., 2008). ATM is required for the efficient completion of CSR and consistent with this, A-T patients have reduced IgA and IgG levels (Pan et al., 2002). Mouse B cells also have reduced CSR when stimulated in vitro. In the absence of ATM, AID induced DSB can persist over several cell division and can lead to abnormal recombination including IgH- Myc translocations (Ramiro et al., 2006). Overall, like in V(D)J recombination, ATM is involved in the organisation of the repair complex and halting the cell cycle in CSR (Callén et al., 2007, Reina-San-Martin et al., 2004).

SHM is a process in which point mutations are introduced into the variable region of the antibody with the intention to refine the specificity of the receptor to antigen (Bross et al., 2000). High rates of transcription are required for it to occur (Peled et al., 2008). Point mutations are generated during the erroneous repair of uracil, introduced into the DNA by the deamination of cytosine by AID, by base excision repair (BER) and mis-match repair (MMR) (Peled et al., 2008).

The germinal centre is the site of T cell specific immune response. The purpose of it is to facilitate the affinity maturation of B cells to generate long lived plasma cells with high affinity antigens (Mcheyzer-Williams and Ahmed, 1999). There are a series of common steps. Firstly the activated B cell migrates to the centre of the follicle where it begins to proliferate. The follicle has two distinct areas: light zone and dark zone. The follicle is mostly made up of T cells, B cells, macrophages and follicular dendritic cells (FDCs) that express larges amounts of antigen. The follicular processes of the FDCs extend into a light zone. The dark zone contains the closely packed proliferating B cells, and very few FDC processes. B cells in the

follicle can been categorised morphologically into small cleaved centrocytes found predominantly in the light zone, and larger round centroblasts, found predominantly in the dark zone (Allen et al., 2007b, Maclennan, 1994, Maclennan, 2005). Centroblasts are rapidly dividing B cells that do not express immunoglobulin as they are undergoing progressive rounds of SHM indicated by high levels of AID protein expression in this region (Cattoretti et al., 2006, Moldenhauer et al., 2006). When centroblasts stop dividing, they become centrocytes and migrate to the light zone. Although more recently it has been proposed that cells in both the light and dark zone undergo mitosis and the cells move back and forth between the light and dark zone (Camacho et al., 1998, Hauser et al., 2010). B cells with a high affinity BCR that interact strongly with T cells and FDCs, are selected for in the GC. Those B cells with a low affinity receptor are eliminated by apoptosis. This process is termed affinity maturation (Kepler and Perelson, 1993, Maclennan, 1994). Positively selected B cells choose to either undergo further rounds of SHM or to exit the germinal centre and differentiate into long lived plasma cells or memory B cells (Meyer-Hermann et al., 2012).

Figure 1.2 The germinal centre
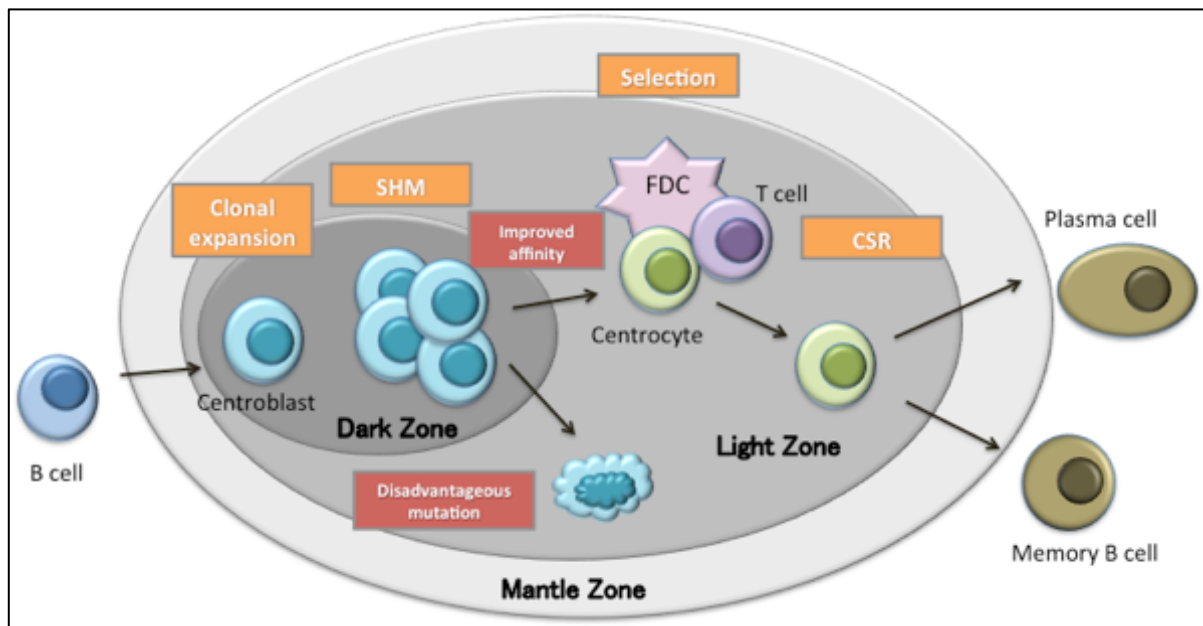
The germinal centre is composed of three zones; light zone, dark zone and mantle zone. Mature B cells that have encountered antigen differentiate into centroblasts in the dark zone. Here, the centroblasts undergo a phase of rapid proliferation. During this phase SHM of the immune gene takes place to generate an antigen receptor that has a high affinity. Those cells with an antigen receptor with weak affinity or are autoreactive undergo apoptosis. The remaining cells leave the dark zone and move into the light zone and become centrocytes. Centrocytes undergo further rounds of editing and selection of their immune genes to increase affinity to antigens presented by FDC and T cells. In the light zone some centrocytes undergo CSR, which changes the effector function of the antigen receptor. Finally the centrocytes differentiate into either a plasma cell or memory B cell and are now ready to leave the germinal centre.

Diffuse large B cell lymphoma is composed mostly of centroblasts B cells. Follicular lymphoma contains both centroblasts and centrocyte B cells.

SHM = Somatic hypermutation

CSR = Class switch recombination

FDC = Follicular dendritic cell

1.5 The role of ATM in tumour development

1.5.1 Tumour development in patients with A-T

It has long been known that patients with A-T have an increased risk of developing cancers (Sedgwick and Boder, 1991). Recent studies suggest between 22 and 40% of A-T patients are likely to develop malignancy (Reiman et al., 2011, Micol et al., 2011, Meyn, 1999). A-T patients develop a range of malignancies mainly lymphoid tumours, but also endocrine and brain tumours, breast cancer, glioblastoma, liver, uterine, ovarian and myeloid leukaemia (Taylor, 1992, Micol et al., 2011). The type of tumour development in A-T patients is closely related to the age of development (Reiman et al., 2011), with lymphoid tumours being more prevalent in young patients (<16 years of age). About 40% of lymphoid malignancies are non-Hodgkin's lymphoma, 25% are acute lymphoblastic leukaemia and 10% are Hodgkin's lymphoma. It is unclear whether A-T patients have a higher proportion of T cell lymphomas than B cell lymphomas.

Bcr-Abl, Tel-AML, MLL translocations are frequently found in paediatric leukaemia in the general population, but the incidence of these translocations is not increased in tumours that develop in A-T patients suggesting that ATM loss is not involved in the development of B precursor ALL (Taylor et al., 1996, Reiman et al., 2011). In the general population paediatric B cell lymphoma usually develops from early B cells that have not yet undergone V(D)J recombination, whereas B cell lymphoma in young A-T patients frequently are of mature B cell origin. T cells from A-T patients frequently have translocations involving chromosomes 7 and 14 with breaks within the T cell receptor genes and these are present at much higher levels that in the general population (Taylor et al., 1996, Reiman et al., 2011). This may be a consequence, either of increased occurrence of such translocations, in the absence of ATM, or

a reduced level of apoptosis of cells with such translocations. T cell prolymphocytic leukaemia (T-PLL) develops from a T cell with a translocation involving the T cell receptor and an oncogene and is associated with old age. However, A-T patients develop these tumours at an early age, probably as a consequence of the high level of the appropriate translocations in their T cells. It is possible that such aberrant translocations play an important part in the development of all lymphoid tumours (both B and T cell origin) seen in A-T patients although this is difficult to document.

In older A-T patients that develop a malignancy there is an increased proportion of solid tumours (Reiman et al., 2011) and this can be associated with the expression of abnormal ATM protein, but with some kinase activity (Reiman et al., 2011), in these patients allowing increased longevity. A possible explanation for this is that the small amount of ATM kinase activity protects the patients from developing lymphoid malignancies at an early age but this ATM activity is not enough to prevent the development of solid tumours later in life (Reiman et al., 2011). The risk of A-T patient developing breast cancer is probably higher than the risk associated with carrying either a *BRCA1* or *BRCA2* mutation.

Heterozygote carriers of an *ATM* mutation are at increased risk of developing cancer; in particular female carriers are twice as likely to develop breast cancer than a non-carrier. Approximately 1% of the population are carriers of an *ATM* mutation, which has implications in the monitoring and management of breast cancer in both A-T families and the general population (Taylor, 1992, Meyn, 1999).

1.5.2 ATM and tumour development in the general population

Somatic *ATM* mutations have been associated with cancer development, particularly chronic lymphocytic leukaemia (CLL) (Stankovic et al., 1999) T cell prolymphocytic leukaemia

(Vorechovský et al, 1997) and Mantle Cell Lymphoma (Schaffner et al., 2000), in the general population. Somatic *ATM* mutations have been detected in several other tumour types including lymphoid, lung and large intestine tissues. *ATM* missense mutations were most common in sporadic lymphoid tumours, in contrast to the situation with germ line mutations, which are most commonly truncating mutations (Cremona and Behrens, 2014). Loss of ATM function can also occur through deletion of chromosomal region distal 11q where the *ATM* gene is located. In a cohort of chronic lymphocytic leukaemias with an *ATM* mutation Skowronska and colleagues found that almost half also had an 11q deletion, leading to biallelic inactivation of *ATM* and consequently loss of ATM function (Skowronska et al., 2012). The association of loss of function of ATM with the development of sporadic lymphoid tumours (eg T-PLL and Mantle cell lymphoma) may be related to the function of ATM in lymphoid cells and particularly in V(D)J recombination and formation of chromosome translocations, although other mechanisms may operate in CLL and other tumours, which remain to be elucidated. Finally, *ATM* has also been shown to be hypermethylated in colorectal tumours, although this was not shown to correlate with a change in ATM protein expression (Beggs et al., 2012).

1.6   The A-T mouse

Several mouse models have been constructed in order to examine the effect of the systemic loss of ATM (Barlow et al., 1996, Elson et al., 1996, Xu et al., 1996), or the consequences of particular ataxia telangiectasia associated mutations for cancer risk (Spring et al., 2001), or targeting *ATM* mutations in order to investigate neurodegeneration in older mice (Borghesani et al., 2000) and the effect of the presence of a normal level of kinase dead ATM (Yamamoto

et al., 2012, Daniel et al., 2012). A summary of these models is given in Table 1.1 and Table

1.2.

Table 1.1 Summary of A-T mouse models

Mouse/ Author	Type of mutation	Atm protein expression	Survival	Neurological abnormalities	Tumour development	Tumour phenotype
Barlow et al., 1996*	Disruption at exon 40/41 (nucleotides 5705–5882)	ND	2-5 months	Slight ataxia[1,2]	Thymoma (nearly all mice)	CD4+CD8+CD3-
Xu and Baltimore, 1996	Disruption of kinase domain at exons 62/63 (nucleotides 8619/8831)	ND (No Atm mRNA expression)	3-4 months	No	Thymoma (nearly all mice)	ND
Elson et al., 1996	Disruption at exon 38 (nucleotides 5460)	No	ND	ND	4/12 mice developed thymoma and died between 3-4 months	CD4+CD8+CD3-
Borghesani et al., 2000	Disruption at exons 51-55 (nucleotides 7279-7818)	No	50% survived over 10 months	Decreased motor learning[2], cerebellar degeneration[3]	Thymoma (incidence unknown)	ND
Spring et al., 2001	Atm knock-in corresponding to the human *ATM* 7636del9	Yes (low levels of full-length Atm protein detected with activity)	30% survived over 16 months	No	Thymoma (mice surviving after 40wks developed B cell, ovarian granulosa cell, epithelial carcinoma, ovarian sex cord, stromal cell)	CD4+CD8+, CD4+CD8-, CD4-CD8+ (Thymoma)

Table summarises the phenotypes of each A-T mouse model. ND= not done. Daniel and Yamamoto homozygote mice were not viable so were excluded from the summary. [1]measured by foot print analysis. [2] measured by rotor rod performance. [3]as seen by histological analysis of cerebellar brain sections. *Wynshaw-Boris mice

Table 1.2 Haematopoietic comparison

Mouse/ Author	Thymus		Spleen			Bone Marrow			
	Proportion of CD4+CD8+	Proportion of CD4+CD8- and CD4-CD8+	Proportion of all T cells	Proportion of B220+/IgM+	Proportion of Granulocytes (Gr1+)	Relative Proportion of B220+ CD43+	Relative Proportion of B220+ IgM+	Relative Proportion of B220+ IgM-	Proportion of granulocytes (Gr1+)
Barlow et al., 1996*	Increased	Decreased	ND	Normal (Loizou et al. 2011)	Normal	ND	Decreased	Decreased	Normal
Xu and Baltimore, 1996	Decreased	Decreased	Decreased	Normal	ND	Normal	Normal	Decreased	Increased
Elson et al., 1996	Increased	Decreased	Decreased	ND	ND	ND	ND	ND	ND
Borghesani et al., 2000	Decreased	Decreased	Decreased	Normal	ND	Decreased	ND	Decreased	ND
Spring et al., 2001	ND (Total thymocytes decreased)	ND	ND	ND	ND	ND	ND	ND	ND

Table summarises the haematological phenotypes of A-T mice. Daniel and Yammoto homozygote mice weren't viable so were excluded from the comparison. ND= not done *Wynshaw-Boris mice

24

1.6.1 Atm null mice

Barlow and colleagues created the first A-T mouse in 1996 (Barlow et al., 1996). Atm protein expression was ablated by insertions of a PKG neo cassette into the Atm gene at position 5790 to create a truncation mutation similar to that seen in A-T patients. This mutation was predicted to lead to absence of ATM protein expression in these mice and southern blotting was used to confirm disruption of the gene. These mice recapitulate A-T in that they are radiosensitive, sterile, smaller than wild type, have immunological abnormalities and a high susceptibility to T cell lymphoma of the thymus (thymoma). All mice develop thymoma of CD4+CD8+ T cell origin, and die between 2 and 4 months of age. The thymomas are genetically unstable and contain chromosome 6, 12, 14 and 15 translocations.

Immunological abnormalities in the Wynshaw-Boris (Barlow) mice included reduced CD4+ and CD8+ T cells. Additional analysis of these mice by Loizou and colleagues (Loizou et al., 2011) showed that pre B and immature B cells are also reduced in these mice. Abnormalities in the B cells in the Barlow mice also include reduced IgG expression, suggesting and impairment in CSR.

No evidence of neurodegeneration can be detected in these mice by histological examination of brain tissues including cerebellum. However, the Barlow A-T mice faired poorly in rota-rod tests and foot print analysis compared to wild type mice, suggesting a neurological deficit in these A-T mice. The mild neurological abnormalities observed in these mice are clearly not as severe as the progressive neurodegeneration that develops in A-T patients (Shiloh and Rotman, 1996).

A-T mice were also generated with disruption of the Atm gene in several other laboratories. Xu and Baltimore generated mice by disrupting the conserved sequence in the kinase domain

that resulted in no protein expression (Xu et al., 1996, Xu and Baltimore, 1996). The Xu and Baltimore mice, like the Wynshaw-Boris mice, nearly all develop T cell lymphoma and die by the age of 4 months. Similarly they also have immunological abnormalities. Double positive (CD4+CD8+) and single positive (CD4+CD8- and CD4-CD8+) T cells, along with immature (B220medium IgM+) and follicular (B220+IgM-) B cells are reduced in the Xu and Baltimore mice. Unlike the Wynshaw-Boris mice, the Xu and Baltimore mice showed no signs of neurological abnormalities.

The Elson (Elson et al., 1996) mice had a disruption in the Atm gene that corresponded to position 5460 of human cDNA. These mice produced two alternative spliced Atm mRNAs but no Atm protein expression (normal or abnormal), could be detected in their tissues. The Elson mice were similar to the Wynshaw-Boris and Xu Atm null mice in that they had growth retardation, hypersensitivity to ionising radiation and reproductive defects. Like the Xu and Baltimore mice, no neurological abnormalities have been observed in the Elson mice. Interestingly, the incidence of thymoma was much lower in the Elson mice compared to the Wynshaw-Boris and Xu and Baltimore mice as only a third (4/12) of mice developed a thymoma.

Some mutations that are found in A-T patients result in the expression of an abnormal ATM protein that retains some activity (Reiman et al., 2011). With this in mind, Borghesani (Borghesani et al., 2000) generated mice with mutations that were intended to express abnormal Atm protein. This mouse had an insertion in the kinase domain that allowed for two Atm transcripts; one that had a premature stop codon and another that would theoretically allow for read through and production of an abnormal Atm protein that had a kinase domain. However no Atm transcript or protein was detected in these mice. Despite this, the Borghesani mice lived longer than the Wynshaw-Boris and Xu mice; 50% of Borghesani

mice were still alive at 10 months of age. The incidence of lymphoma development was also reduced compared to the Wynshaw-Boris and Xu and Baltimore mice suggesting that something was protecting these mice. Despite these differences the Borghesani mice were similar to the Wynshaw-Boris and Xu and Baltimore mice in that all three had reduced T and B cell numbers. Double positive (CD4+CD8+) and single positive (both CD4+CD8- and CD4-CD8+) thymocytes were reduced, indicating a disruption in T cell maturation. Also, immature B cells (B220medium IgM+) in the bone marrow were reduced but the more mature B cells in the spleen were comparable to that of the wild type mice.

Unlike the Wynshaw-Boris, Xu and Baltimore, and Elson mice, the Borghesani mice had detectable neurological defects. In the cerebellum, the molecular layer was reduced and Purkinje cells had an abnormal pathology that was detectable in both young (6 weeks of age) and old (12 months of age) mice. No overt ataxia could be seen in bridge crossing or footprint analysis tests but rota rod performance indicated that the Borghesani mice had decreased motor learning.

A mouse model was made by Spring and colleagues that had residual Atm protein expression (Spring et al., 2001). This model carried a mutation that recapitulated the c.7636del9 mutation found in A-T patients. Like the Atm null mice generated by Wynshaw-Boris, Xu, Elson and Borghesani and colleagues, the Spring mice had growth retardation, radiosensitivity, reproductive defects and immunological abnormalities but they are dissimilar to the models that had no Atm protein expression because they lived longer. Approximately, 30% of Spring mice were still alive at 18 months. These mice developed thymic lymphoma at a lower incidence than the mice with complete loss of Atm protein. The thymic lymphoma developed from a double positive (CD4+CD8+) and single positive (CD4+CD8- and CD4-CD8+) origin whereas the Atm null mice predominantly developed double positive (CD4+CD8+) thymic

lymphoma. In addition the Spring mice also developed malignancies of a non-T cell origin. Mice that died before 40 weeks of age all developed T cell lymphoma, but older mice were susceptible to developing B cell lymphoma as well as ovarian sex cord, epithelial and stromal cell tumours.

The Wynshaw-Boris, Xu and Baltimore, Elson and Borghesani mice all had no detectable Atm transcript or protein expression yet the age of survival and tumour type and incidence in these mice differed greatly. There have been two possible reasons for this proposed; (1) differing husbandry methods: Reduced exposure to pathogens can reduce the incidence of lymphoid tumours in mice and could also be a factor in the development of lymphoid tumours in A-T mice (Reliene and Schiestl, 2006) and (2) Differing background strains: The background strain of the mice can also affect tumour incidence (Genik et al., 2014).

Finally, a further type of *ATM* mutation was modelled in mice. Mice were engineered to express a normal level of ATM protein that was kinase dead; these mice were not viable when the mutation was present in the homozygous state (Daniel et al., 2012, Yamamoto et al., 2012). This suggested that the presence of kinase dead Atm protein was more detrimental to the organism than complete loss of Atm protein. In the Daniel et al work, the authors modelled two ataxia telangiectasia mutations c.8293 G>A; p.(Gly2765Ser) and c.8189A>C;p.(Gln2730Pro), which in patients gave rise to expression of a normal level of ATM protein but without kinase activity (Reiman et al., 2011). Homozygosity for each of these mutations, in mice, was embryonically lethal. A conditional deletion allowed survival of the c.8189A>C;p.(Gln2730Pro) heterozygous mouse. The reason for the presence of kinase dead ATM protein causing embryonic lethality in mice is not known and while there are no known examples of human homozygotes for these particular mutations, there is a published case of another *ATM* mutation, c.9022C>T;p.(Arg3008Cys), present in a patient in the

homozygous state (Angèle et al., 2003). The effects, on the one hand, of kinase dead ATM protein and, on the other, total absence of ATM, in A-T patients remains to be fully investigated.

At the same time, another group generated a mouse that also expressed an Atm protein that lacked Atm kinase activity (Yamamoto et al., 2012). This mouse had a D2880A/N2885K double mutation that corresponds to D2870A/N2875K in humans (Canman et al., 1998, Bakkenist and Kastan, 2003). Mice that were heterozygous for this double mutation were viable, normal in size, fertile and had no discernable lymphocyte abnormalities. However, like the Daniel mice, homozygous mutation led to embryonic lethality. It was concluded that the cause of embryonic lethality was not due to a dominant negative effect, as heterozygous mice had no defects. To overcome this lethality conditional kinase dead (KD) mice were generated. The defect in lymphocyte development was not enhanced in conditional Atm KD mice, as V(D)J recombination and CSR was similar to Atm-/- mice. Conditional KD Atm mice had increased genomic instability after IR compared to Atm-/- mice, which points to an inhibitory involvement of KD Atm in NHEJ and HR.

1.6.2 Lymphoma in A-T mice

A-T mice (excluding the Spring mice), develop DP (CD4+CD8+) T cell thymic lymphoma. These lymphoma harbour recurrent translocations involving chromosomes 12, 14, and 15. The translocations are present in almost all cells in a tumour population (Liyanage et al., 2000). Translocation between chromosomes 12 and 14 (12;14)) are commonly found (Zha et al., 2010). The break point of this translocation on chromosome 14 is at the TCRalpha/ delta locus and this is juxtaposed to the centromeric portion of chromosome 12. This translocation causes loss of the B cell immune gene IgH. The t(12;14) is also concurrent with amplification of a portion of chromosome 14 to generate complex translocations called complicons (Zha et

al., 2010, Liyanage et al., 2000). There are several possibilities as to why chromosome 14 frequently translocate with chromosome 12. The TCR and IgH locus are frequently co localised in the nucleus. This close proximity could allow for increased incidence of erroneous repair of DSB in each of these genes that leads to translocation. The loss of the distal part of chromosome 12 or the juxtaposition of 12 to 14 could also confer an advantage to the cell and therefore this translocation is selected for. T cell lymphomas in A-T mice have another chromosomal abnormality that is likely to confer a selective advantage to the cell. Aberrations involving chromosome 15 frequently results in increased copy number of Myc, although this increased copy number does not result in increased mRNA levels in these cells (Liyanage et al., 2000). The chromosomal locations of immune genes and gene associated with lymphoid tumours in humans and mice are given in Table 1.3.

Table 1.3 Chromosome locations of genes in humans and mice

Human		Mouse		
Name	Location	Name	Location	**Description**
Immune genes				
IGH	14	Igh	12	Immunoglobulin heavy
IGL	22	Igl	16	Immunoglobulin light
IGK	2	Igk	6	Immunoglobulin kappa
TRA	14	Tcra	14	T cell receptor alpha
TRD	14	Tcrd	14	T cell receptor delta
TRB	7	Tcrb	6	T cell receptor beta
TRG	7	Tcrg	13	T cell receptor gamma
Non-immune genes				
MYC	8	Myc	15	Myelocytomatosis oncogene
BCL6	3	Bcl6	16	B-cell CLL/lymphoma 6
BCL2	18	Bcl2	1	B-cell CLL/lymphoma 2

This table gives the location of immune genes and non-immune genes in human and mice. The nomenclature for each species is taken from the NCBI Gene database.

1.7 The origins of B cell lymphoma

1.7.1 An overview of the WHO classification of lymphoid neoplasms

The WHO classification of tumours of haematopoietic and lymphoid origin aims to encompass the all the methodologies available to clinicians in the diagnosis of human tumours. These include morphological, immunophenotypic, cytogenetic and clinical features. The most recent review of the classification system was conducted in 2008. The classification stratifies neoplasms into lineage (myeloid, lymphoid or dendritic cell/ histiocytic cell) and aims to assign a normal cell counterpart to each neoplasm. Lymphoid neoplasms are divided into two groups B and T cell/NK cells. Most T and B cell neoplasms largely resemble the normal cells counterpart and their classification reflects this (Swerdlow, 2008).

To understand B and T cell neoplasm classification an understanding of lymphocyte development is needed. Briefly, progenitor B cells (Immunoblast B cells) in the bone marrow undergo V(D)J recombination and differentiate into Pre- B cells, which become immunoglobulin (IgM+) expressing immature B cells, that leave the bone marrow and finally become mature B cells expressing both IgM and IgD (Lebien and Tedder, 2008). Mature B cells that encounter antigen in secondary lymphoid tissues enter the germinal centre, become rapidly proliferating centroblasts and undergo CSR and SHM. Once they stop dividing, the centroblasts move to the light zone of the germinal centre (GC) and become centrocytes. Centrocytes leave the germinal centre and differentiate into long-lived plasma cells or memory B cells (Maclennan, 1994, Allen et al., 2007a). Some post-germinal centre memory B cells remain in the marginal zone of the follicle and others enter the peripheral blood. Marginal zone B cells express pan B cell markers (CD19 and CD20), IgM and low levels of IgD. Plasma cells travel to the bone marrow where they survive for long periods of time and

31

secrete antibody (Mcheyzer-Williams and Ahmed, 1999). Also see Figure 1.2 for an outline of B cell development in the germinal centre.

There are two types of lymphoma that are of most interest here, diffuse large B cell lymphoma (DLBCL) and follicular lymphoma (FL). DLBCL cells morphologically resemble centroblasts and centrocyte cells. In addition, DLBCL cells have evidence of somatic hypermutation taking place suggesting that they originate from cells that have been exposed to antigen and were part of the GC reaction. FL also originates from GC B cells. They are composed of a mixture of centrocytes and centroblasts. The proportion of each cell type determines the grading of the lymphomas. Lymphoma can also arise from non-germinal centre B cells and include, mantle cell lymphoma, marginal cell lymphoma and plasma cell myeloma. The morphological, immunological and genetic characteristics of these tumours as described in the WHO classification, 2008 will be described in more detail below (Swerdlow, 2008).

1.7.2   Classification of diffuse large B cell lymphoma

DLBCL are a heterogeneous group of tumours and patients may be asymptomatic depending on the tumour location. The most recent nomenclature given to this tumour group is DLBCL, not otherwise specified (NOS). The common variants of this type are centroblastsic, immunoblastic or anaplastic type. The cells in this tumour form a diffuse pattern and are twice the size of a normal lymphocyte. DLBCL, NOS usually arise de novo but can also be a consequence of progression of another, less aggressive type of B cell lymphoma e.g. follicular lymphoma. The centroblastsic variant is the most common variant of DLBCL and is either composed almost entirely of centroblasts (>90% centroblasts) or is a mixture of centroblasts and immunoblasts (<90% centroblasts). DLBCL usually lack expression of one or more common B cell markers. Tumour cells usually express surface immunoglobulin, most

commonly IgM and less frequently IgG and IgA. Other surface markers typical of this lymphoma include; IRF4/MUM1, CD10, BCL6, BCL2. Genetic analysis of DLBCL shows that *MYC* and *IgH* are frequently translocated in these tumours. Aberrant somatic hypermutation of *MYC, BCL6 PAX6* or *RHO/ TIFF* are present and suggested to be involved in tumourigenesis of DLBCL (Swerdlow, 2008).

1.7.3 Classification of follicular lymphoma

Follicular lymphoma is composed of both centrocytes and centroblasts. Most FL have a follicular pattern that differs to a reactive follicle as it has a smaller or non-existent mantle zone and tingible body macrophages are usually absent. FL is graded to aid prognosis and treatment. Grade 1 and 2 are low-grade lymphoma. Grade one predominately consists of centrocytes and 0-5 centroblasts per high power field (hpf). Grade 2 contains 6-15 centroblasts per hpf. Both grades 1 and grade 2 are indolent and the same treatment is prescribed for both. Grade 3 is a high-grade lymphoma that has > 15 centroblasts per hpf. Grade 3 is further subdivided; grade 3A has centrocytes present and grade 3B is solid sheets of centroblasts only. Within a FL, diffuse areas of predominantly centroblasts are given a separate diagnosis of DLBCL with follicular lymphoma, grade 1-2, grade 3A or grade 3B. The number of centroblasts is counted or estimated, in ten neoplastic follicles, and expressed per 40x hpf. Follicular lymphoma usually express surface antigen (IgM+/-, IgD, IgG or IgA) as well as B cell associated antigens. In addition tumour cells in FL are commonly BCL2+, BCL6+, CD10+ CD5- CD43-. FL grade 3B cells may lack CD10 expression but still express BCL6. FL have rearranged immunoglobulin gene and SHM can be ongoing. BCL2 translocations are frequently found in FL, and are more common in grade 1-2 than grade 3 (Swerdlow, 2008).

1.7.4 Classification of marginal zone and mantle cell lymphoma

Splenic marginal zone lymphoma (MZL) is composed of small-medium sized cells that resemble those in the follicular marginal zone. Marginal zone tumour cells replace the white pulp and infiltrate the red pulp. Tumour cells in MZL commonly express surface IgM and sometimes IgD. Most MZL are BCL2 positive, approximately 50% of cases are CD43+ and MZL tumour cells are negative for CD10, BCl6, CD5 and CD23 expression. 50% of cases in MZL tumour cells have a mutated *IgH* gene suggesting that they have been exposed to antigens but otherwise a specific cell type has not been assigned to this type of tumour yet.

Mantle cell lymphoma (MCL) accounts for 10% of NHL in humans. MCL resemble small to medium sized lymphocytes with an irregular nucleus. MCL cannot be distinguished from MZL morphologically and require immunophenotypic analysis to confirm diagnosis. MCL tumour cells express IgM and IgD. In addition they are BCL2+, CD5+, CD43+, CD10-, BCL6, Cyclin D1+. MCL tumour cells have a rearranged *IgH* but do not have evidence of SHM so are likely to develop from a pre-germinal centre B cell. In general, MCL tumours have Cyclin D1 translocations and an additional number of non-random translocations (Swerdlow, 2008).

1.7.5 Classification of Burkitt lymphoma

Morphologically, Burkitt lymphoma is composed of medium irregular shaped tumour cells with round nuclei and prominent nucleoli. Burkitt lymphoma has a high proliferation index and a large amount of visible apoptosis. The large numbers of macrophages that have ingested apoptotic tumour cells creates a starry sky pattern in that is characteristic of Burkitt lymphoma. Burkitt lymphoma tumour cells have a rearranged IgH gene and mutations that are associated with somatic hypermutation (SHM). Burkitt lymphoma tumour cells express the common B cell antigens and also express BCL6, CD38, CD77 and CD43. Tumour cells in

Burkitt lymphoma are usually BCL2 negative. The most common genetic abnormality associated with Burkitt lymphoma is a translocation between *MYC* and *IgH*.

In certain instances, tumours have features that align with both DLBCL and Burkitt lymphoma. These tumours are classified as B cell lymphoma, unclassifiable, with features intermediate between diffuse large B cell lymphoma and Burkitt lymphoma. The tumour cells in these lymphomas can be medium sized cells or a mixture of medium and large blast cells. Other features of tumours in this classification include, a high mitotic index, and either with or without a *MYC* translocation. The *IgH* gene is clonally rearranged in these tumours and expressed. Tumour cells are also CD10+, BCL6+ BCL2- and IRF4/MUM1-. This is a heterogeneous classification group and some transformed FL can be placed in this category (Swerdlow, 2008).

1.7.6 Classification of lymphoid neoplasms in mice

In 2002 the Mouse Models of Human Cancers Consortium (MMHCC) was formed and a haematopathology committee were brought together to develop a scheme for the classification of mouse lymphoma and leukaemia that could be used by pathologists to relate murine malignancies to human counterparts. A goal of studying mouse lymphoid neoplasms is to determine if they truly recapitulated human disease. For the most part, mouse leukaemia and lymphoma are categorised in a similar structure to human leukaemia and lymphoma, but there are a few differences between human and mice that should be taken into consideration. First, mice have on-going haematopoiesis in the spleen throughout adult life, unlike in adult humans where haematopoiesis is restricted to the bone marrow (Wolber et al 2002). Second, the murine germinal centre structure is modestly different in the mouse compared to humans, as the marginal zone is smaller and less distinct. With regards to neoplasm cytology, mouse FL has a more diffuse pattern, whilst still maintaining a follicular character, and also has a higher

proportion of centroblasts than human FL. The final difference to note is murine lymphomas with a high proliferative index and surface Ig expression that resemble human Burkitt lymphoma may lack translocations involving *MYC* and in this instance, it is suggested that, they are categorised as Burkitt-like lymphoma. With consideration of the exceptions mentioned above, classification of DLBCL, FL, marginal zone lymphoma, and classic Burkitt lymphoma is in alignment with the guidelines for the classification of human lymphoid neoplasms (Swerdlow, 2008).

1.7.7   B cell lymphoma tumourigenesis

Through understanding the development of lymphoma better, It is hoped that better tratments can be developed. Chromosome translocations have long been associated with lymphoid tumour development (Lengauer et al., 1998). Lymphoid tumours and B cell lymphoma in particular, have chromosomal translocations that usually involve the immunoglobulin variable or switch region, but non IG gene rearrangements have also be found (Robbiani and Nussenzweig, 2013). Translocations confer a proliferative advantage to the cell. Advantage can be gained through juxtaposition of a proto-oncogene next to a promoter that increases the transcription of this protein or gene translocations can lead to fusion of two genes and the production of an altered gene product that has oncogenic activity (Nussenzweig and Nussenzweig, 2010). The most likely cause of translocation that leads to tumourigenesis is the persistence of unrepaired DNA DSB.

1.7.8   Etiology of DNA double strand breaks in lymphoma

Chromosomal translocations are only able to form when two concurrent DSBs are present. DSBs occur frequently in dividing cells as a consequence of errors in replication (Bartkova et al., 2005). Current estimates predict that approximately 10 double strand breaks occur in dividing fibroblasts per day (Lieber, 2010). The cause of these breaks can be endogenous or

exogenous. Programmed DSB are generated during lymphocyte development by RAG1/2 and AID proteins (Wang et al., 2008a). RAG1/2 generates DSB in the variable region of the *IgH* and *IgL* genes in pro-B cells in the bone marrow during V(D)J recombination (Gostissa et al., 2011). RAG1/2 targets recombination specific sequences (RSS) that flank the V, D and J genes. The RSS sequence consists of a conserved heptamer and an A-T rich nonamer separated by 12 or 23 bases. The specificity of these two signals target RAG to the correct gene families during V(D)J recombination. However this regulation of RAG1/2 is error prone. RAG1/2 also recognises some sequences that are highly similar to RSS as targets and generates DSB in non-immunoglobulin genes. These types of sequences are present in certain oncogenes, including *BCL2*. These off target RAG1/2 breaks can become illicit substrates for V(D)J recombination (Marculescu et al., 2002).

In mature B cells AID is activated and generates DSB breaks for the processes of SHM and CSR. RAG1/2 targets specific sequences whereas AID is more promiscuous in its coding target. AID targets RGYW motifs such as AGCT and although these motifs are enriched in the variable region exons, they are also present throughout the genome. Consequently, non-immunoglobulin genes are also frequently targeted by AID. Genes that are frequently found translocated in cancers such as *Pax5, Il21r, Gas5, Ddx6, Birc3, Ccnd2, Aff3, Grhpr, MYC, Pvt1, Bcl2l11, Socs1, mir142, Junb* and *Pim1*, are AID target hotspots. Translocations involving these genes often confer a selective growth advantage to the cell. In addition to the off-target action of RAG1/2 and AID, physiological factors such as errors in replication and transcription, and certain DNA structures can generate DSBs (Zhao et al., 2010). External factors also cause DSB DNA damage. Common cancer treatments such as topoisomerase inhibitors and IR, or oxidation can also generate DSBs (Felix et al., 2006).

In normal circumstances DSBs break are rapidly repaired and genome integrity is maintained (Robbiani and Nussenzweig, 2013). For a translocation to occur an unrepaired DSB generated by one of the above mechanism must persist long enough to come into close proximity to a second DSB to which it can be joined. In normal cells the DDR leads to cell cycle checkpoint activation and repair of the break by either C-NHEJ or HR (Section 1.3.4, 1.3.6). Impairment in this response by loss of one of the factors involved causes the persistence of DSBs. Unrepaired DSBs are substrates for translocations that can have severe consequences on the cell and organism. B lymphocytes from mice deficient in Atm, a critical activator of cell cycle checkpoints in response to DSBs, harbor persistent DSBs. DSBs generated early on in development can become substrates for translocation later on in development in mature B cells (Isoda et al., 2012, Callén et al., 2007). Translocations and tumour development associated with Atm loss will be discussed below.

1.7.9 Mechanisms promoting translocation in lymphoma

After DSB have been formed and in order for these to result in translocation two DSBs must be brought together and joined. Either two DSBs are generated spatially close together in the nucleus or mobility of the damaged DNA ends brings two distant DSBs proximal allowing for them to be aberrantly joined (Misteli and Soutoglou, 2009). There are several factors that increase the possibility that two DSB will be generated in close proximity and that they may be aberrantly joined. Actively transcribed regions of DNA are localized in the nucleus together. Transcription is error prone, plus AID targets single strand DNA. Both of these factors increase the possibility of co-localised DSB formation occurring. The genome is not randomly organized. The higher organization of DNA into chromatin can lead to certain genes being colocalised with others. In mice two genes that frequently translocate together, *IgH* and *MYC*, are frequently localised near to each other in the nucleus, thus increasing the

possibility of a translocation between the two regions of the genome (Zhang et al., 2012, Klein et al., 2011). In addition mis-repair of DSB on chromosomes of a similar size is also possible.

The mobility of a chromosome can also determine the propensity for translocation. Changes to the chromatin properties such as relaxation, can affect the motion of chromatin and are critical for translocation (Dimitrova et al., 2008, Roukos and Misteli, 2014).

1.7.10 DSB repair and translocation ligation

Once two DSBs are co-localised they need to be ligated together for the translocation to be complete. The key question is what mechanism is responsible for the wrongful joining of these two DSB? DSB generated by RAG1/2 and AID in lymphocyte development are repaired by C-NHEJ. This repair pathway does not require a template and therefore can facilitate the joining of two non-homologous chromosomes such as in V(D)J recombination, SHM, CSR and aberrant translocations. Translocations occur in normal cells but occur at a higher rater in cells deficient for C-NHEJ factors. Mice have been generated that are deficient in each of the C-NHEJ factors and they have a reduced ability to undergo V(D)J recombination. When these mice are also deficient in p53 they develop tumours that harbor translocations (Rooney et al., 2004).

In the absence of C-NHEJ ,breaks can be repaired by a process called alternative end joining. (A-EJ) and it is thought that this mechanism of repair is more prone to chromosomal translocations than C-NHEJ (Chiarle et al., 2011). DSBs joined using A-EJ tend to have higher degree of microhomology at the junction, but in the absence of microhomology blunt ends can also be joined. The search for homologous sequence processing at the broken ends can result in genetic loss or insertions, altering the normal code. C-NHEJ preferentially joins

breaks within the same chromosome; coincidently preventing the occurrence of translocations. Overall, C-NHEJ plays a role in maintaining genome stability and loss of this pathway has severe consequences for the cell (Ferguson et al., 2000, Alt et al., 2013).

1.7.11 The role of NHEJ in B cell lymphoma development

Mice deficient for C-NHEJ factors show a marked decrease in V(D)J recombination, decreased CSR and increased neuronal cell death. Cells from these mice have a high level genomic instability. Activation of the p53 checkpoint prevents tumourigenesis in mice that lack C-NHEJ. Therefore mice deficient for both a C-NHEJ factor and p53 have a high predisposition to the development of lymphoid malignancies (Franco et al., 2006, Lieber et al., 2006).

For example, mice deficient in XRCC4 and p53 develop pro-B cell lymphomas that harbor IgH-Myc translocations. In addition, they also have complex translocations (complicons) that contain amplification of both Myc and IgH gene loci. These complicons are initiated by RAG1/2 induced breaks and joined by A-EJ (Zhu et al., 2002). In mice with XRCC4 and p53 deficiency in mature B cells, tumour development occurs via a slightly different mechanism. Mice developed mature B cell lymphomas that had attempted V(D)J recombination and CSR but lacked surface immunoglobulin expression. The tumors harbored frequent translocations involving IgH, Igκ and Igλ locus. Most of these tumours had reciprocal translocations between IgH and Myc but had no gene amplification or complicons (Wang et al., 2008b). Analysis of the breakpoints of these translocations showed that they arise from RAG1/2 induced breaks and suggested that, like the XRCC4 deficient pro B cell lymphoma, the translocations in the mature B cell lymphoma resulted from abnormal secondary V(D)J recombination in the periphery (Wang et al., 2009). Both XRCC4 deficient Pro B cell lymphoma and mature B cell lymphoma had translocations involving Myc but the up-

regulation of this gene is likely to be caused by different mechanisms and dependent on the differentiation stage of the B cell.

Similar phenotypes were observed in mice deficient for other C-NHEJ factors. Ku80-/-p53-/- mice developed disseminated pro-B cell lymphomas with IgH-Myc translocations and complicons (Difilippantonio et al., 2000). In addition, Lig4-/- p53-/- mice develop pro- B cell lymphomas that have amplification of both IgH and Myc (Orii et al., 2006). These models illustrate that loss of C-NHEJ in the absence of p53 checkpoint allows for the occurrence of tumorigenic translocations and the development of B cell lymphomas.

1.7.12 The mechanisms associated with Atm loss and tumour development

In addition to the components of C-NHEJ, factors responsible for detecting the DSB are also important in lymphocyte differentiation and protecting against tumour development (Nussenzweig and Nussenzweig, 2010, Bartkova et al., 2005). Human patients deficient in the DDR factors ATM, H2AX, 53BP1, MCD1, MRE11 and NBS1 have reduced lymphocyte development due to impaired V(D)J recombination and CSR (Franco et al., 2006).

Loss of the DNA damage response factor, ATM, affects V(D)J recombination and increases tumour development in humans and mice (section 1.1.1,1.1.3). Several studies have sought to understand the role of immune gene rearrangement, and the mechanism for this rearrangement, in the development of tumours in the absence of ATM protein. Like humans, Atm-/-mice have perturbed lymphocyte development and develop T cell lymphomas (thymomas), which frequently harbour translocations involving immune genes (Zha et al., 2010). The reduced capability of successful V(D)J recombination in Atm-/- T cells inhibits differentiation and is the reason for the reduced levels of mature T cells in Atm-/- mice.

Aberrant V(D)J recombination in Atm-/- T cells also results in unresolved DSB that predispose to translocations (Vacchio et al., 2007)

The effect of Atm loss is similar in B cells and T cells. Atm-/- mature B cells have a greater number of unrepaired DSBs in the antigen receptor genes than wild type mature B cells *in vitro*. These breaks are not dependent on AID, which is expressed only in mature B cells, suggesting that the breaks persist from an earlier developmental stage. The DSBs in mature Atm-/- B cells are dependent on RAG1/2 expression and are likely the result of erroneous attempts at V(D)J recombination (Callén et al., 2007). Even though RAG1/2 induced breaks are not critical for tumour development in Atm-/- mice, the high frequency of RAG1/2 breaks and the persistence of these breaks increase the likelihood for erroneous repair of these DSBs and the potential for translocation (Petiniot et al., 2000).

Tumour development in Atm deficient mice is associated with, but not exclusively reliant on RAG1/2 or AID induced breaks in the immune genes (Petiniot et al., 2002, Ramiro et al., 2006). RAG2-/-Atm-/- mice still developed tumours, albeit at a lower frequency than Atm-/- mice. Unlike Atm-/- T cell lymphoma, RAG2-/-Atm-/- tumours did not have translocations involving the TCRα, or TCRδ genes. They did however have increased number of translocations compared to Atm-/- tumours, indicating that Atm-/- tumours develop translocations caused by aberrant repair of DNA DSBs in both immune and non-immune genes (Petiniot et al., 2000, Liao and Van Dyke, 1999).

The persistence of DNA DSBs in Atm-/- mice is the consequence of a checkpoint defect in Atm-/- cells (Chun and Gatti, 2004). In the absence of checkpoint activation, a B or T cell that has a DSB, which is likely to be in one IgH or TCR allele, is able to undergo successive rounds of recombination in the second allele, until a successful V(D)J rearrangement is made.

Signalling through this second IgH or TCR promotes survival of the B or T cell respectively, and thus propagates the DSBs through successive cell divisions and differentiation (Callén et al., 2007).

1.7.13 Translocations associated with B cell lymphoma

Knowing the genetics of a tumour is important for diagnosis and treatment of human malignancies. Recurrent translocations are a hallmark of certain B cell lymphomas. These translocations frequently involve immunoglobulin genes, most commonly the *IgH* gene, which is located on chromosome 14 (Swerdlow, 2008). The translocation partner is usually a proto-oncogene, for which juxtaposition to the IgH enhancers causes up regulation. The most common translocations associated with DLBCL involves *BCL6* (Bastard et al., 1994, Offit et al., 1994). BCL6 is a transcriptional repressor that is involved in B cell development. Up-regulation of this protein via translocation prevents differentiation of the B cell, maintaining it as a GC B cell and predisposing it to neoplastic transformation (Ohno, 2004). The t(14;18) translocations involving *BCL2* is present in 18-20% of DLBCL (Hill et al., 1996). Also present in 85% of follicular lymphoma, the t(14;18) translocation is the major pathogenic mechanism in these lymphomas through up-regulation of *BCL2* (Barrans et al., 2003). Another gene that is frequently associated with translocation is *MYC*. Nearly all cases of Burkitt lymphoma harbour *MYC* translocations with an immunoglobulin gene. The translocation most frequently observed is t(8;14) and but sometimes t(2;8) and t(8;22), involving the light chain genes, are also found (Kramer et al., 1998). Translocations involving *MYC* are also found in other B cell lymphoma, including DLBCL, but in these tumours *MYC* can be found translocated to a non-immune gene (Johnson et al., 2009).

Chromosome translocation is not the only cause of gene deregulation in B cell lymphomas. Mutations have been found in *BCL2, BCL6, MYC, RHOH/TTF, PIM1, PAX5, IRF4,*

ST6GAL1, BCL7A, CIITA, LRMP and *SOC* in DLBCL. These mutations are caused by aberrant SHM and are likely to be involved in lymphomagenesis in the absence of translocations (Khodabakhshi et al., 2012, Pasqualucci et al., 2001).

1.8 The nude mouse

The athymic nude phenotype was first observed in a colony of hooded rats in 1953 at the Rowett Research Institute in England (Vos et al., 1980). The first nude mouse was described by Flanagan in 1996 (Flanagan, 1966). Homozygous mutation in the Foxn1 gene is responsible for the lack of hair, abrogated thymic development and reduced T cells in the nude mice (Nehls et al., 1994, Nehls et al., 1996) . The Foxn1 gene encodes a winged helix domain transcription factor named whn. A single deletion in the coding sequence of the whn gene causes a frame shift and a premature stop codon that prevents transcription of the protein. Whn is highly expressed in the thymus and skin, where is has a role in the inducing the expression of tissue specific genes required for thymic anlage and the hair papilla development (Nehls et al., 1996, Brissette et al., 1996).

Nude mice have reduced levels of T cells in the lymph nodes and spleen and consequently do not reject allografts and some xenografts. Despite having reduced T cell numbers, nude mice a have functional 'post-thymic' T cell repertoire with a cytolytically active CD8+ T cell response. The natural killer cell response is normal, even slightly elevated in nude mice (Belizário, 2009). The B cell population is also normal but the IgH antibody repertoire is reduced (Kaushik et al., 1995).

An observational study by Sharkey and Fogh suggests that the median survival for nude mice is 6 months, but this is dependent on the husbandry conditions (Sharkey and Fogh, 1979). The tumour incidence in nude mice is no different to that of the immunocompetent counterparts of the same strain (Stutman, 1978) and tumour development was observed in 6.8% of nude mice. Therefore nude mice do not have an increased incidence of spontaneous tumour development. Ninety-two per cent of tumours developed in nude mice that were over 5 months of age and

the median age of development was 9 months. The tumours were mostly of lympho-reticular origin, but a small proportion were pulmonary adenomas. Other causes of death in these nude mice included hepatitis and sendai virus infections (Sharkey and Fogh, 1979, Sharkey and Fogh, 1984).

1.9 Aims

The reason for Atm-/- mice developing only T cell lymphoma, whereas A-T patients develop a wide range of lymphoid malignancies has been a long-standing question (Micol et al., 2011). In an attempt to answer this question, Spring and colleagues (2001) developed mice with a hypomorphic Atm mutation. Indeed, in addition to thymoma development, these mice succumbed to B cell and non-lymphoid malignancies, albeit at a low frequency, but no investigation into the development of these tumours was undertaken. There is a need, therefore, for a model in which aggressive T cell lymphoma development is eliminated, allowing the development and investigation of other phenotypes associated with A-T. This model for example, could enable investigation into non-T cell tumour development in the absence of Atm protein expression. The nude (nu-/-) mouse is athymic. If thymic development was abrogated in the Atm-/- mouse, by crossing it with the nu-/- mouse, it could be possible to prevent thymoma development and generate a long-lived Atm-/- mouse in which case these studies could be carried out.

T cell malignancies in A-T patients and Atm-/- mice are associated with translocations within immune genes but little is known about the development of B cell malignancies in A-T patients (Russo et al., 1988, Liyanage et al., 2000, Taylor et al., 1996). Analysis of Atm-/- tumours revealed the role of defective DNA repair in the development of genetic abnormalities that contribute to tumour development. In these tumours loss of Atm caused persistence of unrepaired DSBs that result in translocations as a consequence of abnormal immune gene rearrangements during lymphocyte development (Zha et al., 2010). Whether ATM null B cell lymphomas develop by a similar mechanism remains to be elucidated.

With these questions in mind the aims of this study were;

a. To generate an Atm-/-nu-/- nude A-T mouse in which early thymoma development and subsequent early death was abrogated and in which longer survival might reveal susceptibility to other tumour types.

b. To determine the suitability of this new Atm-/-nu-/- nude A-T mouse as a model for A-T.

c. To investigate the mechanisms associated with the development of any malignancies in these Atm-/-nu-/- nude A-T mice.

CHAPTER 2

MATERIALS AND METHODS

2 MATERIALS AND METHODS

2.1 Generation of A-T mice

2.1.1 Generation of Atm-/- mice

Atm-/- mice were generated by the Wynshaw-Boris laboratory (Barlow et al, 1996). Atm knockout was undertaken by insertion of a PGK-neomycin gene into position 5979 of the murine Atm gene causing a truncating mutation.

We obtained these mice as a breeding pair of heterozygotes from the Jackson laboratory (stock number *129S6/SvEvTac-Atm^{tm1Awb}/J*). These were bred to larger numbers and heterozygote males and heterozygote females mated to generate Atm-/-, Atm+/- and Atm+/+ mice. All work was approved by the Home office under the Animals (scientific procedure) act 1986.

2.1.2 Generation of Atm-/-nu-/- mice.

The generation of Atm-/-nu-/- mice required a series of matings. The proximal mating pairs that produced these double knockout animals were Atm heterozygous nude males (Atm+/-nu-/-) and female Atm/nude double heterozygotes (Atm+/-nu+/-). Some additional preliminary matings were undertaken in order to get to these proximal genotypes and these are given in table 2.1. First, Atm+/-nu+/- males and Atm+/-nu+/- females were obtained by mating an Atm heterozygote female (Atm+/-nu+/+) with a Balbc nude male (Atm+/+nu-/-) (Mating 1). An Atm+/-nu+/- female from the first generation was then mated with a nude male as used in the first cross (Mating 2). From this mating Atm+/-nu-/- males were obtained. The third mating was the proximal one of male Atm+/-nu-/- with female Atm+/-nu+/-. Some of these offspring were Atm-/-nu-/- double knockouts. The breeding strategy is outline in Table 2.1

Table 2.1 Mating strategy for the generation of Atm-/-nu-/- mice

Mating number	Mating Genotypes	Progeny genotype
Mating 1	Atm+/+nu-/- (m) x Atm+/-nu+/+ (f)	Atm+/+nu+/- **Atm+/-nu+/- (f)**
Mating 2	Atm+/+nu-/- (m) x Atm+/-nu+/- (f)	Atm+/+nu+/- Atm+/+nu-/- Atm+/-nu+/- **Atm +/-nu-/- (m)**
Mating 3	Atm+/-nu-/- (m) x Atm+/-nu+/- (f)	Atm+/+nu+/- Atm+/+nu-/- Atm+/-nu+/- Atm+/-nu-/- Atm-/-nu+/- **Atm-/-nu-/- (m & f)**

2.2 Atm genotyping

2.2.1 DNA extraction

Ear clippings from 3 weak old mice were incubated for a minimum of 5 hours, but usually overnight, in lysis buffer (100mM Tris-HCl pH 8.5, 5mM EDTA 0.2% SDS, 200mM NaCl, 100μg/ml proteinase K). Digested tissue samples were centrifuged for 15-20 minutes at 13000rpm. The supernatant was added to 1.5ml micro centrifuge tubes containing 350μl of propan-2-ol. DNA was precipitated by inverting several times and then was centrifuged at 13000rpm for 15-20 minutes. The supernatant was discarded and 500μl of 70% ethanol was added to wash the pellet. The DNA pellet was centrifuged again for 10-15 minutes at 13000rpm/18000g. Once more, the supernatant was discarded and the DNA pellet was air-dried. When completely dry the DNA pellet was resuspended in 20-50ul of 10mM Tris-HCl, 1mMEDTA pH8.0 depending on pellet size, and finally heated at 70-80°C for 10-15 minutes to resuspended the DNA in the buffer.

2.2.2 Atm PCR for identification of Atm-/- mice

Atm knockout in these Atm null mice was caused by the insertion of a PKG neomycin gene into the Atm gene. Mice with the Atm knockout gene were identified using primers between the remaining Atm sequence and the inserted PKGneomycin gene; Atm-A (5' gac ttc tgt cag atg ttg ctg cc -3') and Atm-Neo (5'ggg tgg gat tag ata aat gcc tg -3), that produced a 441-bp PCR product. Wild type Atm was detected using primers between the portion of the Atm gene present in the knockout and the part of the Atm that was deleted in the knockout; Atm-A (5' gac ttc tgt cag atg ttg ctg cc -3') and Atm-B (5' cga att tgc agg agt tgc tga g -3'), that generate a 152 BP PCR product. The thermo cycling protocol used was as follows: 94˚C for 3min; 37x[94˚C for 10 sec, 55˚C for 20sec]; 72˚C for 40sec. PCR products were

separated on a 1% agrose gel made with TBE and 5μl of PCR product was loaded with 2μl

trypan blue (New England Biolabs, Ipswich, UK).

The Atm-/-, Atm+/- and Atm+/+ mice could be distinguished as shown in Figure 2.1

2.2.3   Morbidity assessment

Mice were monitored daily for signs of morbidity. All animal procedures were performed

according to protocol.

Figure 2.1 Atm knockout identification
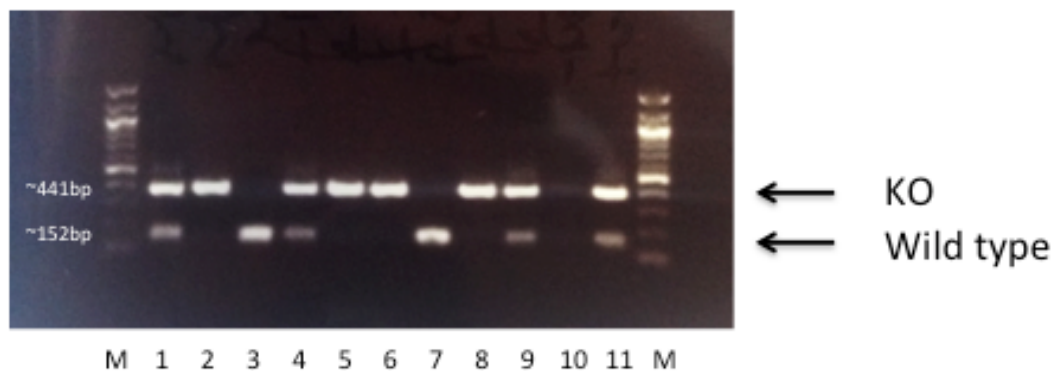
This agrose gel shows the result of an Atm genotyping PCR. Rows 1-9 mice, row 10 is a water control and row 11 is a known genotype control. The top band is the KO (knockout) allele and the bottom band is the wild type allele. A sample with two bands was heterozygote (Atm+/-) (Lanes 1, 4, 9). Lanes 2, 5, 6 and 8 were Atm-/- and lanes 3 and 7 were Atm+/+.

bp =base pair

M =marker

2.3 Analysis of cellular phenotype

2.3.1 Total protein extraction for subsequent Atm analysis

Tissues were isolated from the mouse and snap frozen in liquid nitrogen immediately after culling. All procedures were performed at 4°C or on ice where possible. Tissue was disrupted using a 1ml syringe plunger in 50μl RIPA buffer (Pierce, Illinois, USA) with added Halt protease inhibitor and 0.5M EDTA solution according to manufacturer's instructions (Thermo Scientific), then incubated at 4°C for 5 minutes. Samples were sonicated for 30 seconds and incubated again on ice for 10 minutes. Samples were then vortexed briefly, and centrifuged at 7°C for 20-30 minutes at a speed of 1400rpm. Finally, the supernatant was removed and protein determination was undertaken using Bio-Rad protein determination solution, before being snap frozen in liquid nitrogen and stored at -80°C until needed.

2.3.2 Total protein determination assay

Protein extracts were prepared as above (section 2.3.1). A standard curve was made using BSA diluted in distilled water to 0, 100, 200, 300, 400 and 500μg/ml and an example standard curve is shown in Figure 2.2. The standards were aliquoted in triplicate into a Falcon 96-well plate (Fisher Scientific). Protein samples were diluted 1 in 10 in distilled water and aliquoted in triplicate onto the 96-well plate. Bio-Rad protein determination solution was diluted 1 in 5 in distilled water and 200μl of this diluted solution was added all the samples in the 96-well plate. The reaction was incubated for 5 minutes at room temperature before the absorbance was measured at 595nm. A standard curve was plotted, from which the protein concentration of the samples were determined.

Figure 2.2 Representative BSA standard curve
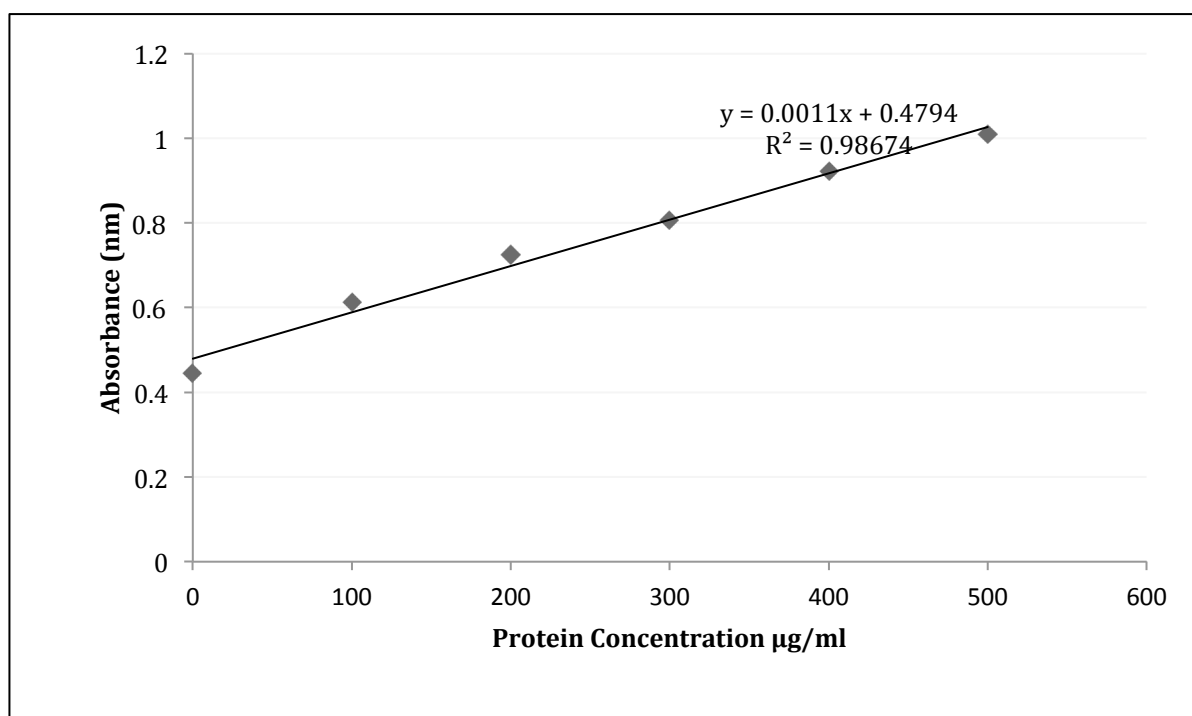
Total protein concentration was calculated using a standard curve like the one shown above.

2.3.3   SDS PAGE

Total protein from thymus, spleen, and brain was separated on a 6% acrylamide gel consisting of 4ml of 1M Tris/1M Biscine, 8 ml 30% acrylamide, 200μL 20% SDS, 80μL TEMED, 27.6ml of distilled water, and 200μL of 10% APS added last to initiate polymerisation. The mixture was poured into the gel apparatus and a well forming gel comb was inserted, ensuring all air bubbles were removed. Once the gel was set, the combs were removed and the wells were washed with running buffer (0.1M Tris/0.1M Biscine, 0.1% SDS).   25μg of human protein and 50μg of mouse protein was diluted 3:1 in 4X sample buffer (0.125 M Tris/HCl pH 6.8, 4% (w/v) SDS, 20% Glycerol, 0.2 M DTT, 0.02% bromophenol blue). Samples were denatured at 100°C for 5 minutes and loaded on to the gel alongside a molecular weight

marker (Thermo Fisher Fermentas). The gel apparatus were filled with running buffer and samples were electrophoresed for 4.5 hours at 30mA per gel.

2.3.4 Electrophoretic transfer of proteins

The gel was carefully removed from the plates and a piece of nitrocellulose membrane, that had been pre-soaked in transfer buffer (0.02 M Tris, 0.19 M glycine and 20% v/v methanol), was overlaid on to it ensuring all air bubbles were removed. The gel and membrane were sandwiched between 2 pieces of Whatman filter paper that were also pre-soaked in transfer buffer, and enclosed in a blotting cassette with two sponges. The whole cassette was placed in a transfer tank filled with transfer buffer and proteins were immunoblotted at 200mA overnight.

2.3.5 Immunodetection of proteins

Once transferred, the membrane was removed from the cassette and incubated with Ponceau stain (Sigma-Aldrich) for 5 minutes to visualise the proteins and check the success of the transfer. The stain was removed and the membrane was rinsed twice in distilled water. Using the molecular weight markers and the Ponceau stained lanes as a guide, the membrane was cut into sections that contained the proteins of interest (Atm is approximately 350kDa and SMC1 is approximately 150kDa). The membranes were then incubated in distilled water, with constant agitation, until there was no stain left on the membranes. To prevent non-specific background binding, the membranes were incubated in 5% Marvel dried milk powder made up in TBS-T, for 2 hours at room temperature with constant agitation. The membranes were then washed 3 times for 5 minutes in TBS-T at room temperature with constant agitation. The membranes were probed with anti-ATM (MAT3) (Sigma-Aldrich) or anti-ATM (2C1) (Abcam, Cambridge, UK) or anti-SCMC1 (Bethyl, Montgomery, Texas, USA) diluted in 5% milk in T-BST, in a sealed bag overnight at 4°C with constant rocking. The following day,

after removing primary antibody and washing thoroughly in TBS-T, the membranes were incubated with either anti-rabbit (1 in 3000) or anti-mouse (1 in 1000) HRP conjugated secondary antibodies (both from Dako, Cambridge, UK) for 1 hour at room temperature. The secondary antibody was removed, and the membrane was washed thoroughly for 3 x 10 minutes in TBS-T with constant agitation to remove any remaining secondary antibody.

For visualisation, the membranes were incubated with Amersham ECL solution (GE healthcare life sciences, Little Chalfont, UK) for 1 minute. Excess solution was removed and the membrane was placed in an X-Ray cassette. The luminescence generated from the HRP catalysed oxidation reaction was detected using X-Ray film (Amersham, GE healthcare) that was developed with a Xograph Imaging Systems Compact X4.

2.3.6 Splenocyte radiosensitivity analysis

A single cell suspension was generated from whole mouse spleen by forcing it through a 70μm strainer (Falcon). Cells were treated with Ammonium-Chloride-Potassium (ACK) lysing solution (Gibco, Life Technologies) to remove red blood cells. Splenocytes were cultured for 3 days in media containing 1% penicillin-streptomycin (Gibco, Life Technologies), 10% FCS (Sigma-Aldrich), 50μM β-mercaptoethanol (Gibco, Life Technologies,) and 150μg/ml E. coli lipopolysaccharide (LPS) (Sigma-Aldrich) at a cell density of $5x10^6$ per ml. After 3 days in culture the sample was divided into two: half was exposed to 1 Gray of radiation and the other was not exposed and used as a control. After irradiation the samples were incubated again at 37°C for 3 hours after which, a couple of drops of colcemid (Gibco, Life Technologies) were added using a 1ml Pasteur pipette. After 1 hour the media was removed and replaced with 2mls of 0.75M KCl solution (BDH, VWR, Pennsylvania, USA), incubated at 37°C for 15-20 minutes, and then fixed in 3:1 methanol:

acetic acid added drop-wise in the first instance. Fixation was repeated twice and after the final fix cells were left in approximately 10mls of fixative at room temperature, overnight.

Metaphase spreads were made by dropping a concentrated cell solution onto a slide that was air-dried and then stained with Geimsa diluted in buffer, pH 6.8 (Gurr®, VWR, Pennsylvania, USA) for 10 minutes. After which the slides were rinsed in pH 6.8 buffer and air-dried before a large cover slip was applied using DPX (VWR, Pennsylvania, USA).

For each mouse 25 metaphases were analysed for the control and irradiated sample, using a Leitz microscope. The quality of a metaphase was assessed to be sufficient for analysis at low power, before the metaphase was assessed for damage at high power (x100). Chromatid breaks, chromosome breaks tri-radial or quadri-radial chromosomes (three or four chromosomes attached together respectively) were quantified and as well as any abnormality that did not fit these standard descriptions, but was clearly abnormal and therefore was described as 'other'. The total number of abnormalities in 25 cells in the control sample was subtracted from the total amount of damage in 25 cells in the irradiated sample; to give the total amount of irradiation induced damage. Two Atm-/- and two Atm+/+ mice were analysed, and one of each Atm-/-nu-/-, Atm+/+nu-/-, and Atm-/- were also analysed.

2.4 Analysis of haematopoietic system in Atm-/- and Atm-/-nu-/- mice

2.4.1 Mouse tissue preparation

Mice were culled by cervical dislocation and a post mortem was undertaken where organs were checked for abnormality and lymph node size was assessed.

Both hind legs were removed, tissue was removed from the bone and then the bone was flushed with PBS or DMEM with 10% FCS to remove the marrow. Both the spleen,

approximately 0.5cm^3 of liver and tumour (when present), were also removed and a single cell suspension was made from these tissues by forcing them through a 70μm cell strainer (Falcon) that was then washed with PBS or DMEM with 10% FCS, collecting the cells in a 50ml falcon tube. The cells were treated with Ammonium-Chloride-Potassium (ACK) buffer (Gibco, Life Technologies) to remove red blood cells, except for erythrocyte analysis in the bone marrow cells were removed prior to ACK treatment. At this point cells were either stained for FACS analysis or frozen viably in FCS containing 10% DMSO (Sigma-Aldrich) for analysis at a later point. Comparison was always undertaken between fresh, or frozen samples only.

2.4.2   Cell staining with fluorophore conjugated antibodies

At least 1x10^6 cells were used for each panel of antibodies that was used. If using frozen cells, these were revived by thawing the cells at 37°C and diluting in 10ml of cold PBS or DMEM with 10% FCS, followed by spinning the cells at 1,100 RPM for 5 minutes. The cells were washed once more and finally re-suspended in 1ml of PBS or DMEM with 10% FCS in a 1.5ml eppendorf tube, and stored on ice ready to begin staining.

Staining was done on ice in a volume of 100μl in a V- bottom 96-well plate. Non-specific antibody binding was prevented by blocking the cells with 5μg/ml of anti- mouse CD16/32, except when CD16/32 expression was being analysed. Cocktails of antibodies were made for analysis of each cell type. Cells were incubated with the antibodies for 1 hour on ice in the dark (see Table 2.2). To stop the staining 100μl of PBS or DMEM with 10% FCS was added to the cells to dilute the antibody, before the plate was spun and then all the media was removed. Cells were resuspended in 300μl PBS or DMEM with 10% FCS and transferred into FACS tubes for analysis.

2.4.3 FACS analysis

Cells were analysed using a CyAn ADP analyser. All flow cytometry data was analysed using Summit software (Version 4.3). 20,000 (50,00 for stem cells) events were analysed for each sample. Control cells stained with a single antibody was used to compensate for spectral overlap. Gates were set on live cells for all analysis, which was determined by known size and density of live cells.

Cell populations were identified based on surface marker expression. The most pluripotent progenitor cells, the KSL (Lin-Sca-1+c-Kit+) population was subdivided into; (in order of decreasing pluripotency) long- term progenitors (LTP) (Flt3- CD34-), short-term progenitors (STP) (Flt3- CD34+) and multipotent progenitors (MPP) (Flt3+ CD43+). The Lin- Sca-1- c-Kit+ population was subdivided into common myeloid progenitors (CMP) (CD16/32+CD34med), GMP (CD16/32- CD34-) and MEP (CD16/32+CD34+).

T cell populations were identified as follows; immature double positive (DP) T cells (CD4+CD8+) and more mature single positive T cells; T- helper cells (CD4+ CD8-) and T-cytotoxic cells (CD4-CD8+).

B cell populations were identified as follows; Pro-B cells (CD43+B220+), Pre B cell (CD43-B220+) and immature B cells (CD43-B220med IgM+), transitional B cells (CD43-B220high IgM+) and follicular B cells (CD43-B220high IgM-) were also analysed. For measurement of IgM expression, B220 positivity was measured as medium and high to distinguish between immature and re-circulating B cells in the bone marrow and transitional and follicular B cells in the spleen.

For the myeloid cell populations, macrophage (CD11b+ Gr-1-) and granulocytes (CD11b+Gr-1+) were measured. The following erythrocyte populations were measured; pro erythroblast

(CD71+ TER-119-), erythroblast (CD71+ TER-119+) and mature erythrocyte (CD71-TER119+). Platelets and mature megakaryocytes (c-Kit-CD41+) megakaryocyte progenitors (c-Kit+CD41+) and all progenitors (c-Kit+CD41-). All populations except where stated, were expressed as a proportion of the total bone marrow cells or total spleen cells. A list of the all cell types and surface marker expression can be found in Table 2.2.

2.4.4   Antibodies

The antibodies used for FACS analysis are listed here and summarised in Table 2.3; **CD4-PE** (12-0041; clone GK1.5), **CD8a-APC** (17-0081; clone 53-6.7), **B220-APC** (17-0452; clone RA3-6B2), **Gr-1-APC** (17-5931; clone PB6-8C5), **CD11b-APC** (17-0112; clone M1/70), **CD5-APC** (17-0051; clone 53-7.3), **TER119-APC** (17-5921; clone TER-119), **CD71-PE** (12-0711; clone R17217), **c-Kit- Pe-Cy5** (15-1171; clone 2B8), **B220-E450** (48-0452; clone RA3-6B2), **CD11b-Pe-Cy7** (25-0112; clone M1/70), **Gr-1-FITC** (11-5931; clone RB6-8C5), **CD41-PE** (12-0411: clone eBioMWReg30), **CD34- FITC** (11-0341; clone RAM34), **Flt3-PE** (12-1351; clone A2F10), **Sca-1 -PeCy7** (25-5981; clone D7), **CD16/32-PE** (12-0161; clone 93), **CD43-PE** (12-0431; clone ebioR2/60), **CD16/32** (purified)(14-0161; clone 93), **CD5-APC** (17-0051; clone 53-7.3) and **CD19-PE** (eBio-D3, 12-0193). Lin+ cells were identified using lineage cocktail of the following APC conjugated antibodies B220, CD8a, Gr-1, CD11b, CD5 and TER-119. LSK cells were identified as Lin- Sca1+ c-Kit+.

Table 2.2 Categorisation of cell type by surface marker expression for FACS analysis

Cell Type	Cell markers
Progenitors:	
LSK	Lin-Sca-1+c-Kit+
Long term progenitor	Lin-Sca-1+c-Kit+Flt3- CD34-
Short term progenitor	Lin-Sca-1+c-Kit+Flt3- CD34+
Multipotent progenitor	Lin-Sca-1+c-Kit+Flt3+CD34+
Common myeloid progenitor	Lin-Sca-1-c-Kit+ CD16/32+CDCD34med
Granulocyte monocyte progenitor	Lin-Sca-1-c-Kit+ CD16/32-CDCD34-
Megakaryocyte erythrocyte progenitor	Lin-Sca-1-c-Kit+ CD16/32+CDCD34+
T cells:	
Double positive T cells	CD4+CD8+
Helper T cell	CD4+CD8-
Cytotoxic T cell	CD4-CD8+
B cells:	
Pro B cell	CD43+B220+
Pre B cell	CD43-B220+
Immature B cell	CD43-B220mediumIgM+
Transitional B cell	CD43-B220+IgM+
Follicular B cell	CD43-B220+IgM-
IgM+IgD+ B cells	B220+IgM+IgD+
IgD+ B cell	B220+IgM-IgD+
Myeloid Cells:	
Monocyte	CD11b+ Gr-1-
Granulocyte	CD11b+ Gr-1+
Pro-erythroblast	CD71+ TER-119-
Erythroblast	CD71+ TER-119+
Erythrocyte	CD71- TER-119+
All progenitors	c-Kit-CD41-
Megakaryocyte progenitors	c-Kit+CD41+
Mature megakaryocytes and platelets	c-Kit-CD41+

Table 2.3 Antibodies used for FACS analysis

Antibody	Cell Type	Conjugate	Lot number	Clone
Flt3	Progenitor	PE	12-1351	A2F10
CD16/32	Progenitor	PE	12-0161	93
c-Kit	Progenitor	PE-Cy5	15-1171	2B8,
Sca-1	Progenitor	PE-CY7	25-5981	2 D7
CD34	Progenitor	PE-CY7	11-0341	RAM34
CD43	B cell	PE	12-0431	ebioR2/60
CD19	B cell	PE	12-0193	eBio1D3
B220	B cell	E450	48-0452	RA3-6B2
B220	B cell*	APC	17-0452	RA3-6B2
CD4	T cell	PE	12-0041	GK1.5
CD5	T cell*	APC	17-0051	53-7.3
CD8a	T cell*	APC	17-0081	53-6.7
CD71	Erythrocyte	PE	12-0711	R17217
TER119	Erythrocyte*	APC	17-5921	TER-119
CD41	Megakaryocyte	PE	12-0411	eBioMWReg30
Gr-1	Myeloid*	APC	17-5931	PB6-8C5
CD11b	Myeloid	PE-Cy7	25-0112	M1/70
CD11b	Myeloid*	APC	17-0112	M1/70
CD16/32	*Block*	Purified	14-0161	93

All antibodies were purchased from eBioscience, San Diego, California, USA

* these antibodies were used in the lineage cocktail to identify Lin+ cells.

2.4.5   Side population analysis

Higher levels of multi-drug resistance (mdr) protein on the surface of haematopoietic stem cells (HSC) compared to other cell lineages, causes a faster rate of Hoechst 33342 dye efflux from HSC. This difference has been utilised as an alternative method of isolating HSC from mouse bone marrow. Bone marrow was removed from the mouse and prepared as described for FACS analysis. Cells were resuspended at a concentration of 1x 10^6/ml in pre-warmed DMEM. Hoechst 33342 dye was added to a final concentration of 5μg/ml, the sample was mixed well and incubated at 37°C for 90 minutes mixing regularly. To ensure that the correct population of cells was analysed the cells were co-stained with lineage cocktail, c-Kit and Sca-1 antibodies as previously done for FACS analysis. Analysis was done on a BD flow cytometer with UV a channel.

2.4.6   Colony forming assay

The ability of haematopoietic stem cells (HSCs) in the spleen and bone marrow to differentiate into different myeloid cell lineages was measured using a colony forming unit (CFU) assay. Myeloid differentiation is outlined in Figure 2.3. Single HSCs can differentiate and grow to form a colony of mature myeloid cells, termed a CFU, that can be identified morphologically. The colony forming assay was carried out in order to detect a range of different colony types. 2x 10^4 bone marrow cells or 2x 10^5 splenic cells were added to 1 ml of semi-solid methylcellulose (M3434, Stem cell technologies, Manchester, UK), in duplicate. M3434 contains recombinant mouse-stem cell factor, recombinant human- IL-3, recombinant human- IL-6 and recombinant human- erythropoietin along with added thrombopoietin (TPO) to a concentration of 6.25ng/ml (Peprotech, London, UK) to stimulate megakaryocyte growth. After incubation at 37°C for 10-14 days, colonies were counted. Colonies were visualised on an inverted microscope and given one of the following colony descriptions; CFU-G, CFU-

GM, CFU-M, CFU-MK, CFU-M/MK, BFU-E and CFU-GEMM based on the criteria defined by Stem Cell Technologies and is outlined in Figure 2.4 and Table 2.4. After the colony type was determined, cells were removed from the plate by diluting in cold DMEM, washed by spinning down and resuspending in DMEM, and the total number of cells was counted.

Figure 2.3 Haematopoietic differentiation
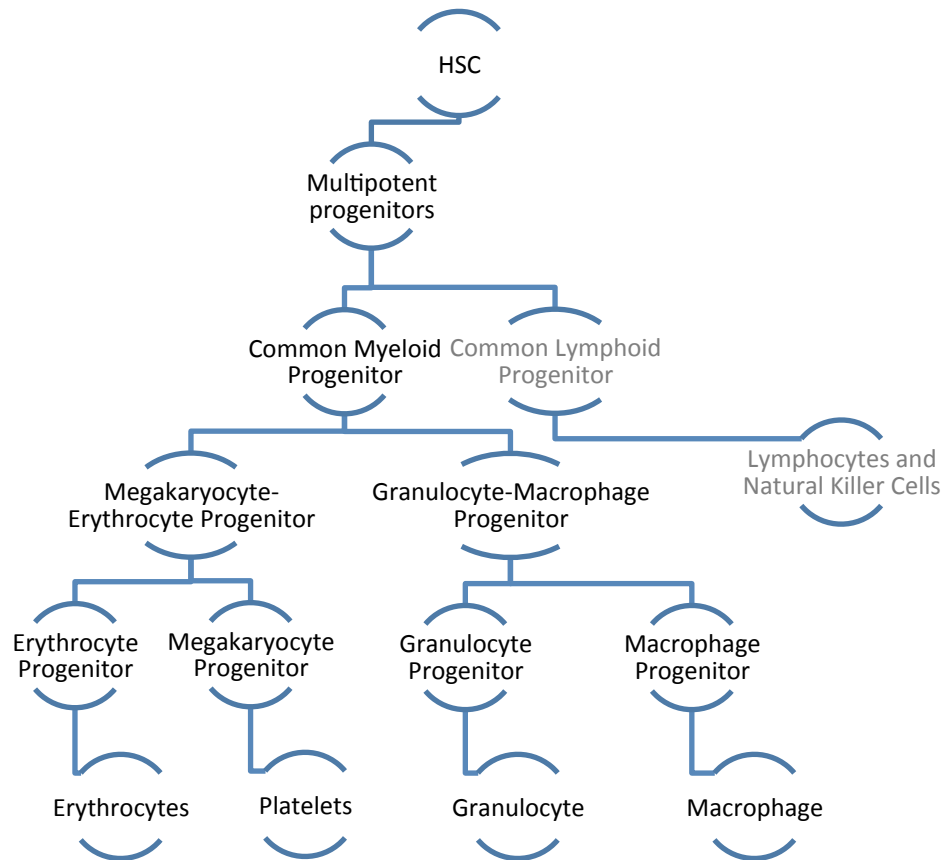
Haematopoietic stem cells (HSC) have the potential to differentiate into all haematopoietic cell types. Differentiation occurs in a stepwise manner, as outlined above, and is guided by a series of signals, such as growth factors. The colony forming unit (CFU) assay can be used to analyse the functional ability of HSCs and multipotent progenitors to differentiate into the different myeloid lineages *in vitro*. Growth and differentiation was supported by a cocktail of growth factors specific to myeloid cell lineages.

Figure 2.4 Representative colony types
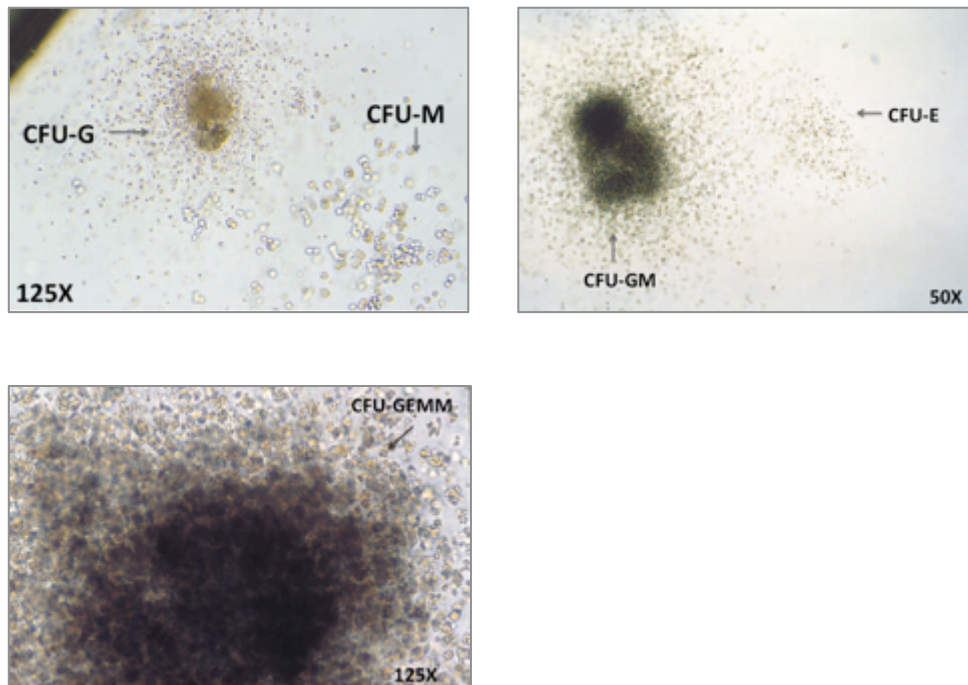
Pictures were taken from 'Stem Cell Technologies Technical Manual'. For CFU analysis, colonies were identified using these pictures, along with the written descriptions given Table 2.4 for guidance.

Table 2.4 Colony forming unit (CFU) descriptions

Colony type (Cell type)	Description
CFU-G (Granulocyte)	Bright small cells, uniform in size, form dense clusters of cells
CFU-GM (Granulocyte, macrophage)	Mixture of GM and M cells. A dense core of cells surrounded by larger brighter cells
CFU-M (Macrophage)	Large oval/ round cells, bright with a grainy centre.
CFU-MK (Megakaryocyte)	Large cells with visible budding or surrounded by very small cells, form small colonies of 5-10 cells.
CFU-M/MK (Macrophage, Megakaryocyte)	Mixture of CFU-M and CFU-MK. Medium-large colonies of M interspersed with MK cells.
CFU-GEMM (Granulocyte, erythroid, macrophage, megakaryocyte)	Mixture of all cell lineages. Have a dense core. Erythrocyte clusters and MK cells are easily distinguished around the periphery.
BFU-E (Burst forming unit-erythroid)	Very small cells, irregular in shape, can appear red/pink in colour
CFU-Undifferentiated (Undetermined)	Large colony of small- medium cells with no distinguishable characteristics.

Descriptions are adapted from the 'Stem Cell Technologies Technical Manual'.

2.4.7 Peripheral blood counts

60-90μl of blood was taken from the tail vein of mice prior to being sacrificed. 30μl of acid citrate dextrose (ACD) (citric acid 6.8 mM, trisodium citrate 11.2 mM, glucose 24 mM, Atm-/- bleeding) or heparin (Sigma-Aldrich) (Atm-/-nu-/- comparison at 6, 24 and 48+ weeks) was used to prevent coagulation. Total volume was measured and then the blood was analysed using an ABX Pentra 60 haematology analyser. The dilution factor was accounted for to give the actual blood cell count.

2.5 Atm-/-nu-/- tumour phenotyping

2.5.1 Tissue preservation

At post mortem, tissues removed from the mice for histological analysis were fixed immediately in neutral buffered formaldehyde, 10% v/v (Surgipath, Leica Microsystems, Milton Keynes, UK). After a minimum of 24 hours, the tissues were embedded in paraffin wax using an automated system either at the Biobank, University of Birmingham or the histopathology department at the Queen Elizabeth Hospital Birmingham (QEHB). Tissue sections were cut at 4μm for H&E staining and immunohistochemistry.

H&E staining was done according to standard protocols by the Biobank at the University of Birmingham, or the histopathology department at the QEHB. H&E section analysis was undertaken by histopathologists Dr Zbigniew Rudzki, at Birmingham Heartlands hospital and Dr Maha Ibrahim, University of Birmingham, as outlined in the results section, with guidance from the WHO classification of tumours of haematopoietic and lymphoid tissue, 4th edition (Swerdlow, 2008).

2.5.2   Sectioning tissues

For immunohistochemical analysis slides were prepared as follows. FFPE blocks were chilled for approximately 20 minutes on ice. Blocks were cut 4μm in thickness and placed on X-tra Adhesive micro-slides (Surgipath, Leica Microsystems, Milton Keynes, UK). Slides were heated to 60°C for 60 minutes to completely dry the section.

2.5.3   Preparation of tissue sections

For analysis of antigen expression analysis heat induced antigen retrieval was used prior to visualisation using the HRP-DAB technique and sections were counterstained with haematoxylin as follows. Firstly, to remove paraffin wax, tissue sections were incubated in histoclear (National Diagnostics, UK), for a minimum of 20 minutes and until all wax was removed. To rehydrate the sections, they were immersed in IMS for 2x 5 minutes, followed by rinsing under tap water for 5 minutes. Slides were then blocked with 3% H_2O_2 (Sigma-Aldrich) for 15 minutes to inactivate any endogenous peroxidase, followed by rinsing under running tap water again.

2.5.4   Antigen retrieval

Antigen retrieval was done by heating the slides in a beaker containing pre-heated sodium citrate buffer (1.26g of sodium citrate (VWR, Pennsylvania, USA) 0.25g citric acid (VWR, Pennsylvania, USA) in 1L, pH 6.0) in the microwave for 10 minutes on medium power, followed by 10 minutes on low power. The slides were left to cool before they were removed and then rinsed under running tap water for 5 minutes.

2.5.5   Detection of antigen by immunohistochemistry

Prior to staining, tissue sections were outlined with a wax pen (Sigma-Aldrich) and conditioned with Tris-buffered saline with 0.1% Tween-20 (TBS-T) for 5 minutes. Tissue

sections were blocked with 1X casein (Vector Labs, Peterborough, UK) diluted in TBS-T for 10 minutes to prevent non-specific background staining. Tissue sections were incubated overnight at 4°C, with an adequate volume of primary antibody to cover the sections. The primary antibodies were used as follows; anti-B220 (RA3, BD Biosciences, Oxford, UK) (dilution 1:400, 1:800 and 1:1600), anti CD3 (A0452, Dako, Cambridge, UK) (dilution: 1:250. 1:500 and 1:1000) and anti MAC-1 (CL8941AP, Cederlane, Gateshead, UK) (dilution: 1:50). In certain cases a sample was tested with 3 different antibody concentrations to account for variation in fixation and paraffin block preparation.

The following day, the slides were washed 3 times in TBS-T before incubation with anti-rabbit (K4010, Dako, Cambridge, UK) or anti- rat secondary antibody (P0450, Dako, Cambridge, UK) both used at a 1:100 dilution, at room temperature for 30 minutes. After which the slides were washed 3 times in TBS-T. For visualisation Dako, (Cambridge, UK) DAB+ liquid (K3467) was used, and the staining development was observed using an inverted microscope. When the staining was saturated, the reaction was stopped by dilution with TBS-T, and the slides were rinsed in tap water for 5 minutes. Counterstaining was done using Meyers haematoxylin incubated for 1- 5 minutes, then immersed in warm running water until the colour turned blue. Finally, the slides were dehydrated in two changes of IMS and then incubated in histoclear for 10 minutes. Immediately prior to mounting the slides were immersed in xylene (Sigma-Aldrich) and air-dried before the cover slip was applied with DPX (VWR, Pennsylvania, USA). All staining was repeated twice on separate occasions.

Staining of FOXP1, IRF4/MUM1 and CD10 along with B220 and CD3 was done in the lab of Dr Teresa Marafiott, at the University College London hospitals according to local procedures.

2.6   V(D)J recombination analysis

2.6.1   V(D)J recombination PCR

V(D)J rearrangements were amplified by polymerase chain reaction (PCR) from normal and tumour genomic DNA extracted using a Qiagen (Manchester, UK) DNA easy blood and tissue kit, according to manufacturers instructions for cells in culture. The PCR reaction mix contained 200ng of DNA, 5μL of 10X PCR buffer, 0.2mM dNTP's, 10pM each of forward and reverse primer, 2.5mM magnesium chloride and 2.5units hot-start Taq polymerase (Promega, Southampton, UK) in a total volume of 50μl. The JH-4 (5' CTC CAC CAG ACC TCT CTA GAC AGC 3') reverse primer was used along with one of the following forward primers VH7183 (5' GAA SAM CCT GTW CCT GCA AAT GAS C 3') (where S = C and G and M= A and C), VHQ52 (5'CAG GTG CAG CTG AAR CAG TCA 3'), or J558 (5'CAG CCT GAC ATC TGA GGA CTC TGC 3'). The three forward primers correspond to the 3 most common V gene families and JH-4 being the most distal J gene. Thermocycling was done at 95°C for 3 minutes, 35x(95°C for 30 seconds, 61/63°C for 30 seconds, 72°C for 2 minutes), and 72°C for 7 minutes. The annealing temperature was 63°C for J558 and 61°C for VH7183 and VH52Q. PCR products were separated on a 1.5% agrose gel. A single PCR product was determined to be indicative of a monoclonal rearrangement in the V(D)J gene in the sample. A smear, or 4 fuzzy bands was present in polyclonal sample that correspond to multiple different rearrangements involving the same J genes.

2.6.2   Sequencing of V(D)J

To confirm a single PCR product was indeed a monoclonal rearrangement it was sequenced. dNTP's were removed from the PCR reaction using Exosap (1μL PCR product, 1μL Exosap (Affymetrix, High Wycombe, UK)) and 8μl water). After which the entire 10μL of reaction

mix was added to a sequencing reaction mix containing 1μ 2.5X Big Dye, 3.5μ Buffer, 10pM primer, made up to 20μL with water. The forward primer used in the PCR reaction was used with one of each JH-4, JH-3 (5' GTC ACT GAC CCT GAA ATT GTC 3') and JH-2 (5' AGA TGG AGG CCA GTG AGG GAC 3'), depending on the re-arrangement at least one of these reverse primers would enable amplification. The DNA produced in this reaction was precipitated from the mix using sodium acetate; then it was cleaned with EtOH and air-dried. The pellet was re-suspended in Hi-Di (BD Biosciences, Oxford UK) for sequencing using an Applied Biosystems 3500XL sequencer.

The sequence obtained was analysed using the NCBI Ig Blast software to confirm a rearrangement and to identify what V, D and J genes were used in the rearrangement.

2.7 Sub-cutaneous transplant of tumour cells in to immunocompromised mice.

5×10^6 cells were injected sub-cutaneously into the right flank of a NOG (NOD/Shi-scid/IL-2Rγ null) immunocompromised mouse. The NOG mice used here were obtained from a colony bred and maintained in house. The strain was originally derived at the Central Institute for Experimental Animals, CIEA, Japan by cross breeding three mouse strains: 1) non-obese diabetic - NOD/Shi; 2) severe combined immune deficiency – SCID; 3) interleukin 2 receptor-gamma-null - IL-2Rγnull. As a consequence of this genetic background, NOG mice have defective macrophage, T and B lymphocyte and natural killer cell function. The experiment was done in triplicate. Mice were monitored daily for tumour growth and once tumour was detected, the size of the tumour was measured twice weekly using calipers, until the tumour neared the maximum size permissible by the project license. At this point the mice were culled, and a post mortem was undertaken. The tumour was removed, along with the

spleen and liver if tumour was visible in these organs also. For each sample cells were frozen viably, fixed in formalin and DNA was extracted. The fixed tissue was processed into paraffin blocks from which sections were cut and stained with H&E and immunohistochemically stained as described in section 2.5.2 to2.5.5 with anti-CD3 and anti-B220. V(D)J recombination was also analysed by PCR as described in section 2.6.

2.8 Chromosome analysis

2.8.1 T cell culture

Frozen viable thymoma cells were revived and cultured at a density of $2x\ 10^7$ cells/ml in media containing 20% FCS, 100units/ml IL-2, penicillin / streptomycin (1 in 100) (Gibco, Life Technologies) for 24 to 48 hours. The cells were harvested as described in section 2.3.6 for splenocyte radiosensitivity analysis.

2.8.2 B cell culture

Tumour cells and normal B cells were cultured in media containing 15μg/ml LPS, penicillin-streptomycin (1 in 100), 50μM β-mercaptoethanol and 10% FCS for up to 72 hours. Cells were harvested as described for splenocyte radiosensitivity analysis in section 2.3.6.

2.8.3 Multicolor fluorescence in situ hybridisation

Slides were aged overnight before hybridisation. 7μl of mouse 21X Metasystems (Bicester, UK) M-FISH probe was applied to the slide and covered with an 18x18mm coverslip and sealed. Hybridisation was done on a Vysis HyBright (Abbot Molecular, Illinois, USA) at a melting temperature of 73°C for 2 minutes followed by hybridisation at 37°C for 16 hours.

After removing the coverslip, the slide was washed in pre-warmed 0.4x SSC at 73°C for 2 minutes followed by 2X SSCT at room temperature for 30 seconds. Slides were

counterstained with 7.5µl of DAPI and a cover slip was applied. Images of metaphases were automatically captured using a Zeiss Axio imager Z.1, with Metasystems Metafer slide scanning software. Analysis of karyotype was done using ISIS software for multicolour FISH. All suitable metaphases, up to a maximum of 40 metaphases, were analysed. Chromosome gains, losses, duplications and translocations were counted and an aberration was determined to be clonal if it was present in two or more cells.

2.8.4   Targeted fluorescence in situ hybridisation

FISH probes were custom made using the following BACS; IgH alpha- 5-ROX dUTP (RP23-455J10), IgH V1 5-Fluorescein dUTP (RP23-303N6), c-Myc 5-ROX dUTP (RP23-307D14) (Empire Genomics, Buffalo, New York, USA).

Slides were prepared as described in section 2.8.3 for M-FISH. For IgH analysis 0.5µL of IgH alpha and 0.5µL IgH V1 were added to 5µL of buffer. For c-Myc 0.5µL of probe was added to 4.5µL of buffer. For IgH or c-Myc analysis, the probe mixture was added to the slide and a cover slip placed on top and sealed. Hybridisation was undertaken using a Vysis HyBright (Abbot Molecular, Illinois, USA) with a melting temperature of 75°C for 2 minutes followed by hybridisation at 37°C for 16 hours.

After hybridisation was complete the coverslip was removed and the slide was washed in pre warmed 0.4 SSC/ 0.3%NP-40 at 73°C for 2 minutes followed by 2xSSC/0.1% NP-40 for 1 minute. Slides were counterstained with 7.5µl of DAPI before cover slipping. Analysis was done on a Zeiss fluorescence microscope using ISIS software.

CHAPTER 3

THE SUITABILITY OF THE ATM-/-NU-/-

MOUSE AS A MODEL FOR ATAXIA

TELANGIECTASIA

3 THE SUITABILITY OF THE ATM-/-NU-/- MOUSE AS A MODEL FOR ATAXIA TELANGIECTASIA

3.1 Generation of the Atm-/-nu-/- mouse

Nude Atm heterozygous (Atm+/-nu-/-) males were mated with Atm+/-nu+/- double heterozygote females to generate Atm-/-nu-/- mice. An eighth of the offspring of this mating would be expected to be nude Atm-/- mice (Atm-/-nu-/-) another quarter expected to be Atm-/- and half expected to be nude. The genotypes of animals expected from this mating are given in Table 3.1. Since 2012, a record of each mouse born from these pairings and its genotype was recorded on an ARMIS database and a summary of these records can be found in Table 3.1. In total 490 offspring were born to these matings between 15/05/2012 and 07/03/2013. The number of Atm-/-nu-/- mice that survived until genotyping at 2-3 weeks of age was roughly a quarter of the predicted Mendelian frequency (15 compared to 61, Table 3.1). The frequency of Atm-/-nu+/- mice was also roughly half and Atm+/+nu-/- mice were two thirds of the expected number also.

Pups were genotyped at weaning which clearly excluded those that did not survive until this point. Pre-wean losses calculated for 20 litters in Table 3.2 was 11%. If this value is extrapolated to all of the colonies of this mating type, 11% of pups born in this mating were likely to have died before weaning. It therefore can be estimated that for the 490 mice recorded in Table 3.1 there would have been an additional 60 that died before weaning. This pre-weaning loss could be one of the reasons for reduced number of Atm-/-nu-/- and Atm-/-nu+/- mice than predicted. Another explanation for this reduced number is that these mice died *in utero*; this however has not been investigated.

3.2 Survival of the Atm-/-nu-/- mouse

In total, 103 mice (in both matings to produce double knockouts and also in the Atm heterozygote colony) in this study were culled because of morbidity. Of these 16/103 were Atm-/-nu+/- or Atm-/- (from the heterozygote colony), 18/103 were nude Atm+/+nu-/- and 69/103 were double knockouts Atm-/-nu-/- Figure 3.1. Atm+/+nu+/- are not included in this group because no Atm+/+nu+/- mice developed morbidity, they were mostly culled when healthy and used as controls during the analysis of Atm-/-nu-/- mice. Nevertheless, 2 Atm+/+nu+/- and 1 Atm+/-nu+/- mice were allowed to age and reached over 90 weeks old before they were culled, and post mortem revealed no abnormalities. Similarly, only 18 Atm+/+nu-/- mice are included in the survival analysis because they were also used alongside Atm+/+nu+/- mice as controls and therefore few remained that could be included.

Atm-/-nu-/- mice lived longer than Atm-/- mice. Atm-/-nu-/- mice had a mean age of 25 ±16 weeks (range = 6-90 weeks), compared to single knockout Atm-/- mice, from the heterozygote colony, which had a mean age of 13 ±1 weeks (range = 11-15 weeks). The mean age of Atm+/+nu-/- mice was 32 ±15 weeks (range = 12-72 weeks). The age of death for Atm+/+nu+/- and Atm+/+ mice could not be calculated as these mice were only culled when healthy as controls.

3.3 Morbidity in the Atm-/-nu-/- mouse

All 16/16 Atm-/-nu+/- and Atm-/- mice developed laboured, rapid breathing and a starry coat, which indicated a mouse in pain and these were immediately culled (Table 3.3). In Atm+/+nu-/- mice, 10/18 were culled as a consequence of showing symptoms indicating poor body condition, 4/18 an eye abscess and 2/18 a prolapsed bowel (Table 3.3). In Atm-/-nu-/- mice 31/69 had poor body condition, 17/69 had an eye abscess, 3/69 had a prolapsed bowel,

8/69 had a swollen abdomen, 1/69 had a growth on its front right limb and 1/69 had hind leg paralysis and were culled as a consequence of these morbidities but for 8/69 the cause of death was unknown (Table 3.3).

For the mice with declining body condition, H&E sections from tissues from 6 mice (4 Atm-/-nu-/- and 2 Atm+/+nu-/-) were analysed by a consultant histopathogist Zbigniew Rudski, to try and elucidate the cause of death. Pictures of these sections are found in Figure 3.2. Briefly, 2/4 Atm-/-nu-/- mice had evidence of pneumonia with pneumocystis in the lungs. 1/4 Atm-/-nu-/- mouse had granulocytes present in the portal tract of the liver, which is indicative of hepatitis and 1/4 had reactive bone marrow, which could indicate infection. 1/2 Am+/-nu-/- mice had pneumocystis in the lungs and the remaining one had focal pneumonia.

3.4   Cellular Atm protein expression

Atm-/-nu-/- mice would not be expected to have any ATM protein in their cells. The expression of Atm protein in extracts from Atm-/- single knockout and Atm-/-nu-/- tissue was measured using western blotting with two anti-Atm antibodies. Figure 3.3a (lane 1) and Figure 3.3b (lane 1) shows the recognition of ATM in a normal human lymphoblastoid cell line by antibodies MAT3 and 2CI but not in a lymphoblastoid cell line from a classical ataxia telangiectasia patient without any ATM protein (Figure 3.3a& b, lane 2). Figure3.3a also shows that these same antibodies recognised murine Atm in all tissues tested from Atm+/+ mice (Figure 3.3a, lanes, 3, 5, 7) but not in Atm-/- single knockout mice (lanes 4, 6 & 8). Figure 3.3a shows expression of Atm in Atm+/+nu+/- mice (lanes 3 & 6) and in Atm+/+nu-/- mice (lanes 4 & 7). For both antibodies, no Atm protein was detected in the spleen and brain of the Atm-/-nu-/ - mouse (Figure 3.3b lanes 5 & 8).

3.5   Cellular radiosensitivity of the Atm-/-nu-/- mouse

Cells from ataxia telangiectasia patients and Atm-/- single knockout mice are unusually radiosensitive. Splenocytes from Atm-/-nu-/- and Atm-/- mice were assessed for their chromosomal sensitivity to ionising radiation. After exposure to ionising radiation the cells were arrested in metaphase and spread on slides and stained. Metaphases were examined on high power, by light microscopy, for the presence of induced damage (see Figure 3.4 for representative examples). Cells from 2 Atm+/+ and 2 Atm-/- mice were tested. Atm-/- splenocytes had more than three times the amount of damage as Atm+/+ cells (124.5 ± 29 bits of damage and 37.5 ± 9 bits of damage respectively (Figure 3.4). In both Atm-/- and Atm+/+ cells the damage was mostly chromatid breaks, and chromatid gaps were the second most frequent type of damage to be present (Table 3.4).

Using the same method, the radiosensitivity of cells from a single Atm-/-nu-/- mouse spleen was tested. Atm-/-nu-/- and Atm-/- cells had more damage than Atm+/+nu-/- cells (78 and 82 compared to 31 bits of damage). Again, like Atm-/- cells, Atm-/-nu-/- cells the most common type of damage to be present was chromatid breaks and the second most common being chromatid gaps (Table 3.5 and Figure 3.4).

3.6   Discussion

The number of Atm-/-nu-/- mice born was lower than expected using Mendelian ratios. Whether Atm-/-nu-/- mice died in utero, or shortly after birth but prior to weaning cannot be known for certain. However, there was a significant pre-wean loss in litters from Atm+/+nu-/-, Atm+/-nu+/- pairings that could account for the mice dying shortly after birth. To generate Atm+/-nu-/- males that are required to generate Atm-/-nu-/- mice, a nude (nu-/-) BALBc male was mated with Atm+/- females. The Mendelian ratio was most reduced in the mice that were

homozygous for Atm loss. Atm-/- 129S6/SvEvTac were born at the expected frequency but a lower than the expected birth rate has been observed for Atm-/- BALBc mice, although this reduction was not significant (χ^2=5.886, P=0.0527, df= 2) (Genik et al., 2014). Therefore the lower than expected numbers of Atm-/-nu-/- mice could be in part a consequence of the BALBc phenotype inherited from the nude male founder of the colony.

The Atm-/- mice used in this study survived between 11 and 15 weeks of age. These mice had the same mutation in the Atm gene as those used by Barlow and colleagues that survived between 8 and 20 weeks of age (Barlow et al., 1996). The age range of Atm-/- mice in the Barlow study was larger than that was observed here. Differences in the survival between Atm null mouse models have been observed previously and were attributed to differing husbandry conditions or strain background. Like the mice in the Barlow study, the Atm-/- mice used in this study were housed in specific pathogen free (SPF) conditions but variation could occur between housing facilities and local environmental factors could account for the small difference in survival between the two studies (Reliene and Schiestl, 2006). The mice used in this study were the same strain background as those used by Barlow and colleagues in 1996 and therefore the age of survival should be similar.

The median age of survival for Atm-/-nu-/- was 25 weeks, which was almost double that of my Atm-/- mice that had a median survival of 13 weeks. Therefore the Atm-/-nu-/- model has achieved the objective of increasing the survival of A-T mice. Schubert and colleagues noted a median survival of the Atm-/- Barlow mouse of 30 weeks (Schubert et al., 2004). Petiniot and colleagues reported a similar median survival of 30 weeks for a mouse containing the same mutation in Atm as the Wynshaw-Boris mice, but had a C57BL/6 genetic background as a consequence of being heterozygote for a Rag knock-out gene (Petiniot et al., 2002). The C57BL/6 Atm-/- mouse has been shown to have an increased survival compared to the

129S6/SvEvTac Atm-/- mouse and therefore genetic background could cause the increased longevity of the mice in the Petiniot study (Genik et al., 2014).

The most common reason for having to cull the Atm-/-nu-/- mice in my study was a declining body condition. This was also the most common cause of death for the Atm+/+nu-/- mice and therefore this morbidity is may be associated with the nude phenotype. Analysis of histological sections from a selection of mice that had declining body condition by a histopathologist revealed evidence of pneumonia, pneumocystis and hepatitis. These diseases are all cause by infection. Bone marrow from one mouse analysed was reactive, which is also indicative of an infection (Swerdlow, 2008). Nude mice are prone to hepatitis virus and Sendai virus infections further suggesting that the declining body condition could be cause by an infection (Sharkey, 1978). Nude-mice are immunocompromised and the immune system of Atm-/-nu-/- mice is further compromised by the loss of Atm causing reduced T and B lymphocytes (Barlow et al., 1996). It is therefore plausible that declining body condition observed in Atm-/-nu-/- and Atm+/+nu-/- mice was the consequence of an infection. None of hairy mice (nu+/-) developed an eye abscess or prolapsed bowel so it is possible that these conditions are a consequence of the nude (nu-/-) phenotype. These conditions developed in 20/69 nude mice and therefore made over one quarter of the Atm-/-nu-/- mice unsuitable to be used for investigation into the A-T phenotype.

The mutation in the Barlow Atm-/- mice is predicted to lead to truncation of the Atm protein, which in humans causes instability and loss of Atm protein from the cell (Reiman et al., 2011). In 1996, due to not having a suitable antibody available, Barlow and colleagues confirmed knock out of the Atm gene in the Barlow Atm-/- mice using functional assays, such as testing cell cycle checkpoint analysis. Since then, several human ATM antibodies have been found to cross-react with murine Atm. Using two of these, no Atm protein was observed in the spleen

or brain of my Atm-/- and Atm-/-nu-/- mice by western blotting. However, these findings are contrary to a report by Li and colleagues that detected mutant Atm protein in the brains of the Atm-/- Barlow mice (Li et al., 2011). The same anti-Atm antibody (2C1A1) that was used to detect Atm in the brain of Atm-/- Barlow mice in the study by Li and colleagues was unable to detect Atm protein in the brains of my Atm-/- and Atm-/-nu-/- mice. In this report Li and colleagues used two antibodies, 5C2 and Y170, in addition to 2C1A1 and Atm protein could be also detected in the brain of Barlow Atm-/- mice using 5C2 but not Y170.

Cells from my Atm-/-nu-/- mice lacked Atm protein expression and were chromosomally radiosensitive like the Atm-/- single knockout animals. For these two crucial reasons the Atm-/-nu-/- mice can be regarded as A-T mice. The Atm-/-nu-/- mice survived longer than Atm-/- mice, but they also developed morbidities possibly associated with the nude phenotype.

Table 3.1 Expected and observed genotypes of offspring from mating Atm+/-nu-/- males with Atm+/-nu+/- females

Genotype	Atm+/+ nu+/-	Atm+/- nu+/-	Atm-/- nu+/-	Atm+/+ nu-/-	Atm+/- nu-/-	Atm-/- nu-/-
Expected genotype frequencies	1/8	2/8	1/8	1/8	2/8	1/8
Expected number of each genotype (n=490)	61	123	61	61	123	61
Actual number	71	181	34	43	146	15

Based on a total of 490 offspring in 103 litters from matings between 15/05/2012 and 07/03/13. The numbers of observed genotypes differ from the number expected (χ^2=85.2, with 5 degrees of freedom, P> 0.001).

Table 3.2 Pre-wean losses in 20 litters from mating Atm+/-nu-/- males with Atm+/-nu+/-

females

Litter number	Litter size	Pre-wean loss
121	1	0
120	5	3
119	7	0
118	8	0
117	6	1
116	6	2
115	8	0
114	6	0
113	9	1
111	4	0
110	13	0
109	10	3
107	7	2
106	6	2
105	10	0
104	10	1
103	7	0
102	10	0
101	13	0
100	1	1
Total	147	16
Average	7.35	0.8

In 20 litters, 147 mice were born and 16 died before weaning (loss of 11%).

Extrapolating the 11% pre wean loss to the population of 490 mice genotyped between 15/05/2012 and 07/03/13, 60 mice would have died after birth and before genotyping was done at weaning.

Figure 3.1 Survival of the Atm-/-nu-/- mouse
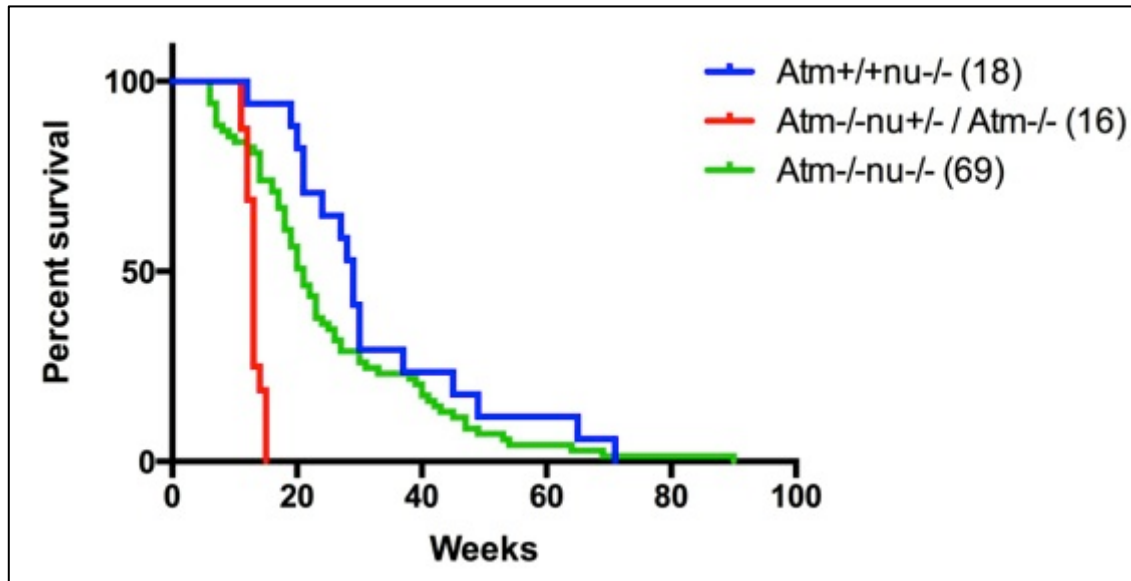
Atm-/-nu-/- mice lived longer than Atm-/- or Atm-/-nu+/- mice

Mean age of Atm-/-nu-/- = 25 ± 16 weeks

Mean age of Atm-/-nu+/- and Atm-/- (from Atm heterozygote colony) single knockout mice =13± 1 weeks.

Table 3.3 Morbidity associated with Atm-/-nu-/- mouse

Genotype	Number of mice	Mean age of death (Weeks)	Morbidity						
			Difficulty breathing	Poor body condition	Abscess	Prolapse	Swollen abdomen	Unknown	Other
Atm-/-nu+/-, Atm-/-	16	13	16	0	0	0	0	0	0
Atm+/+nu-/-	18	33	0	10	4	2	1	1	0
Atm-/-nu-/-	69	25	0	31	17	3	8	8	2

Atm-/-nu-/- mice lived longer than Atm-/-nu+/- and Atm-/- mice.

Death associated morbidity was recorded for 105 mice.
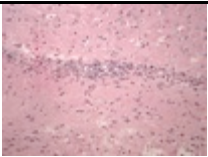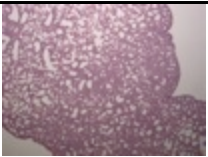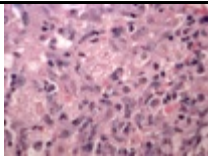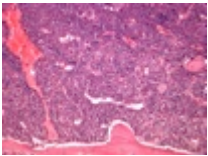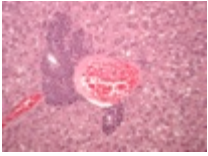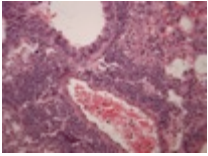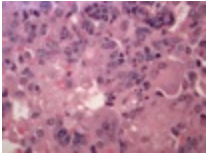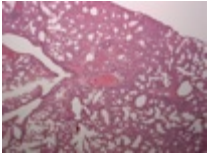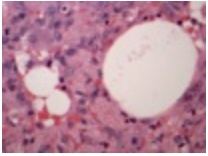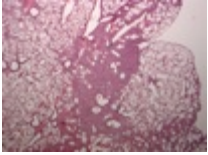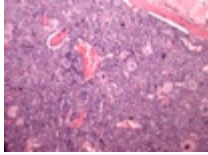
Mean age of death:

Atm-/- nu+/- and Atm-/- mice =13±1 weeks

Atm-/-nu-/- = 25 ±16 weeks

Atm+/+nu-/- = 18 ±15 weeks

Figure 3.2 Pathological analysis of mice that were culled because of poor body condition

Mouse:	H&E analysis:		
39M1 Atm-/-nu-/-	*Brain: inflammation around vessel in 20x*	*Lung: Massive pneumonia, looks like pneumocystis 20X*	*Lung: massive pneumonia, looks like pneumocystis 63X*
46M2 Atm-/-nu-/-	*Reactive bone marrow*		
40F3 Atm-/-nu-/-	*Liver: Mild acute hepatitis granulocytes in the portal tract 20X*		
40M2 Atm-/-nu-/-	*Lung: Acute bronchopneumonia with pneumocystis 20X*	*Lung: Acute bronchopneumonia with pneumocystis 63X*	
46F1 Atm+/-nu-/-	*Lung: Pneumocystis 20X*	*Lung: Pneumocystis 63X*	
40F2 Atm+/+nu-/-	*Lung: Focal pneumonia 20X*	*Lung: Focal pneumonia 20X*	*Lung: Increased neutrophils 20X*

Atm-/-nu-/- and Atm+/+nu-/- mice, which had a poor body condition, were investigated for cause of death. Sections from spleen, liver, lung, brain, bone marrow, kidney, gut, and lung were H&E stained and analysed by histopathologist Dr Zbigniew Rudski to identify possible abnormalities associated with the declining health of the mouse. The mice analysed had evidence of hepatitis pneumonia or pneumocystis. It is possible that infections were the cause of morbidity in these mice.

Figure 3.3 Cellular Atm protein expression in the Atm-/- and Atm-/-nu-/- mouse
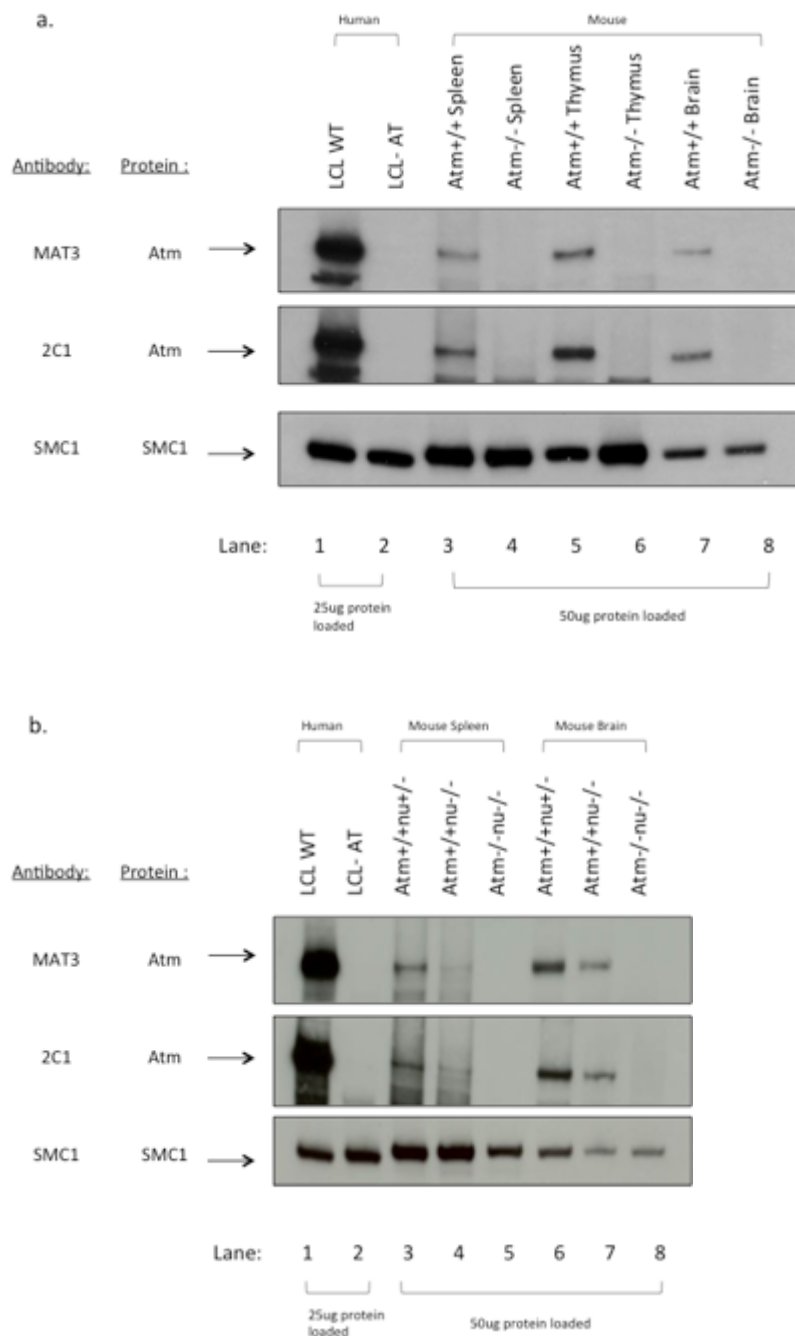
Western blot analysis of Atm protein expression in;

a. Atm+/+ and Atm-/- (from the Atm +/- heterozygote colony) spleen, brain and thymus.

b. Atm-/-nu-/-, Atm+/+nu-/-, Atm+/+nu+/- spleen and brain.

Human and mouse Atm was identified using two monoclonal antibodies (MAT3 and 2CI) which recognise human ATM.

Table 3.4 Radiosensitivity of Atm+/+ and Atm-/- splenocytes

Mouse	Chromatid break	Chromosome breaks	Tri-radial	Quadri-radial	Other	Total Damage
Atm+/+ 1	12	31	0	1	2	46
Atm+/+ 2	12	12	3	0	2	29
Mean	12	22	2	1	2	37.5
s.d	0	10	2	1	0	9
Atm-/- 1	18	74	6	2	4	104
Atm-/- 2	37	104	3	0	1	145
Mean	28	89	5	1	3	124.5
s.d	13	21	2	1	2	29

25 metaphases were analysed for each mouse. The experiment was carried out twice.

s.d= standard deviation

Table 3.5 Radiosensitivity of Atm-/-nu-/- splenocytes

Mouse	Chromatid break	Chromosome breaks	Tri-radial	Quadri-radial	Other	Total Damage
Atm+/+nu-/-	14	16	0	0	1	31
Atm-/-	36	43	0	0	3	82
Atm-/-nu-/-	25	40	10	0	3	78

25 metaphases were analysed for each mouse.

Figure 3.4 Graphical representation of radiosensitivity analysis

a.

b.

c.
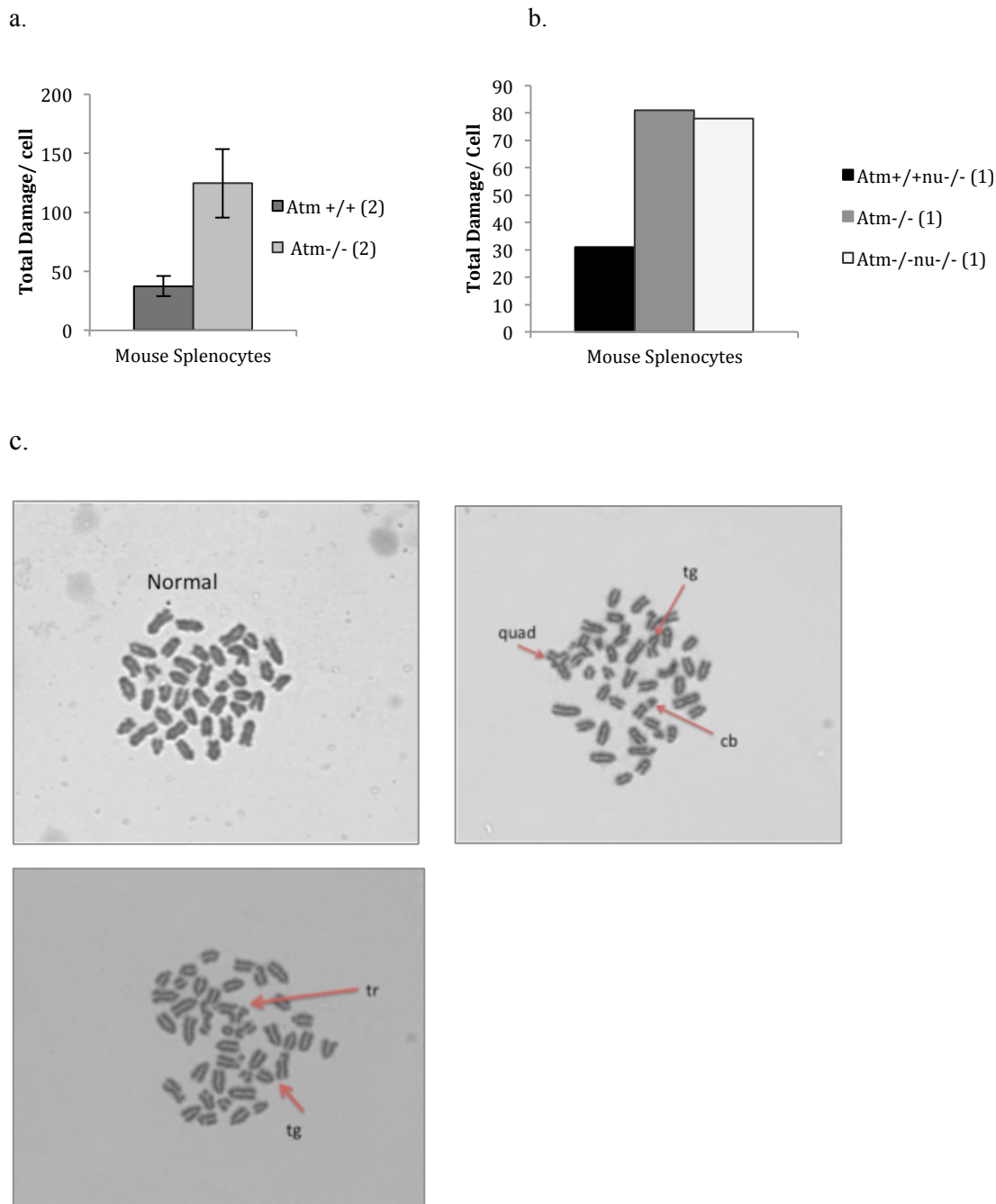
a. Atm-/- splenocytes described in table 3.4 and b. Atm-/-nu-/- splenocytes described in table 3.5.

c. Representative metaphases showing normal chromosomes, chromatid gap (tg), chromosome breaks (cb), triradial (tr) and quadriradial (quad).

Mouse splenocytes were stimulated in culture with LPS. After 3 days, splenocytes were irradiated, incubated for 3 hours and colcemid was added for 1-2 hrs. Cells were spread on slides and stained with Giemsa. 25 cells were analysed for each mouse (except Atm+/+ 1 =10)

CHAPTER 4

THE HAEMATOPOIETIC SYSTEM IN ATM-/-, ATM-/-NU-/- AND ATM+/+NU-/- MICE

4 THE HAEMATOPOIETIC SYSTEM IN ATM-/-, ATM-/-NU-/- AND ATM+/+NU-/- MOUSE

4.1 Immunological phenotyping of Atm-/- bone marrow and spleen by FACS.

Atm-/- mice have been shown to have altered lymphocyte populations (see section 1.6.1). To determine if we could replicate these findings and determine if there were any additional changes in the immune system as a consequence of Atm loss, immunological phenotyping of Atm-/- and Atm+/+ bone marrow and spleen was undertaken at age six weeks of age, before thymoma development occurred. Details are given in 'Materials and Methods' (section 2.4), but briefly, the proportions of progenitor cells, lymphocyte and myeloid cell populations, were measured based on expression of the following cell surface markers, Progenitors; LSK (Lin-Sca-1+c-Kit+), long- term progenitors (LTP) (Flt3- CD34-), short-term progenitors (STP) (Flt3- CD43med), multipotent progenitors (MPP) (Flt3+ CD43+), common myeloid progenitors (CMP) (CD16/32+CDCD34med), granulocyte macrophage progenitors (GMP) (CD16/32- CD34-) and megakaryocyte erythrocyte progenitors (MEP) (CD16/32+CD34+). T cells; double positive T cell (CD4+CD8+), helper T cell (CD4+CD8-), cytotoxic T cells (CD4-CD8+). B cells; pro B cell (B220+CD43+), pre B cell (B220+CD43-), immature B cell (CD43-B220medium IgM+), transitional B cell (CD43- B220high IgM+) and follicular B cell (CD43- B220high IgM-), plus B220+ IgM+IgD-) and (B220+IgM+IgD+) also. Myeloid cells; monocytes/ macrophages (CD11b+ Gr-1-) and granulocytes (CD11b+ Gr-1+). Erythrocytes; pro-erythroblast (CD71+TER-119-), erythroblast (CD71+ TER-119+) and mature erythrocyte (CD71- TER119+). Megakaryocytes; all progenitors (c-Kit+ CD41-), megakaryocyte progenitor (c-Kit+ CD41+) and mature megakaryocyte and platelets (c-Kit- CD41+) . The

gating strategies used for the different populations for the bone marrow and spleen, are shown in Figure 4.1 and Figure 4.3.

Atm-/- bone marrow was compared to Atm+/+ bone marrow and the results are shown in Figure 4.2. No difference was seen in early progenitor (LSK, LT, ST progenitors) and late progenitor (MPP, GMP, MEP) cell populations in these two genotypes.

Lymphoid cell populations were altered in the bone marrow of Atm-/- mouse. The numbers of single positive (SP) T cells, both cytotoxic-T cells (CD4- CD8+) and helper-T cells (CD4+ CD8-), were significantly reduced in the Atm-/- mice although the more immature double positive (DP) (CD4+CD8+) T cells were normal (Figure 4.2 d, e &f).

The progenitor B cells; pro B (B220+ CD43+), pre-B (B220+ CD43-) and immature B cells (B220med IgM+) cells, were also altered in Atm-/- mice. The pro B cell population was increased and pre B and immature B cells were significantly reduced but the most mature B cell population analysed here, the transitional B cells (B220high IgM-), were not significantly different (Figure 4.2 g, h, i & j).

Comparison of myeloid cell populations in the bone marrow showed that the proportion of macrophages (CD11b+ Gr-1 -) was normal in Atm-/- mice bone marrow but the proportion of granulocytes (CD11b+ Gr-1+) was significantly increased. Considering the erythrocyte populations, pro erythroblast (CD71+ TER-119-), erythroblast (CD71+ TER-119+) and mature erythrocyte (CD71- TER119+) cells were normal in Atm-/- mice (Figure 4.2 m, n, o). Finally, megakaryocyte cell populations were analysed. All progenitors (c-Kit+ CD41-), megakaryocyte progenitor (c-Kit+ CD41+) and mature megakaryocyte and platelets (c-Kit- CD41+) cell populations were normal in Atm-/- bone marrow (Figure 4.2 p, q, r).

Overall, only lymphocyte and granulocyte cell populations were altered in Atm-/- bone marrow. Atm-/- bone marrow lymphocyte population differed from normal Atm+/+ bone marrow in that mature single positive T cells were reduced in these mice. B cell populations were also changed; the more immature pro B cells were increased whereas the proportion pre B cells, which differentiate from pro B cells, were reduced.

FACS analysis of splenic T cells showed that the proportion of both DP and SP T cells were reduced in the Atm-/- spleen compared to Atm+/+ spleen. Unlike the bone marrow, there was no significant change in the B cell population in the Atm-/- mouse spleen. In the Atm-/- spleen, the immature B cell population was normal, and the more differentiated transitional and follicular B cell populations were also unchanged. The proportion of macrophage and granulocyte populations in the spleen of Atm-/- mice were increased at 6 weeks compared to Atm+/+. Finally, there was no statistical difference observed in erythrocyte or megakaryocyte populations in the spleen (Figure 4.4)

Analysis of both Atm-/- bone marrow and spleen showed that the proportion of single positive T cells was reduced. In the spleen only, early B cell populations (Pro, Pre and immature B cell) were altered but the more differentiated B cells (transitional and follicular) were normal. Changes were observed in the myeloid cells also, granulocytes cells were increased both in the bone marrow and spleen, and macrophages were increased in the spleen only.

4.2 Analysis of Atm-/- peripheral blood

After changes were observed in the spleen and bone marrow of Atm-/- mice, peripheral blood was analysed to see if loss of Atm altered this haematological compartment. Comparison of Atm-/- and Atm+/+ peripheral blood cells was undertaken using a blood counter (ABX Pentra

60 haematology analyser, see section 2.4.7). The results are shown in Figure 4.5. The platelet count was not significantly different in Atm-/- mice compared to Atm+/+ mice. The mean white blood cell (WBC) count was lower in Atm-/- blood compared to Atm+/+ blood, however this was not a significant change.

When considering sub-types of WBC independently, differences were seen between Atm-/- and Atm+/+ control mice. Both the total lymphocyte count and proportion of lymphocytes were reduced in Atm-/- mice. Conversely myeloid cell populations were increased in Atm-/- mice compared to Atm+/+ mice. The mean monocyte count and proportion of monocytes was increased in Atm-/- mice, although only the increase in the proportion was significant. Of the granulocyte population, the proportion of neutrophils was significantly increased; the mean proportion of eosinophils and basophils was also increased (but not significantly). In summary, like the spleen and bone marrow, Atm-/- peripheral blood had a reduced proportion of lymphocytes, and an increased proportion of monocytes and granulocytes. Overall, these abnormalities were the most marked in the spleen.

4.3 Determination of normal Atm-/- stem cell function using side population analysis

Side population analysis refers to a method of identifying the most primitive haematopoietic stem cells population. These cells efflux Hoechst dye faster than other cell in the bone marrow and therefore can be sorted by FACS due to their low fluorescence level (see materials and methods). Co-staining for LSK markers was done to confirm that the side population was in fact within the stem cell compartment.

After observing the changes in the bone morrow, spleen and peripheral blood cell populations, side population analysis was used to determine if a change in the character of stem cells was

responsible for an increase in myeloid cells in the spleen of Atm-/- mice. FACS analysis of stem cell populations LSK, LT and ST progenitors using cell surface markers; Lin-, Sca-1, c-Kit, CD34, Flt3 and CD16/32, showed no difference in the proportions of these cells, so side population analysis was used in addition to cell surface marker expression, as another measurement of stem cell populations. The proportion of cells in the side population was comparable between Atm-/- and Atm+/+ mice showing no difference stem cell phenotype by this test and therefore the change in Atm-/- myeloid cell population is unlikely to be the result of abnormal stem cell function (Figure 4.6).

4.4 Measuring Atm-/- bone marrow and spleen cell proliferation and differentiation using an in vitro colony forming unit (CFU) assay.

Side population analysis indicated it was unlikely that there was a defect in stem cell function causing a change in the myeloid population in Atm-/- mice. Therefore, the differentiation potential of myeloid cell progenitors was tested using a colony forming unit assay. Atm-/- and Atm+/+ bone marrow cells were grown in methylcellulose with added cytokines that stimulate myeloid growth and differentiation, and the number and type of colonies were quantified. Examples of the different types of colony morphology expected are shown in Figure 4.7.

In Atm-/- bone marrow the total number of colonies per plate were significantly reduced compared to Atm+/+ bone marrow and the total number of cells per plate were also reduced, however this was not significant (Figure 4.8a). This suggests that fewer cells in Atm-/- bone marrow had the potential to form colonies than in Atm+/+ bone marrow, but the colonies that were formed were possibly larger and had more cells than Atm+/+ bone marrow colonies. The number of different types of colony was expressed as a proportion of the total number of

colonies counted per plate. CFU-GM and CFU-M were both decreased in Atm-/- bone marrow compared to Atm+/+ bone marrow and no difference was seen in the proportion of the remaining colony types (Figure 4.8). The most striking difference between Atm-/- and Atm+/+ bone marrow was that Atm-/- bone marrow formed more colonies which were unable to be identified morphologically and were therefore categorised as 'CFU-undetermined'. This could be a result of reduced differentiation in these colonies as a consequence of a slower growth rate, which would also cause a reduced total colony number.

In Atm-/- spleen the number of colonies per plate was decreased and Atm-/- spleen had a reduced proportion of CFU-M colonies along with increased BFU-E and CFU-GEMM colonies. Undetermined colonies were more frequent in Atm-/- spleen, although this was not statistically significant (Figure 4.9).

In summary, the CFU potential of Atm-/- bone marrow and spleen was similar in that both Atm-/- bone marrow and spleen had reduced potential to form colonies, formed more unidentifiable colonies, and CFU-M colonies were less frequent. However unlike the Atm-/- bone marrow, no difference was seen in the proportion of CFU-GM colonies in spleen and conversely no change in BFU-E and CFU-GEMM colony formation was seen in bone marrow that was present in the spleen. These results highlight an altered myeloid proliferation potential *in vitro* in Atm-/- bone marrow and spleen cells but is not consistent with the observation of the increased proportion of monocytes and or granulocytes detected in the bone marrow, spleen and peripheral blood of Atm-/- mice.

4.5 FACS analysis of Atm-/-nu-/- bone marrow, spleen and liver, at 6, 24 and 48 weeks of age

Comparison of Atm-/- mice with Atm+/+ mice suggested changes in lymphocytes and myeloid cell populations in the bone marrow and spleen of these mice. A limitation of the Atm-/- single knock out model meant that changes in these populations could not be studied beyond the age of 8 weeks. In order to determine if Atm loss affects these cell populations with age, the Atm-/-nu-/- model was utilised. Atm-/-nu-/- mice were compared to Atm+/+nu-/- and Atm+/+nu+/- mice to determine the effect of Atm loss on the haematopoietic cell populations. The same gating strategy was used for the Atm-/-nu-/- analysis as the Atm-/- analysis and can been seen in Figure 4.1 (bone marrow) and Figure 4.3 (spleen).

Like the Atm-/- mouse no difference was seen in Atm-/-nu-/- early progenitor cells at 6-8 weeks (Figure 4.10a). This did not change significantly with age, although the proportion of MPP cells decreased between 6 and 48+ weeks (not significant).

Comparison of the lymphocyte populations showed similar changes in Atm-/-nu-/- bone marrow cells as Atm-/- mice (Figure 4.10b). The immature, DP T cell population was normal at 6, 24 and 48+ weeks and did not vary with age. With regards to the more mature single positive T cells, CD4+ CD8- T cell proportions were normal until 48+ weeks, where they were reduced in Atm-/-nu-/- compared to Atm+/+nu+/- bone marrow. The CD4- CD8+ Atm-/-nu-/- T cell population was reduced compared to Atm+/+nu+/- at 6 weeks but was comparable to Atm+/+nu-/- and Atm+/+nu+/- at 24 and 48+ weeks. In addition both CD4+CD8- and CD4-CD8+ populations in Atm+/+nu-/- bone marrow were also reduced compared to Atm+/+nu+/-, which is expected of the nude phenotype (Figure 4.10b.i).

Therefore, apparently, loss of Atm does not significantly reduce the proportion of T cells further in the nude mice.

Pro-B cells were comparable to Atm+/+nu-/- and Atm+/+nu+/- mice at 6 and 24 weeks, but in the eldest mice analysed (48+ weeks), there was a significant reduction in the proportion of Atm-/-nu-/- pro-B cells compared to Atm+/+nu+/- pro-B cells. Atm+/+nu-/- pro B cells were also reduced.

Pre-B cells were reduced in Atm-/-nu-/- bone marrow compared to Atm+/+nu+/- bone marrow at 6 weeks and at 48+ weeks. At 24 weeks Atm-/-nu-/- pre-B cells were also reduced in the bone marrow compared to Atm+/+nu-/- and Atm+/+nu+/- but this was not statistically significant. Immature B cells were significantly reduced in Atm-/-nu-/- compared to Atm+/+nu-/- mice, but no differences were seen at older ages. Similarly, transitional-B cells were significantly reduced in Atm-/-nu-/- bone marrow at all ages compared to Atm+/+nu-/- and Atm+/+nu+/-, but this reduction was not statistically significant at 24 and 48 weeks (Figure 4.10b.ii).

With regard to the myeloid cells, the monocyte population in Atm-/-nu-/- bone marrow was normal at all ages. On the other hand granulocytes were increased in Atm-/-nu-/- mice compared to Atm+/+nu+/- mice at 6 and 48+ weeks, but no difference was seen between Atm-/-nu-/- bone marrow and Atm+/+nu-/- at any age. Therefore both the Atm+/+nu-/- mice and Atm-/-nu-/- mice had increased granulocytes compared to Atm+/+nu+/- mice (Figure 4.10c).

The erythroid populations were unchanged in Atm-/-nu-/- bone marrow compared to Atm+/+nu-/- and Atm+/+nu+/- bone marrow. All three populations measured, CD71+ TER-119-, CD71+ TER-119+ and CD71- TER-119+, were comparable in Atm-/-nu-/-, Atm+/+nu-

/- and Atm+/+nu+/- bone marrow at 6, 24 and 48 weeks of age. The erythroid population was also unchanged in Atm-/- bone marrow compared to Atm+/+ (Figure 4.10d).

At 6, 24 and 48+ weeks the proportion of megakaryocytes and their progenitors were comparable between Atm-/-nu-/-, Atm+/+nu-/- and Atm+/+nu+/- bone marrow. A noteworthy observation is that mature megakaryocytes (c-Kit- CD41+) from all genotypes were lower at 48 weeks compared to 6 and 24 (Figure 4.10e).

In Atm-/-nu-/- spleen, unlike Atm-/-nu-/- bone marrow where the DP T cell population is normal, DP- T cells are reduced compared to Atm+/+nu+/- at 48 weeks. In contrast, Atm-/-nu-/- and Atm+/+nu-/- spleen single positive CD4+ and CD8+ T cell populations were reduced at 6 and 48 weeks, which was consistent with what was found in Atm-/-nu-/- bone marrow (Figure 4.11a.i).

For the most part, B cell populations in Atm-/-nu-/- spleen were comparable to Atm+/+nu-/- and Atm+/+nu+/- spleen. Although there was one exception, Atm-/-nu-/- transitional B cells (B220high IgM+) were reduced in 6-week-old Atm-/-nu-/- mice compared to Atm+/+nu+/- mice (Figure 4.11a.ii). Mature follicular IgM and IgD expressing B cells were also reduced in the Atm-/-nu-/- mouse compared to both the Atm+/+nu-/- and Atm+/+nu+/- mouse at 6 weeks. This is unlike the Atm-/- mouse in which the pre B (B220+CD43+), pro B (B220+CD43-) cells and immature B (B220medIgM+) but not the transitional (B220high IgM+) and follicular cell (B220high IgM-) population are changed (Figure 4.2 and Figure 4.4).

Myeloid cell pupations were altered in Atm-/-nu-/- spleen. At 6 weeks monocytes were increased in Atm-/-nu-/- and Atm+/+nu-/- spleen compared to Atm+/+nu+/-. Granulocytes were increased in the Atm-/-nu-/- and Atm+/+nu-/- spleen compared to Atm+/+nu+/- at 6 and

48 weeks. Importantly, there was no difference in myeloid cells between the Atm-/-nu-/- and Atm+/+nu-/- (nude) mouse spleen (Figure 4.11b).

Megakaryocyte populations were unchanged in Atm-/-nu-/- spleen compared to Atm+/+nu-/- and Atm+/+nu+/- at 6, 24 and 48+ weeks of age. This reflects the normal population of megakaryocytes that was found in the Atm-/- spleen, Atm-/- bone marrow and Atm-/-nu-/- bone marrow (Figure 4.11c).

Haematopoietic populations in the liver were analysed and the results are shown in Figure 4.12. As the liver is not associated with haematopoiesis in adulthood, any change in the populations of this tissue is likely to suggest an abnormality in the haematopoietic system in Atm-/-nu-/- mice.

T cell populations in the liver were normal apart from Atm-/-nu-/- and Atm+/+nu-/- CD4+ T cells in 6-week-old mice, which were reduced. There was no significant change in any other T cell populations in the liver (Figure 4.12a).

Analysis of immature, transitional and follicular B cell populations in the liver of 6, 24 and 48+ week old Atm-/-nu-/- mice showed these B cell populations were comparable to Atm+/+nu-/- and Atm+/+nu+/- mice (Figure 4.12a).

Finally in the liver of Atm-/-nu-/- mice, monocytes and granulocytes were increased compared to Atm+/+nu+/- mice. In 24 and 48+ week old mouse liver these cell populations were also increased but these differences were not statistically significant. An increase in Atm-/-nu-/- and Atm+/+nu-/- monocytes and granulocytes in the liver, along with the observed increase in monocytes and granulocytes in the bone marrow and spleen shown above, suggests that there could be an abnormality in these cell populations in these mice (Figure 4.12b).

Finally, megakaryocytes were comparable between Atm-/-nu-/-, Atm+/+nu-/- and Atm+/+nu+/- liver cell population in 6, 24 and 48+ week old mice. In addition, no difference was seen in megakaryocyte cell populations in the bone marrow and spleen of Atm-/-nu-/- mice and therefore it is likely that megakaryocyte cells are normal in Atm-/-nu-/- mice (Figure 4.12c).

4.6 Atm-/-nu-/- peripheral blood analysis with age

Peripheral blood counts were taken to determine if Atm loss caused any changes in the blood cell population and are shown in Figure 4.13. The red blood cell count was comparable between Atm-/-nu-/-, Atm+/+nu-/- and Atm+/+nu+/- mice. There was also no difference in platelet and total white blood cell count (WBC).

At 6 weeks both the lymphocyte count and proportion of lymphocytes was significantly reduced in Atm-/-nu-/- peripheral blood compared to both Atm+/+nu+/-, and–Atm+/+nu-/- mice. At 24 and 48 weeks there was no significant difference in lymphocyte populations.

The proportion of monocytes in the peripheral blood of Atm-/-nu-/- mice was increased at 6 weeks, although there was no significant difference in the monocyte count in the peripheral blood. Considering granulocyte cell populations, the proportion of neutrophils was significantly increased in the peripheral blood of Atm-/-nu-/- mice compared to Atm+/+nu+/- mice. There was also an increase in the proportion of neutrophils compared to Atm+/+nu-/- mouse peripheral blood, but this was not significant. In older mice, the proportion of neutrophils is comparable to Atm+/+nu-/- and Atm+/+nu+/- peripheral blood and is therefore likely to be normal in these mice.

In summary the proportions of both lymphocytes and granulocytes were altered in 6-week-old Atm-/-nu-/- mice in a similar way to the Atm-/- mouse but no differences in these populations were seen in the peripheral blood of older Atm-/-nu-/- mice.

4.7 Measuring Atm-/-nu-/- bone marrow and spleen cell proliferation and differentiation using an in vitro CFU assay

The growth and differentiation of Atm-/-nu-/- bone marrow was assessed by CFU assay analysis. Due to the limited number of mice available, the analysis was carried out on three 6-week-old mice, two mice at 24 weeks old and 2 mice at 48+ weeks old. Therefore the results here give an indication of the potential of Atm-/-nu-/- bone marrow cells, but the statistical significance of these results cannot be determined for the 24 and 48 week old mice. The results of the Atm-/-nu-/- CFU analyses are presented in Figure 4.14. The total number of colonies was slightly reduced in 6 and 24 week Atm-/-nu-/- mouse bone marrow; the number of colonies formed from 48+ week old mice bone marrow was comparable to controls. The total number of cells per plate derived from Atm-/-nu-/- bone marrow was reduced in 6-week mice, but at 24 and 48 week old the number of cells was normal. The proportion of CFU-G cells derived from Atm-/-nu-/- bone marrow was also normal, along with the proportion of CFU-M and CFU-E colonies. Atm+/+nu+/- CFU-GM colony frequency increased with age, whereas Atm-/-nu-/- was stable. Conversely CFU-MK cell proportions decreased in Atm-/-nu-/- bone marrow with age, while the frequency of CFU-MK colonies produced by Atm+/+nu+/- bone marrow was stable (Figure 4.14).

CFU analysis of Atm-/-nu-/- spleen showed similar results to Atm-/-nu-/- bone marrow. The number of colonies formed and number of cells per plate were normal in Atm-/-nu-/- spleen. All colonies types were normal in Atm-/-nu-/- spleen apart from the proportion of CFU-

M/MK which was higher in Atm-/-nu-/- and Atm+/+nu-/- spleen produced a than Atm+/+nu+/- spleen (Figure 4.15.

In summary, CFU analysis of Atm-/-nu-/- bone marrow and spleen suggests that Atm-/-nu-/- bone marrow and spleen differentiation *in vitro* is comparable to Atm+/+nu-/- and Atm+/+nu+/- at 6, 24 and 48 weeks of age. It is worth noting here that there were differences observed between Atm-/- and Atm+/+ bone narrow and spleen at 6 weeks of age although these differences were not consistent with the abnormalities found in the bone marrow and spleen of the Atm-/- mouse (Figure 4.8 and Figure 4.9).

The Atm-/-nu-/- mouse was made with the intention of overcoming the limitations of the existing single knock out models that only develop a single type of cancer and die before 4 month of age. In abrogating the thymus in the A-T mouse, by crossing the Atm-/- with the athymic nude mouse, thymoma development was prevented, and thus this early death due to thymoma development the Atm-/- mouse was overcome allowing any other phenotypes associated with Atm loss to develop. Despite this clear benefit, the consequence of the addition of nu-/- mutation to the Atm-/- A-T mouse was evaluated to determine the validity of the Atm-/-nu-/- mouse as a model of A-T. A summary of the evaluation of the haematopoietic system in the Atm-/-nu-/- mouse is shown in Table 4.1.

4.8 Discussion

The haematopoietic system of the Atm-/-nu-/- mouse is phenotypically similar to the Atm-/- mouse and both are distinguishable from the nude mouse.

An important objective was to compare the components of the haematopoietic system, particularly B and T cell development, in the Atm-/-nu-/- mouse, the single knockout (Atm-/-)

but also with the nude mouse (Atm+/+nu-/-). In the Atm-/- single knockout and nude mouse, thymic development is severely curtailed for different underlying reasons (see Introduction, Section 0). At age 6 weeks in BM and spleen in Atm-/- and Atm-/-nu-/- mice there is a large reduction in CD8+ T cells. A similar reduction in CD4+ T cells was seen in spleen cells in all three genotypes. This is in agreement with previously published work on this Atm-/- mouse that had reduced CD4+ and CD8+ T cells in the spleen (Barlow et al, 1996) and another A-T mouse generated by Elson et al., that had reduced CD4+ and CD8+ cells in the spleen also (Elson et al., 1996). CD4+ and CD8+T cells were also reduced in the Atm+/+nu-/- spleen. This is consistent with observations that T cell development is perturbed in the nude mouse due to the absence of a thymus, the main organ where T cell development and maturation takes place (Ikehara et al., 1984). Thus the A-T mice and nude mice had similar defects in T cells.

B cells are produced in the bone marrow and they mature in peripheral lymph nodes such as the spleen (Lebien and Tedder, 2008). Pre, pro and immature B cell development occurs in the bone marrow. At age 6 weeks there was a similar level of Pro B (B220+ CD43+) but a reduction in pre B (B220+ CD43-) and immature (B220med IgM+), B cells in both Atm-/- and Atm-/-nu-/- mice. This observation in the Atm-/- and Atm-/-nu-/- mouse is consistent with the analysis of the Atm-/- mouse by Loizou and colleagues (Loizou et al., 2011) who noted a reduction in pre and immature B cells. No reduction was seen in the nude mouse of any B cell population in the spleen or bone marrow at age 6 weeks. Antigen dependent differentiation occurs in the peripheral compartments such as the spleen (Allen et al., 2007b). In the spleen of Atm-/- mice the more mature B cell populations, transitional (B220high IgM+) and follicular (B220high IgM-) B cells were normal but the transitional B cells were reduced in the Atm-/-nu-/- spleen. The Atm-/-nu-/- have a reduced ability to undergo class

switch recombination as a consequence of the loss of Atm protein and nude mice have reduced functional T cells, which combined could perturb B cell differentiation in the spleen greater than in the Atm-/- mouse (Lumsden et al., 2004, Ikehara et al., 1984).

The reduction in both T and B lymphocytes in the A-T mice but not the nude was also reflected in the reduced lymphocyte count in the peripheral blood of the Atm-/- and Atm-/-nu-/- mouse but not the Atm+/+nu-/- mouse. The absence of B cell defect in the nude mouse bone marrow at 6 weeks of age highlighted a crucial difference between the A-T mice (Atm-/- and Atm-/-nu-/-) and nude (Atm+/+nu-/-).

Altered B cell development in the A-T mice but not the nude is likely to be due to the involvement of Atm in B cell development. Pro B cells differentiate into pre B cells and undergo V(D)J recombination which requires Atm, and therefore the changes in the cell population observed in the A-T mice could be a consequence of perturbed development due to Atm loss (Petiniot et al., 2000).

In the spleen and bone marrow of A-T mice (Atm-/- and Atm-/-nu-/-) the proportion of T and B cells did not change significantly between age 6 weeks and at age 48 weeks. In the bone marrow the pre and pro B cell populations are decreased in the Atm+/+nu-/- mice at age 48 weeks. This age related decline in early B cells in the nude mouse could be a consequence of decreased expression of RAG-1 and RAG-2 proteins with age. These proteins are involved in V(D)J recombination in developing B cells. Aging and thymic involution are both associated with reduced levels of RAG-1 and RAG-2 and therefore could be a contributing factor in the reduction in pre and pro B cells in age 48 week nude mice (Szabo et al., 1998, Szabo et al., 1999).

With regard to myeloid defects, an increase in granulocytes and monocytes was found in the Atm-/- and Atm-/-nu-/- mouse at 6 week of age suggesting that in addition to lymphocyte defects, A-T mice were susceptible to myeloid defects. Monocytes and granulocytes are part of the innate immune system. They are produced in the bone marrow and released into the blood system and from here they migrate to sites of inflammation and infection (Summers et al., 2010).

The proportion of monocytes and granulocytes were increased in the bone morrow of the both the Atm-/- and Atm-/-nu-/- mouse at 6 weeks of age. This suggests either there was an increase in the production of monocytes and granulocytes in the bone marrow or a decrease in loss, either though reduced release from the bone marrow compartment or reduced cell death. Monocyte and granulocytes differentiate from granulocyte monocyte progenitor (GMP) cells. FACS analysis showed that the proportion of GMP cells, along with other stem cells populations in the Atm-/- and Atm-/-nu-/- bone marrow were normal, so it is unlikely that increased production of granulocytes and monocytes is caused by an abnormality in the progenitor cells. In addition, *in vitro* culture of bone marrow cells showed no abnormality in the differentiation into myeloid colonies, and reduced proliferation of the bone marrow cells, suggesting that it is unlikely that increased cell production by progenitors is causing increased granulocytes and monocytes in the A-T mice. As *in vitro* development was normal, the increased proportion of monocytes and granulocytes could be the result of stimulation from the bone marrow environment to promote the survival of the monocytes and granulocytes or to increase the production of new cells from progenitors. Monocytes and granulocytes were also increased in the peripheral blood and spleen suggesting that the migration of monocytes and granulocytes from the bone marrow is not impaired and thus not producing an increase in cells in the bone marrow. It is worth noting here that the granulocyte cell population increased

in the peripheral blood was the neutrophils. The markers used for FACS analysis of the spleen and bone marrow could did not distinguish between granulocytic subpopulations, but the increased neutrophils in the peripheral blood may suggest that it could have been the neutrophil population that were increased in the bone marrow and spleen.

The increase of monocytes and granulocytes in the spleen suggest that more monocytes and granulocytes were homing to the spleen more than normal. This could be due to abnormal cytokine signalling or infection/inflammation. Abnormal cytokine signalling was not investigated here so this possibility cannot be excluded, but A-T mice are immunocompromised due to the reduced lymphocytes, and therefore it is possible that infection was resulting in increased monocytes and granulocytes in these mice. An increase in granulocytes and monocytes was also seen in the liver. As the increase was seen in multiple organs, the cause of increased monocyte and granulocyte numbers could be due to systemic infection or inflammation.

Myeloid abnormalities were less marked in the nude mouse. At age 6 weeks monocytes were increased in the spleen only but they also developed increased granulocytes at age 48 weeks. Nude mice are mice are also immunocompromised, plus as the immune system declines with age, both increase the likelihood of susceptibility to infection and could be a possible cause for increased granulocytes and monocytes in these older nude mice. All mice were in good health when analysed, therefore if an infection was present and causing an increase in monocyte and granulocyte levels, it could only have been underlying and did not affect the overall health of the animal. In addition the mice were kept in a pathogen-controlled environment, and so risk to infection was minimised but not fully eliminated.

Overall, both the Atm-/- and Atm-/-nu-/- mouse have myeloid abnormalities but in comparison, the Atm+/+nu-/- mouse does not share this phenotype at 6 weeks of age. In all three genotypes there was a reduction in the lymphocyte population, which are part of adaptive immunity, and therefore it is possibly that the innate immunity (macrophage and granulocytes) is stepped up to control pathogens in these mice when the effectiveness of the adaptive immune system is reduced. This isn't the first report of myeloid defects in A-T mice, Gr-1+ cells were also increased in the A-T mouse made by Xu and Baltimore but no further investigation was made into this defect (Xu et al., 1996).

Comparison of the Atm-/-nu-/- mouse at a 24 and 48 weeks of age were undertaken to determine any change in the haematopoietic system with age. Only two mice were available at 24 weeks of age for analysis, as the limited numbers of Atm-/-nu-/- mice available were also required for observation for tumour development. Nevertheless, the comparison of haematopoietic cells in the bone marrow, spleen and peripheral blood followed the same pattern as seen at 6 weeks and/ or 48 weeks of age in most instances and therefore, along with the data compiled from 48 week old mice, is included to give an indication of any haematopoietic abnormalities that may develop with age in the Atm-/-nu-/- mouse. In the Atm-/-nu-/- and Atm+/+nu-/- mouse peripheral blood cell populations did not change significantly with age. Some changes were seen in the Atm-/-nu-/- mouse bone marrow; both pro B cell and CD4+ T cells were reduced at age 48 weeks. Similarly in the Atm+/+nu-/- mouse bone marrow CD4+ T cells and both pro and pre B cells were reduced, along with an increase in granulocytes in the bone marrow and spleen at age 48 weeks.

Immunodeficiency in patients with A-T is mostly stable; it does not worsen with age. Defects are primarily seen in T and B cells and include reduced immunoglobulin levels, particularly IgA and IgG subtypes. Patients have increased respiratory tract infections but do not generally

succumb to opportunist viral infections because of residual functioning lymphocytes (Nowak-Wegrzyn et al., 2004, Micol et al., 2011). To my knowledge there are no reports of defects in myeloid cells in A-T patients. Therefore the increased monocytes and granulocytes in the Atm-/- and Atm-/-nu-/- mice could be unique to A-T mice.

To summarise, the reduced B and T cell defects associated with A-T and that are recapitulated in the Atm-/- mouse model are also present in the Atm-/-nu-/- mouse. Atm+/+nu-/- mice also have reduced T lymphocytes, but no defect was detected in B cells. Also, the Atm+/+nu-/- mouse did not have any of the myeloid defects that were associated with the Atm-/- and Atm-/-nu-/- mice. Taking the B and T lymphocyte and myeloid abnormalities all into consideration, the Atm-/-nu-/- phenotype is most similar to the Atm-/- mouse and is therefore a suitable model of A-T.

Figure 4.1 Representative FACS chromatograms of Atm-/- and Atm+/+ bone marrow cells at 6 weeks of age

a.

b.

c.

d.i

e.

d.ii

f.

g.
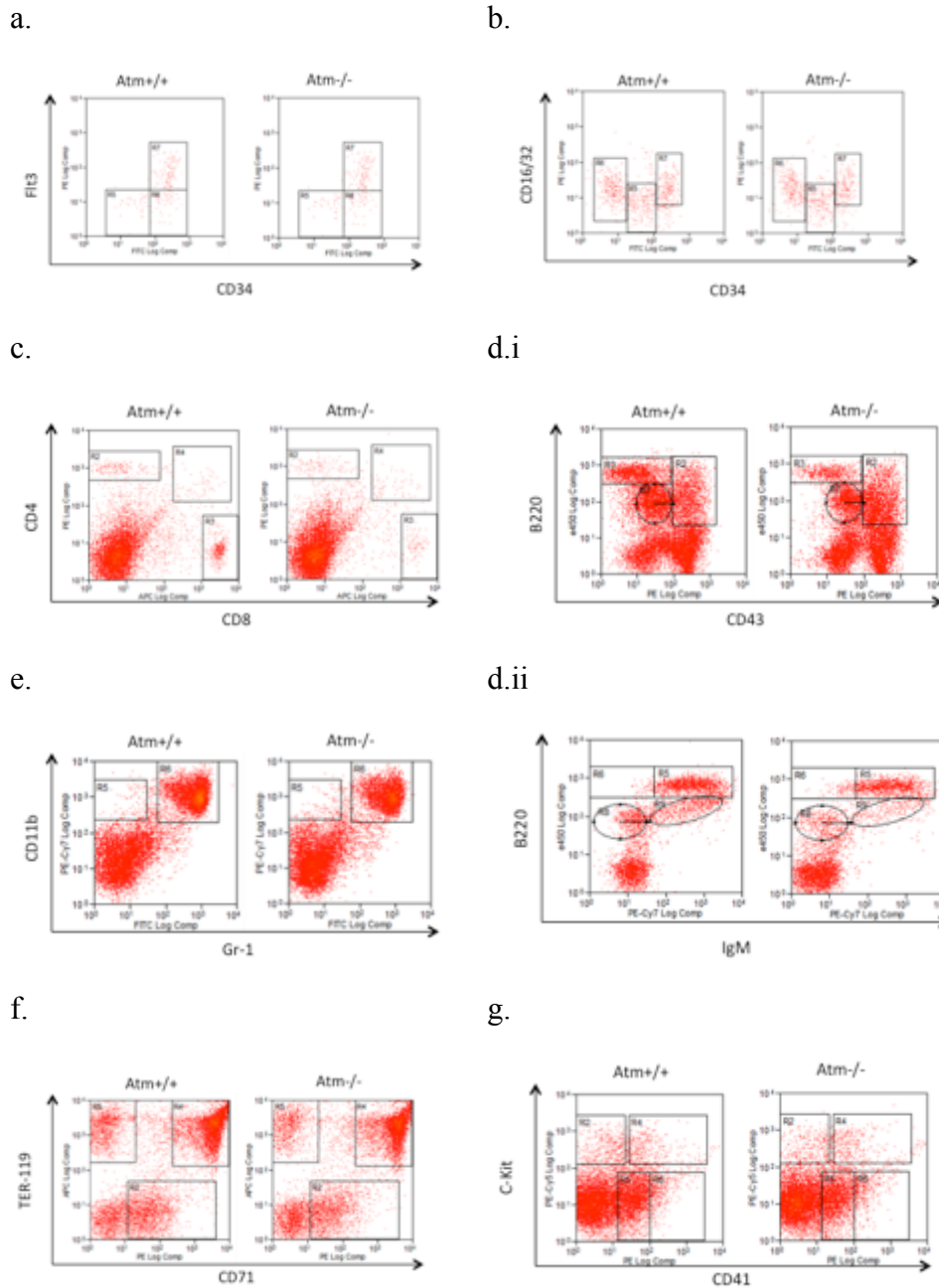
Representative chromatograms for FACS analysis in Figure 4.2. Boxes represent gates used to measure a particular cell population.

a. Early progenitors
b. Late progenitors
c. T cells
d. (i). Pre and pro B cells, (ii). Immature B cells

e. Monocytes and granulocytes
f. Erythrocytes
g. Megakaryocytes

Figure 4.2 FACS comparison of Atm-/- and Atm+/+ bone marrow cells at 6 weeks of age

a.
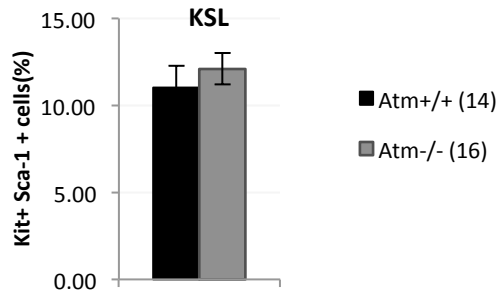
b.
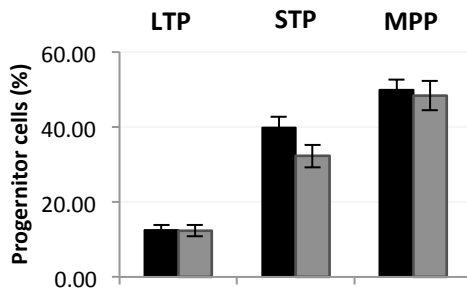
c.
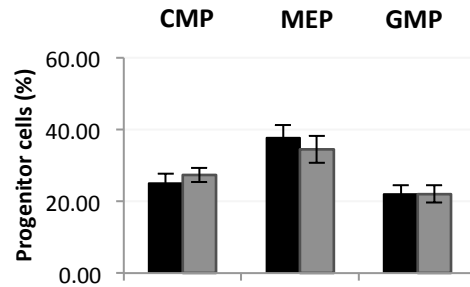
d.
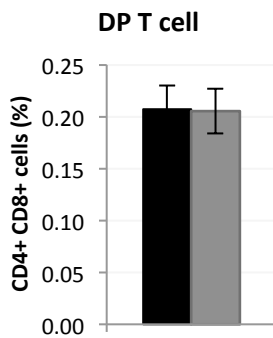
e.
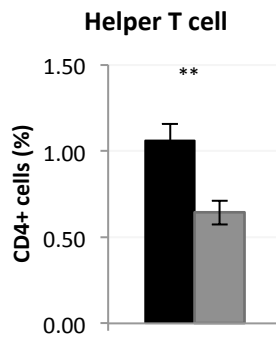
f.
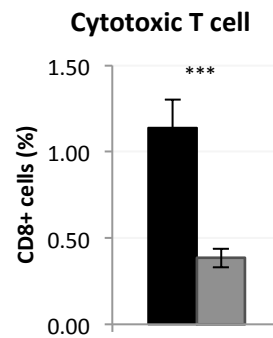
Grey =Atm-/- (n=14), black =Atm+/+ (n=15)

Error bar =S.E.M, *=p< 0.05, ** =p<0.01, *** =p<0.001

a. Haematopoietic stem cells: Lin-kit+ Sca-1+ cells (LSK)

b. Early progenitors: long-term progenitors (LTP) short-term progenitors (STP), multipotent progenitors (MPP)

c. Late progenitors: common myeloid progenitor (CMP), megakaryocyte and erythrocyte progenitor (MEP), granulocyte and monocyte progenitor (GMP)

d. Double positive (DP) T cells, e. single positive CD4 T cells, f. single positive CD8 T cells

Figure 4.2 continued FACS comparison of Atm-/- and Atm+/+ bone marrow cells at 6 weeks of age

g.

h.

Pro-B cell

Pre-B cell

i.

j.

Immature B cell
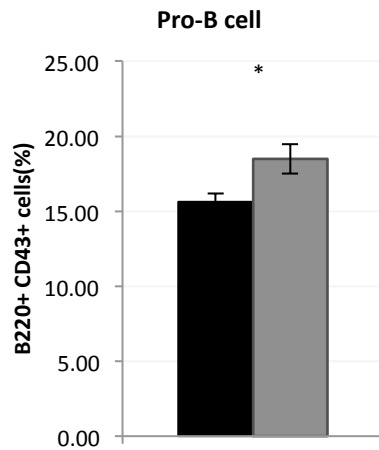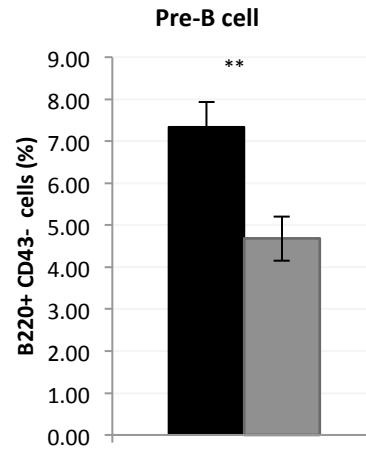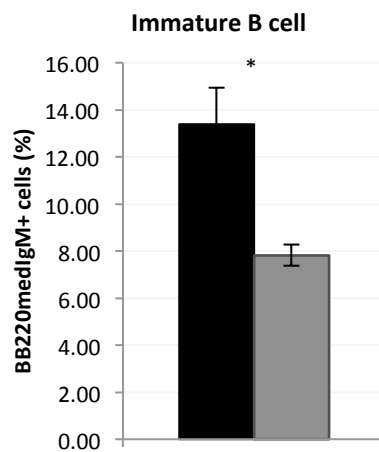
Transitional B cell
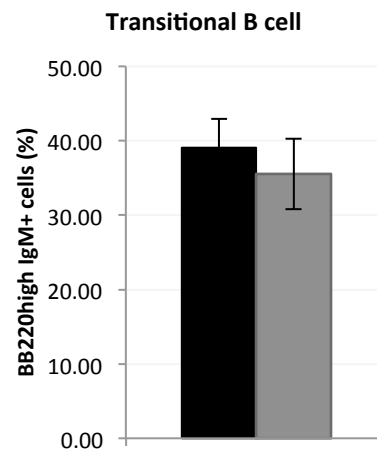
Grey =Atm-/- (n=14), black = Atm+/+ (n=15)

Error bar = S.E.M, *=p< 0.05, ** = p<0.01, *** =p<0.001

g, h, i and j. Pro B, Pre B, immature and transitional B cells respectively

Figure 4.2 continued FACS comparison of Atm-/- and Atm+/+ bone marrow cells at 6 weeks of age

k.

Macrophages

l.

Granulocytes

m.

Pro-erythroblast

n.

Erythroblast

o.

Mature Erythrocyte

p.

**All Progenitors**

q

Meg. Progenitors

r.

Mature Meg./ Platelets
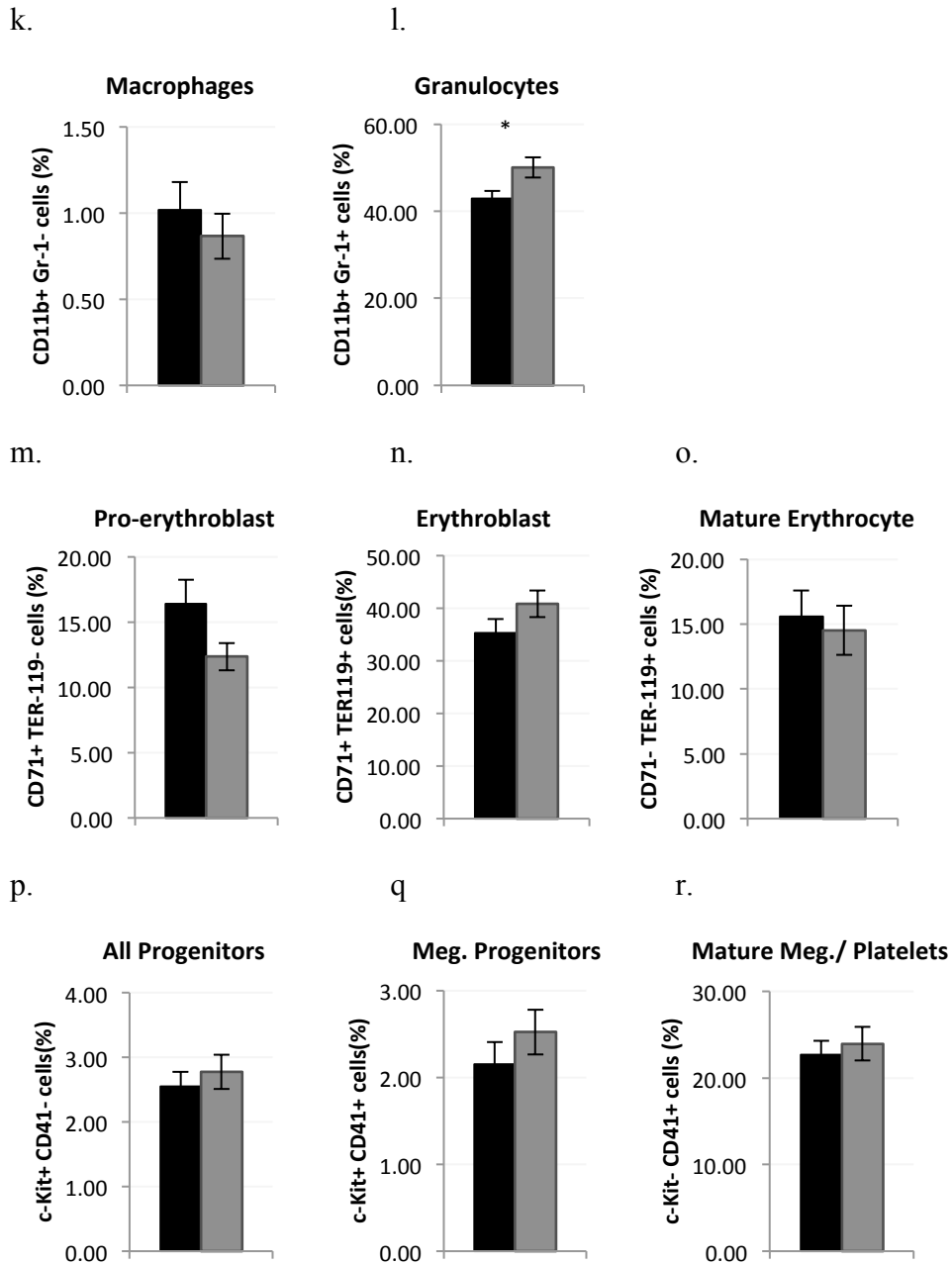
Grey =Atm-/- (n=14), black = Atm+/+ (n=15)

error bar = S.E.M. *=p< 0.05, ** = p<0.01, *** = p<0.001

k & l. myeloid cells: macrophages and granulocytes respectively

m, n & o. Pro-erythroblasts, erythroblasts and mature erythrocytes respectively

p, q & r. c-Kit+ progenitor cells, megakaryocyte (meg.) progenitor and mature megakaryocytes and platelets cell populations respectively

Figure 4.3 Representative FACS chromatograms of Atm-/- and Atm+/+ spleen at 6 weeks of age

a.

b.

c.
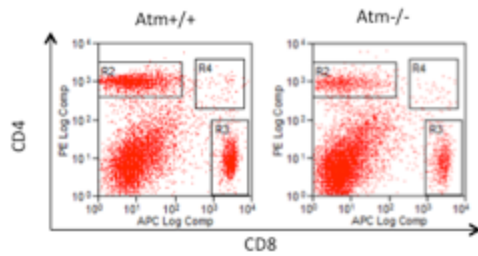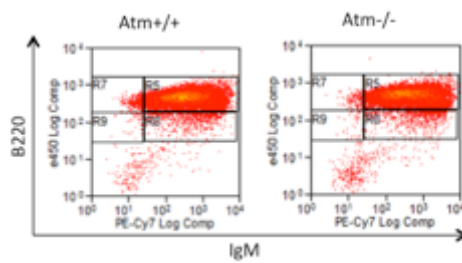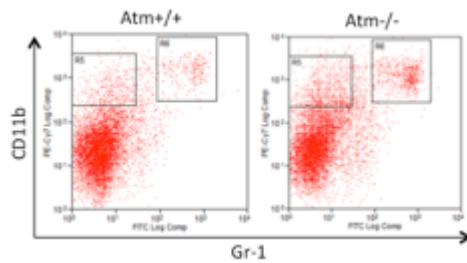
d.
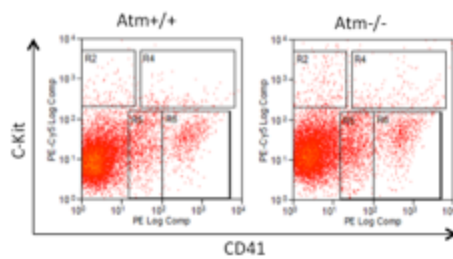
Representative chromatograms for FACS analysis in figure 3.3 Boxes represent gates used to measure a population.

e. T cells
f. Immature, transitional and follicular B cells

g. Monocytes and granulocytes
h. Megakaryocytes

Figure 4.4 FACS comparison of Atm-/- and Atm+/+ spleen cells at 6 weeks of age
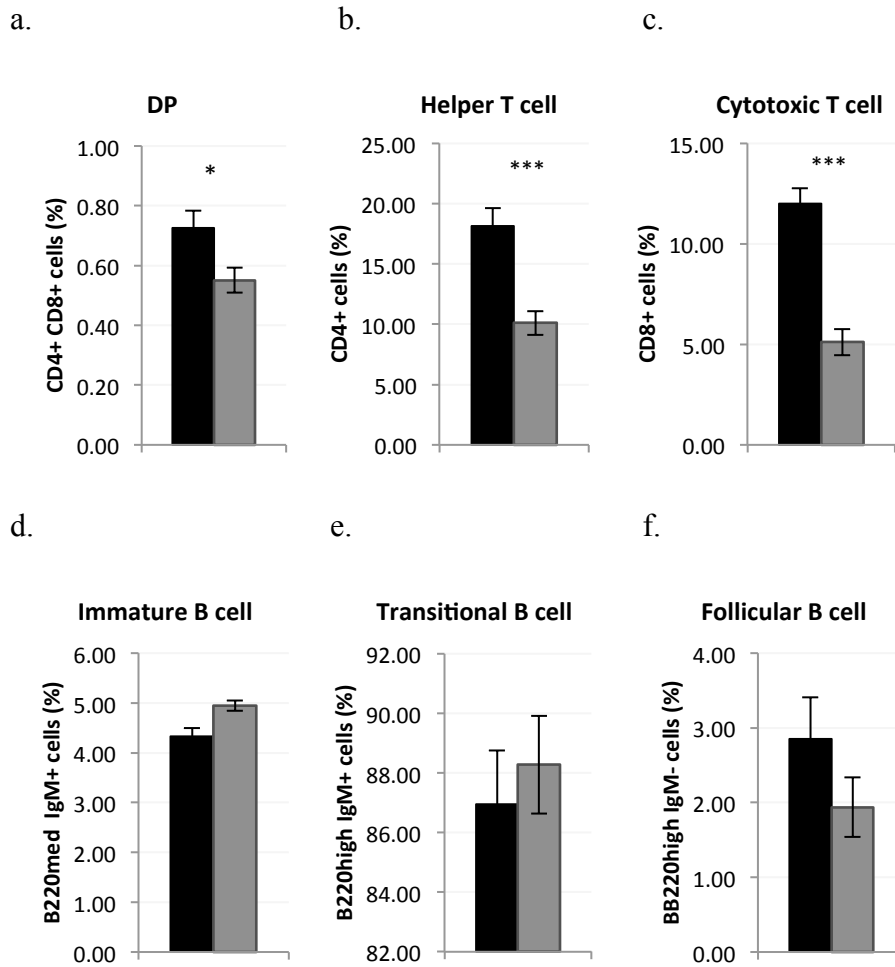
Grey =Atm-/- (n=14), black = Atm+/+ (n=15)

Error bar = S.E.M. *=p< 0.05, ** = p<0.01, *** =p<0.001

a, b & c. double positive (DP) T cells, single positive CD4 T cells, single positive CD8 cells respectively

d, e & f. immature B cells, Transitional B cells and Follicular B cells respectively

Figure 4.4 continued FACS comparison of Atm-/- and Atm+/+ spleen cells at 6 weeks of age

g.   h.

i.   j.   k.
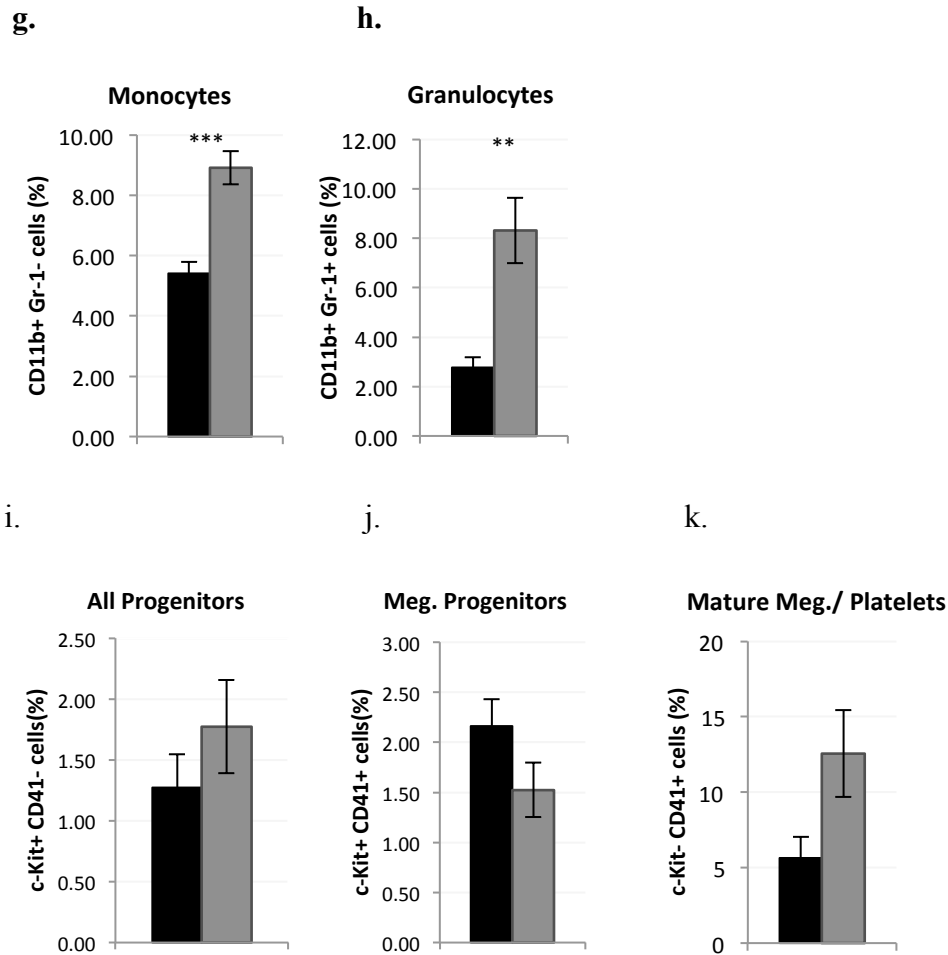
Grey =Atm-/- (n=14), black = Atm+/+ (n=15)

error bar = S.E.M, *=p< 0.05, ** = p<0.01, *** =p<0.001.

g &h. myeloid cells: macrophage and granulocytes respectively

i, j & k. c-Kit+ progenitor cells, megakaryocyte (meg.) progenitors and mature megakaryocytes and platelets cell populations

Figure 4.5 Atm-/- peripheral blood counts at 6 weeks of age

a.

b.

c.

d.

e.

f.

g.
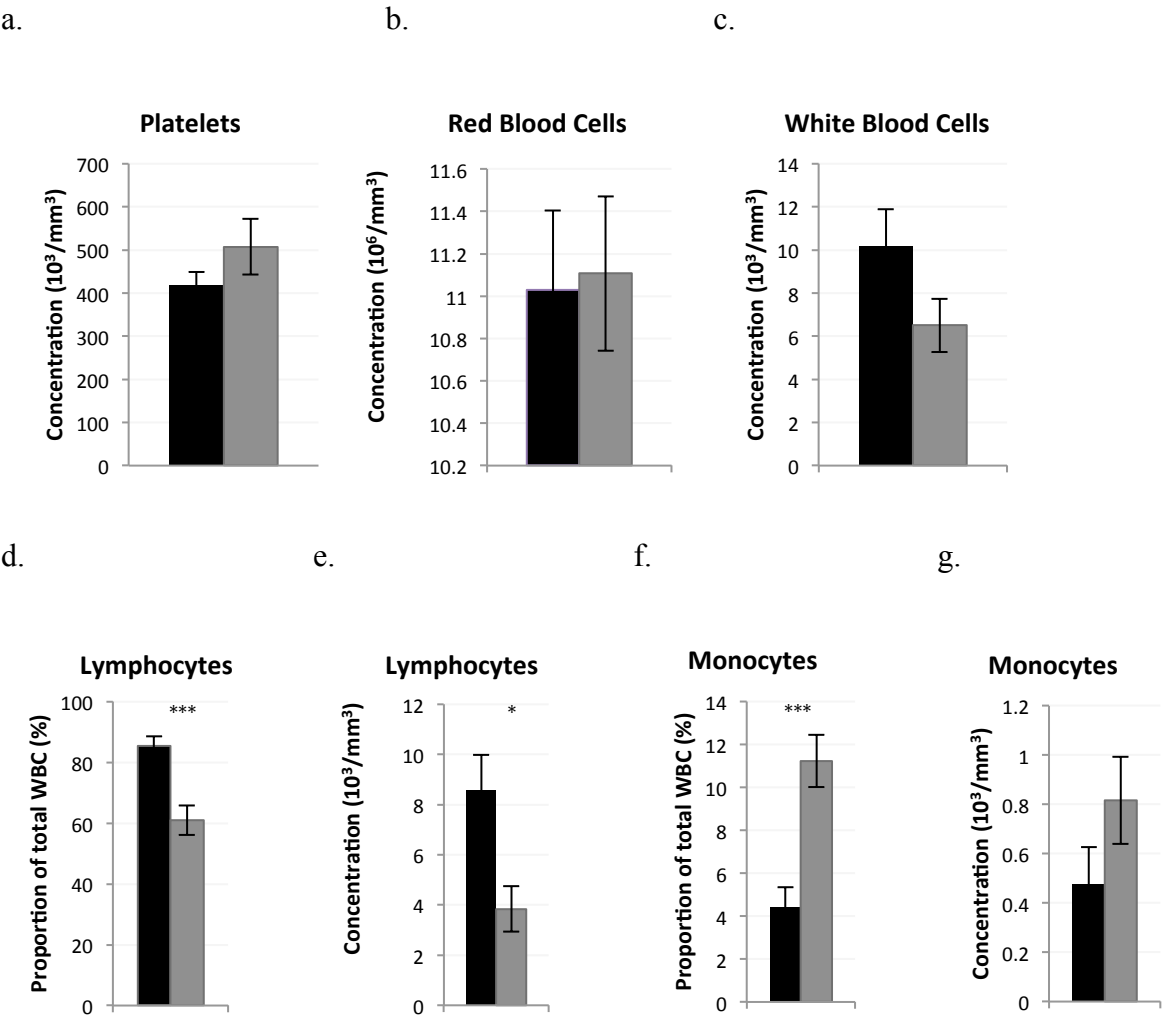
Grey =Atm-/- (n=9), black = Atm+/+ (n=8)

Error bar = S.E.M. *=p< 0.05, ** = p<0.01, *** =p<0.001

a. Platelet count

b. Red blood cell count

c. White blood cell count

d and e. Lymphocyte proportion and count respectively

f and g. Monocyte proportion and count respectively

Figure 4.5 continued Atm-/- peripheral blood counts at 6 weeks of age

h.   i.   j.

k.   l.   m.
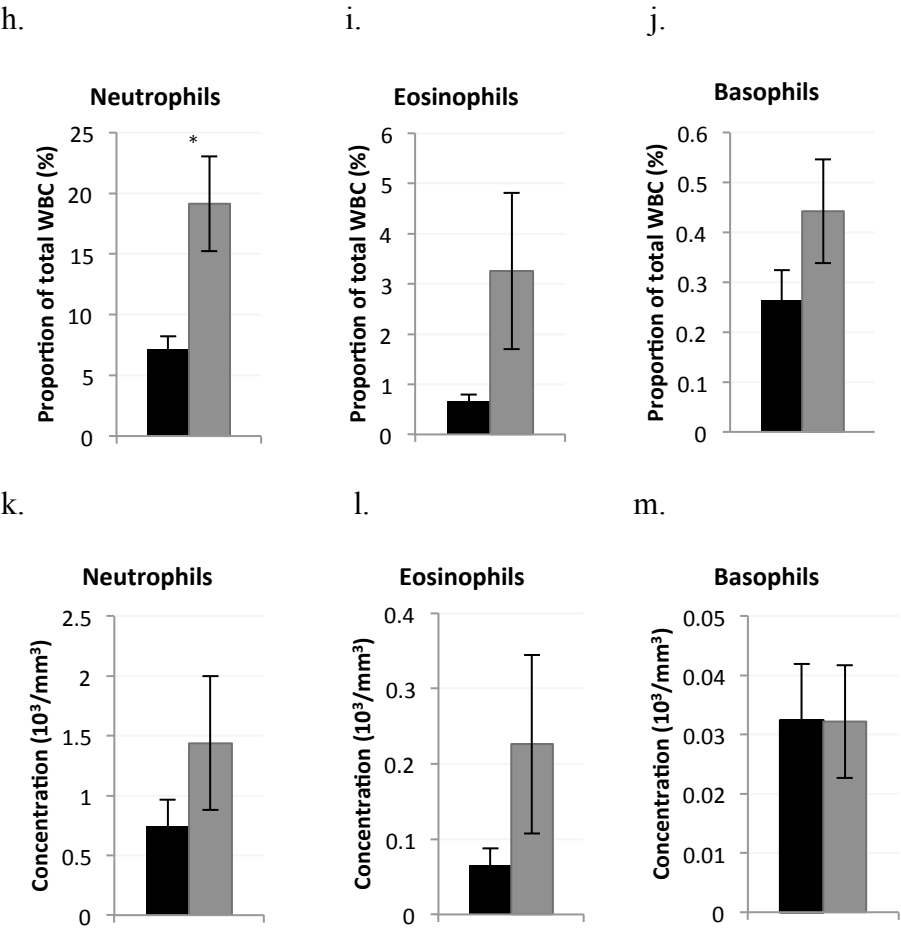
Grey =Atm-/- (n=9), black = Atm+/+ (n=8)

Error bar = S.E.M. *=p< 0.05, ** = p<0.01, *** =p<0.001

h, i & j. neutrophils, eosinophil and basophil proportion

k, l & m. neutrophils, eosinophil and basophil count

Figure 4.6 Atm-/- side population analysis

a.
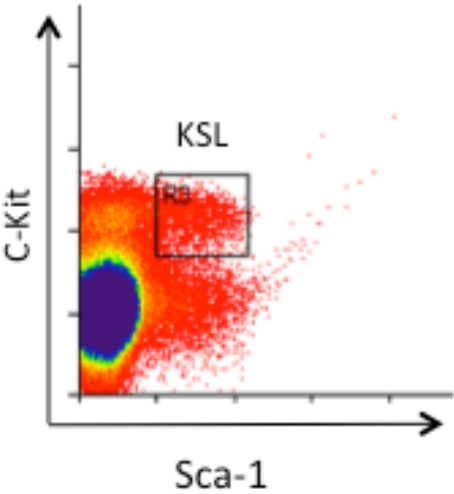
b.
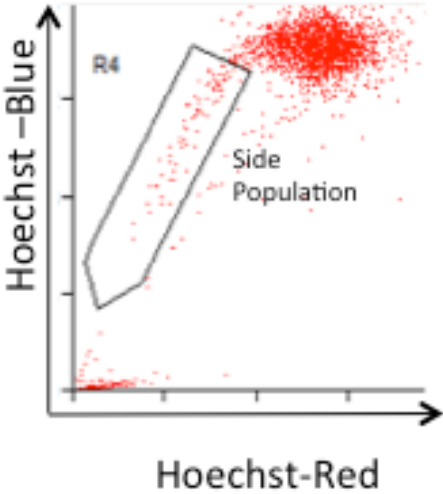
c.
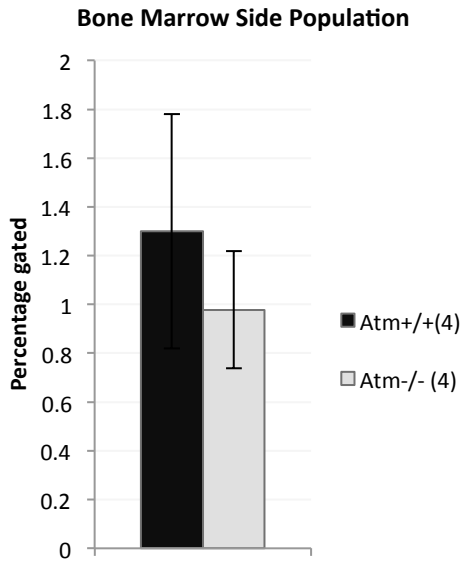
Black bar = Atm+/+ (n=4), grey bar= Atm-/- (n=4), Error bars = S.E.M

a. Gating of LSK cells

b. Gating of side population

c. Proportion of side population

Figure 4.7 Colony forming unit (CFU) morphology

a.

b.

c.
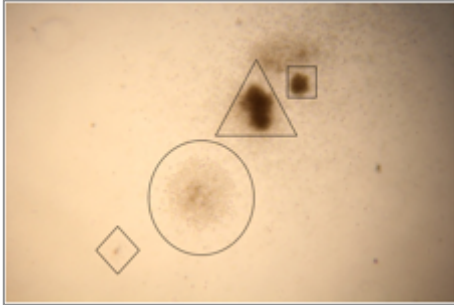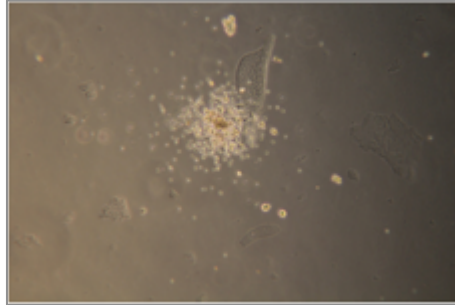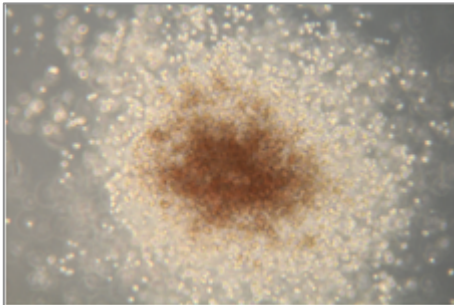
d.
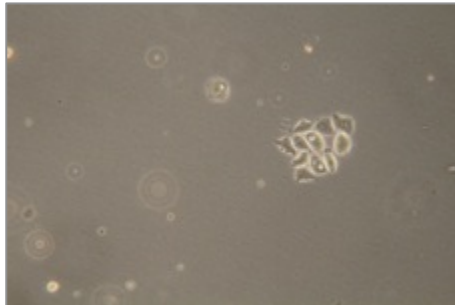
Representative pictures of different colony types that grow on M3434 media.

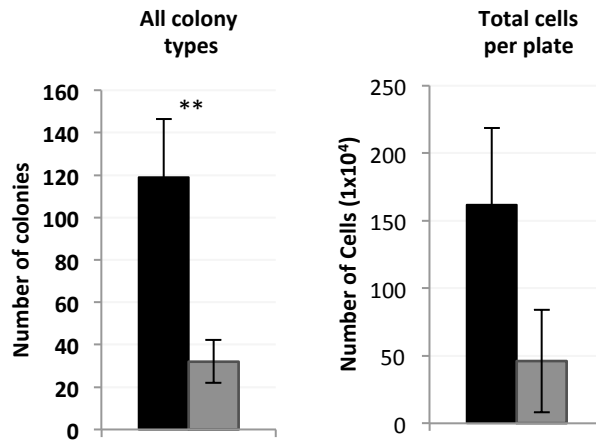a. Diamond is CFU-E, circle is CFU-M, triangle is CFU-GM, square is CFU-G (x20)
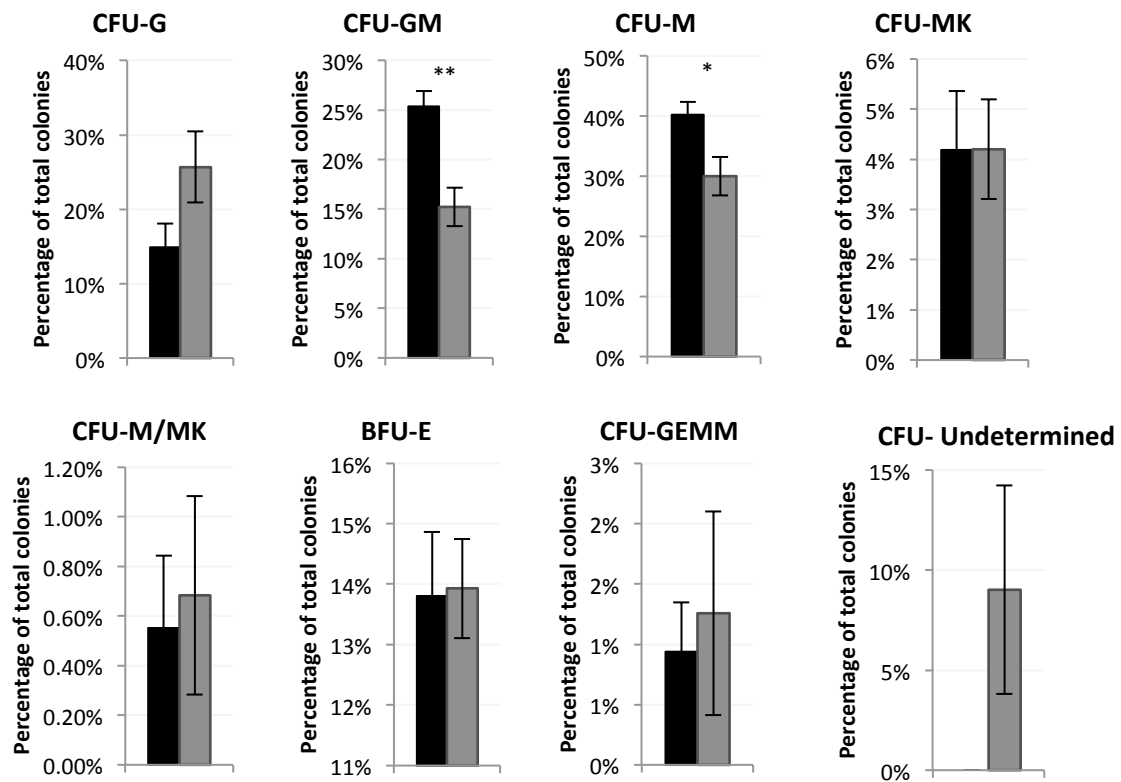
b. CFU-GEMM (x40)

c. CFU-E (x100)

d. CFU-MK (x40)

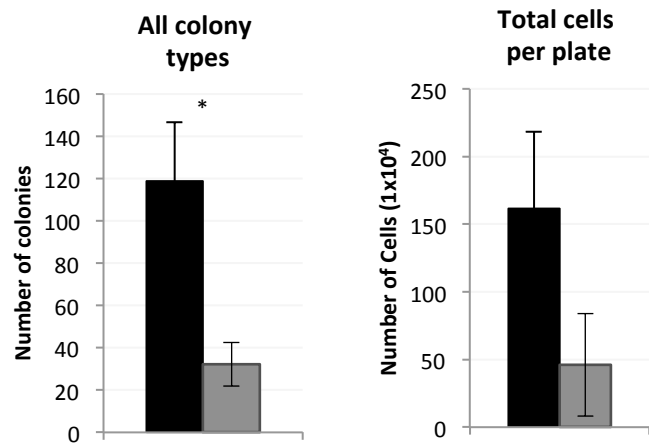**Figure 4.8 Atm-/- bone marrow CFU potential at six weeks of age**

a.

b.

Black= Atm+/+ (n=4), grey= Atm-/- (n=4), error bar = S.E.M, *=$p < 0.05$, ** = $p < 0.01$, *** = $p < 0.001$

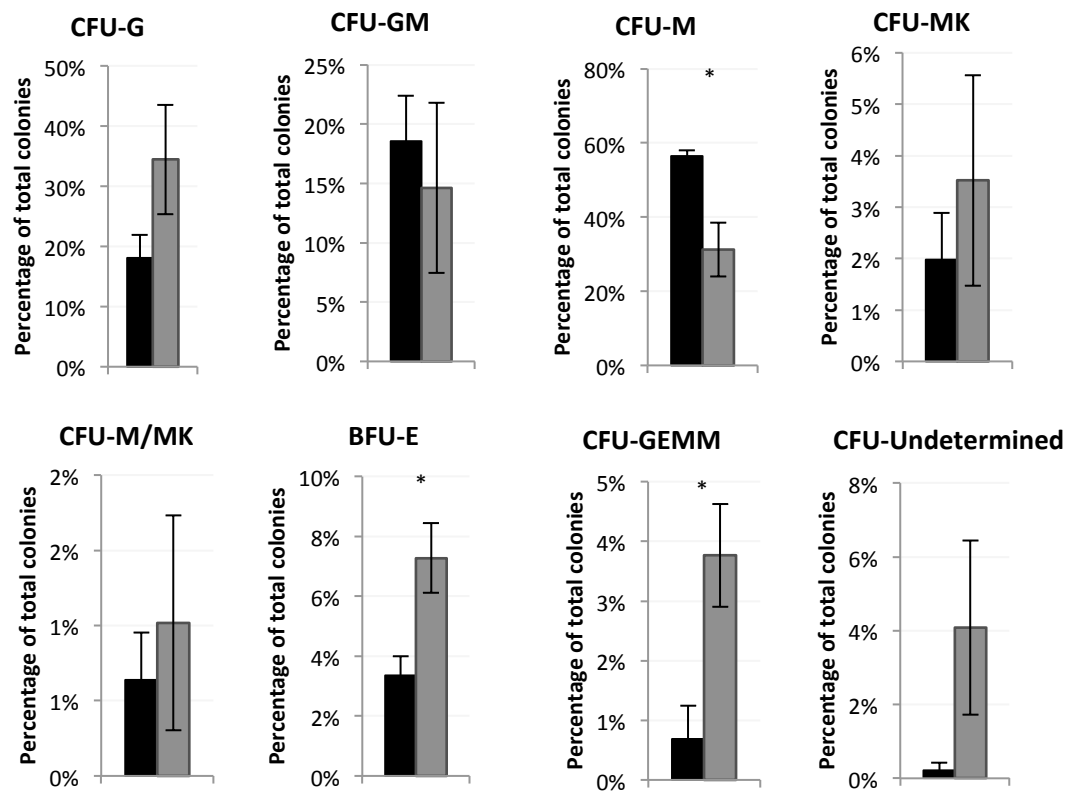a. Total number of colonies per plate and total cells per plate

b. Differentiation potential expressed as a proportion of the total number of colonies formed per plate

Figure 4.9 Atm-/- spleen CFU potential at six weeks of age

a.

b.
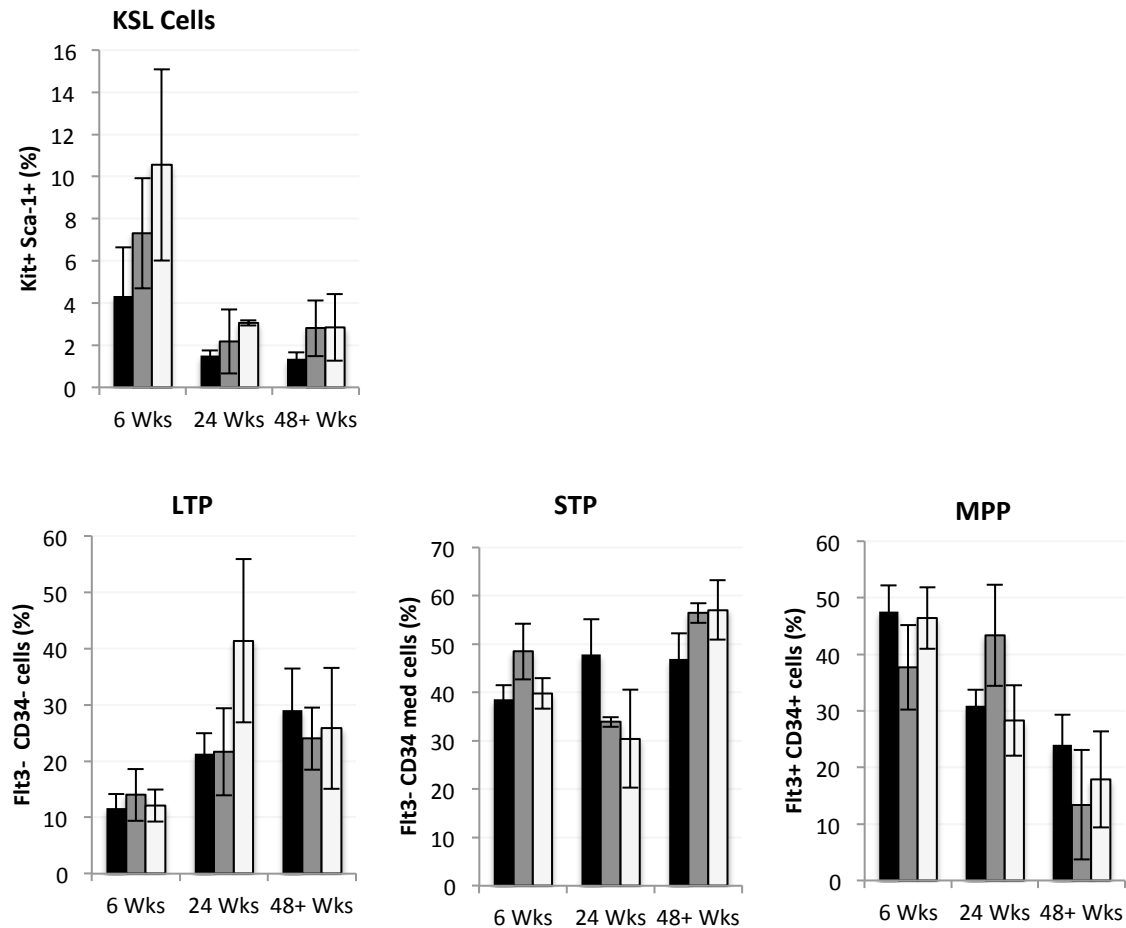

Black= Atm+/+ (n=4), grey= Atm-/- (n=4), error bar = S.E.M, *=p< 0.05, ** = p<0.01, *** = p<0.001

a. Total number of colonies per plate and total cells per plate

b. Differentiation potential expressed as a proportion of the total number of colonies formed per plate

Figure 4.10 FACS comparison of Atm-/-nu-/-, Atm+/+nu-/- and Atm+/+nu+/- bone marrow at 6, 24 and 48+ weeks of age
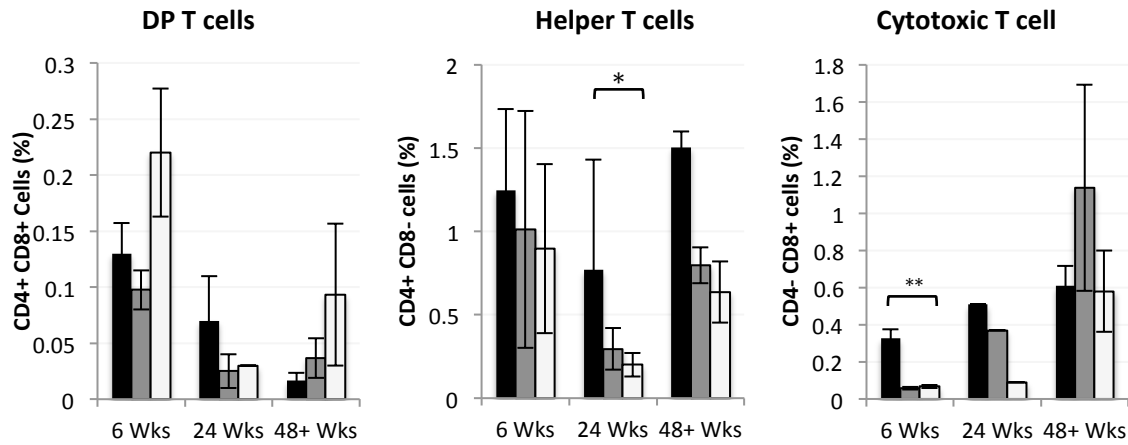
a.

Black = Atm+/+nu+/-, grey=Atm+/+nu-/- and white = Atm-/-nu-/-

Error bar = S.E.M, *=p< 0.05, ** = p<0.01, *** = p<0.001.

At 6 weeks, 4 mice of each genotype were analysed, at 24 weeks 2 mice of each genotype were analysed and at 48+ weeks 3 mice of each genotype were analysed.

a. Progenitor cells; LSK (lin-, Sca-1-, c-Kit-), long term (Flt3-CD34-) (LTP), short term (Flt3- CD34 med)(STP) and multipotent progenitors (Flt3+, CD34+) (MPP).

Figure 4.10 continued FACS comparison of Atm-/-nu-/-, Atm+/+nu-/- and Atm+/+nu+/-bone marrow at 6, 24 and 48+ weeks of age

b.i

Black = Atm+/+nu+/-, grey=Atm+/+nu-/- and white = Atm-/-nu-/-, error bar = S.E.M, *=p< 0.05, ** = p<0.01, *** = p<0.001

At 6 weeks 4 mice of each genotype were analysed, at 24 weeks 2 mice of each genotype were analysed and at 48+ weeks 3 mice of each genotype were analysed.

b.i T and B lymphocytes: Double positive (DP) T cell (CD4+CD8+), Helper T cell (CD4+Cd8-), Cytotoxic T cells (CD4-CD8+).

**Figure 4.10 continued FACS comparison of Atm-/-nu-/-, Atm+/+nu-/- and Atm+/+nu+/-
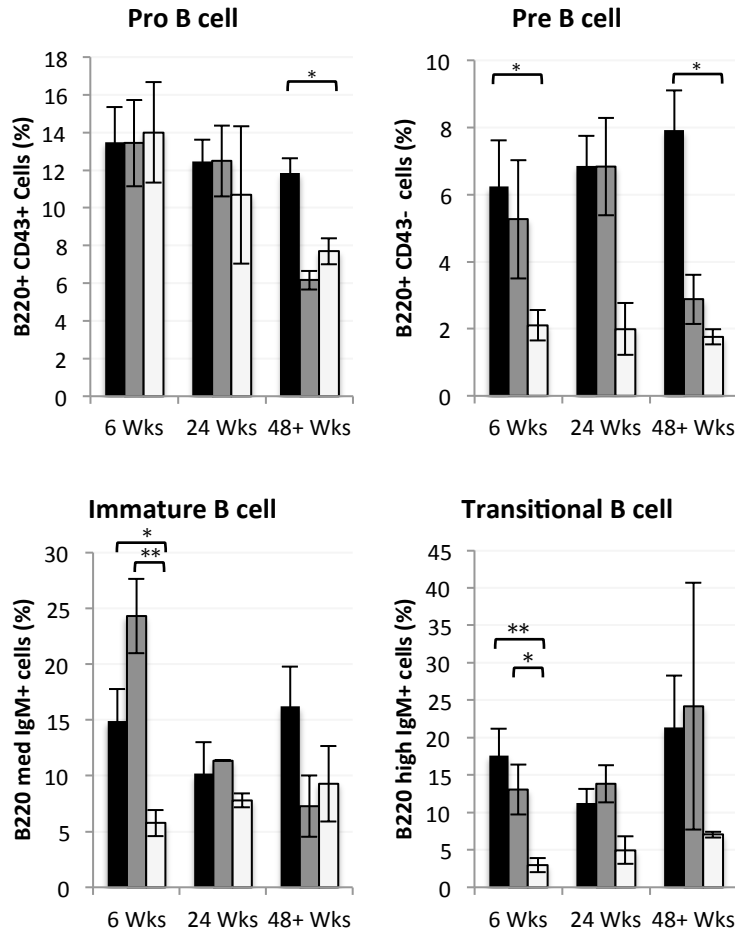bone marrow at 6, 24 and 48+ weeks of age**

b.ii

Black = Atm+/+nu+/-, grey=Atm+/+nu-/- and white = Atm-/-nu-/-, error bar = S.E.M, *=p< 0.05, ** = p<0.01, *** = p<0.001

At 6 weeks 4 mice of each genotype were analysed, at 24 weeks 2 mice of each genotype were analysed and at 48+ weeks 3 mice of each genotype were analysed.

b.ii Pro B cell (B220+CD43+), pre B cell (B220+CD43-), Immature B cell (B220medium IgM+), transitional B cell (B220medium IgM+).

Figure 4.10 continued FACS comparison of Atm-/-nu-/-, Atm+/+nu-/- and Atm+/+nu+/-bone marrow at 6, 24 and 48+ weeks of age

c.

d.
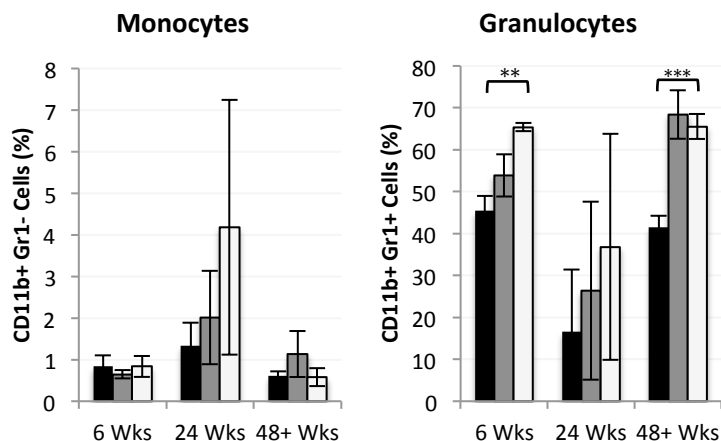

Black = Atm+/+nu+/-, grey=Atm+/+nu-/- and white = Atm-/-nu-/-

Error bar = S.E.M, *=p< 0.05, ** = p<0.01, *** = p<0.001

At 6 weeks 4 mice of each genotype were analysed, at 24 weeks 2 mice of each genotype were analysed and at 48+ weeks 3 mice of each genotype were analysed.
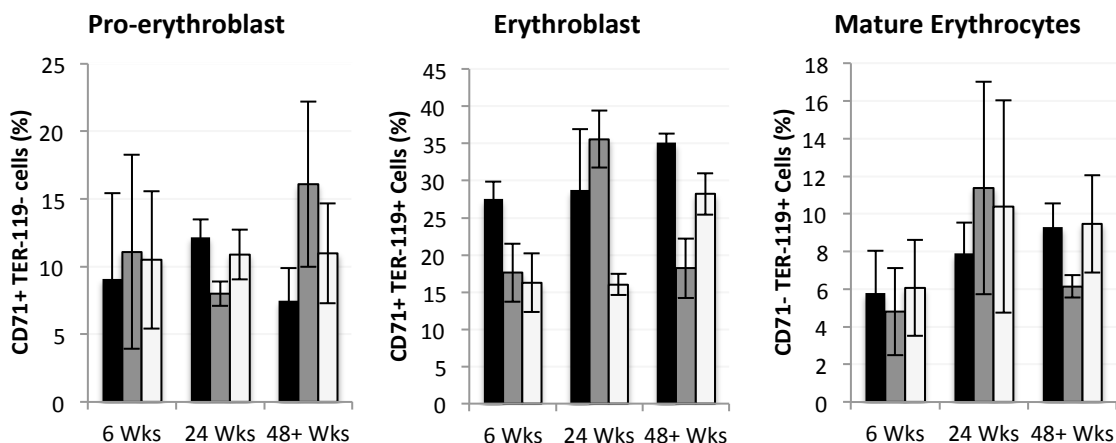
c. Myeloid cells: monocytes (CD11b+ Gr-1-) and granulocytes (CD11b+ Gr-1+)

d. Erythrocyte populations: pro-erythroblast (CD71+ TER-119-), erythroblast (CD71+ TER-119+) and mature erythrocytes (CD71- TER119+)

Figure 4.10 continued FACS comparison of Atm-/-nu-/-, Atm+/+nu-/- and Atm+/+nu+/-bone marrow at 6, 24 and 48+ weeks of age

e.

Black = Atm+/+nu+/-, grey=Atm+/+nu-/- and white = Atm-/-nu-/-

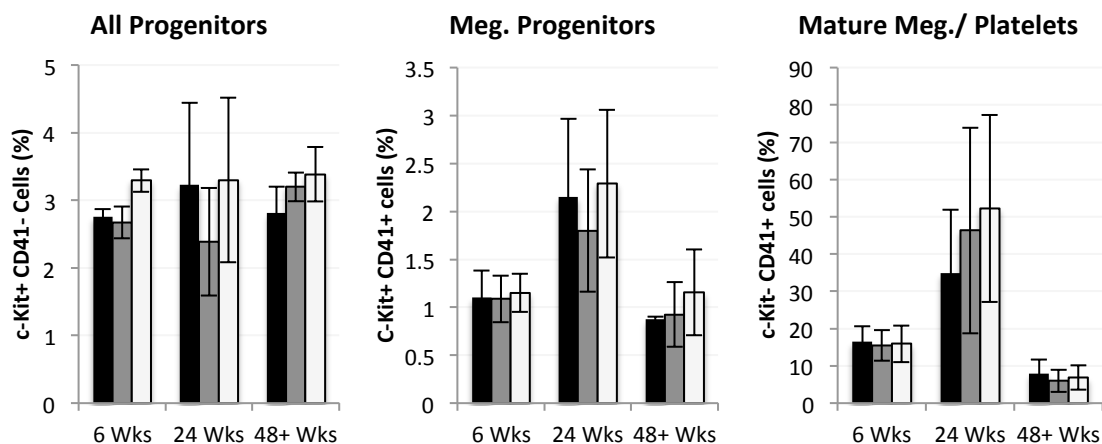Error bar = S.E.M, *=p< 0.05, ** = p<0.01, *** = p<0.001

At 6 weeks 4 mice of each genotype were analysed, at 24 weeks 2 mice of each genotype were analysed and at 48+ weeks 3 mice of each genotype were analysed.

e. Megakaryocyte population: all progenitors (c-Kit+ CD41-), megakaryocyte progenitor (c-Kit+ CD41+) and mature megakaryocyte and platelets (c-Kit- CD41+)

Figure 4.11 FACS comparison of Atm-/-nu-/-, Atm+/+nu-/- and Atm+/+nu+/- spleen at 6, 24 and 48+ weeks of age

a.i.

Black = Atm+/+nu+/-, grey=Atm+/+nu-/- and white = Atm-/-nu-/-, error bar = S.E.M, *=p< 0.05, ** = p<0.01, *** = p<0.001

At 6 weeks 4 mice each genotype were analysed, at 24 weeks 2 mice of each genotype were analysed and at 48+ weeks 3 mice of each genotype were analysed.

a.i. T lymphocytes: Double positive (DP) T cell (CD4+CD8+), helper T cell (CD4+Cd8-) and cytotoxic T cells (CD4-CD8+)

Figure 4.11 continued FACS comparison of Atm-/-nu-/-, Atm+/+nu-/- and Atm+/+nu+/-spleen at 6, 24 and 48+ weeks of age

a.ii.
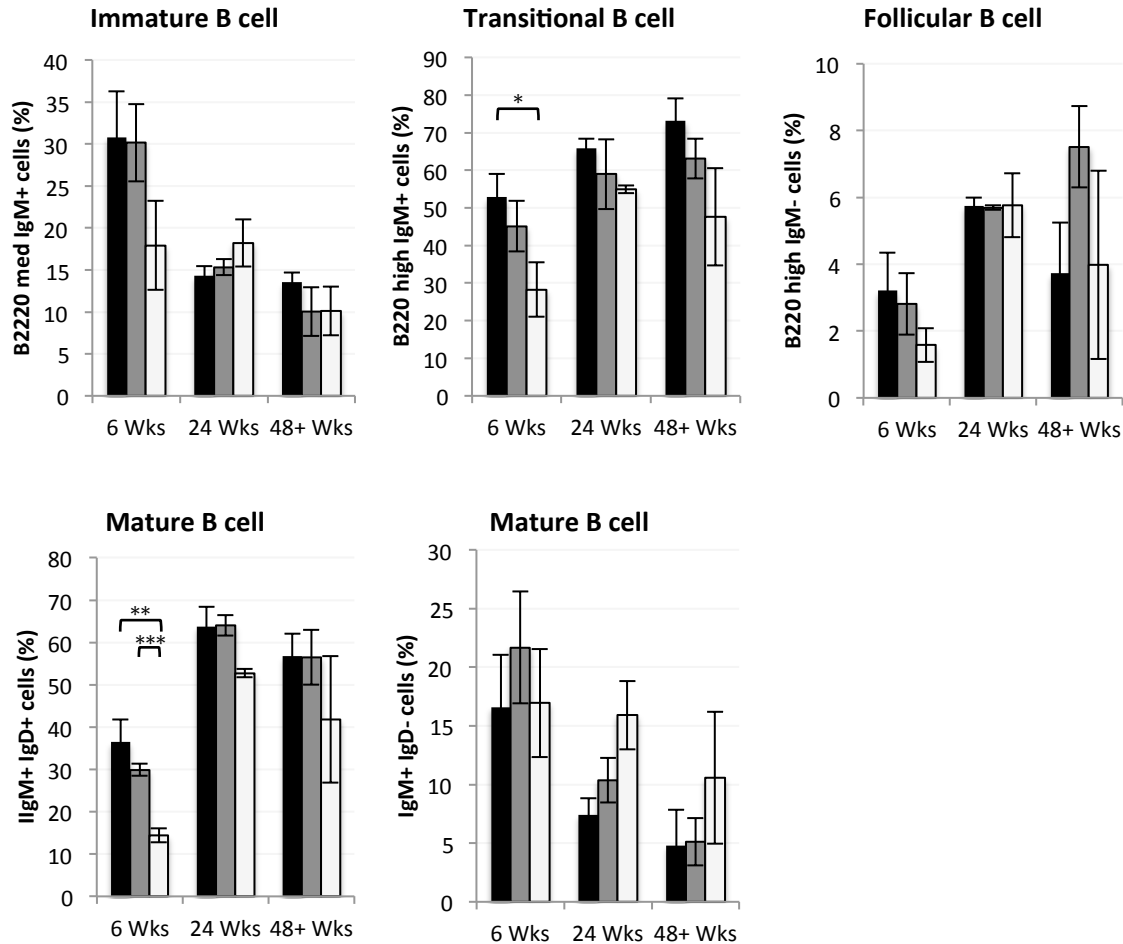
Black = Atm+/+nu+/-, grey=Atm+/+nu-/- and white = Atm-/-nu-/-, error bar = S.E.M, *=p< 0.05, ** = p<0.01, *** = p<0.001
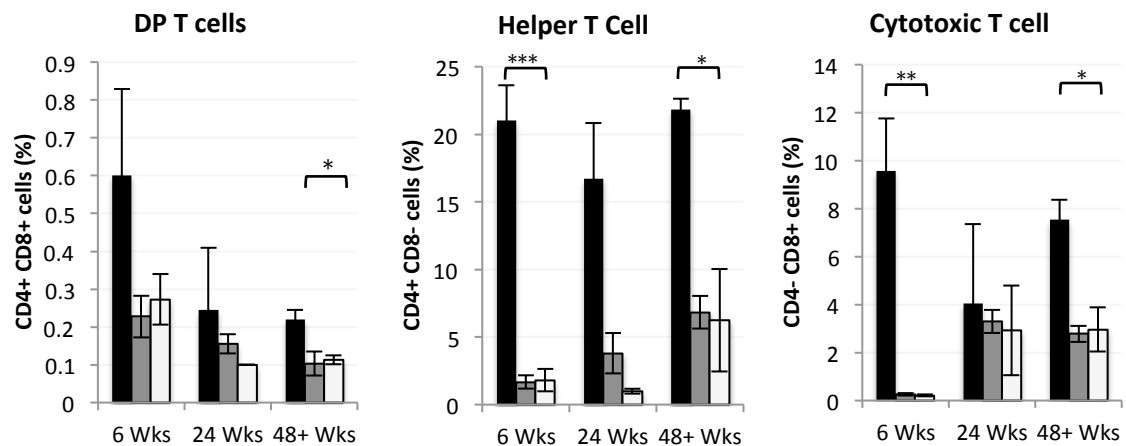
At 6 weeks 4 mice each genotype were analysed, at 24 weeks 2 mice of each genotype were analysed and at 48+ weeks 3 mice of each genotype were analysed.

a.ii. B lymphocytes: immature B cell (B220medium IgM+), transitional B cell (B220high IgM+), follicular B cells (B220high IgM-) and mature B cells (IgM+ IgD+ and IgM-IgD+)

Figure 4.11 continued FACS comparison of Atm-/-nu-/-, Atm+/+nu-/- and Atm+/+nu+/-

spleen at 6, 24 and 48+ weeks of age

b.

c.

Black = Atm+/+nu+/-, grey=Atm+/+nu-/- and white = Atm-/-nu-/-, error bar = S.E.M, *=p< 0.05, ** = p<0.01, *** = p<0.001

At 6 weeks 4 mice each genotype were analysed, at 24 weeks 2 mice of each genotype were analysed and at 48+ weeks 3 mice of each genotype were analysed.

b. Myeloid cells: monocytes (CD11b+ Gr-1-) and granulocytes (CD11b+ Gr-1+)

c. Megakaryocyte population: all progenitors (c-Kit+ CD41-), megakaryocyte progenitor (c-Kit+ CD41+) and mature megakaryocyte and platelets (c-Kit- CD41+)

Figure 4.12 FACS comparison of Atm-/-nu-/-, Atm+/+nu-/- and Atm+/+nu+/- liver at 6, 24 and 48+ weeks of age

a.
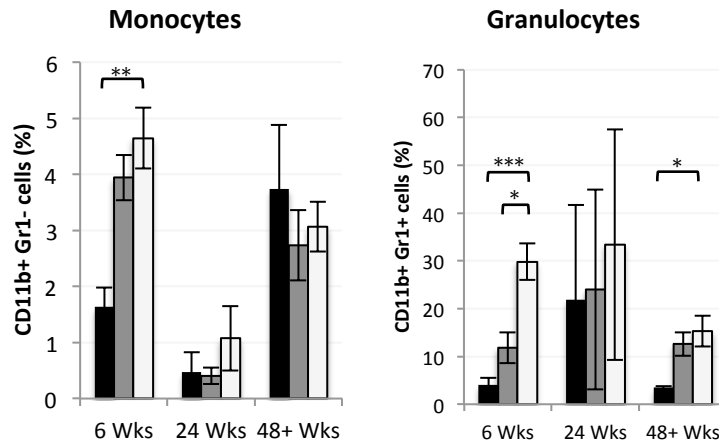

Black= Atm+/+nu+/-, grey=Atm+/+nu-/- and white = Atm-/-nu-/-

Error bar = S.E.M, *=p< 0.05, ** = p<0.01, *** = p<0.001

At 6 weeks 4 mice each genotype were analysed, at 24 weeks 2 mice of each genotype were analysed, and at 48+ weeks 3 mice of each genotype were analysed.
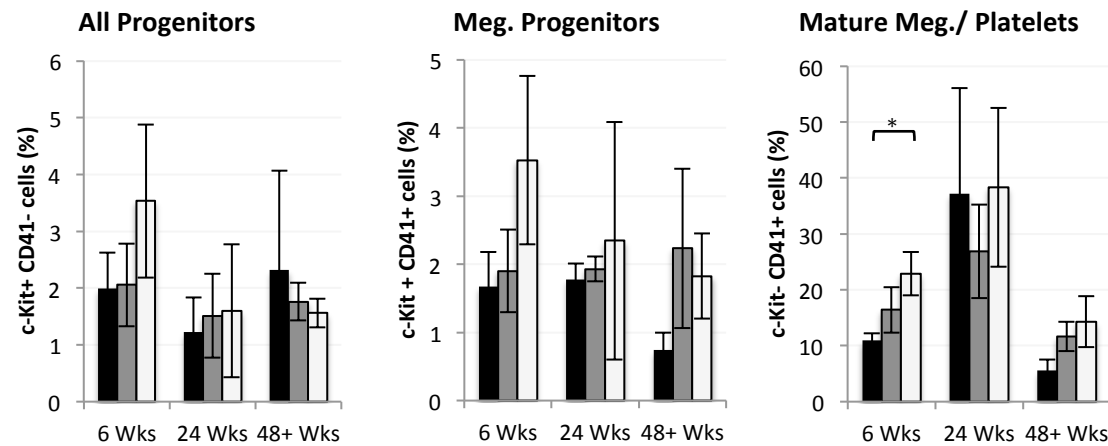
a. T and B lymphocytes: Double positive (DP) T cell (CD4+CD8+), helper T cell (CD4+Cd8-), cytotoxic T cells (CD4-CD8+), immature B cell (B220medium IgM+), transitional B cell (B220high IgM+), follicular B cells (B220high IgM-)

Figure 4.12 continued FACS comparison of Atm-/-nu-/-, Atm+/+nu-/- and Atm+/+nu+/- liver at 6, 24 and 48+ weeks of age

b.

c.

Black = Atm+/+nu+/-, grey=Atm+/+nu-/- and white = Atm-/-nu-/-, error bar = S.E.M, *=p< 0.05, ** = p<0.01, *** = p<0.001
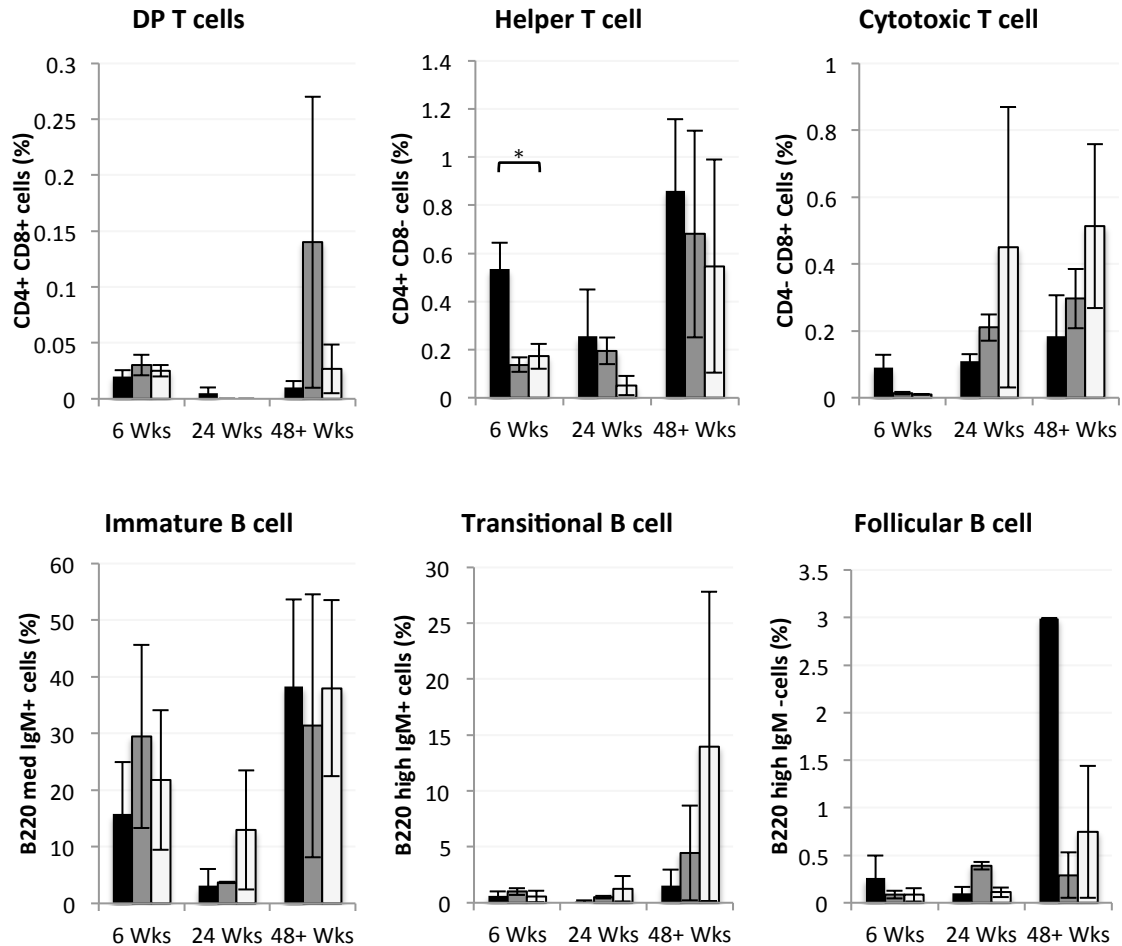
At 6 weeks 4 mice each genotype were analysed, at 24 weeks 2 mice of each genotype were analysed, and at 48+ weeks 3 mice of each genotype were analysed.

b. Myeloid cells: monocytes (CD11b+ Gr-1-) and granulocytes (CD11b+ Gr-1+)

c. Megakaryocyte population: all progenitors (c-Kit+ CD41-), megakaryocyte progenitor (c-Kit+ CD41+) and mature megakaryocyte and platelets (c-Kit- CD41+)

Figure 4.13 Atm-/-nu-/- peripheral blood analysis at 6, 24 and 48 weeks of age
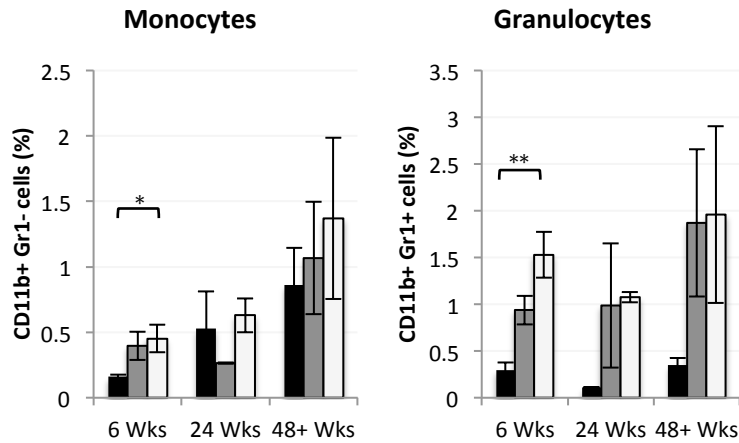

Black = Atm+/+nu+/-, grey=Atm+/+nu-/- and white = Atm-/-nu-/-, error bar = S.E.M, *=p< 0.05, ** = p<0.01, *** = p<0.001

Four mice each of genotype were analysed at 6 weeks of age, 2 mice of each genotype were analysed at 24 weeks and at 48+ weeks 3 mice of each genotype were analysed.

a. Platelet count

b. Red blood cell count

c. White blood cell count

d and e. Lymphocyte proportion and count respectively

f and g. Monocyte proportion and count respectively

Figure 4.13 continued Atm-/-nu-/- peripheral blood analysis at 6, 24 and 48 weeks of age

h.

i.
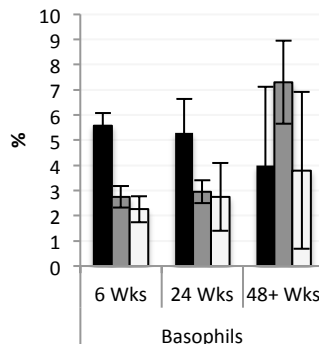
j.
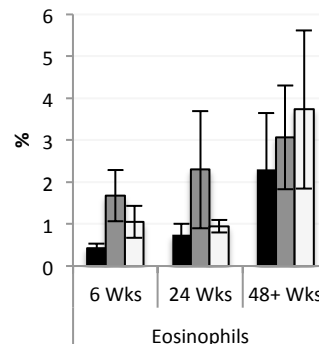
k.
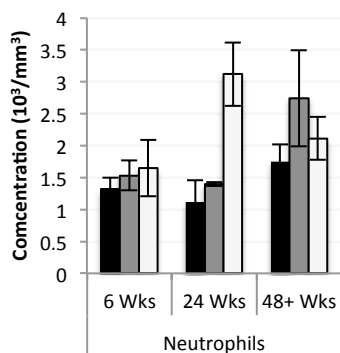
l.
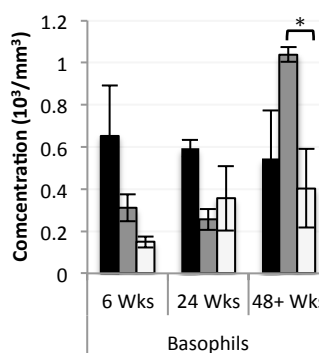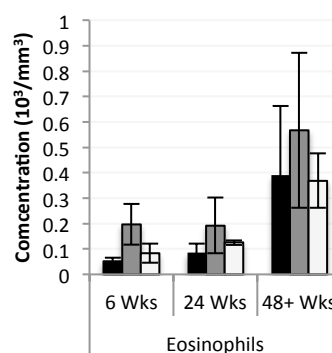
m.

Black = Atm+/+nu+/-, grey=Atm+/+nu-/- and white = Atm-/-nu-/-

Error bar = S.E.M, *=p< 0.05, ** = p<0.01, *** = p<0.001

Four mice each of genotype were analysed at 6 weeks of age, 2 mice of each genotype were analysed at 24 weeks and at 48+ weeks 3 mice of each genotype were analysed.
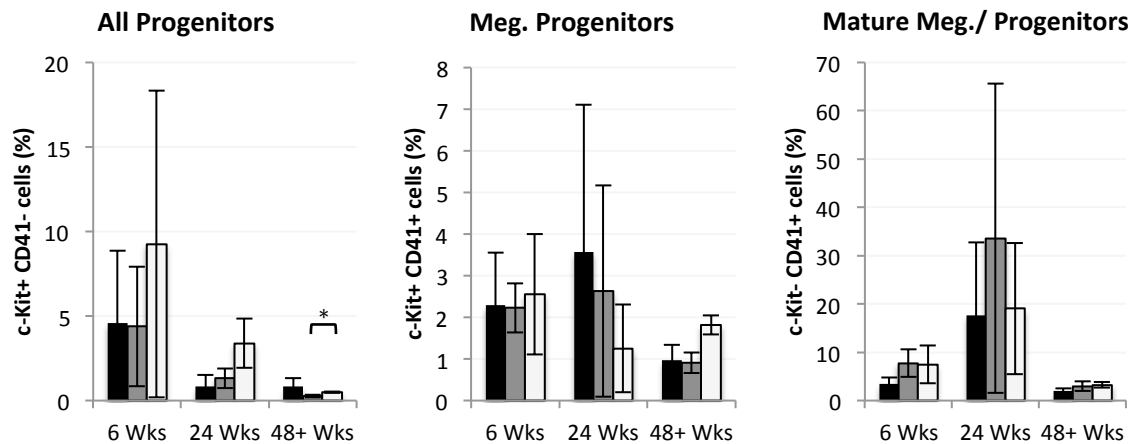
h, I and j. neutrophils, eosinophil and basophil proportion

k, l and m. neutrophils, eosinophil and basophil count

Figure 4.14 Atm-/-nu-/- bone marrow CFU potential at 6, 24 and 48 weeks of age

a.
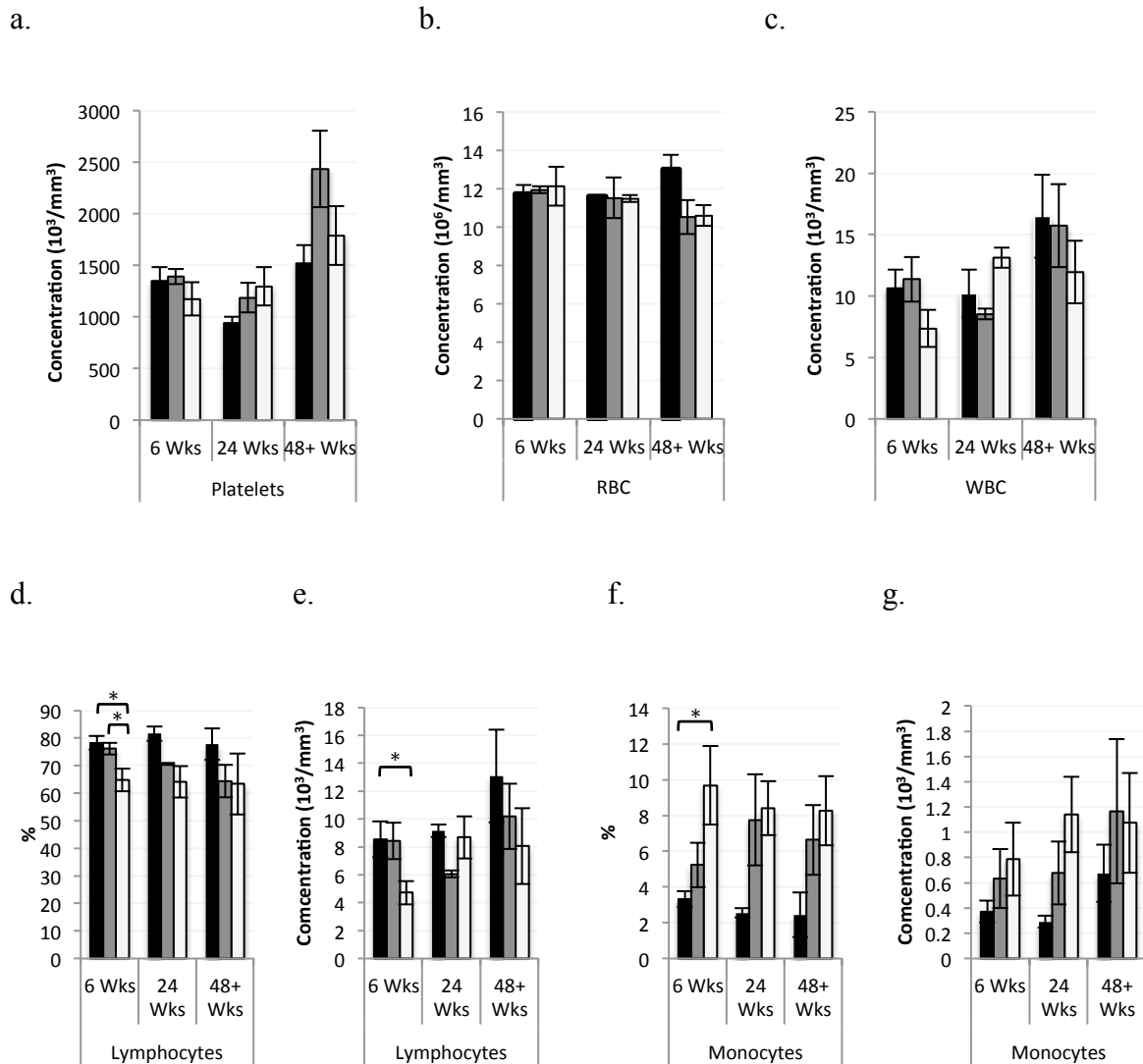

Black= Atm+/+nu+/-, grey=Atm+/+nu-/- and white = Atm-/-nu-/-

Error bar = S.E.M, *=p< 0.05, ** = p<0.01, *** = p<0.001

Four mice each of genotype were analysed at 6 weeks of age, 2 mice of each genotype were analysed at 24 weeks and at 48+ weeks 3 mice of each genotype were analysed.

a. Total number of colonies per plate and total cells per plate

b.

Black= Atm+/+nu+/-, grey=Atm+/+nu-/- and white = Atm-/-nu-/-

Error bar = S.E.M, *=p< 0.05, ** = p<0.01, *** = p<0.001

Four mice each of genotype were analysed at 6 weeks of age, 2 mice of each genotype were analysed at 24 weeks and at 48+ weeks 3 mice of each genotype were analysed.

b. Differentiation potential expressed as a proportion of the total number of colonies formed per plate

Figure 4.15 Atm-/-nu-/- spleen CFU potential at 6, 24 and 48 weeks of age
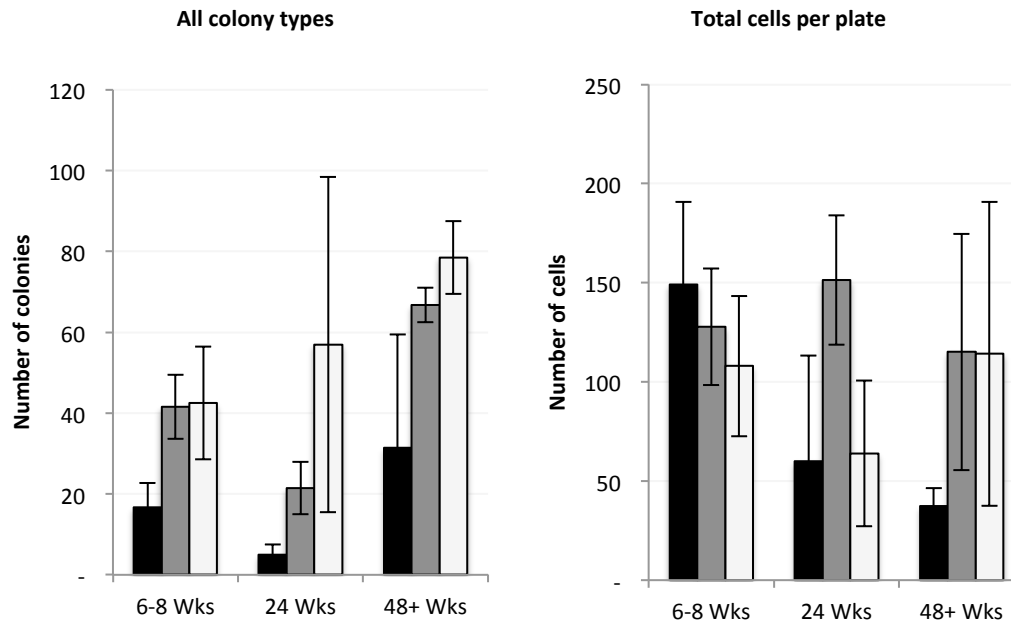
a.

Black= Atm+/+nu+/-, grey=Atm+/+nu-/- and white = Atm-/-nu-/-

Error bar = S.E.M, *=p< 0.05, ** = p<0.01, *** = p<0.001

Four mice each of genotype were analysed at 6 weeks of age, 2 mice of each genotype were analysed at 24 weeks and at 48+ weeks 3 mice of each genotype were analysed.

a. Total number of colonies per plate and total cells per plate
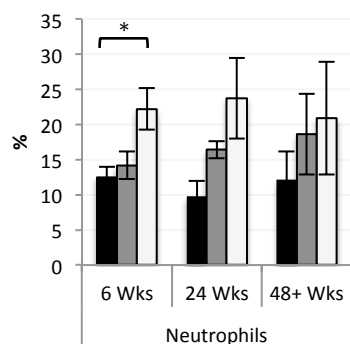
Figure 4.15 continued Atm-/-nu-/- spleen CFU potential at 6, 24 and 48 weeks of age
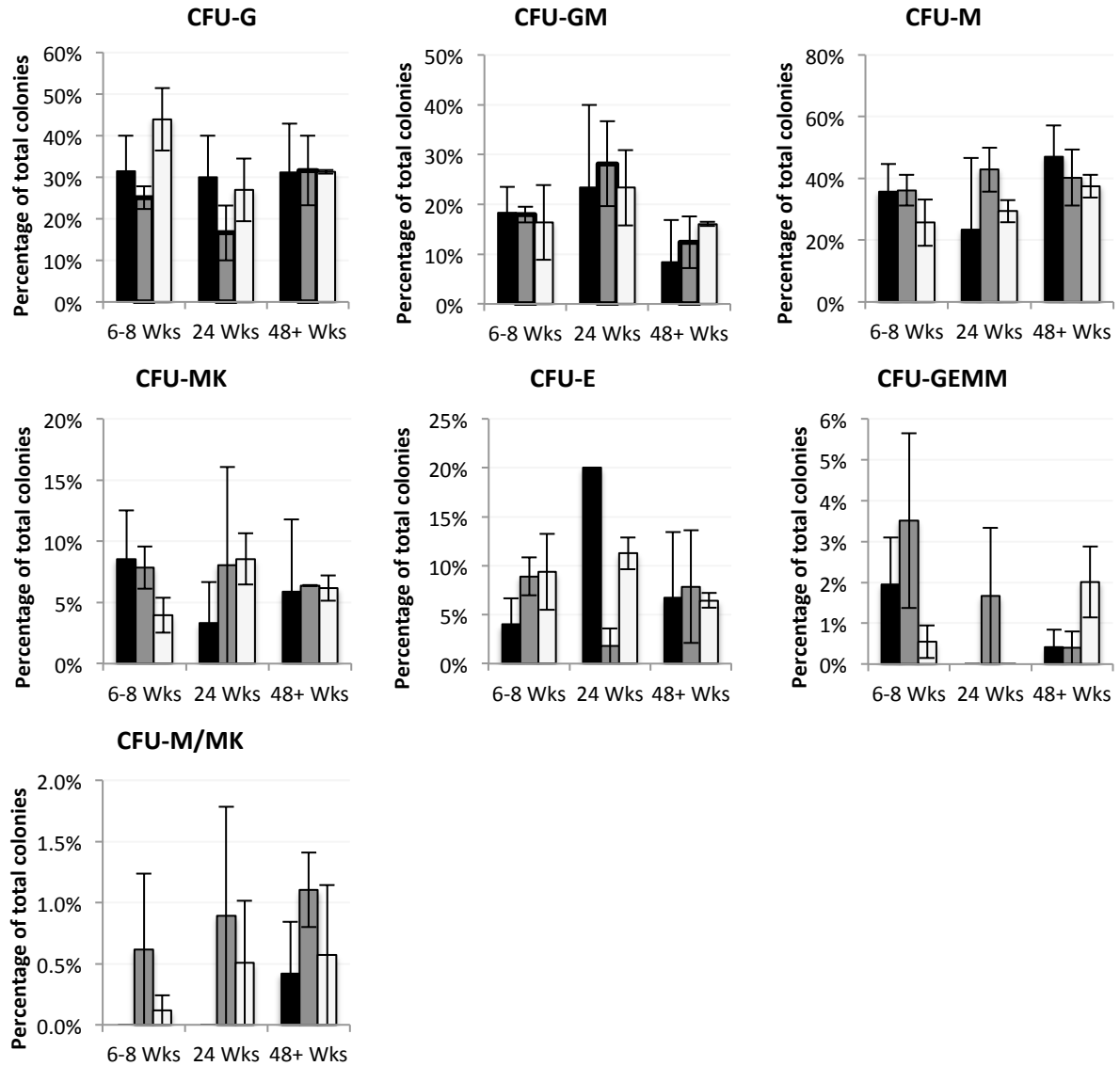
b.

Black= Atm+/+nu+/-, grey=Atm+/+nu-/- and white = Atm-/-nu-/-

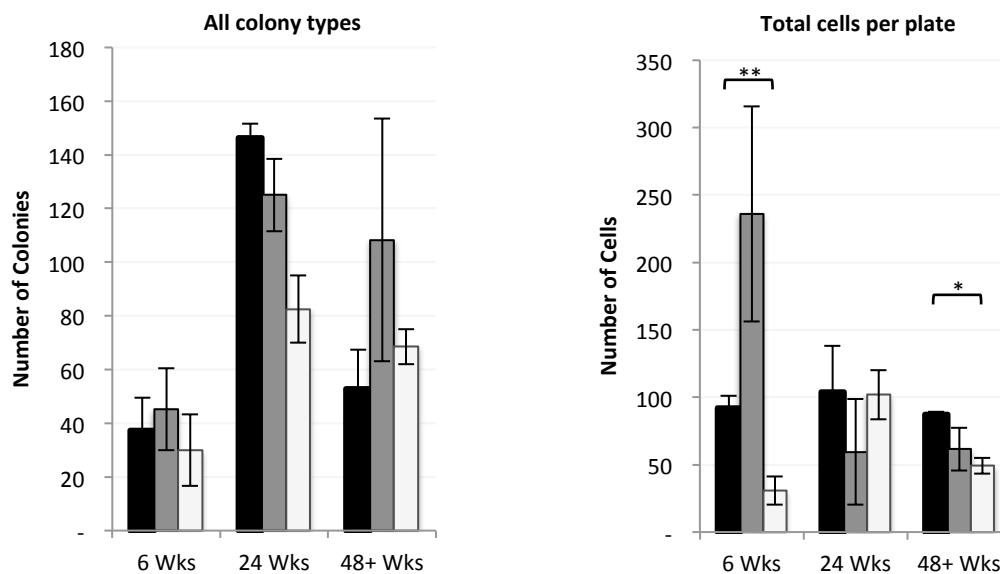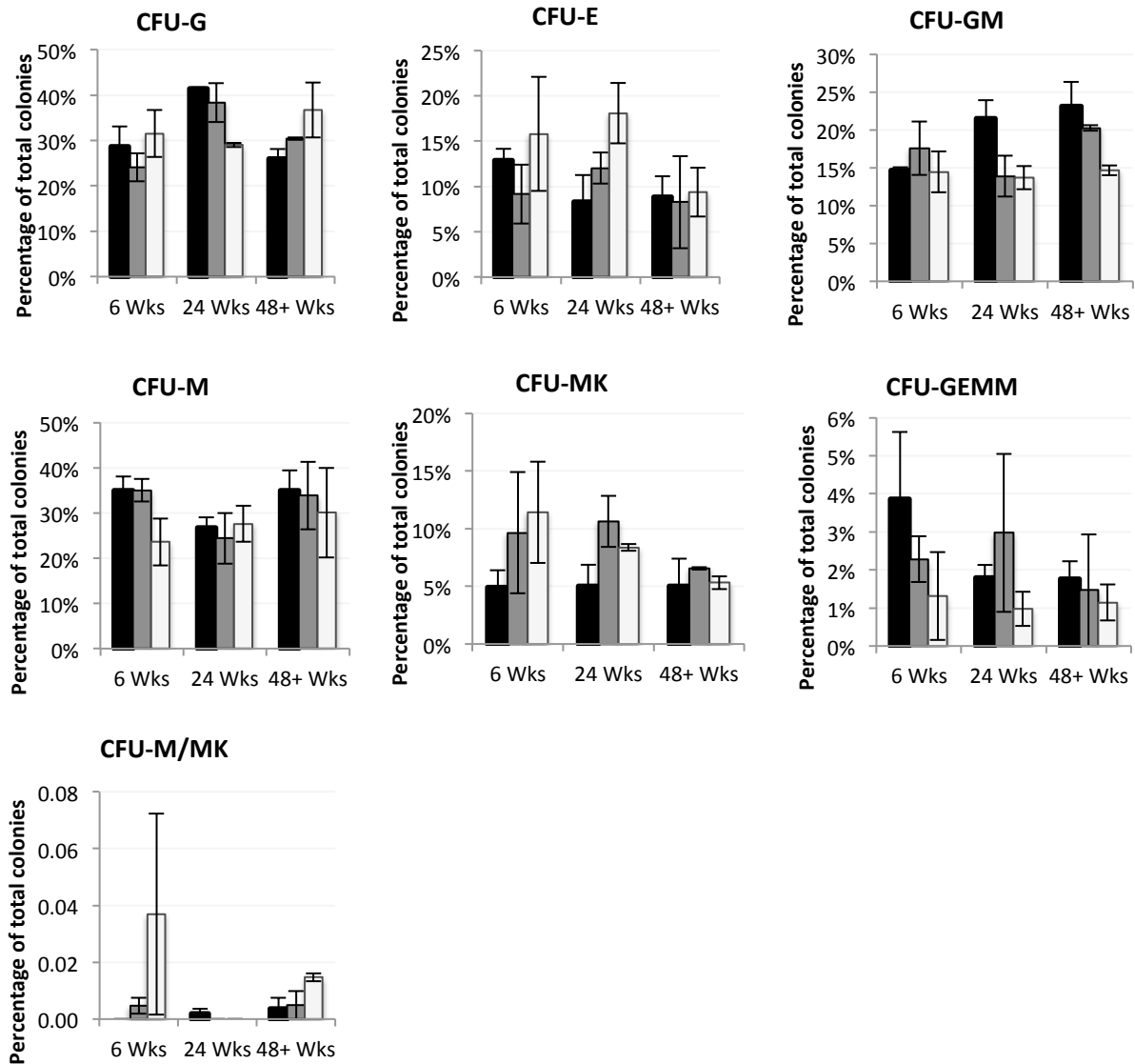Error bar = S.E.M, *=p< 0.05, ** = p<0.01, *** = p<0.001

Four mice each of genotype were analysed at 6 weeks of age, 2 mice of each genotype were analysed at 24 weeks and at 48+ weeks 3 mice of each genotype were analysed.

b. Differentiation potential expressed as a proportion of the total number of colonies formed per plate

Table 4.1 Summary of hematopoietic comparison of Atm-/-, Atm-/-nu-/- and Atm+/+nu-/- mice

	Atm-/-	Atm-/-nu-/-	Atm+/+nu-/-
FACS: Bone Marrow	Normal stem cells ⬇ CD4+ T ⬇ CD8+ T ⬆ Pro B ⬇ Pre B ⬇ Immature B ⬆ granulocytes	Normal stem cells ⬇ CD4+ at 48 weeks ⬇ CD8+ at 6 weeks ⬇ Pro B at 48 weeks ⬇ Pre B at 6 and 48 weeks ⬇ Immature B ⬇ Transitional B at 6 weeks ⬆ Granulocytes at 6 and 48 weeks	Normal stem cells ⬇ CD4+ at 48 weeks ⬇ CD8+ at 6 weeks ⬇ Pro B at 48 weeks ⬇ Pre B at 48 weeks ⬆ granulocytes at 48 weeks
FACS: Spleen	⬇ DP ⬇ CD4+ T ⬇ CD8+ T B cells normal ⬆ Macrophages ⬆ Granulocytes Megakaryocytes normal	⬇ DP at 6 and 48 weeks ⬇ CD4+ T at 6 and 48 weeks ⬇ CD8+ T at 6 and 48 weeks ⬇ Transitional B cell ⬇ IgM+ IgD+ B cells ⬆ Macrophages at 6 weeks ⬆ Granulocytes at 6 and 48 weeks ⬆ mature meg/ platelets at 48 weeks	⬇ DP at 6 and 48 weeks ⬇ CD4+ T at 6 and 48 weeks ⬇ CD8+ T at 6 and 48 weeks B cells normal ⬆ Macrophages at 6 weeks ⬆ Granulocytes at 48 weeks Megakaryocytes normal
Peripheral blood analysis	⬇ Lymphocytes ⬆ Monocytes ⬆ Neutrophils	⬇ Lymphocytes ⬆ Monocytes 6 weeks ⬆ Neutrophils 6 weeks ⬇ Basophils 48 weeks	Normal
CFU: Bone marrow	⬇ Number colonies ⬇ CFU-GM ⬇ CFU-M	Normal	Normal
CFU: Spleen	⬇ Colony number ⬇ CFU-M ⬆ CFU- E ⬆ CFU-GEMM	Normal	Normal

Levels relative to Atm+/+ and Atm+/+nu+/- mice

CHAPTER 5

TUMOUR DEVELOPMENT IN THE

ATM-/-NU-/- MOUSE

5 TUMOUR DEVELOPMENT IN THE ATM-/-NU-/- MOUSE

5.1 Type of tumour development in the Atm-/-nu-/- mouse

5.1.1 *Post mortem* analysis of Atm-/-nu-/- mice.

The longevity of Atm-/-nu-/- mice was examined in a cohort of 71 mice and 17/71 Atm-/-nu-/- mice found to have a tumour at post mortem. These mice died aged between 7 and 69 weeks, with a median age of 25 weeks compared with a median age of 13.5 weeks for the Atm-/- and 13 weeks for the Atm-/-nu+/- mice (Figure 5.1).

Figure 5.2 details the occurrence of tumours in 17 Atm-/-nu-/ mice, with a summary of locations of each tumour given in Table 5.1. 15/17 mice had a tumour in the spleen. Five of these 17 mice had tumour at one site only (4 in the spleen and 1 axillary). The remaining 12 mice had tumours in multiple locations, 6 in the spleen and liver, 2 mice had tumour in the spleen, liver and abdomen, 2 mice had tumour in spleen, liver, abdomen and thorax, 1 mouse had tumour in the abdomen and thorax and 1 mouse had a tumour in the liver and abdomen. Two mice did not have detectable tumour in the spleen.

5.1.2 H&E analysis of Atm-/-nu-/- tumours

H&E stained sections were made from all 17 Atm-/-nu-/- tumours. Ten were analysed by consultant histopathologist, Dr Zbigniew Rudski (ZR), Birmingham Heartlands Hospital, who made a diagnosis of lymphoma in all 10 cases. Histopathologist Dr Maha Abd El Kalek Hafez, School of Cancer Sciences, University of Birmingham, confirmed the diagnosis in these 10 and also diagnosed lymphoma in a further 7 lymphomas. The WHO classification of human haematopoietic malignancies considers the morphology, immunophenotype, genetic features

and clinical features of the disease and the Atm-/-nu-/- lymphomas were assessed according to these criteria.

Firstly, H&E stained sections of all 17 Atm-/-nu-/- tumours were evaluated and given a preliminary classification based solely on morphological appearance. Details of this analysis are given in Table 5.2 and summarised in Table 5.3. 17/17 tumours were Non-Hodgkin's lymphomas (NHL). Of these 17, one tumour (68F2) was a low-grade lymphoma and 16/17 were high grade lymphomas. The low-grade lymphoma was a small cell lymphoma, possibly of either mantle cell or marginal zone type. Of the 16 high-grade lymphomas one (656) was an anaplastic large–cell lymphoma (ALCL), one (519) was NHL (unclassifiable), with features intermediate between diffuse large B cell lymphoma (DLBCL) and Burkitt lymphoma, 11 were DLBCL (NOS) and 3 were follicle centre cell lymphomas, predominantly diffuse, grade 3A. Another noteworthy observation was that, one of the DLBCLs contained tingible body macrophages and had a 'starry sky' appearance, which suggested an aggressive nature and is also characteristic of Burkitt lymphoma.

In summary, analysis of H&E sections indicated that 16/17 Atm-/-nu-/- lymphoma were high grade NHL with most (11/16), being diffuse large cell lymphoma that have morphological features consistent with DLBCL and therefore were assigned this classification pending immunophenotypic analysis. Also, one of these high grade NHL (case 656), an ALCL, could be a T cell tumour because >70% of ALCL tumours are of this origin.

5.1.3   Discussion

Secondary lymphoid tissue consists of follicles, the most obvious of which is the germinal centre (GC) follicle. Within these follicles B cells respond to antigen stimulation and undergo maturation, which involves a process of immune receptor gene editing called somatic

hypermutation, to enhance antigen specificity. The outer portion of the follicle, the mantle, contains re-circulating B cells. The dark inner section is composed of densely packed large B cells (centroblasts), and a lighter inner section is composed of smaller B cells (centrocytes derived from centroblasts) interspersed by dendritic cells (Maclennan, 1994) (Summarised in Figure 1.2).

Tumour cell morphology is considered when classifying lymphoid tumours. DLBCL is composed of large centroblasts cells only. Follicular lymphoma (FL) contains mostly smaller centrocytes and a variable number of large centroblasts. The proportion of centroblasts in the lymphoma determines the grade of FL. Grade 1: 0-5 centroblasts per high power field (hpf), grade 2: 5-15 centroblasts per hpf, grade 3A: some centrocytes still present and 3B: sheets of centroblasts with no centrocytes present per hpf. (High power field of $0.159mm^2$ 40x objective lens, 18mm field of view ocular) (Maclennan, 1994, Swerdlow, 2008, Kogan et al., 2002).

Morphological analysis suggested that 1 Atm-/-nu-/- tumour could be of T cell origin and the remaining 16/17 were all of B peripheral cell origin, albeit not all the same classification of B cell lymphoma. Typically, FL develops from a germinal centre cell, and DLBCL can develop from a GC or post-GC B cell. Therefore, the Atm-/-nu-/- lymphomas described here are likely to have a GC or post-GC origin. In contrast, the small cell lymphoma is likely to be derived from marginal zone or mantle zone B cells, outside the germinal centre.

For both Burkitt and DLBCL the normal cellular origin is GC or post-GC and consequently this may be the cellular origin of tumour 519, (B Cell lymphoma, unclassifiable, with features intermediate between DLBCL and Burkitt lymphoma). In humans it has been seen that FL

can progress to this type of B cell lymphoma, and therefore tumour 519 could have a common origin as FL, and have therefore have developed from a GC B cell.

5.2 Phenotyping of the Atm-/-nu-/- tumours as B cell tumours

5.2.1 Immunohistochemical staining of Atm-/-nu-/- tumours

Immunohistochemical (IHC) staining of the Atm-/-nu-/- tumours was undertaken to further define the cell type of these tumours. Tumour sections were stained with antibodies against B cell marker B220, T cell marker CD3 and monocyte marker CD11b (Figure 5.3).

Control tissues from Atm+/+nu+/- and Atm+/+nu-/- mice were stained alongside the 17 Atm-/-nu-/- tumours. Because, B220 was a rat antibody, control tissues were stained with a rat isotype control and no staining was detected; similarly as anti-CD3 was a rabbit antibody, tissues were stained with no primary plus anti-rabbit secondary and again no staining was detected indicating that both secondary antibodies (anti-Rat and anti-Rabbit) did not cross react with mouse tissue. As an additional negative control, Atm-/- T cell lymphoma stained with B220 antibody also showed no positive staining, indicating that the anti-B220 did not bind to mouse thymocytes.

Figure 5.3 shows the results of IHC staining and a summary of staining is given in Table 5.4. With regard to B220 staining of Atm-/-nu-/- tumours, 10/17 were B220+ and 6/17 were B220-. B220 staining in tumour 36F1 was positive, however it was weaker than normal B cells within the same histological section.

11/11 Atm-/-nu-/- tumours tested were CD11b- (Figure 5.3).

Further immunophenotypic analysis undertaken for one Atm-/-nu-/- tumour (519) is shown in Figure 5.4. Expression of B cell associated transcription factor PAX5 is often used to confirm

B cell origin of lymphoid neoplasms. No PAX5 expression could be detected in tumour 519, despite positive staining for B220.

Large B cell lymphomas can be classified further depending on the expression of CD10, BCL6 and IRF4/MUM1. Foxp1 can also be a prognostic indicator in patients. It is expressed in activated B cells, prior to the germinal centre (GC) reaction and is commonly overexpressed in DLBCL. Cells in tumour 519 stained positively for Foxp1. These Atm-/-nu-/- tumour cells also stained negatively for CD10 and IFR4/MUM1. In DLBCL negative staining of CD10 and IRF4/MUM1 along with BCL6 positivity normally indicates a germinal centre cell origin. No BCL6 staining was undertaken with tumour 519 and, therefore, without this confirmation a germinal centre cell origin for tumour 519 cannot be confirmed.

14 /17 tumours with suitable material were also analysed for surface marker expression by flow cytometry (Figure 5.5 with results summarised in Table 5.4). Five of the six tumours that had no detectable B220 expression by IHC were tested using FACS; 1/5 (5F1) also had no detectable B220 expression by FACS; for another 2/5 tumours (55F1 and 319M1), the bulk of the total cell population were B220- and only a subpopulation were positive and the remaining 2/5 (107F2 and 656) were B220+ despite no B220 expression being detected by IHC. B220 positivity by FACS and not detected IHC could be the result of normal B cell in the cell population or could be the result of technical limitations.

All 10 tumours tested expressed B cell marker CD19, 4 of these 10 were B220 negative by IHC including 1 that had no B220 expression by FACS either. For one tumour, 37F3, staining of tumour cells could not be distinguished from normal spleen.

One Atm-/-nu-/- tumour (656) was CD3+ and the remaining were CD3-. Expression of another T cell surface marker, CD5 was measured using FACS for 10/17 tumours, of which 1/10 was CD5+, 1/10 was CD5[normal] and 8/10 were CD5- (Figure 5.5 and Table 5.4).

5.2.2 Identifying the developmental origin of Atm-/-nu-/- B cell lymphoma - FACS profiling of tumours

The 14 /17 tumours with suitable material were analysed for surface marker expression by flow cytometry, to further elucidate the developmental origin of the Atm-/-nu-/- tumours (Figure 5.5 and summarised in Table 5.4). In addition to CD5 and CD19 discussed above, CD43, IgM, IgD, CD4 and CD8 surface marker expression was also measured. 11/14 Atm-/-nu-/- tumours expressed CD43. In seven of these 11 Atm-/-nu-/- tumours CD43 was only expressed by a small proportion of the total cell population, but for the other 4 Atm-/-nu-/- tumours (656, 593, 69F5 and 107F2), CD43 expression was detected on the majority of the total cell population. Interestingly, ALCL lymphomas express CD43, which further supported the diagnosis of tumour 656 as an ALCL.

11/14 Atm-/-nu-/- tumours expressed IgM; including 2/14 that expressed both IgM and IgD. Surface immunoglobulin expression is expected on DLBCL and FL. Atm-/-nu-/- lymphoma surface IgM or IgD expression could not be distinguished from normal cells in 1/14 (37F3) and the remaining two (5F1 and 107F2) tumours had no detectable expression. These two tumours may not express surface immunoglobulin or have undergone class switch and therefore expression would not be detected with the antibodies used here. Two tumours of 13 tested had a population of CD8+ cells, likely to be associated with tumour infiltrating CD8 T cells. Overall, most Atm-/-nu-/ lymphomas are IgM expressing B cell lymphoma.

5.2.3 Discussion

In summary, 16/17 tumours were either B220 or CD19 expressing and therefore of B cell origin. 11/17 these were also diffuse large cell lymphomas and because these are now identified as B cells they can be confirmed as diffuse large B cell lymphoma (DLBCL) (Table 5.4 Summary of morphological and immunophenotypic analysis of Atm+/+ nu-/- lymphoma

Table 5.5).

Interpretation of this staining to determine the cellular origin of Atm-/-nu-/- lymphoma 519 was difficult. FOXP1 expression suggested a non-GC origin whereas CD10 and IRF4/MUM1 negativity suggested a GC origin. The WHO classification system does not consider FOXP1 to be a marker of a non-GC B cell and rather uses it as a prognostic factor in patients. Taking these considerations into account, the additional staining undertaken of Atm-/-nu-/- tumour 519 suggested that it is likely to have an activated B cell origin and may be of GC origin.

In addition one Atm-/-nu-/- tumour, 55F1, expressed CD5, a marker of normal T cells but also can be aberrantly expressed on DLBCL, where it is associated with an aggressive phenotype. As 55F1 expressed B cell associated antigens CD19, IgM and IgD, the classification of DLBCL (NOS) was still applicable to this tumour.

The only non B cell tumour, therefore, was an anaplastic large cell lymphoma (656), that had no B220 expression by IHC and had only a sub population of B220+ staining cells by FACS; it also stained positively for T cell marker, CD3. Positive expression for a T cell marker in this tumour further suggested that this tumour was a T cell ALCL.

5.3 IgH V(D)J rearrangements in Atm-/-nu-/- lymphomas - their clonal nature

5.3.1 Results

To detect V(D)J rearrangement and ascertain clonal status in the Atm-/-nu-/- lymphomas, PCR amplification of IgH V(D)J was undertaken. Three forward primers corresponding to the three most commonly used V gene families were used along with a single reverse primer downstream of the most proximal J gene, JH-4. Normal Atm-/-nu-/-, Atm+/+nu-/- and Atm+/+nu+/- spleen was used as a positive control. Figure 5.6 shows the PCR reaction products of a representative selection of control and tumour DNA samples. Amplification of V(D)J from normal spleen produced four major bands, relating to the mixed population of B cells with V(D)J rearrangements within the spleen. DNA extracted from mouse ear clipping was used as a germline control. No V(D)J rearrangements could be amplified from this DNA (Figure 5.6, lane 11).

16/17 Atm-/-nu-/- tumours, for which DNA was available, were analysed for IgH V(D)J rearrangements. Table 5.6 shows that 11/16 tumours had detectable monoclonal V(D)J rearrangements determined by the amplification and sequencing of a single product with primers that span the V, D, and J genes. Conversely, PCR amplification of this region in 5/16 Atm-/-nu-/- lymphomas produced products of multiple sizes, similar to that of normal spleen, and were provisionally termed 'polyclonal' tumours. Tumours with a monoclonal rearrangement were sequenced and the V, D and J gene to which there was the highest sequence similarity was identified. The IgBlast alignments are shown in Figure 5.7. Sequence analysis of one of the 11 Atm-/-nu-/- tumours (40F1) with a monoclonal rearrangement showed that the rearrangement contained a V and J gene, but between these two gene

sequences there were 6 nucleotides which could not be assigned to a D gene family. Also, 1/16 Atm-/-nu-/- tumour (319M1) had two different detectable V(D)J rearrangements within the same tumour.

In 4/16 tumours (36F2, 69F5, 319M1 and 61M3) with a monoclonal rearrangement, and where there was DNA available from multiple tumour sites, the V(D)J rearrangement was the same at all tumour sites.

The V, D, and J families used in V(D)J recombination in the Atm-/-nu-/- tumours were varied. 4 different V gene families were used in the rearrangements found in the 16 tumours tested; V1, V2, V3, and V5, 3 different D gene families were used; D1, D2, and D3. Equally varied, J1, J2, J3, and J4 were used in the Atm-/-nu-/- tumour rearrangements. Therefore no single gene rearrangement is associated with Atm-/-nu-/- tumour development.

5.3.2 Discussion

In summary, 11/16 Atm-/-nu-/-tumours had a single detectable rearrangement by sequencing suggesting that each of these lymphomas was clonal. During B cell development, pre-B cells undergo V(D)J gene rearrangement in the bone marrow, therefore the tumours with a detectable V(D)J rearrangement are likely to originate from a cell which has reached this stage of development. The Atm-/-nu-/- mice which had tumours at more than one site and that had the same V(D)J rearrangement are likely to have developed from a primary tumour that has spread to multiple sites as a result of metastasis.

For the 5/11 tumours from this analysis, for which a monoclonal rearrangement could not be detected, and were therefore termed 'polyclonal' there could be one of several explanations; (1) they may not have undergone V(D)J rearrangement and their origin was from a B cell that had not reached this stage of development, (2) the tumour cell population was contaminated

with normal B cells and therefore a monoclonal rearrangement could not be distinguished in this mixed population, (3) the B cell had undergone V(D)J recombination but the rearrangement was not amplifiable with the primer combinations used here. These five tumours are DLBCL, which are peripheral mature B cell origin, and therefore are expected to have undergone V(D)J rearrangement. Therefore, it is likely that these tumours are monoclonal, but with clonality undetected by this method.

5.4 Validating the malignant character of Atm-/-nu-/- B cell lymphoma by subcutaneous transplant into immunocompromised mice

5.4.1 Results

Cells from Atm-/-nu-/- DLBCL case 593, were injected subcutaneously into the right flank of 3 immunocompromised NOG mice. Normal Atm+/+nu-/- splenic cells were also injected subcutaneously in the right flank of a NOG mouse. Subcutaneous tumour growth was detected 48 days post injection, at the site of injection, in all 3 mice injected with Atm-/-nu-/- DLBCL cells (Figure 5.8a). Ten days post detection, the average tumour volume had tripled, almost reaching maximum permissible by the licence, so the experiment was ended (Figure 5.8c). No tumour growth was detected in the mouse injected with normal spleen cells. At post mortem, 2/3 mice injected with Atm-/-nu-/- DLBCL, also had tumour growth in the liver and spleen, visible as white patches. A photograph of the spleen from one mouse is shown in Figure 5.8b. The pathologist's analysis of H&E stained tissue sections from each of the three recipient mice showed the subcutaneous tumour to be a large cell lymphoma (the same as the injected tumour) and confirmed the presence of lymphoma cells in the spleen and liver in two of these animals (Figure 5.8d). In addition, the cells from the subcutaneous tumour could be seen to be infiltrating nearby skeletal muscle. IHC staining of these sections showed that the

subcutaneous tumour had low expression of B220 and no expression of CD3. The clusters of infiltrating lymphoid cells in the liver had expression of both B220 and CD3 (Figure 5.8e). PCR amplification and sequencing of IgH V(D)J using DNA extracted from the primary tumour, Atm-/-nu-/- DLBCL 593, and from the tumour growth in the donor mouse showed these two samples had the same rearrangement (Figure 5.8f).

5.4.2 Discussion

In summary, the ability to propagate the tumour in an immune compromised host confirmed the malignant character of Atm-/-nu-/- tumour 593. Metastasis to the host organs suggested that the lymphoma was aggressive. IgH V(D)J rearrangement in the primary tumour and the subcutaneous secondary tumour was the same and therefore the subcutaneous tumour was derived from the Atm-/-nu-/- tumour cells injected into the mouse.

5.5 Investigating the mechanism of tumour development using multicolour-fluorescence in situ hybridisation (M-FISH)

5.5.1 Results

Development of B cell lymphomas is frequently associated with chromosomal translocation. In order to establish if chromosomal abnormalities were involved in Atm-/-nu-/- B cell lymphoma development, tumours were karyotyped using multicolour florescence in situ hybridisation (M-FISH).

A normal Atm+/+ spleen was analysed and no clonal chromosomal abnormalities were detected (Figure 5.9).

Before examining the B cell lymphomas in the Atm-/-nu-/- mice, thymomas from Atm-/- single knockout animals were examined, as these have been shown, previously to have clonal

chromosomal rearrangements. Three Atm-/- T cell lymphomas (F1, F2 and 58M4) were karyotyped. Each tumour had multiple chromosomal translocations; the most frequent rearrangements involved chromosomes 12, 14 and 15 (Figure 5.10 and summarised in Table 5.7). Other chromosomes that were involved in clonal rearrangements included 1, 4, X, and Y. Two of the three Atm-/- T cell lymphomas (F1 and 58M4) had a clonal translocation that was present in all cells; the remaining tumour (F2) had two clones with different chromosome abnormalities exclusive to each clone (Table 5.7).

Like Atm-/- T cell lymphomas, M-FISH analysis of Atm-/-nu-/- B cell lymphomas revealed several types of chromosome abnormalities, including chromosomal duplications, balanced and unbalanced translocations, whole chromosome loss and also whole chromosome gain. 2/6 tumours (cases 5F3 and 593) (Table 5.8) each had an abnormality that was present in most cells and in both tumours the abnormality involved a derivative chromosome 17, although involving a different second chromosome (Figure 5.11 and Figure 5.12). Both tumours had additional aberrations that were detected at a lower frequency than the chromosome 17 translocations and in varied combinations. The predominance of the chromosome 17 translocations within the tumour cell population, suggested that the chromosome 17 translocations may have arisen earlier on in tumour development and may have conferred a selective advantage to the tumour, over other abnormalities, which appeared at a lower frequency i.e. these additional changes represent a subclone as a consequence of selection. It is also worth noting that in tumour 5F3, apparently two different chromosome 18 translocations, der(18)t(15;12;18) and der(18)t(15;18) were detected in 10/20 and 8/20 cells respectively. The part of chromosome 12 involved in the first translocation is relatively small, and therefore due to the limitations of M–FISH analysis, it is possible, even likely that all 18/20 cell could have either der(18)t(15;12;18) or der(18)t(12;18). Therefore, tumour 5F3

could also have both a chromosome 17 and also a chromosome 18 abnormality present at a high frequency.

On the other hand, 3/6 tumours (37F3, 50F2 and 703) had multiple clonal aberrations, with none being present in the majority of cells (Figure 5.13, Figure 5.14 and Figure 5.15). These tumours may be in an earlier state of maturity, when a single clone, representing cells with a clear growth advantage, had not arisen. In each of these tumours, the most common aberration involved an unbalanced translocation of chromosome 18. However, the translocation involved a different partner chromosome in each tumour (3, 7, 13 and X). Each tumour also had a mixture of additional abnormalities and no two cells in these tumours contained the same combination of abnormalities. Also, there was no evidence to suggest that the abnormalities were acquired as a result of successive clonal selection. Interestingly, one Atm-/-nu-/- lymphoma (case 37F3) had chromosome 18 translocations in 35/40 cells analysed, but in many of these cells the recipient chromosomes were different. The most common translocation, der(18)t(3;18) was present in 10/40 cells and the second most common, der(18)t(12;18) was found in 6/40 cells, the remaining clonal chromosome 18 translocations were detected in three or fewer cells.

Finally, 1/6 tumour (case 68F2) had der(12)t(12;15) present in 8/12 cells, the remaining 4/12 cells were normal. In addition to this der(12)t(12;15), the abnormal cells had either an abnormal chromosome 12 or der(19)t(12;19) (Figure 5.16) consistent with the notion that, since all the tumour cells had a der(12)t(12;15), this translocation could be associated with tumour initiation.

5.5.2 Discussion

Chromosome 17 translocations were present at a high frequency in 2/6 tumours and Chromosome 18 abnormalities are present in 4/6 Atm-/-nu-/- tumours. One explanation for the recurring involvement of chromosome 18 suggests that the abnormalities confer an advantage to the tumour, possibly by an up regulation of an oncogene gene or a down regulation of a tumour suppressor. However the presence of a multiple different chromosome 18 aberrations in one Atm-/-nu-/- tumour suggests that the chromosome 18 translocations are due to genetic instability, and this area of the genome may be easily prone to translocation. Translocations of one chromosome with multiple recipients in a single tumour are termed jumping translocations. These are rare genetic events where part of a donor chromosome is fused to two or more different recipient chromosomes within the cell line. Jumping translocations are thought to not be causative in the development of the tumour, but a by-product of the genetic instability. In human patients they are thought to indicate a poor prognosis. Evidence suggests that they may be caused by the shortening of telomeres in the tumour (Mills et al., 2003, Manola et al., 2008).

5.6 Confirming the absence of IgH and Myc involvement in Atm-/-nu-/- B cell lymphoma using targeted FISH

5.6.1 Results

Using targeted FISH analysis, normal Atm+/+ spleen cells were shown to have 2 copies of Myc. 4/6 Atm-/-nu-/- tumours tested (703, 593, 50F2, 37F3) had a normal copy number of Myc, and 2/6 had 3 copies of Myc (5F3 & 68F2). In the tumour cells with 3 copies of Myc, the Myc directed probe was found on 3 different chromosomes (Figure 5.17to Figure 5.22).

Targeted FISH of the IgH locus in normal Atm+/+ spleen cells showed two intact IgH genes, represented by a 'fusion' or close localisation of the red IgH constant alpha and green IgH v1 probe, in all cells. Splitting of the red and green probes would indicate an IgH translocation. This was demonstrated using Atm Δ/Δ B cells, which undergo IgH translocation at a rate of 1 in 4 cells (personal communication, Monica Gostissa). I found an IgH translocation in 2/11 Atm Δ/Δ B cells (Figure 5.23).

5/6 of the Atm-/-nu-/-B cell lymphomas (703, 5F3, 593, 50F2, 37F3) did not have a translocation involving breakage within IgH. However, 2/5 (5F3, 593) of these had loss of IgH v1 or loss of both IgH constant alpha (IgHa) and IgH v1 in one allele. 1/6 tumour (68F2) had an IgH translocation shown by splitting of the IgH constant alpha and IgH v1 probes along with amplification of IgH constant alpha (Figure 5.24 to Figure 5.29) (Summarised in Table 5.8).

5.6.2   Discussion

Previous studies have found that Atm-/- T cell lymphomas are associated with abnormalities in chromosome 12, 14, and 15. In mice chromosome 12 contains IgH, chromosome 14, TCR alpha and delta, and chromosome 15 carries Myc. T cell lymphoma has been associated with aberrant immune gene rearrangement and Myc amplification (Liyanage et al., 2000, Barlow et al., 1996). The analysis of Atm-/- T cell lymphoma undertaken here replicated previous findings that showed that Atm-/- T cell lymphoma development was associated with abnormalities involving the chromosome that contain TCR and Myc genes. Specificity of T cells to antigen is established by rearrangement of the T cell receptor and aberrant rearrangement can lead to translocations.

In B cells antigen specificity is established by the rearrangement of the immunoglobulin genes IgH and IgL. IgH has also been shown to be involved in translocations in B cell lymphoma (Nussenzweig and Nussenzweig, 2010).

In addition, IgH, Myc translocations have been found in B cell lymphoma from DNA repair protein XRCC4 deficient mice (Wang et al., 2008b). However, in Atm-/-nu-/- lymphoma chromosome 12 translocations were only detected here in 2/6 cases using M-FISH. To determine if an IgH translocation or Myc amplification had taken place targeted FISH was performed, which has a greater sensitivity than M-FISH. Only 1/6 B cell lymphoma was found to contain an IgH translocation using FISH probes that span the IgH locus. This suggested that IgH translocations were not essential for Atm-/-nu-/- tumour development and that there may be more than one mechanism of development associated with Atm-/-nu-/- B cell lymphoma. In two tumours either part or all of IgH could not be detected, which may indicate instability in this region.

The targeted FISH results can be related to the M-FISH analysis. The 2/6 cells with 3 copies of Myc had additional chromosome 15 material; the consequence of an unbalanced translocation involving chromosome 15. As only 2/6 tumours analysed had an increase Myc it is unlikely that Myc amplification is essential for Atm-/-nu-/- B cell lymphoma development.

In Atm-/-nu-/- B cell lymphoma case 5F3, M-FISH detected an aberration involving chromosome 18, 12 and 15. However, the IgH gene is not likely to be translocated, as IgH v was completely lost from the cell. The chromosome 12 translocation in this tumour could have been caused by fusion of the vulnerable distal end of chromosome 12, generated by the loss of the region of chromosome 12 containing IgH v, to another double strand break in chromosome 18 or 15.

Loss of both IgH a and IgH v in Atm-/-nu-/- B cell lymphoma 593 suggested that this tumour lost a single copy of IgH. M-FISH analysis of this tumour suggested that this loss of IgH could be caused by an unbalanced translocation involving chromosome 12. M-FISH analysis of chromosome 12 detected a translocation involving a small part of chromosome 12 in 2/20 cells. This low frequency translocation suggested that it could be possible that this loss of 1 copy of IgH is associated with this chromosome 12 translocation.

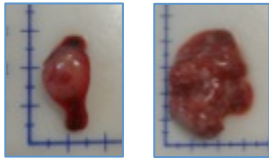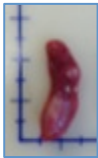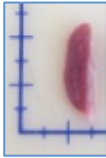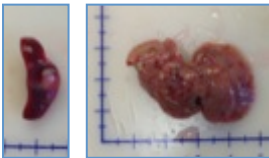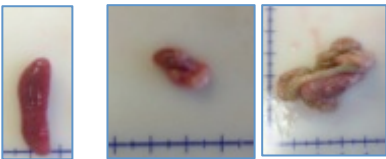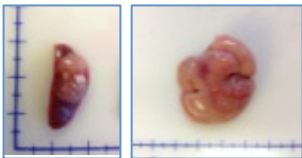In summary, IgH translocation and Myc amplification was only detected in 1 Atm-/-nu-/- B cell lymphoma (68F2) so development of the other 5/6 Atm-/-nu-/- lymphoma is likely to be associated with another mechanism, possibly involving chromosome 17 and or 18.

Figure 5.1 Tumour free survival in Atm-/-nu-/- mice
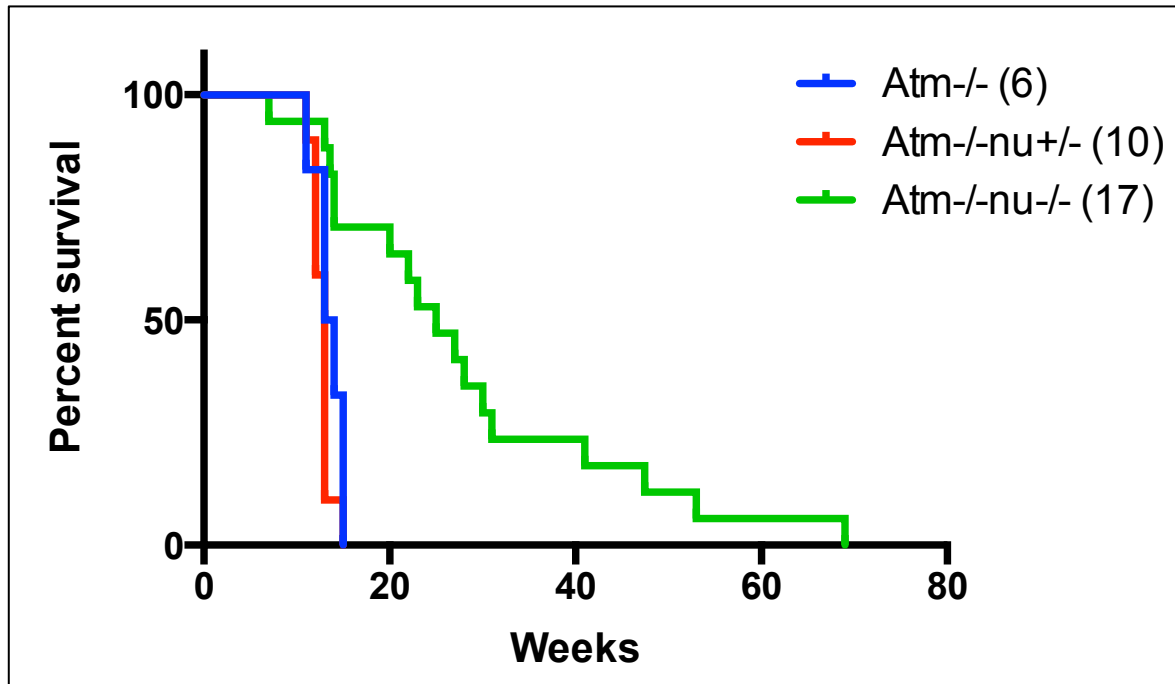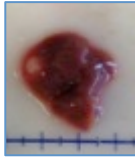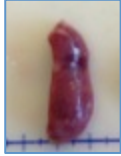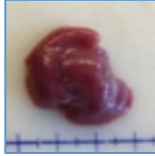
Survival of Atm-/-nu-/-, Atm-/-nu+/- and Atm-/- mice that developed tumours only; analysis excludes mice that died of non-tumour related cause. Age of tumour free survival is longer in Atm-/-nu-/- mice compared to Atm-/- and Atm-/-nu+/- mice (Median survival Atm-/- = 13.5 weeks, Atm-/-nu+/- = 13 weeks and Atm-/-nu-/- =25 weeks).

Figure 5.2 Post mortem analysis of 17 Atm-/-nu-/- tumours

Mouse	Age (weeks)	Tumour sites	Tumour
519	13	Spleen, liver	
703	7	Spleen	
656	27	Spleen, liver, abdomen, thorax	
5f3	25	Spleen, liver	
593	53	Spleen, liver, abdomen, thorax	
5F1	31	Spleen, abdomen, thorax	
37M 3	22	Spleen, liver	
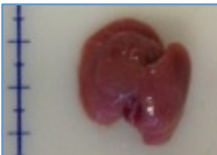
Atm-/-nu-/- mice were culled when moribund. At post mortem, all organs were examined for signs of abnormality. The table details the age of death, location of tumours found and photograph of tumours in the 17 Atm-/-nu-/- mice.

Figure 5.2 continued post mortem analysis of 17 Atm-/-nu-/- tumours

Mouse	Age (weeks)	Tumour sites	Tumour
50F2	14	Spleen, liver, abdomen x2 (near gut & spine)	
40F 1	20	Liver, abdomen,	
53M 7	14	Axillary tumour	
36F1	41	Spleen, liver	
69F5	23	Spleen, liver	

Atm-/-nu-/- mice were culled when moribund. At post mortem, all organs were examined for signs of abnormality. The table details the age of death, location of tumours found and photograph of tumours in the 17 Atm-/-nu-/- mice.

Figure 5.2 continued Post mortem analysis of 17 Atm-/-nu-/- tumours

Mouse	Age (weeks)	Tumour sites	Tumour
68F2	30	Spleen	
319M1	69	Spleen, liver, abdomen	
61M3	38	Spleen, liver	
55F1	47	Spleen	
107F2	14	Spleen	

Atm-/-nu-/- mice were culled when moribund. At post mortem, all organs were examined for signs of abnormality. The table details the age of death, location of tumours found and photograph of tumours in the 17 Atm-/-nu-/- mice.

Table 5.1 Summary of 17 Atm-/-nu-/- tumour locations

	Location				
Mouse	Spleen	Liver	Abdomen	Thorax	Axillary
703	X				
68F2	X				
55F1	X				
107F2	X				
519	X	X			
5F3	X	X			
37F3	X	X			
36F1	X	X			
69F5	X	X			
61M3	X	X			
319M1	X	X	X		
50F2	X	X	X		
656	X	X	X	X	
593	X	X	X	X	
5F1	X		X	X	
40F 1		X	X		
53M 7					X

Tumours were most commonly found in the spleen.

Table 5.2 Detailed cellular morphological examination of 17 Atm-/-nu-/- tumours

Mouse	ZR comments:	MH comments: Diffuse/ Nodular	Size	Cleaved?	Anaplastic?	Grade	Classification
519	Spleen: Lymphoma (Diffuse)	Diffuse	Medium	No	No	High grade (Tingible bodies, Starry sky)	B cell lymphoma, unclassifiable, with features intermediate between DLBCL and Burkitt lymphoma
703	Spleen: lymphoma (Diffuse), increased erythropoiesis.	Diffuse	Large	No	No	High grade	DLBCL, NOS
656	Spleen: Lymphoma (Nodular), residual red pulp	Red pulp still present – looks nodular	Large	No	Anaplastic	High grade	ALCL
5F3	Lymphoma, Infarct, unstructured white pulp, lots of erythrocytes BM: normal	Diffuse	Large	No	No	High grade	DLBCL, NOS
593	Spleen: Lymphoma (Diffuse)	Diffuse	Large	No	No	High grade	DLBCL, NOS
5F1	Spleen: Lymphoma (Diffuse)	Predominantly diffuse	Large	Yes	No	High grade	Follicle centre cell lymphoma, predominantly diffuse, Grade 3A

Table 5.2 continued Detailed cellular morphological examination of 17 Atm-/-nu-/- tumours

Mouse	ZR comments:	MH comments: Diffuse/ Nodular	Size	Cleaved?	Anaplastic?	Grade	Classification
37F3	Spleen: Lymphoma (Diffuse), few remaining nodules of red pulp	Diffuse	Large	No	No	High grade	DLBCL, NOS
50F2	Spleen: Lymphoma	Diffuse-predominantly	Large	Yes	No	High grade	Follicle centre cell lymphoma, predominantly diffuse, Grade 3A
40F 1	Spleen: Normal, Liver and abdominal tumour: Lymphoma, BM: Possible neoplasm	Diffuse tumour & reactive follicle	Large	No	No	High grade	DLBCL, NOS
53M7	Axillary tumour: Lymphoma, no histiocytes, Liver: tumour present, not massive involvement	Diffuse tumour infiltrating red pulp	Large	No	No	High grade	DLBCL, NOS
36F1	Spleen: Large lymphoma, morphologically like Burkitt's Liver: Lymphoma infiltration	Diffuse	Large	No	No	High grade (Tingible body macrophages)	DLBCL, NOS

166

Table 5.2 continued Detailed cellular morphological examination of 17 Atm-/-nu-/- tumours

Mouse	ZR comments:	MH comments: Diffuse/Nodular	Size	Cleaved?	Anaplastic?	Grade	Classification
69F5	Spleen: Lymphoma, very little normal spleen remaining. Liver: Infiltrate of lymphoma	Diffuse	Large	No	No	High grade	DLBCL, NOS
68F2	ND		Medium - Small	Yes	-	Low grade	Small cell lymphoma, possibilities include mantle cell or marginal zone lymphoma
319M1	ND	Diffuse	Large	Yes	No	High grade	Follicle centre cell lymphoma, predominantly diffuse, Grade 3A
61M3	ND	Diffuse	Large	No	No	High grade	DLBCL, NOS
55F1	ND	Diffuse	Large	No	No	High grade	DLBCL, NOS
107F2	ND	Diffuse	Large	No	No	High grade	DLBCL, NOS

H&E stained sections of tumour tissue were analysed by consultant histopathologists Zbigniew Rudski (ZR), Birmingham Heartlands Hospital and Maha Abd El Kalek Hafez (MH), University of Birmingham. Preliminary classification was assigned based on morphological description according to WHO 2008 classification of lymphomas, (Swerdlow, 2008). Immunophenotyping is required to confirm diagnosis. Possible classifications for small cell lymphomas are Mantle cell and Marginal zone lymphoma.
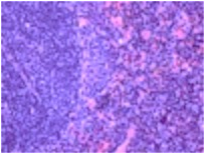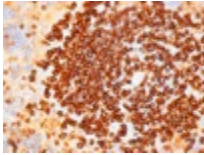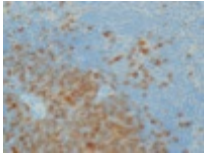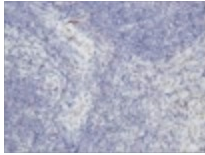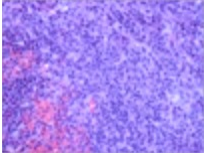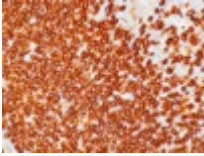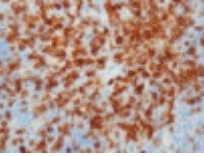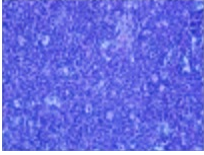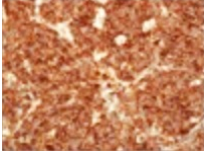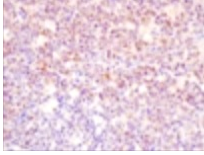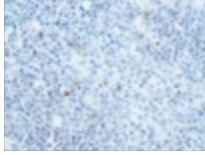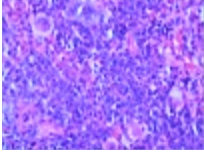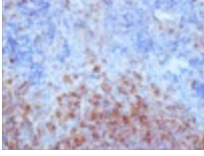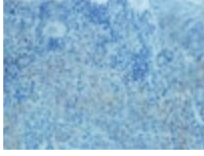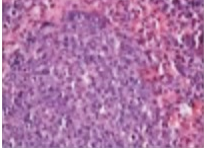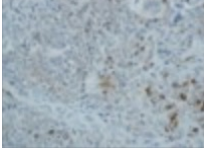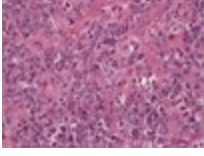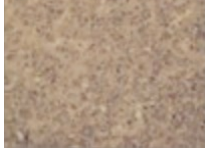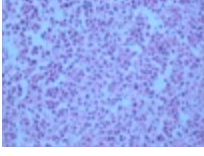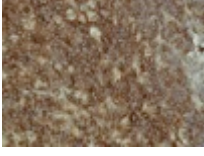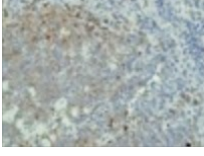
Abbreviations: DLBCL=Diffuse large B cell lymphoma, NOS=not otherwise specified, ALCL= anaplastic large cell lymphoma, ND = not done. [1]Further Immunophenotyping required to confirm this, BM=Bone marrow.

Table 5.3 Summary of Atm-/-nu-/- tumour classification

Mouse	Classification
High Grade:	
703	DLBCL, NOS
5F3	DLBCL, NOS
593	DLBCL, NOS
37M 3	DLBCL, NOS
40F 1	DLBCL, NOS
53M 7	DLBCL, NOS
36F1	DLBCL, NOS
69F5	DLBCL, NOS
61M3	DLBCL, NOS
55F1	DLBCL, NOS
107F2	DLBCL, NOS
5F1	Follicle centre cell lymphoma, predominantly diffuse, Grade 3A
50F2	Follicle centre cell lymphoma, predominantly diffuse, Grade 3A
319M1	Follicle centre cell lymphoma, predominantly diffuse, Grade 3A
519	B cell lymphoma, unclassifiable, with features intermediate between DLBCL and Burkitt lymphoma
656	ALCL
Low Grade:	
68F2	Small cell lymphoma

Summary of Table 5.2. Atm-/-nu-/- tumours were assigned a preliminary lymphoma classification based on the criteria assessed by the histopathologist during morphological examination of H&E stained sections.
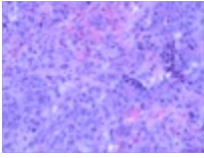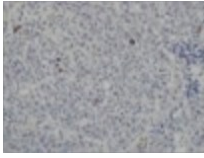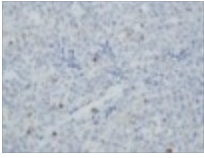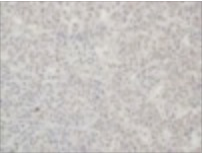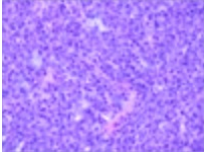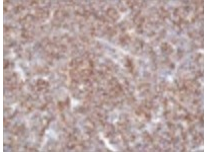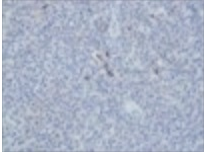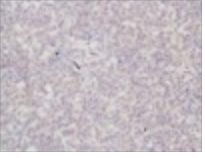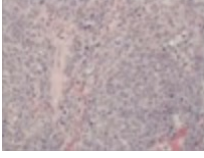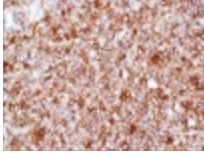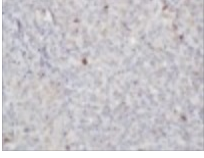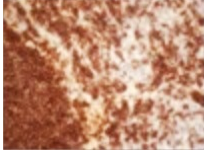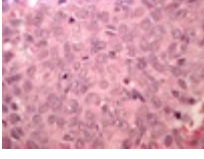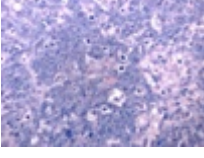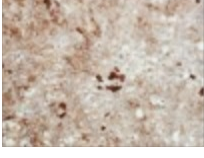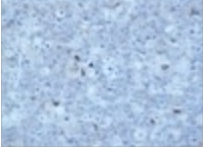
Figure 5.3 Histological analysis of Atm-/-nu-/- tumours

Mouse	H&E	B220	CD3	CD11b
Atm+/+ nu+/-				
Atm+/+ nu-/-				ND
519				
703				
656				
5f3 (Liver)				
593				

Sections of 17 Atm-/-nu-/-lymphoma, along with normal Atm+/+nu-/- and Atm+/+nu+/- spleen, were H&E stained and immunohistochemically stained for B220, CD3 and CD11b. The antigen stained brown and images of stained sections were taken at x40 magnification

ND = not done
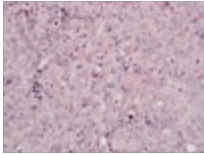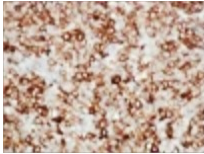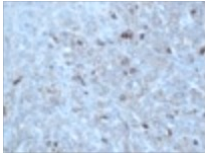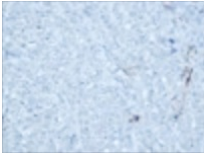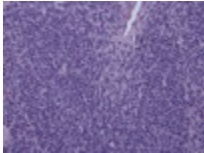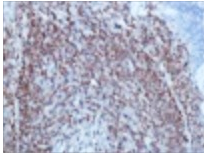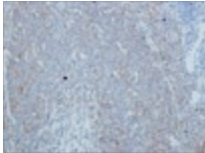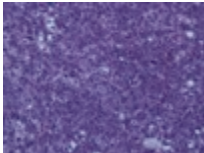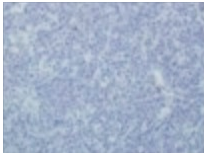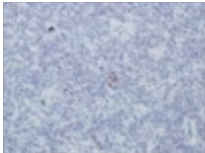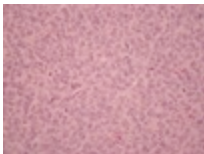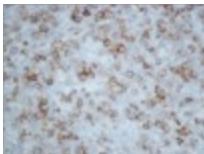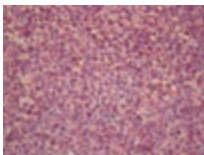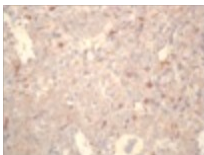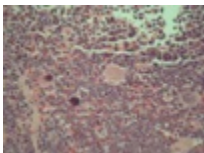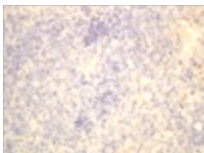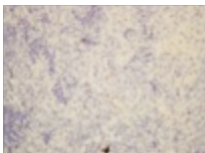
Figure 5.3 continued Histological analysis of Atm-/-nu-/- tumours

Mouse	H&E	B220	CD3	CD11b
5F1				
37M 3				
50F2				
40F 1			ND	
53M7				
36F1				

Sections of 17 Atm-/-nu-/-lymphoma, along with normal Atm+/+nu-/- and Atm+/+nu+/- spleen, were H&E stained and immunohistochemically stained for B220, CD3 and CD11b. The antigen stained brown and images of stained sections were taken at x40 magnification.

ND= not done

Figure 5.3 continued Histological analysis of Atm-/-nu-/- tumours

Mouse	H&E	B220	CD3	CD11b
69F5				
68F2				ND
319M1				ND
61M3				ND
55F1				ND
107F2				ND

Sections of 17 Atm-/-nu-/-lymphoma, along with normal Atm+/+nu-/- and Atm+/+nu+/- spleen, were H&E stained and immunohistochemically stained for B220, CD3 and CD11b. The antigen stained brown and images of stained sections were taken at x40 magnification.

ND= not done

Figure 5.4 Additional immunophenotyping of Atm-/-nu-/-, Atm+/+nu-/- and Atm+/+nu+/- mice
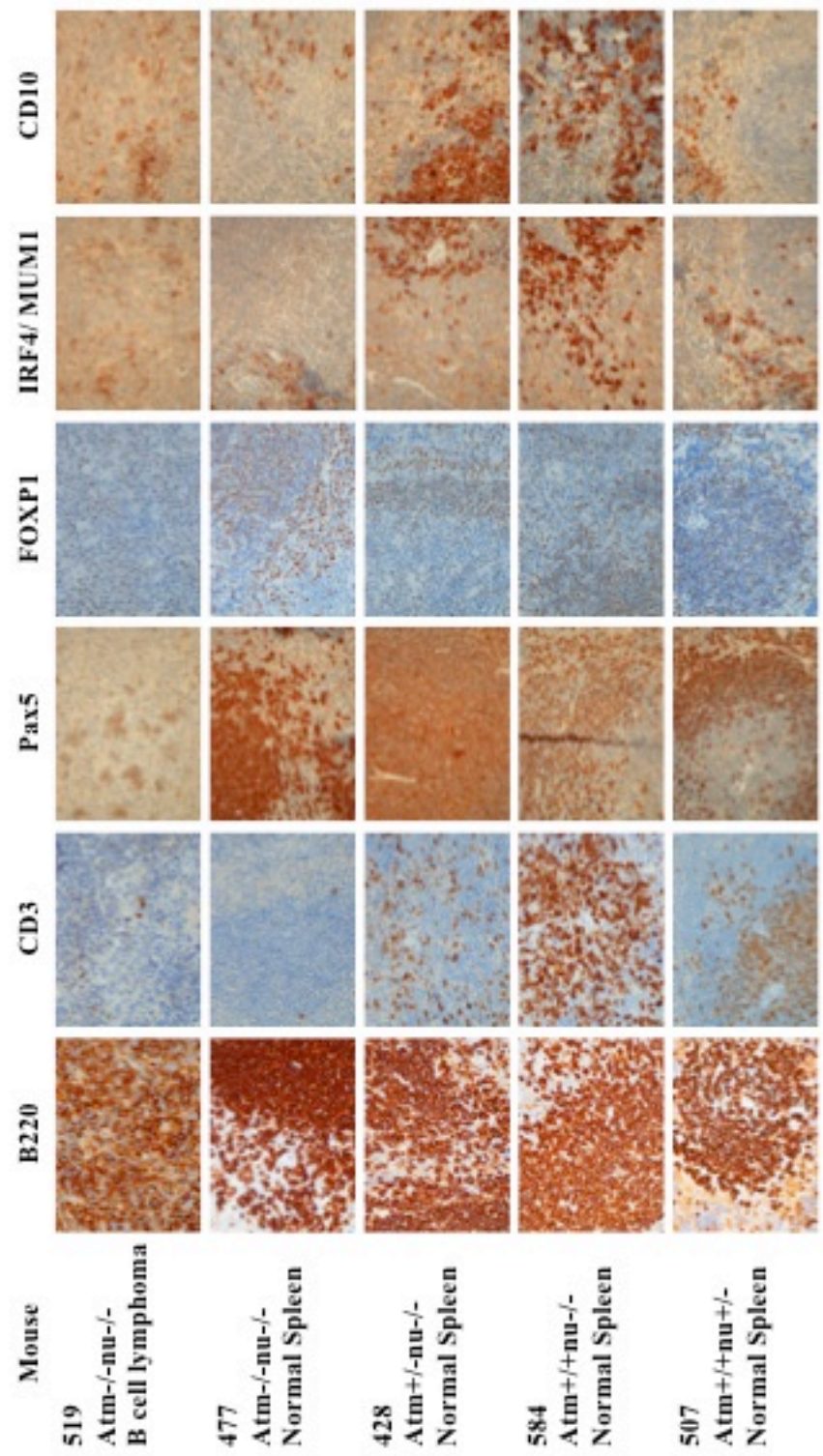
Staining was undertaken in the laboratory of Dr Teresa Marafiotti at University College Hospital, London to evaluate additional properties of the tumour. Atm-/-nu-/- B cell lymphoma was B220+, CD3-, Pax5-, FOXP1+, IRF4/MUM1- and CD10-.

Figure 5.5 FACS profiling of Atm-/-nu-/- lymphomas

173

Figure 5.5 continued FACS profiling of Atm-/-nu-/- lymphomas

Figure 5.5 continued FACS profiling of Atm-/-nu-/- lymphomas
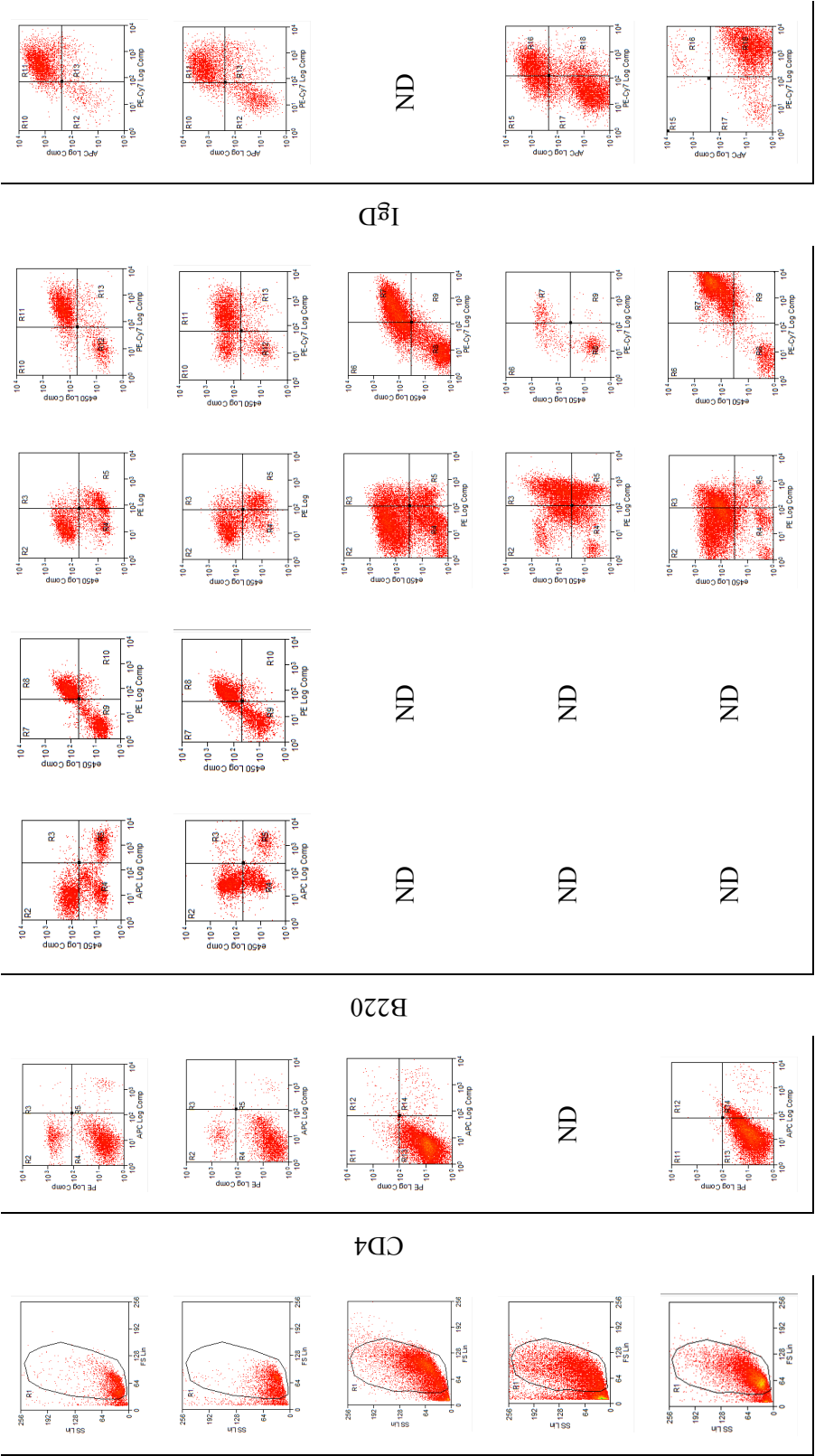
The expression of T cell associated markers CD5, CD4, CD8, B cell markers B220, CD19, CD43, IgM and IgD on Atm+/+nu-/-, Atm+/+nu+/-, Atm+/+nu+/- normal spleen and Atm-/-nu-/- lymphoma cells was measured using FACS. FS/SS profile gated around live cells.

Table 5.4 Summary of morphological and immunophenotypic analysis of Atm+/+nu-/- lymphomas

Mouse	Histology	IHC			Flow Cytometry						
		B220	CD3	CD11b	B220	CD19	CD43	IgM	IgD	CD5	CD4/ CD8
703	DLBCL, NOS	+	-	-	+	ND	+	+	ND	ND	-
5F3	DLBCL, NOS	+	-	-	+	ND	+	+	-	ND	-
593	DLBCL, NOS	+	-	-	+	ND	+	+	-	ND	-
61M3	DLBCL, NOS	+	-	ND	+	+	+	+	-	-	-
36F1	DLBCL, NOS	+#	-	-	+	+	+	+	-	-	-
69F5	DLBCL, NOS	+	-	ND	+	+	+	+	-	-	CD8+
37F3	DLBCL, NOS	+	-	-	N	N	N	N	N	N	N
40F 1	DLBCL, NOS	+	-	-	+	+	-	+	+	-	-
53M7	DLBCL, NOS	-	-	-	ND	ND	ND	ND	ND	ND	ND
55F1	DLBCL, NOS	-	-	ND	+	+	+	+	+	+	-
107F2	DLBCL, NOS	-	-	ND	+	+	+	-	-	-	-
50F2	FL*	+	-	-	+	+	-	+	-	-	-
5F1	FL*	-	-	-	-	+	+	-	-	-	-
319M1	FL*	-	-	ND	+	+	+	+	-	-	CD8+
519	B cell lymphoma, unclassifiable+	+	-	-	ND	ND	ND	ND	ND	ND	ND
656	ALCL	-	+	-	+	ND	+	+	+	ND	ND
68F2	Small cell lymphoma	+	+	ND	ND	ND	ND	ND	ND	ND	ND

Summary of surface marker expression analysis by immunohistochemistry and flow cytometry in figure 5.3 and figure 5.5. Sample 37F3 staining of tumour cells could not be distinguished from normal spleen.

FL= Follicular lymphoma, DLBCL, NOS = Diffuse large B cell lymphoma, not otherwise specified, IHC= Immunohistochemistry, ND= not done, N= normal * follicle centre cell lymphoma, predominantly diffuse, Grade 3A , + B cell lymphoma, unclassifiable, with features intermediate between DLBCL and Burkitt lymphoma. #B220 staining of tumour cells was weaker than normal B cells.

Table 5.5 Atm-/nu-/- lymphoma developmental origin

Mouse	Histology	Developmental Type
703	DLBCL, NOS	Mature B Cell: GC/ Non- GC
5F3	DLBCL, NOS	Mature B Cell: GC/ post GC
593	DLBCL, NOS	Mature B Cell: GC/ post GC
61M3	DLBCL, NOS	Mature B Cell: GC/ post GC
36F1	DLBCL, NOS	Mature B Cell: GC/ post GC
69F5	DLBCL, NOS	Mature B Cell: GC/ post GC
37M 3	DLBCL, NOS	Mature B Cell: GC/ post GC
55F1	DLBCL, NOS	Mature B Cell: GC/ post GC
40F 1	DLBCL, NOS	Mature B Cell: GC/ post GC
107F2	DLBCL, NOS	Mature B Cell: GC/ post GC
53M 7	DLBCL, NOS	Mature B Cell: GC/ post GC
50F2	FL[*]	Mature B Cell: GC
5F1	FL[*]	Mature B Cell: GC
319M1	FL[*]	Mature B Cell: GC
519	B cell lymphoma, unclassifiable[+]	Mature B Cell: GC
656	ALCL	B/T cell**
68F2	Small cell lymphoma	Peripheral B cell: Marginal Zone or Mantle cell

Atm-/-nu-/- lymphomas were assigned to a developmental group based on human morphology and immunophenotype. The postulated normal counterpart cell types are as follows:

DLBCL, NOS = mature B cell, germinal centre (GC) or post-GC B cell

Follicular lymphoma = mature B cell, GC;

Small cell lymphoma = Mantle cell or Marginal zone cell origin.

** Further Immunophenotyping is needed to confirm the origin of this tumour.

Figure 5.6 PCR analysis of IgH V(D)J rearrangements in Atm-/-nu-/- lymphomas

Lane: 1 2 3 4 5 6 7 8 9 10 11 12
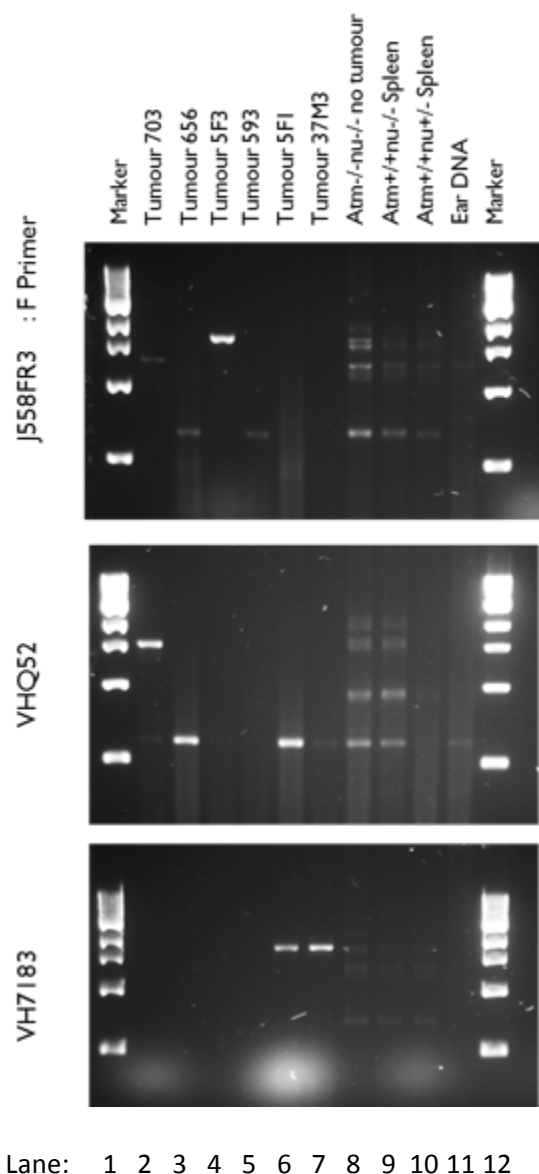
Agrose gel with representative tumours 703, 656, 593, 5F1 and 37M3 showing a single gene product from PCR amplification of IgH V(D)J, which indicates monoclonality. Forward primers J558, VHQ52 and VH7183 were used with reverse primer JH4. DNA from normal spleen of Atm-/-nu-/- and Atm+/+nu-/- and Atm+/+nu+/- spleen cells were used as positive control. Multiple bands present in these lanes correspond to the presence of multiple B cells in spleen each having a different rearrangement. DNA extracted from ear clippings was used as a negative control; no band was present in genomic ear DNA.

Table 5.6 Sequence analysis of IgH V(D)J rearrangement of Atm-/-nu-/- lymphoma

Mouse	Tissue	V(D)J rearrangement			Sequencing		
		J558	VHQ52	VH7183	V Gene	D Gene	J Gene
519	-	ND	ND	ND	ND	ND	ND
703	Tumour	Monoclonal	Monoclonal		V1	D2	J3
656	Spleen	Monoclonal	Monoclonal		V1	D2	J4
5F3	Tumour	Monoclonal			V1	D1	J2
593	Spleen	Monoclonal			V1	D3	J4
5F1	Spleen		Monoclonal	Monoclonal	V5	D2	J2
37M 3	Spleen	Monoclonal		Monoclonal	V5	D2	J2
50F2	Spleen	Monoclonal	Monoclonal		V1	D1	J4
40F1	Liver		Monoclonal		V3	None	J1
53M 7	Tumour	Polyclonal	Polyclonal	Polyclonal	-	-	-
36F1	Spleen & Liver	Polyclonal	Polyclonal	Polyclonal	-	-	-
69F5	Spleen & Liver	Polyclonal	Monoclonal	Polyclonal	V2	D2	J3
68F2	Spleen	Polyclonal	Polyclonal	Polyclonal	-	-	-
319M1	Spleen, Liver,	Monoclonal	Polyclonal	Monoclonal	V1, V2	D1, D1	J4, J2
61M3	Spleen, Liver		Monoclonal		V5	D2	J3
55F1	Spleen	Polyclonal	Polyclonal	Polyclonal	-	-	-
107F2	Spleen	Polyclonal	Polyclonal	Polyclonal	-	-	-

Summary of PCR amplification and sequencing of IgH V(D)J for 16 Atm-/-nu-/- lymphomas with DNA available. Tumours with a monoclonal rearrangement were sequenced. The NCBI IgBlast tool was used to align each sequence to the closest matching V, D and J gene family. Tumour 319M1 had two different rearrangements.

For mice with tumours at multiple locations and that there was DNA was available, all tumours were tested and found to have the same IgH V(D)J rearrangement.

ND=Not done.

Figure 5.7 IgH V(D)J sequence analysis

Mouse: 703

```
                                        <----------------------------FR1-IMGT----------------------------><------CDR1-IMGT---
                         703 reversed 17 CCAGCTGAAGCAGTCAGGACCTGAGCTGGTGAAACCTGGGGCCTCAGTGAAGATATCCTGCAAGGCTTCTGGATACACATTCACTGACTA 106
V  96.9% (281/290)  IGHV1S29*02       6 CCAGCTTCAGCAGTCAGGACCTGAGCTGGTGAAACCTGGGGCCTCAGTGAAGATATCCTGCAAGGCTTCTGGATACACATTCACTGACTA  95

                                        --->><--------------------FR2-IMGT--------------------><-------CDR2-IMGT------><---------
                         703 reversed 107 CAACATGCACTGGGTGAAGCAGAGCCATGGAAAGAGCCTCGACCCCCATTGGATATATTTATCCTTACAATGGTGGTACTGGCTACAACC 196
V  96.9% (281/290)  IGHV1S29*02       96 CAACATGCACTGGGTGAAGCAGAGCCATGGAAAGAGCCTTGAGTGG-ATTGGATATATTTATCCTTACAATGGTGGTACTGGCTACAACC 184

                                        --------------------------------------------FR3-IMGT-------------------------------------
                         703 reversed 197 AGAAGTTCAAGAGCAAGGCCACATTGACTGTAGACAATTCCTCCAGCACAGCCTACATGGAGCTCCGCAGCCTGACATCTGAGGACTCTG 286
V  96.9% (281/290)  IGHV1S29*02      185 AGAAGTTCAAGAGCAAGGCCACATTGACTGTAGACAATTCCTCCAGCACAGCCTACATGGAGCTCAGCAGCCTGACATCTGAGGACTCTG 274

                                        ------------->
                         703 reversed 287 CAGTCTATTACTGTGCAAGAAGGGGGGATGGTTACGGGTTTGCTTACTGGGGCCAAGGGACTCTGGTCACTGTCTCTGCAG 367
V  96.9% (281/290)  IGHV1S29*02      275 CAGTCTATTACTGTGCAAGA----------------------------------------------------------------- 294
D  100.0% (9/9)     IGHD2-9*01         7 -------------------------ATGGTTACGG-------------------------------------------------- 15
J  100.0% (45/45)   IGHJ3*01           4 ----------------------------------GGTTTGCTTACTGGGGCCAAGGGACTCTGGTCACTGTCTCTGCAG 48
```

Mouse: 656

```
                                        <-----------FR3-IMGT----------->
                         656 reversed  6 CCCGACATCTGAGGACTCTGCAGTCTATTATTGTGGAAAGGGCTATGGTAACTACGCTATGGACTACTGGGGTCAAGGAACCTCAGTCAC 95
V  94.7% (36/38)    IGHV1-20*01      255 CCTGACATCTGAGGACTCTGCAGTCTATTATTGTGCAA---------------------------------------------------- 292
D  100.0% (13/13)   IGHD2-1*01         5 ---------------------------------------CTATGGTAACTAC---------------------------------- 17
J  98.0% (50/51)    IGHJ4*01           4 ---------------------------------------------------ACTATGCTATGGACTACTGGGGTCAAGGAACCTCAGTCAC 43

                           reversed 96 CGTCTCCTCAG 106
J  98.0% (50/51)    IGHJ4*01          44 CGTCTCCTCAG 54
```

Mouse: 5F3

```
                                        <-----------FR3-IMGT------------->
                         5F3 reversed  4 GCCTGACATCTGAGGACTCTGCGGTCTATTACTGTGCAAGAAGGGAAATTACTACGGTAGTATCTGACTACTGGGGCCAAGGCACCACTC 93
V  100.0% (41/41)   IGHV1S126*01     254 GCCTGACATCTGAGGACTCTGCGGTCTATTACTGTGCAAGA------------------------------------------------- 294
D  100.0% (15/15)   IGHD1-1*01         4 ------------------------------------------------ATTACTACGGTAGTA-------------------------- 18
J  100.0% (41/41)   IGHJ2*01           8 --------------------------------------------------------------TGACTACTGGGGCCAAGGCACCACTC 33

                         5F3 reversed 94 TCACAGTCTCCTCAG 108
J  100.0% (41/41)   IGHJ2*01          34 TCACAGTCTCCTCAG 48
```

Mouse: 593

```
                                        <-----------FR3-IMGT----------->
                         593 reversed  7 TGACATCTGAGGACTCTGCGGTCTATTTCTGTGCAAGACACGAAGAGACGAGGGCTATGGACTACTGGGGTCAAGGAACCTCAGTCACCG 96
V  97.8% (45/46)    IGHV1-62-2*01    257 TGACATCTGAAGACTCTGCGGTCTATTTCTGTGCAAGACACAGAAGA------------------------------------------- 302
D  100.0% (6/6)     IGHD3-3*01        10 -----------------------------------------------------------AGGGCT---------------------------------- 15
J  100.0% (46/46)   IGHJ4*01           9 ------------------------------------------------------GCTATGGACTACTGGGGTCAAGGAACCTCAGTCACCG 45

                         593 reversed 97 TCTCCTCAG 105
J  100.0% (46/46)   IGHJ4*01          46 TCTCCTCAG 54
```

Mouse: 69F5

```
                         69F5         37 GAGCCTGTCCATAACCTGCACAGTCTCTGGTTTCTCATTAACTAGCTATGGTGTACACTGGGTTCGCCAGTCTCCAGGAAAGGGTCTGGA 126
V  100.0% (246/246) IGHV2-5*01        48 GAGCCTGTCCATAACCTGCACAGTCTCTGGTTTCTCATTAACTAGCTATGGTGTACACTGGGTTCGCCAGTCTCCAGGAAAGGGTCTGGA 137

                                        ------------><-----CDR2-IMGT-----><-------------------------------------------------FR3
                         69F5        127 GTGGCTGGGAGTGATATGGAGAGGTGGAAGCACAGACTACAATGCAGCTTTCATGTCCAGACTGAGCATCACCAAGGACAACTCCAAGAG 216
V  100.0% (246/246) IGHV2-5*01       138 GTGGCTGGGAGTGATATGGAGAGGTGGAAGCACAGACTACAATGCAGCTTTCATGTCCAGACTGAGCATCACCAAGGACAACTCCAAGAG 227

                                        -IMGT----------------------------------------------------->
                         69F5        217 CCAAGTTTTCTTTAAAATGAACAGTCTGCAAGCTGATGACACTGCCATATACTACTGTGCCAAAAAAAAACTATAGGTACGCCTGGTTTGC 306
V  100.0% (246/246) IGHV2-5*01       228 CCAAGTTTTCTTTAAAATGAACAGTCTGCAAGCTGATGACACTGCCATATACTACTGTGCCAAAAA----------------------- 293
D  100.0% (12/12)   IGHD2-14*01        4 ------------------------------------------------------------------------ACTATAGGTACG---------- 15
J  100.0% (48/48)   IGHJ3*01           1 -----------------------------------------------------------------------------CCTGGTTTGC 10

                         69F5        307 TTACTGGGGCCAAGGGACTCTGGTCACTGTCTCTGCAG 344
J  100.0% (48/48)   IGHJ3*01          11 TTACTGGGGCCAAGGGACTCTGGTCACTGTCTCTGCAG 48
```

Mouse: 50F2

```
                                        <--------FR3-IMGT-------->
                         50F2 reversed 19 CTGAGGACTCTGCGGTCTATTACTGTACAAAGCTATTACTACGGTAGTAGCTACTGGTACTTCGATGTCTGGGGCGCAGGGACCACGGTC 108
V  100.0% (30/30)   IGHV1S36*01      263 CTGAGGACTCTGCGGTCTATTACTGTACAA--------------------------------------------------------- 292
D  100.0% (21/21)   IGHD1-1*01         3 ----------------------------------TATTACTACGGTAGTAGCTAC----------------------------------- 23
J  100.0% (53/53)   IGHJ1*01           1 -----------------------------------------------CTACTGGTACTTCGATGTCTGGGGCGCAGGGACCACGGTC 40

                         50F2 reversed 109 ACCGTCTCCTCAG 121
J  100.0% (53/53)   IGHJ1*01          41 ACCGTCTCCTCAG 53
```

DNA from 11 Atm-/-nu-/- lymphoma with monoclonal V(D)J PCR products were sequenced and the sequence was aligned to most similar V,D,J genes using IgBlast tool from NCBI.

Figure 5.7 continued IgH V(D)J sequence analysis

Mouse: 319M1 (1)

```
                    319M1    30   ACCGAGCCTGTCCATAACCTGCACAGTCTCTGGTTTCTCATTAACTAGCTATGGTGTACACTGGGTTCGCCAGTCTCCAGGAAAGGGTCT  119
V  99.6% (245/246)  IGHV2-5*01  45   ACAGAGCCTGTCCATAACCTGCACAGTCTCTGGTTTCTCATTAACTAGCTATGGTGTACACTGGGTTCGCCAGTCTCCAGGAAAGGGTCT  134

                                     --------------><-----CDR2-IMGT-----><------------------------------------------------------
                    319M1   120   GGAGTGGCTGGGAGTGATATGGAGAGGTGGAAGCACAGACTACAATGCAGCTTTCATGTCCAGACTGAGCATCACCAAGGACAACTCCAA  209
V  99.6% (245/246)  IGHV2-5*01  135   GGAGTGGCTGGGAGTGATATGGAGAGGTGGAAGCACAGACTACAATGCAGCTTTCATGTCCAGACTGAGCATCACCAAGGACAACTCCAA  224

                                     FR3-IMGT---------------------------------------------------->
                    319    210   GAGCCAAGTTTTCTTTAAAATGAACAGTCTGCAAGCTGATGACACTGCCATATACTACTGTGCCAATTACTACGGTAGTAGTACTACTTT  299
V  99.6% (245/246)  IGHV2-5*01  225   GAGCCAAGTTTTCTTTAAAATGAACAGTCTGCAAGCTGATGACACTGCCATATACTACTGTGCCAA------------------------  290
D  100.0% (16/16)   IGHD1-1*01   4   ------------------------------------------------------------------------ATTACTACGGTAGTAG---------  19
J  100.0% (48/48)   IGHJ2*01     1   -------------------------------------------------------------------------------------ACTACTTT  8

                    319    300   GACTACTGGGGCCAAGGCACCACTCTCACAGTCTCCTCAG  339
```

(2)

```
                                     <------------FR3-IMGT------------->
                    319M1 reversed   3   GCCTGACATCTGAGGACTCTGCAGTCTATTACTGTGCAAGTTACTACGGTAGTAGCTATGCTATGGACTACTGGGGTCAAGGAACCTCAG  92
V  100.0% (40/40)   IGHV1-39*01    254   GCCTGACATCTGAGGACTCTGCAGTCTATTACTGTGCAAG-------------------------------------------------  293
D  100.0% (18/18)   IGHD1-1*01      5   ----------------------------------------TTACTACGGTAGTAGCTA-----------------------------  22
J  100.0% (50/50)   IGHJ4*01        5   ----------------------------------------------------CTATGCTATGGACTACTGGGGTCAAGGAACCTCAG  39

                    319M1 reversed  93   TCACCGTCTCCTCAG  107
J  100.0% (50/50)   IGHJ4*01       40   TCACCGTCTCCTCAG  54
```

Mouse: 61M3

```
                                     <------------------------FR3-IMGT------------------------->
                    61M3 reversed    2   GAACAACCTGTTCCTGCAAATGAGCAGTCTGAAGTCTGAGGACACGGCCATGTATTACTGTGCAAGACGGGCATATGGTAAAGGGAGCCT  91
V  97.1% (66/68)    IGHV5-12-2*02  195   GAACACCCTGTACCTGCAAATGAGCAGTCTGAAGTCTGAGGACACGGCCATGTATTACTGTGCAAGAC----------------------  262
D  100.0% (8/8)     IGHD2-1*01      6   -----------------------------------------------------------------------TATGGTAA---------  13

                    61M3 reversed   92   GGCCTGGTTTGCTTACTGGGGCCAAGGGACTCTGGTCACTGTCTCTGCAG  141
J  100.0% (48/48)   IGHJ3*01        1   --CCTGGTTTGCTTACTGGGGCCAAGGGACTCTGGTCACTGTCTCTGCAG  48
```

Mouse: 5F1

```
                                     <-------------------FR3-IMGT-------------------->
                    5F1 reversed    21   CCTGCAAATGAGCAGTCTGAGGTCTGAGGACACGGCCATGTATTACTGTGCAAGACATAAGGACTGGTACTACTTTGACTACTGGGGCCA  110
V  100.0% (57/57)   IGHV5-9-3*01   240   CCTGCAAATGAGCAGTCTGAGGTCTGAGGACACGGCCATGTATTACTGTGCAAGACA--------------------------------  296
D  100.0% (5/5)     IGHD2-1*01      8   ----------------------------------------------------------------TGGTA--------------------  12
J  100.0% (48/48)   IGHJ2*01        1   --------------------------------------------------------------------ACTACTTTGACTACTGGGGCCA  22

                    5F1 reversed   111   AGGCACCACTCTCACAGTCTCCTCAG  136
J  100.0% (48/48)   IGHJ2*01       23   AGGCACCACTCTCACAGTCTCCTCAG  48
```

Mouse: 37F3

```
                                     <------------------------FR3-IMGT------------------------->
                    37M3 reversed    2   GAACAACCTGTTCCTGCAAATGAGCAGTCTGAGGTCTGAGGACACGGCCATGTATTACTGTGCAAGACATAAGGACTGGTACTACTTTGA  91
V  98.6% (68/69)    IGHV5-9-3*01   228   GAACACCCTGTACCTGCAAATGAGCAGTCTGAGGTCTGAGGACACGGCCATGTATTACTGTGCAAGACA----------------------  296
D  100.0% (5/5)     IGHD2-1*01      8   --------------------------------------------------------------------------TGGTA---------  12
J  100.0% (48/48)   IGHJ2*01        1   -----------------------------------------------------------------------------ACTACTTTGA  10

                    37M3 reversed   92   CTACTGGGGCCAAGGCACCACTCTCACAGTCTCCTCAG  129
J  100.0% (48/48)   IGHJ2*01       11   CTACTGGGGCCAAGGCACCACTCTCACAGTCTCCTCAG  48
```

Mouse: 40F1

```
                                     <-------------------FR1-IMGT-------------------><-------CDR1-IMGT-------><---------------
                    40F1 reversed   44   CCTCGTGAAACCTTCTCAARACTCTGTCCCTCACYTGTTCTGKTCACTGGCGACTCCCATCACCCAGTGGTTACKGRAACTGGATCCSGG  133
V  93.7% (251/268)  IGHV3-8*02      30   CCTCGTGAAACCTTCTCA-GACTCTGTCCCTCACCTGTTCTG-TCACTGGCGACTCC-ATCACC-AGTGGTTACTGGAACTGGATCC-GG  114

                                     ------FR2-IMGT---------------------><-----CDR2-IMGT-----><---------------------------
                    40F1 reversed  134   AAATTCCCAGGGAAWAAACTTGAATACATGGGGTACATAAACTACAGTKGTAGCACTTACTACAATCCATCTYYCAAAARTMGAATCTCC  223
V  93.7% (251/268)  IGHV3-8*02     115   AAATTCCCAGGGAATAAACTTGAGTACATGGGGTACATAAGCTACAGTGGTAGCACTTACTACAATCCATCTCTCAAAAGTCGAATCTCC  204

                                     ------------------FR3-IMGT------------------------------------------->
                    40F1 reversed  224   ATCACTCGAGACACATCCAAGAACCAGTACTACCTGCAGTTGAATTCTGTGACTACTGAGGACACAGCCACATATTACTGTGCAAGATGG  313
V  93.7% (251/268)  IGHV3-8*02     205   ATCACTCGAGACACATCCAAGAACCAGTACTACCTGCAGTTGAATTCTGTGACTACTGAGGACACAGCCACATATTACTGTGCAAGAT--  292

                    40F1 reversed  314   GGGAACTGGTACTTCGATGTCTGGGGCGCAGGGACCACGGTCACCGTCTCCTCAG  368
J  100.0% (51/51)   IGHJ1*01        3   ----ACTGGTACTTCGATGTCTGGGGCGCAGGGACCACGGTCACCGTCTCCTCAG  53
```

DNA from 11 Atm-/-nu-/- lymphoma with monoclonal V(D)J PCR products were sequenced and the sequence was aligned to most similar V,D,J genes using IgBlast tool from NCBI.

Figure 5.8 Subcutaneous transplant into immunocompromised mice.

a.
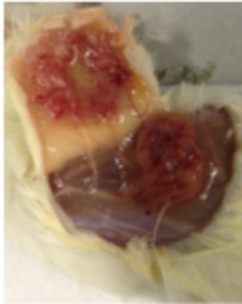
b.

c.
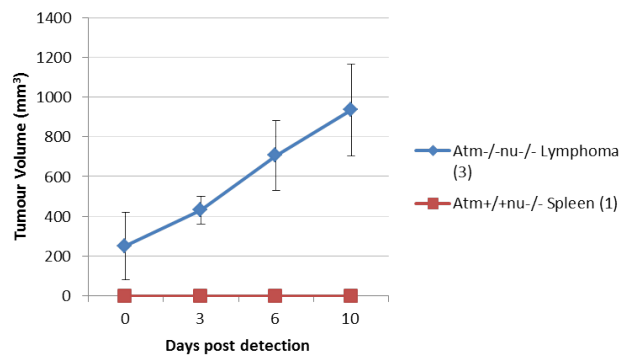
d.
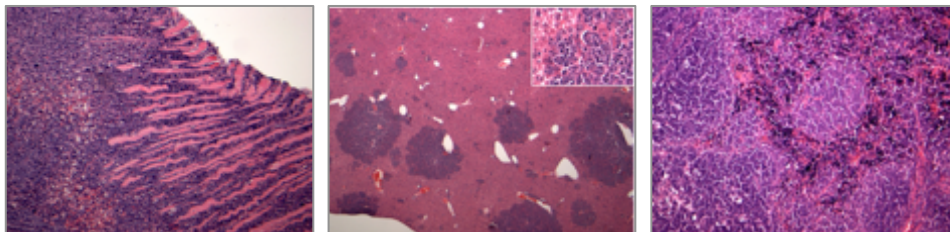
a. photograph of subcutaneous tumour

b. tumour infiltration of recipient spleen

c. subcutaneous tumour growth

d. H&E analysis showing tumour infiltrate into skeletal muscle (top left), metastasis to the liver (top right), and spleen (bottom left)

Figure 5.8 continued Subcutaneous transplant into immunocompromised mice

e.
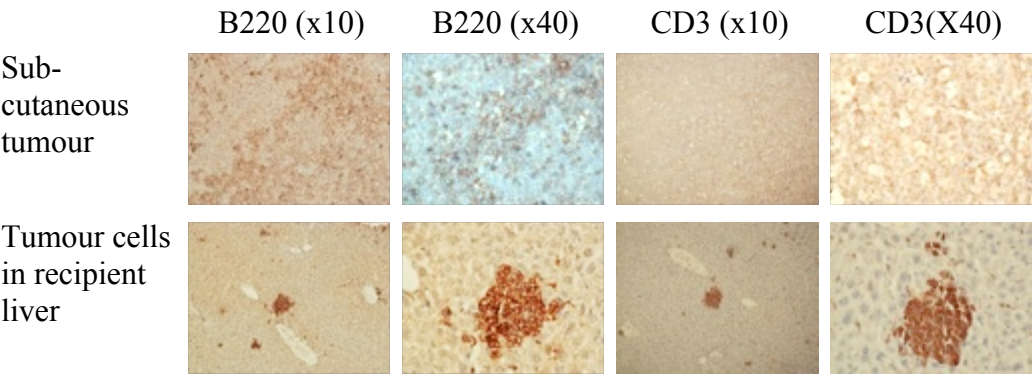
f.
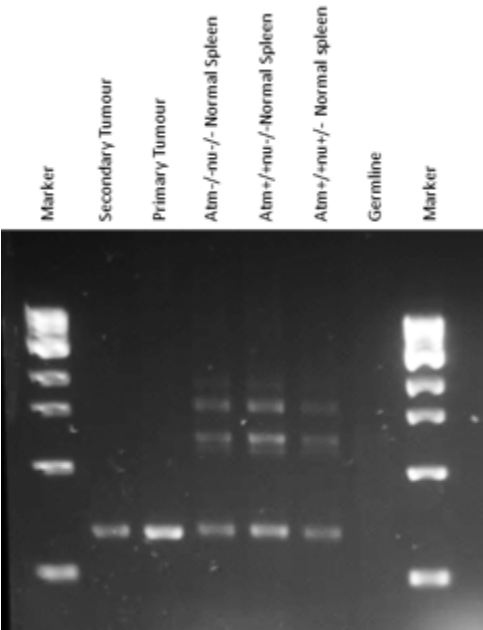
e. Immunohistochemical analysis of subcutaneous tumour and recipient liver

f. Amplification of the same IgH V(D)J from primary tumour and secondary transplant (confirmed by sequencing)

Table 5.7 Clonal abnormalities detected by M-FISH analysis of Atm-/- T cell lymphomas

Mouse	Description	Number of cells
Atm-/- F1	der(14)t(1;14)	15/15
	+15	14/15
	der(12)t(12;14)	14/15
F1 Clone is der(14)t(1;14), der(12)t(12;14), +15		
Atm-/- F2	dup(1)	11/22
	t(2;14)	11/22
	der(12) t(12,15)	11/22
F2 Clone 1 is der(12)t(12;15), t(2;14), dup1.		
	der(14)t(14;15)	10/22
	der(12)t(12;14)	11/22
	dup (4)	9/22
	dup (X)	6/22
F2 Clone 2 is der(12)t(12;14), der(14)t(14;15), dup(4) dup(X)		
Atm-/- 58M4	der(12)t(12;15)	18/18
	der(12)t(Y;12)	16/18
	t(2;14)	16/18
	-15	8/18
	t(1;14)	8/18
58M4 clone is der(12)t(12;15),der(12)t(Y;12).t(2;14), -15, t(1;14)		

Table describes abnormalities detected in each tumour. An abnormality was considered clonal if it was present in 3 or more cells. The number of cells each abnormality is shown out of the total number of cells analysed. Aberrations involving chromosome 12, 14 and 15 were the most frequent. Atm-/- tumour F2 contains two clones with mutually exclusive translocations.

Figure 5.9 Representative karyograms showing no clonal aberrations detected by M-FISH analysis of normal Atm+/+ spleen

Atm+/+ Spleen
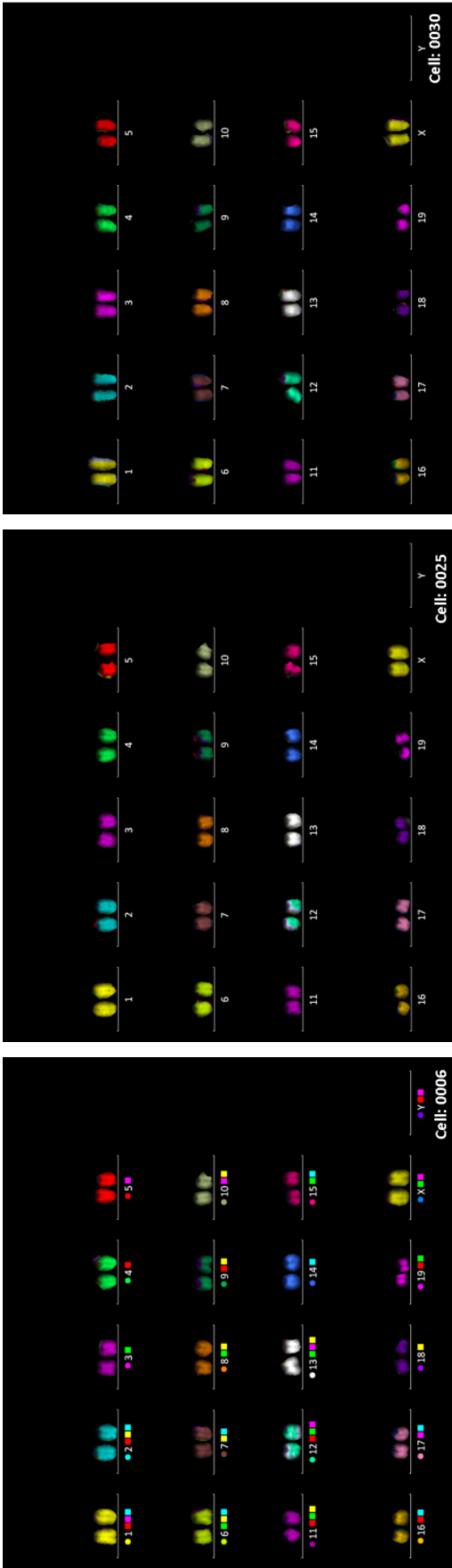
Figure 5.10 Representative karyograms showing clonal aberrations detected by M-FISH analysis of Atm-/- thymoma

Atm-/- thymoma F1
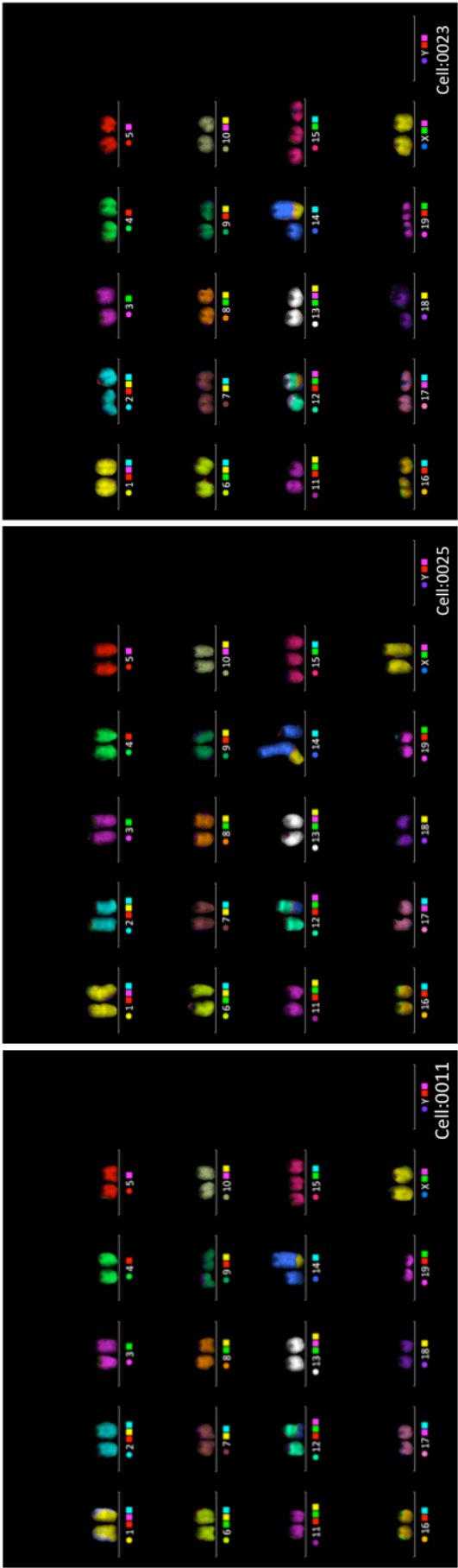
Figure 5.10 continued Representative karyograms showing clonal aberrations detected by M-FISH analysis of Atm–/– thymoma

Atm–/– thymoma F2 clone A
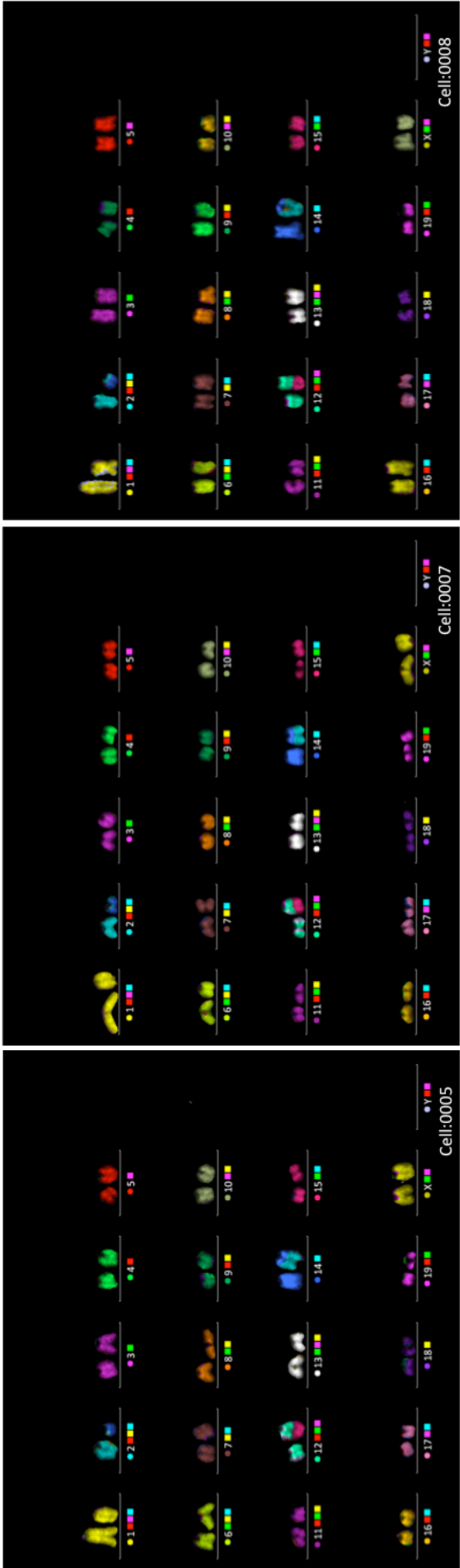
Figure 5.10 continued Representative karyograms showing clonal aberrations detected by M-FISH analysis of Atm-/- thymoma

Atm-/- thymoma F2 clone B
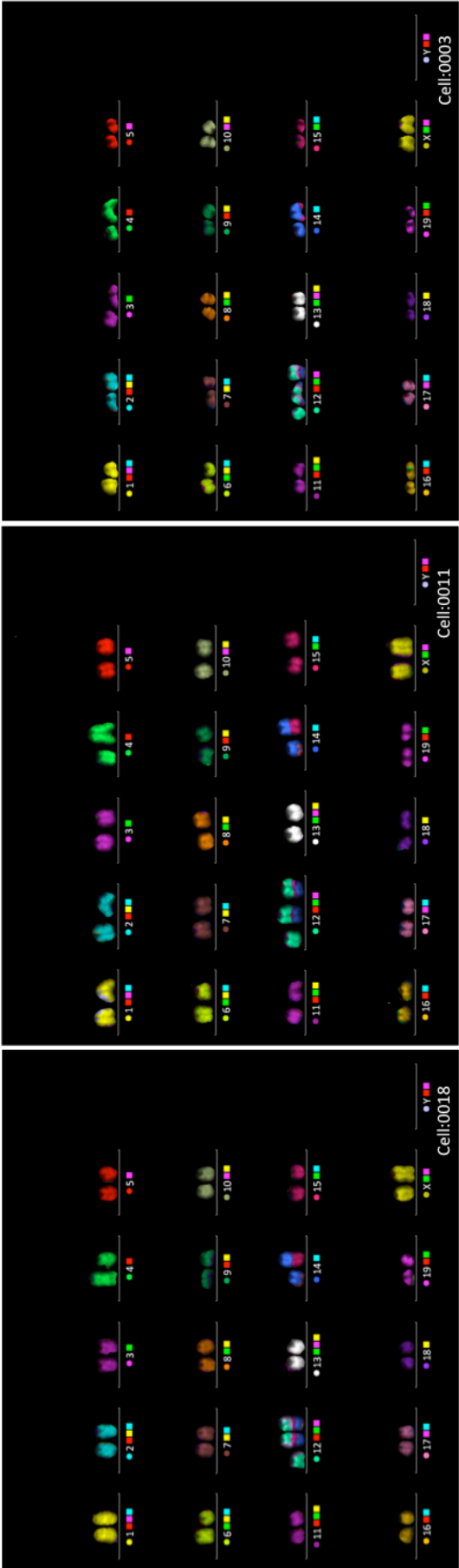
Figure 5.10 continued Representative karyograms showing clonal aberrations detected by M-FISH analysis of Atm–/– thymoma

Atm–/– thymoma 58M4
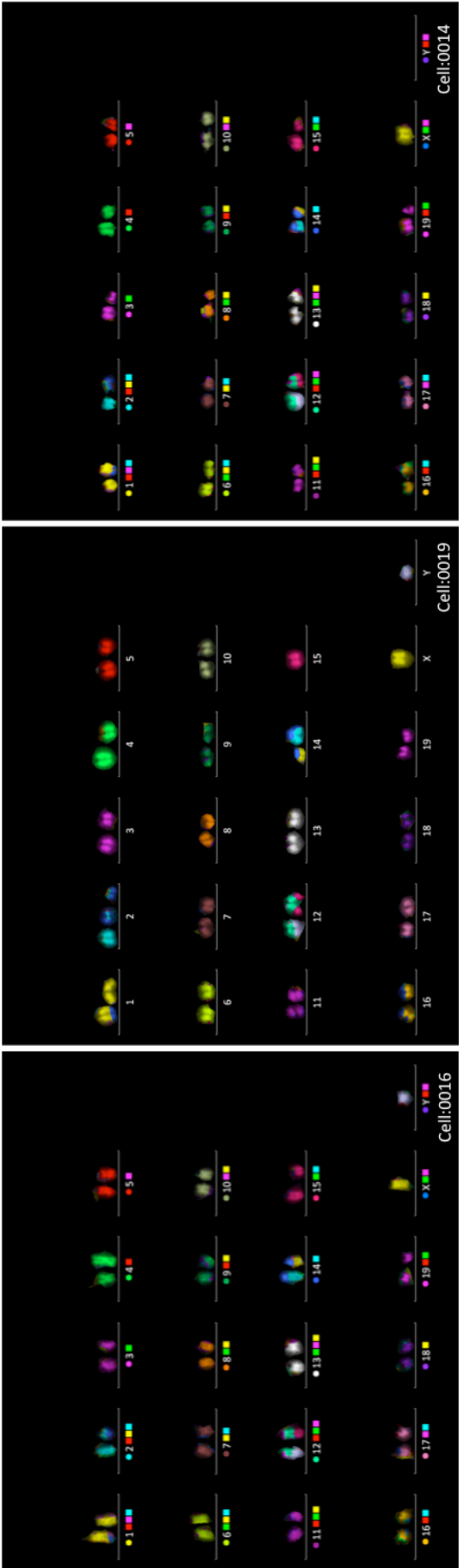
Table 5.8 Clonal abnormalities detected by M-FISH analysis of Atm-/-nu-/- B cell

lymphomas

	M-FISH		Targeted FISH	
Mouse	**Description**	**Number of Cells**	**Copies of Myc**	**IgH translocation**
5F3	39~40, XX		3	No (Loss of IgH v1 in 1 allele)
	der(17)t(11;17)	19/20		
	-11	17/20		
	add (6)	15/20		
	der(18)t(15;12;18)*	10/20		
	der(18)t(15;18)*	8/20		
	dup(14)	5/20		
	der(6)t(1;6)	5/20		
	-16	4/20		
	der(1)t(1;16)	3/20		
5F3 clone is 39~40, XX, der(17)t(11;17),-11, -16, add (6), dup(14), der(18)t(15;12;18), der(18)t(15;18), der(6)t(1;6), der(1)t(1;16)				
593	39~40, XY		2	No (Loss of IgH)
	der(17)t(15;17)	19/20		
	der(13)t(3;13)	7/20		
	-Y	6/20		
	dup(4)	6/20		
	add(4)	4/20		
	der(5)t(5;4)	4/20		
	-1	3/20		
	-11	3/20		
593 clone is 39~40, XY, der(17)t(15;17), -Y, -1, -11, dup(4), add(4), der(13)t(3;13), der(5)t(5;4)				

* It is possible that these two abnormalities are the same but due to the technical limitations of the M-FISH analysis, have been noted separately.

Table 5.8 continued Clonal abnormalities detected by M-FISH analysis of Atm-/-nu-/- B cell

	M-FISH		Targeted FISH	
Mouse	Description	Number of Cells	Copies of Myc	IgH translocation
37F3	30~41, XY		2	No
	der(18)t(3;18)	10/40		
	der(18)t(12;18)	6/40		
	-12	5/40		
	t(1,2)	5/40		
	dup(18)	4/40		
	der(18)t(8,18)	4/40		
	der(18)t(5;18)	3/40		
	der(18)t(7;18)	3/40		
	add(1)	3/40		
	add(3)	3/40		
	add(5)	3/40		
	add(11)	3/40		
	37F3 clone is 30~41, XY, der(18)t(3;18), der(18)t(12;18), der(18)t(8;18), der(18)t(5;18), der(18)t(7;18) -12, dup(18), add(1), add(3), add(5), add(11), t(1;2)			
50F2	37~41, XX		2	No
	dup(18)der(18)t(7;18)	12/20		
	-19	5/20		
	-5	4/20		
	-7	4/20		
	-8	4/20		
	-9	4/20		
	-2	3/20		
	-12	3/20		
	-16	3/20		
	50F2 clone is 30~41, XX, dup(18)der(18)t(7;18), -19, -5, -7, -8, -9, -2, -12, -16			

Table 5.8 continued Clonal abnormalities detected by M-FISH analysis of Atm-/-nu-/- B cell

Mouse	M-FISH Description	Number of Cells	Targeted FISH Copies of Myc	IgH translocation
703	36~41, XX		2	No
	40XX (Normal)	4/36		
	der(X)t(X;13)	11/36		
	der(13)t(13;18)	9/36		
	der(18)t(18;X)	8/36		
	-X	8/36		
	-5	5/36		
	-17	5/36		
	-4	4/36		
	-16	4/36		
	-18	4/36		
	+6	4/36		
	add (6)	4/36		
	der(X)t(X;6)	3/36		
	-3	3/36		
	-13	3/36		
	-15	3/36		
	-19	3/36		
703 clone is d36~41, XX, der(X)t(X;13), der(13)t(13;18), der(18)t(18;X), +6, -X, -4, -3, -5, -13, -15, -16, -17, -18, -19, add(6), der(X)t(X;6)				
68F2	40~41, XX		3	Yes
	40, XX (Normal)	4/12		
	der(12)t(12;15)	8/12		
	-19	5/12		
	+3	5/12		
	+12 (Abnormal)	5/12		
	der(19)t(12;19)	3/12		
68F2 clone is 40~41, XX, der(12)t(12;15), -19, +3, +12, der(19)t(12;19)				

Figure 5.11 Representative karyograms depicting clonal aberrations detected by M-FISH analysis of Atm-/-nu-/- lymphoma 5F3

Atm-/-nu-/- B cell lymphoma 5F3
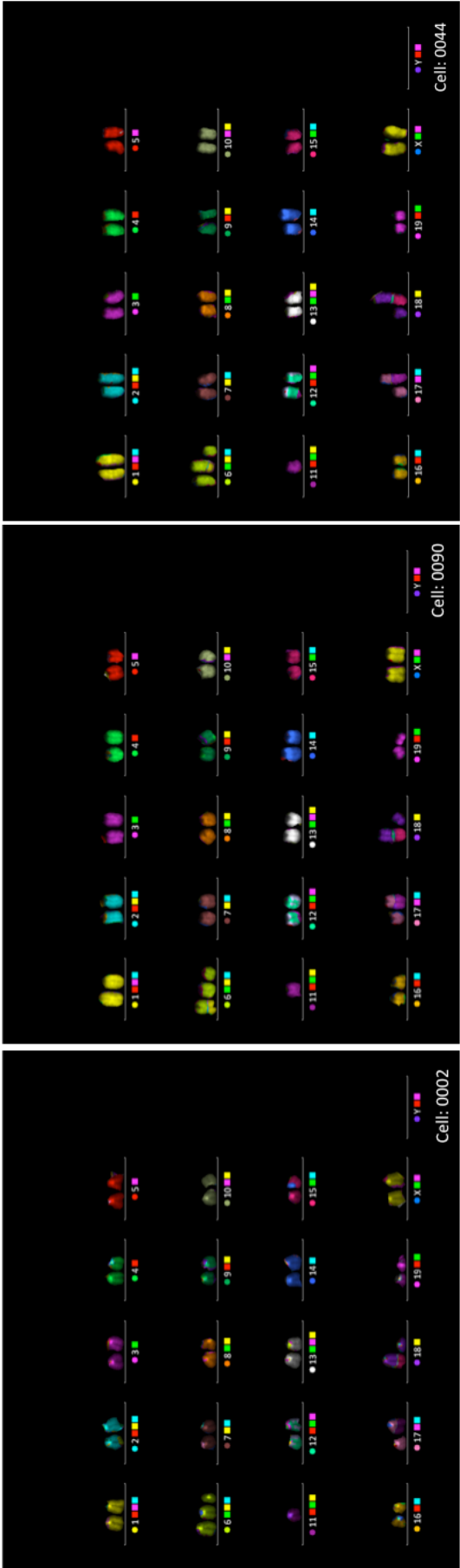
Figure 5.12 Representative karyograms depicting clonal aberrations detected by M-FISH analysis of Atm–/–nu–/– lymphoma 593

Atm–/–nu–/– B cell lymphoma 593
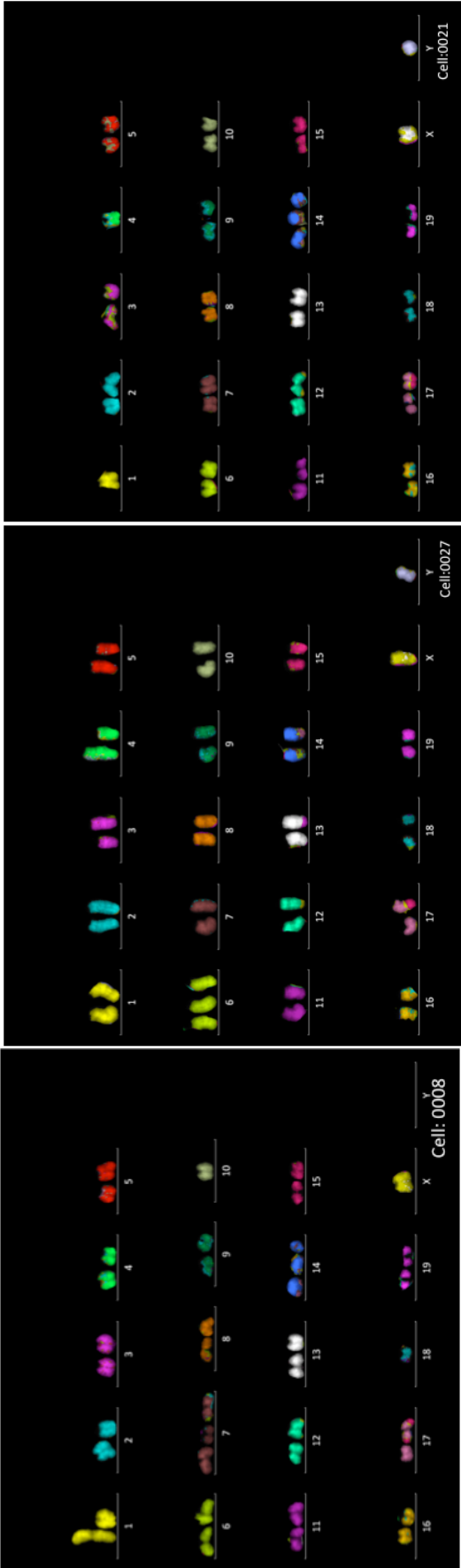
Figure 5.13 Representative karyograms depicting clonal aberrations detected by M-FISH analysis of Atm-/-nu-/- lymphoma 37F3

Atm-/-nu-/- B cell lymphoma 37F3
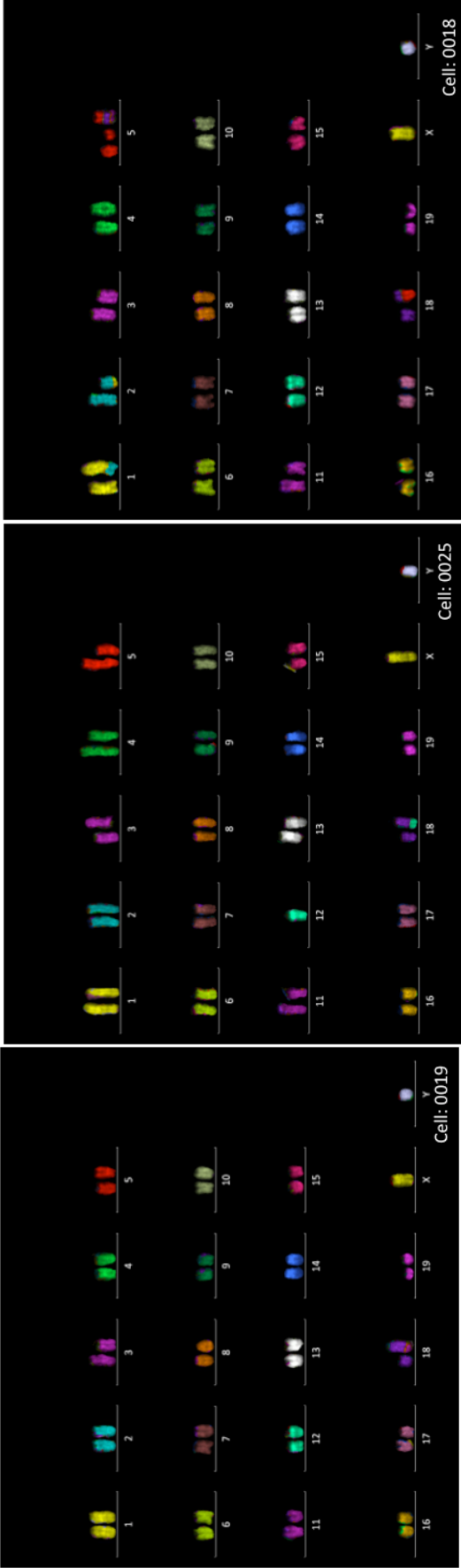
Figure 5.14 Representative karyograms depicting clonal aberrations detected by M-FISH analysis of Atm-/-nu-/- lymphoma 50F2

Atm-/-nu-/- B cell lymphoma 50F2
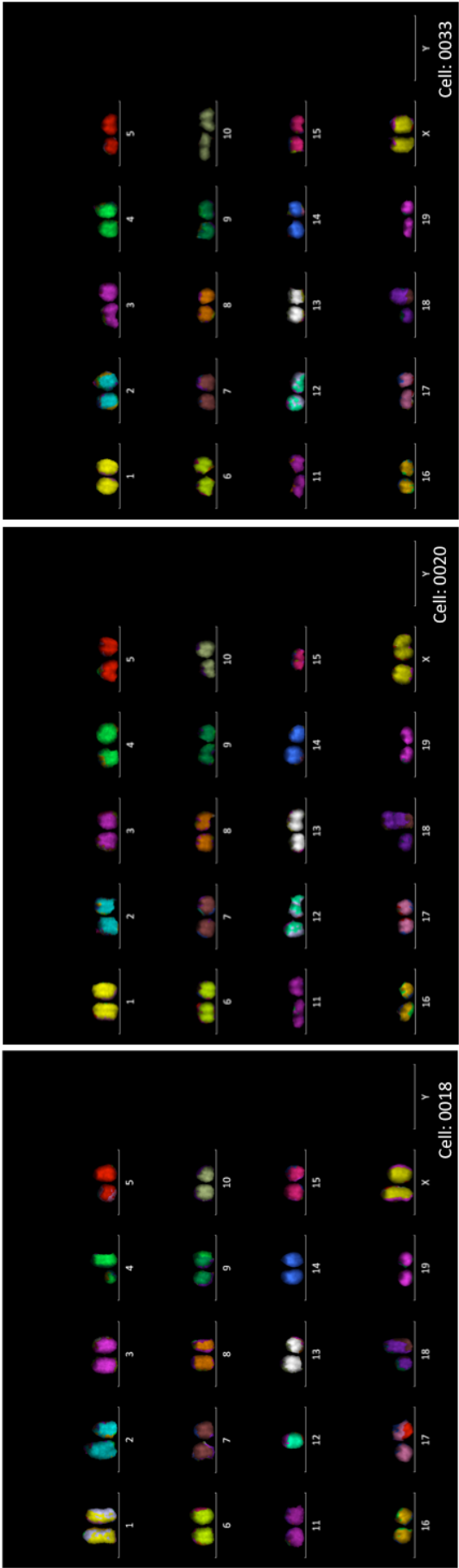
Figure 5.15 Representative karyograms depicting clonal aberrations detected by M-FISH analysis of Atm-/-nu-/- lymphoma 703

Atm-/-nu-/- B cell lymphoma 703
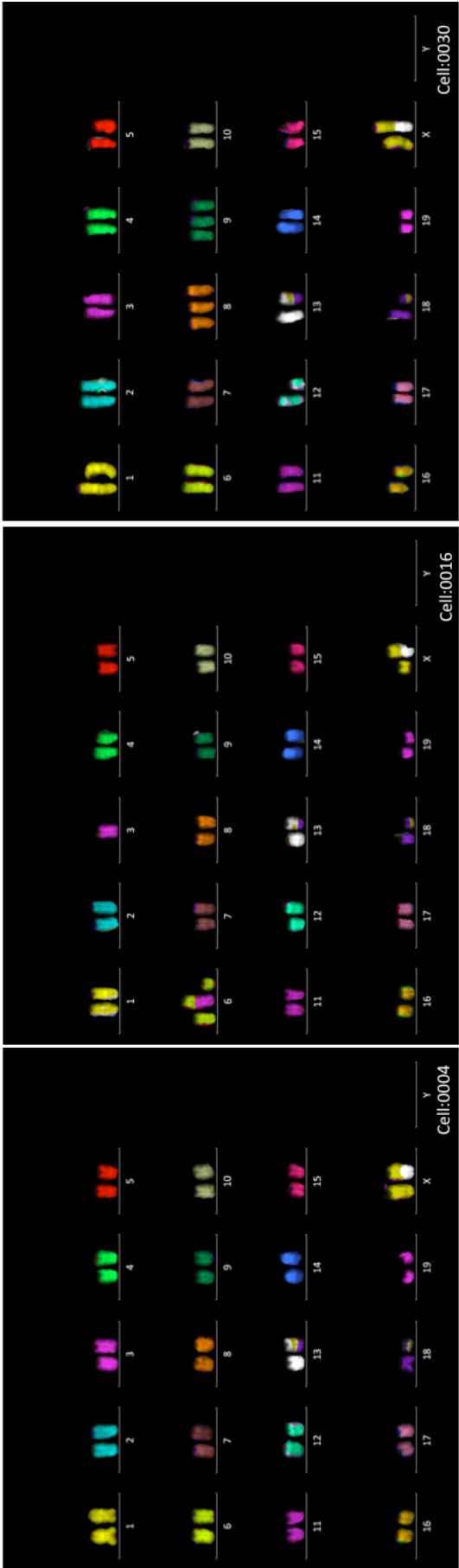
Figure 5.16 Representative karyograms depicting clonal aberrations detected by M-FISH analysis of Atm−/−nu−/− lymphoma 68F2

Atm−/−nu−/− B cell lymphoma 68F2
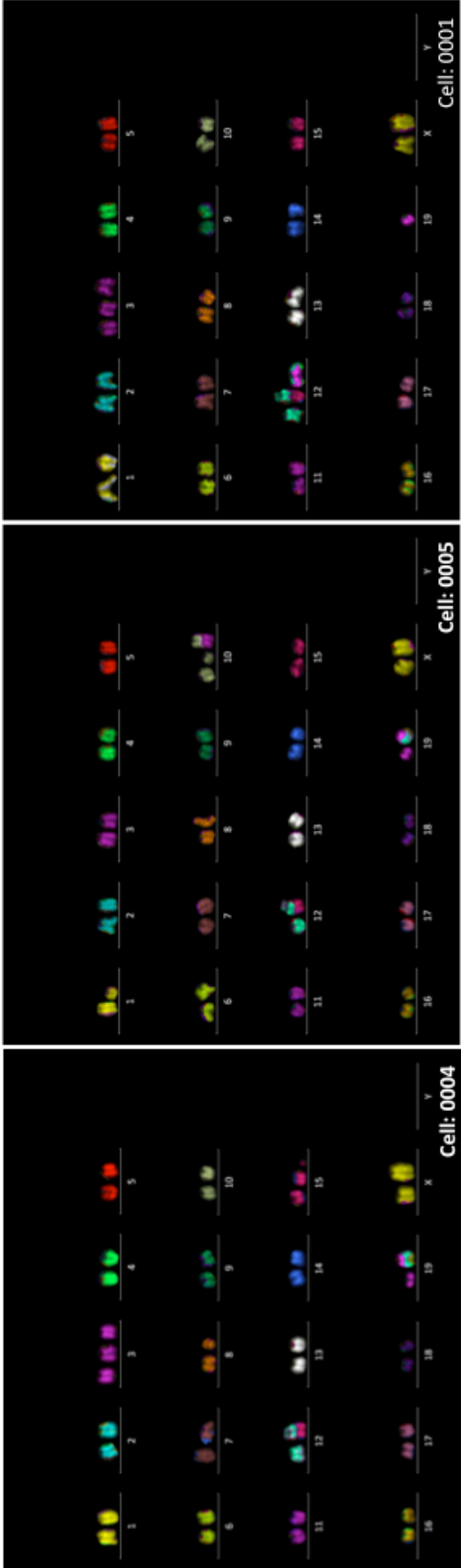
Figure 5.17 Representative cells for Atm-/-nu-/- B cell lymphoma c-Myc targeted FISH analysis

Atm-/-nu-/- B cell lymphoma 703   Result: 2R
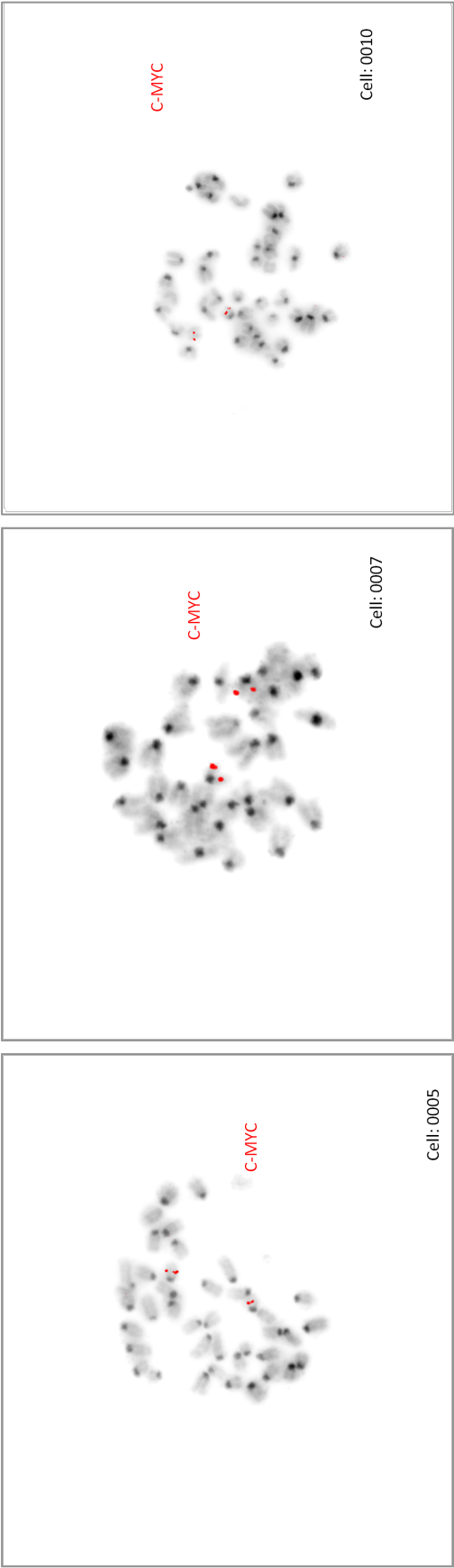
Red: 'C-MYC' probe hybridises within the c-Myc gene

R= Red probe

Figure 5.18 Representative cells for Atm-/-nu-/- B cell lymphoma c-Myc targeted FISH analysis

Atm-/-nu-/- B cell lymphoma 5F3 **Result: 3R**

C-MYC

Cell: 0001

C-MYC

Cell: 0009

C-MYC

Cell: 0012
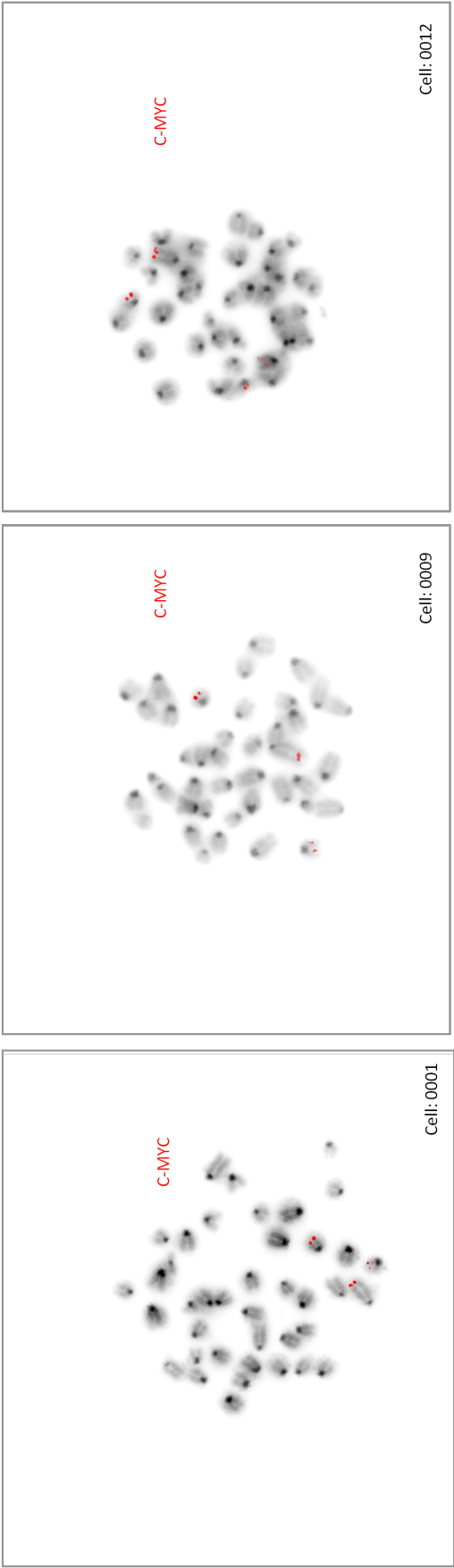
Red: 'C-MYC' probe hybridises within the c-Myc gene

R= Red probe

Figure 5.19 Representative cells for Atm-/-nu-/- B cell lymphoma c-Myc targeted FISH analysis

Atm-/-nu-/- B cell lymphoma 593   **Result: 2R**
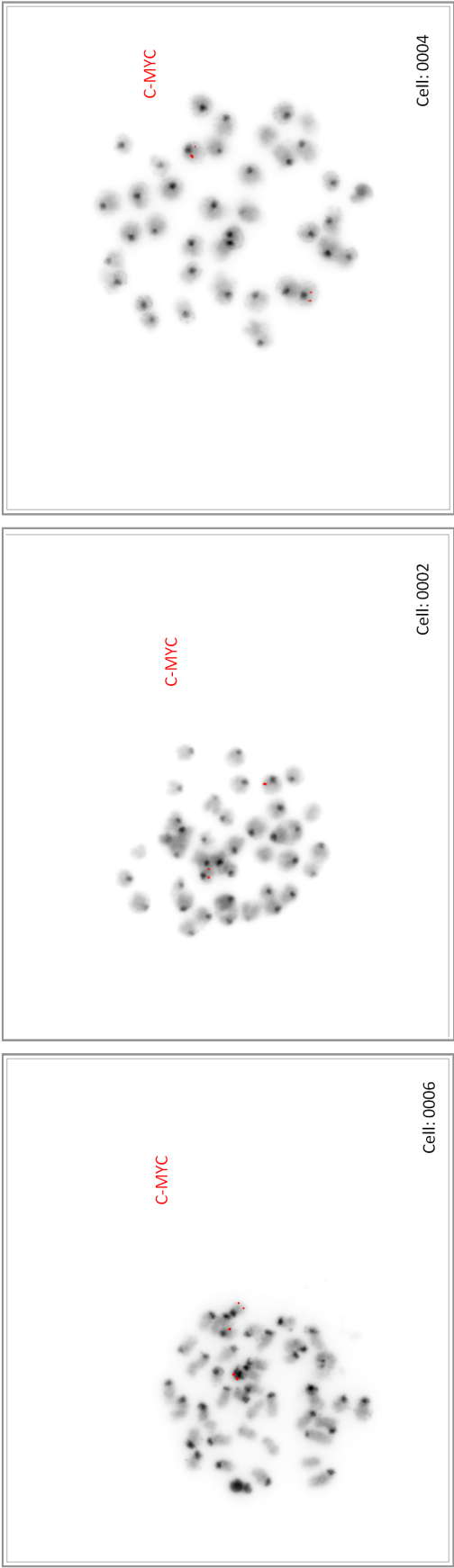
Red: 'C-MYC' probe hybridises within the c-Myc gene

R= Red probe

Figure 5.20 Representative cells for Atm-/-nu-/- B cell lymphoma c-Myc targeted FISH analysis

Atm-/-nu-/- B cell lymphoma 37F3   Result: 2R
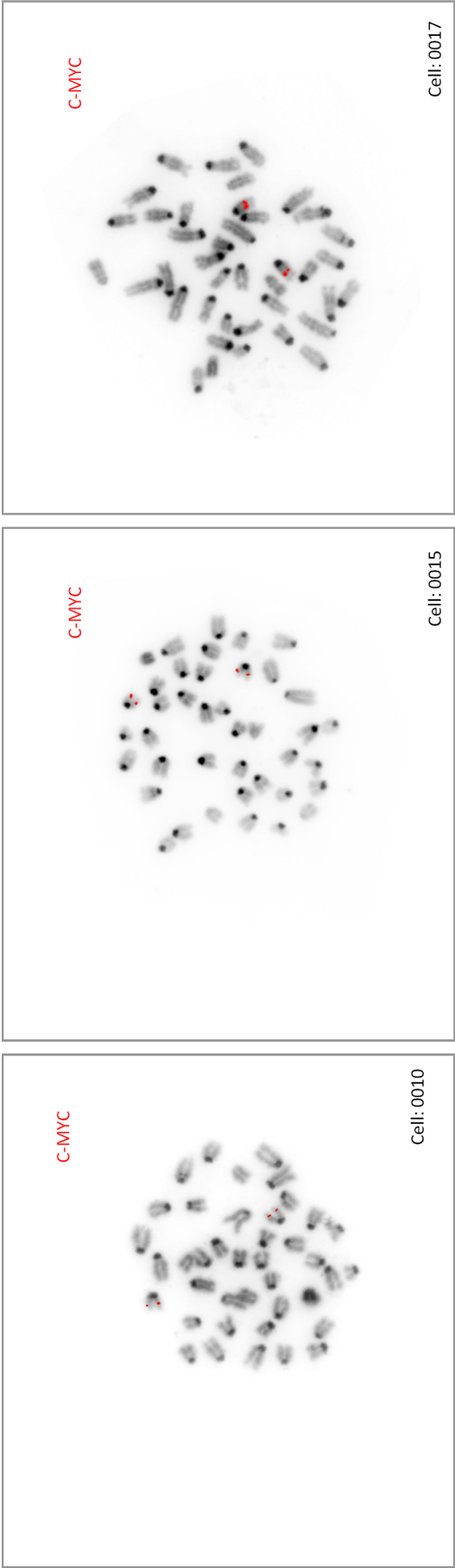
Red: 'C-MYC' probe hybridises within the c-Myc gene

R= Red probe

Figure 5.21 Representative cells for Atm-/-nu-/- B cell lymphoma c-Myc targeted FISH analysis

Atm-/-nu-/- B cell lymphoma 68F2   **Result: 3R 2G**
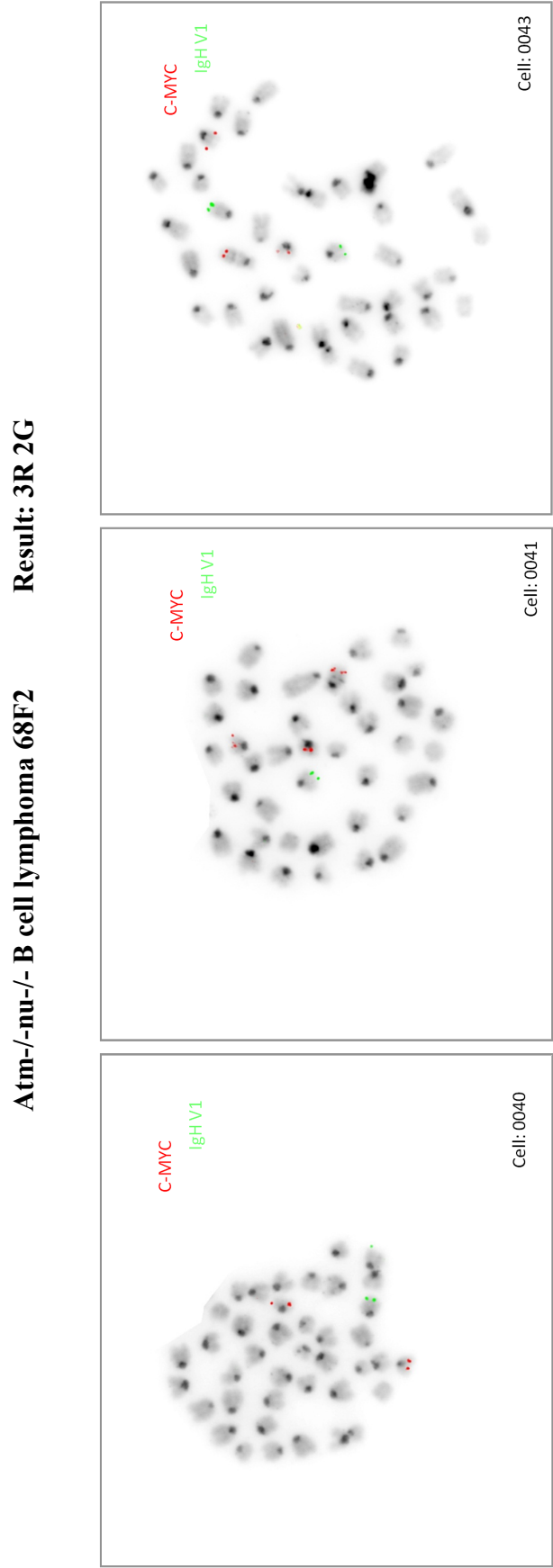
Red: 'C-MYC' probe hybridises within the c-Myc gene. Green: IgH v1 hybridises 5' of the variable region of IgH (Distal).

R= Red probe

G= Green probe

Figure 5.22 Representative cells for Atm–/–nu–/– B cell lymphoma c-Myc targeted FISH analysis

Atm-/-nu-/- B cell lymphoma 50F2   Result: 2R
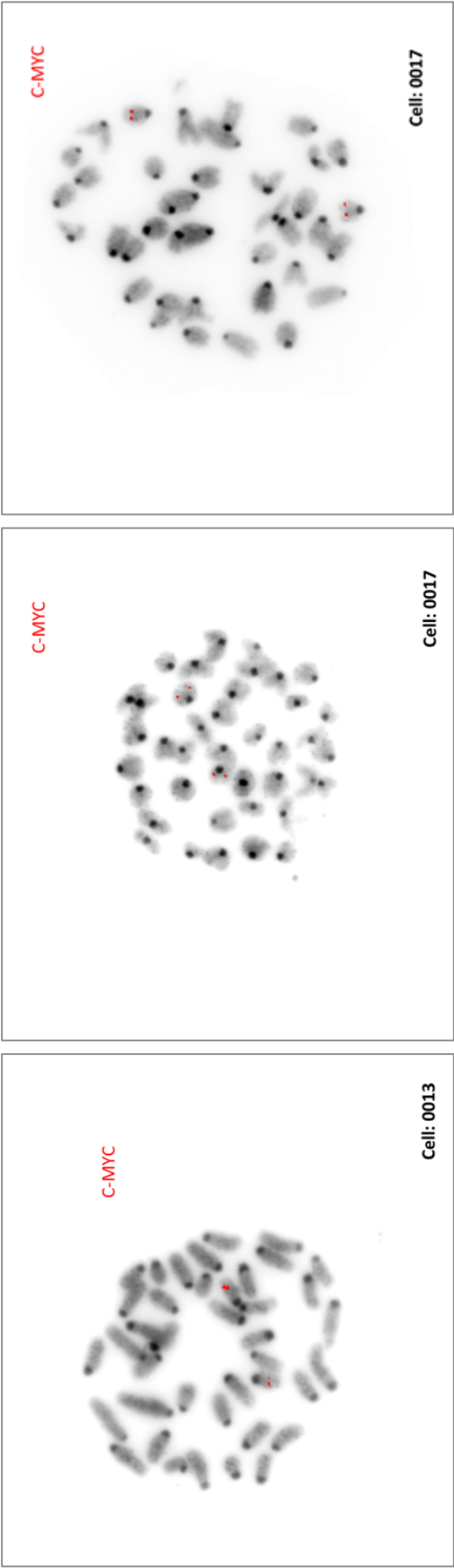
Red: 'C-MYC' probe hybridises within the c-Myc gene

R= Red probe

Figure 5.23 Representative cells for Atm Δ/Δ control B cells IgH targeted FISH analysis

Atm Δ/Δ splenocytes   Result: 1F 1R1G and 2F (Not shown)
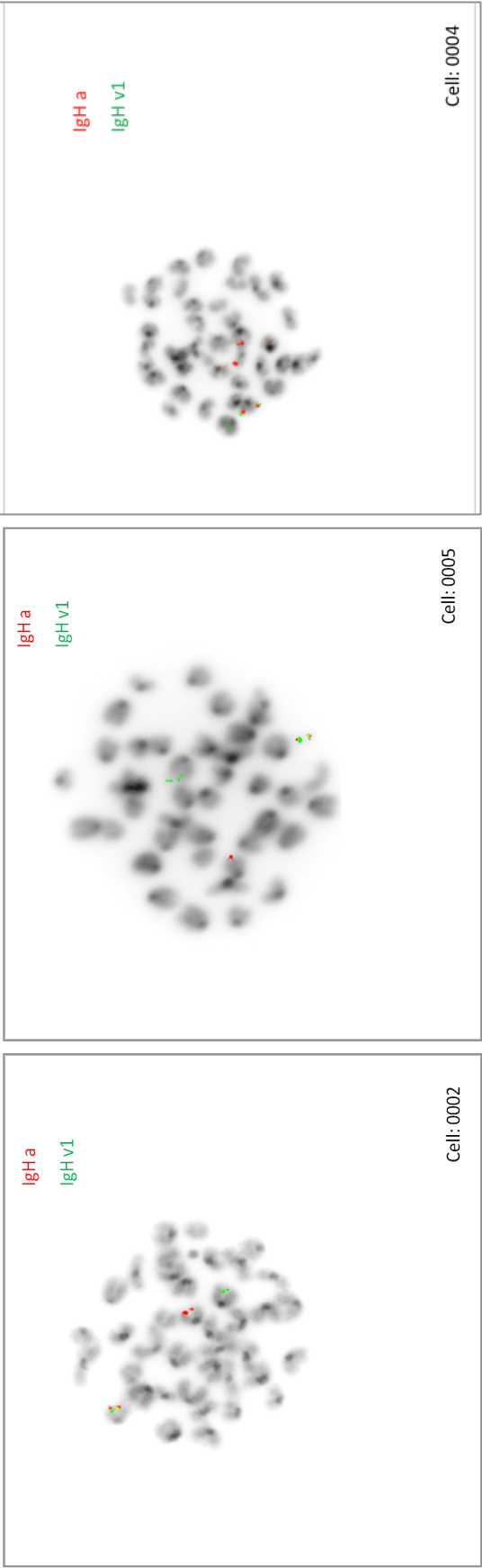
Red: IgH a probe hybridises with the alpha constant region of IgH (Proximal).

Green: IgH v1 hybridises 5' of the variable region of IgH (Distal).

F= fusion. Both red (R) and green (G) probe in close proximity to each other and represents a normal IgH gene.

Figure 5.24 Representative cells for Atm-/-nu-/- B cell lymphoma IgH targeted FISH analysis

Atm-/-nu-/- B cell lymphoma 703   **Result: 2R**
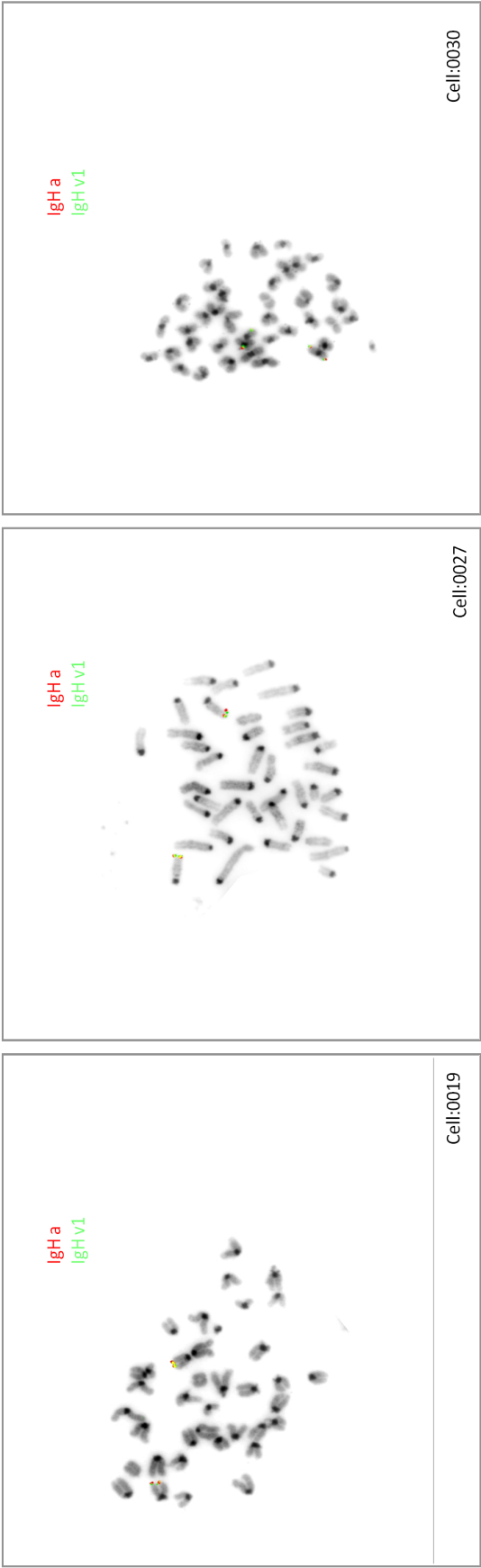
Red: IgH a probe hybridises with the alpha constant region of IgH (Proximal).

Green: IgH v1 hybridises 5' of the variable region of IgH (Distal).

F= fusion. Both red (R) and green (G) probe in close proximity to each other and represents a normal IgH gene.

Figure 5.25 Representative cells for Atm-/-nu-/- B cell lymphoma IgH targeted FISH analysis

Atm-/-nu-/- B cell lymphoma 5F3   Result: 1F1R
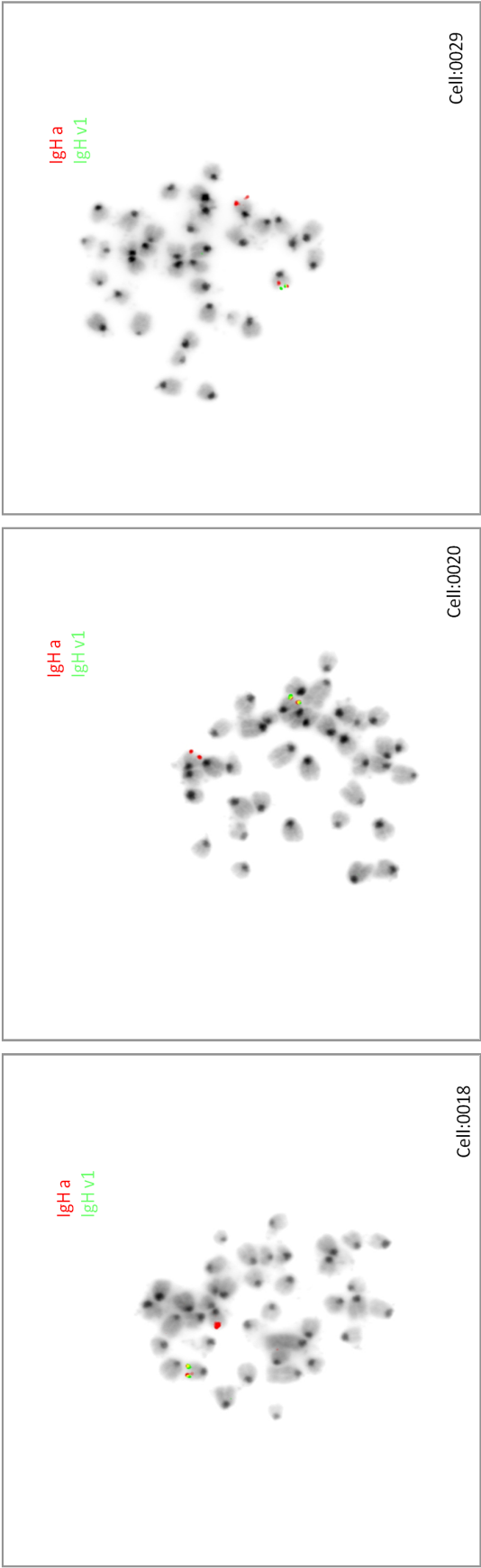
Red: IgH a probe hybridises with the alpha constant region of IgH (Proximal).

Green: IgH v1 hybridises 5' of the variable region of IgH (Distal).

F= fusion. Both red (R) and green (G) probe in close proximity to each other and represents a normal IgH gene.

Figure 5.26 Representative cells for Atm–/–nu–/– B cell lymphoma IgH targeted FISH analysis

Atm–/–nu–/– B cell lymphoma 593   Result: 1F
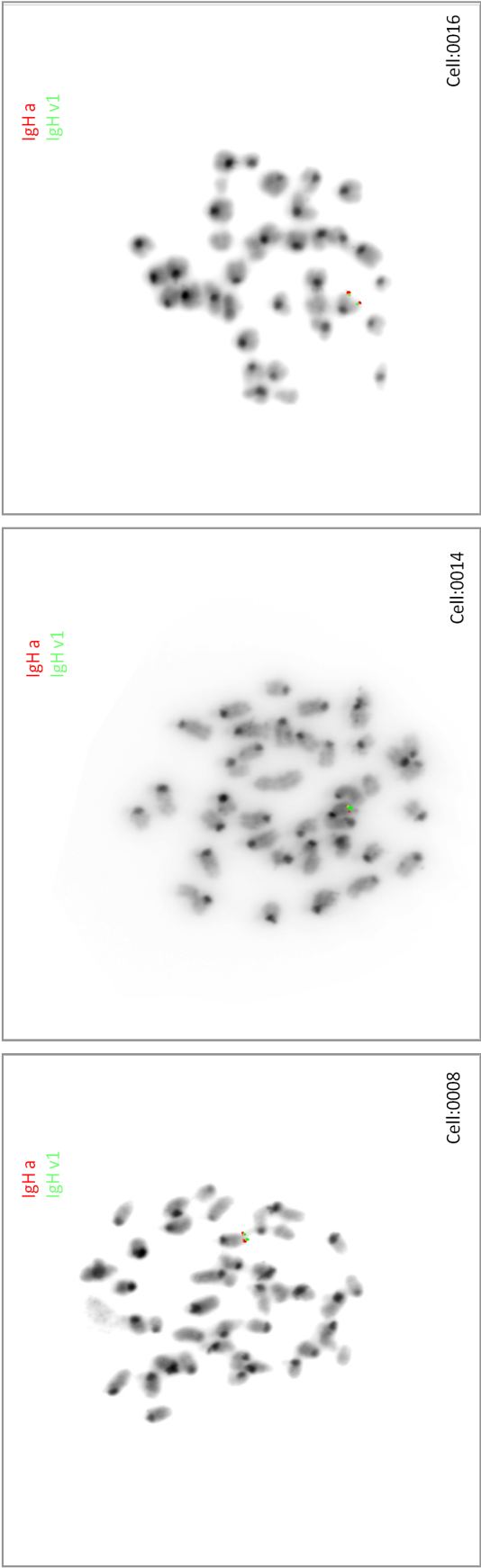
Red: IgH a probe hybridises with the alpha constant region of IgH (Proximal).

Green: IgH v1 hybridises 5' of the variable region of IgH (Distal).

F= fusion. Both red (R) and green (G) probe in close proximity to each other and represents a normal IgH gene.

Figure 5.27 Representative cells for Atm−/−nu−/− B cell lymphoma IgH targeted FISH analysis

Atm−/−nu−/− B cell lymphoma 50F2   **Result: 2F (1F)**
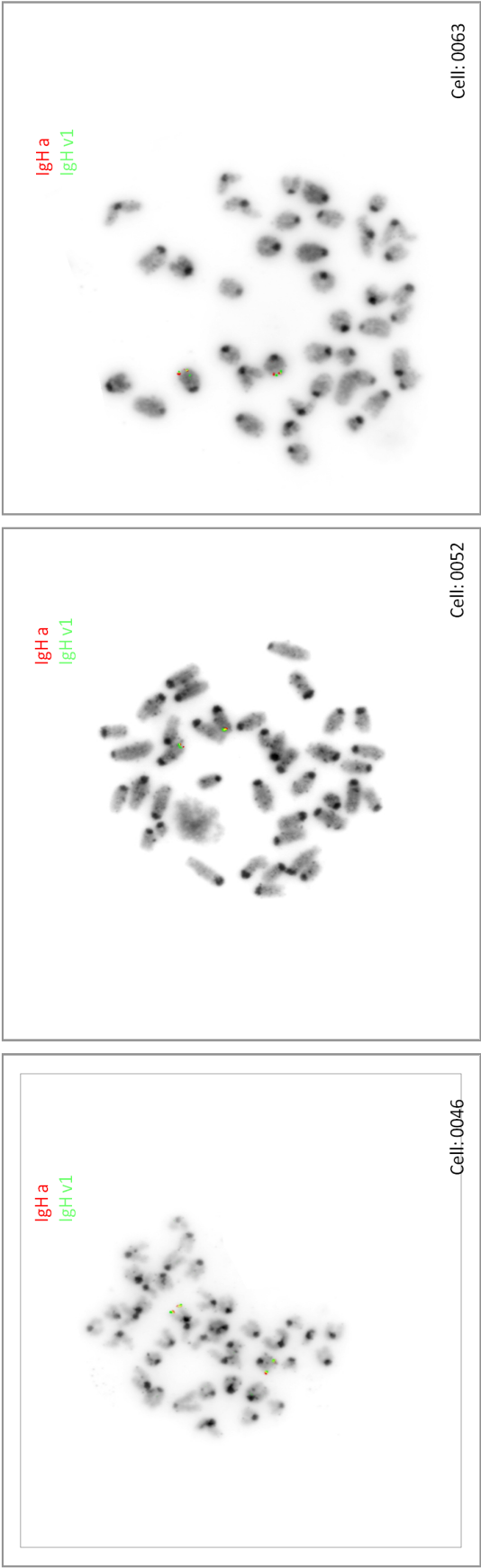
Red: IgH a probe hybridises with the alpha constant region of IgH (Proximal).

Green: IgH v1 hybridises 5' of the variable region of IgH (Distal).

F= fusion. Both red (R) and green (G) probe in close proximity to each other and represents a normal IgH gene.

Figure 5.28 Representative cells for Atm−/−nu−/− B cell lymphoma IgH targeted FISH analysis

Atm−/−nu−/− B cell lymphoma 37F3   **Result: 2F**
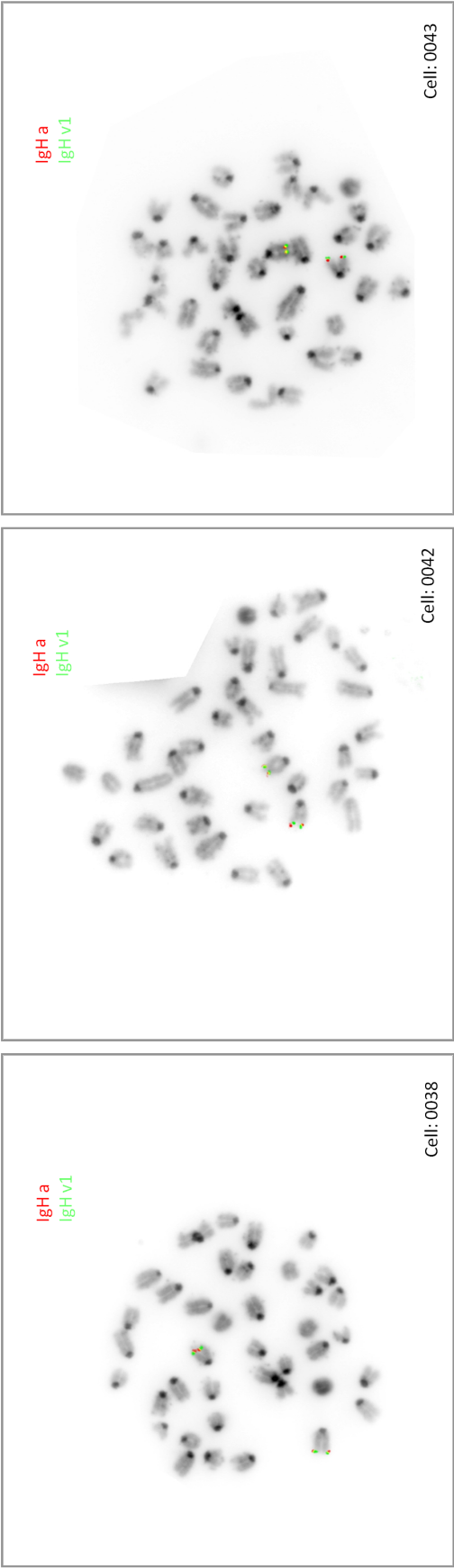
Red: IgH a probe hybridises with the alpha constant region of IgH (Proximal).

Green: IgH v1 hybridises 5' of the variable region of IgH (Distal).

F= fusion. Both red (R) and green (G) probe in close proximity to each other and represents a normal IgH gene.

Figure 5.29 Representative cells for Atm-/-nu-/- B cell lymphoma IgH targeted FISH analysis

Atm-/-nu-/- B cell lymphoma 68F2   Result: 1F 2R* 1R
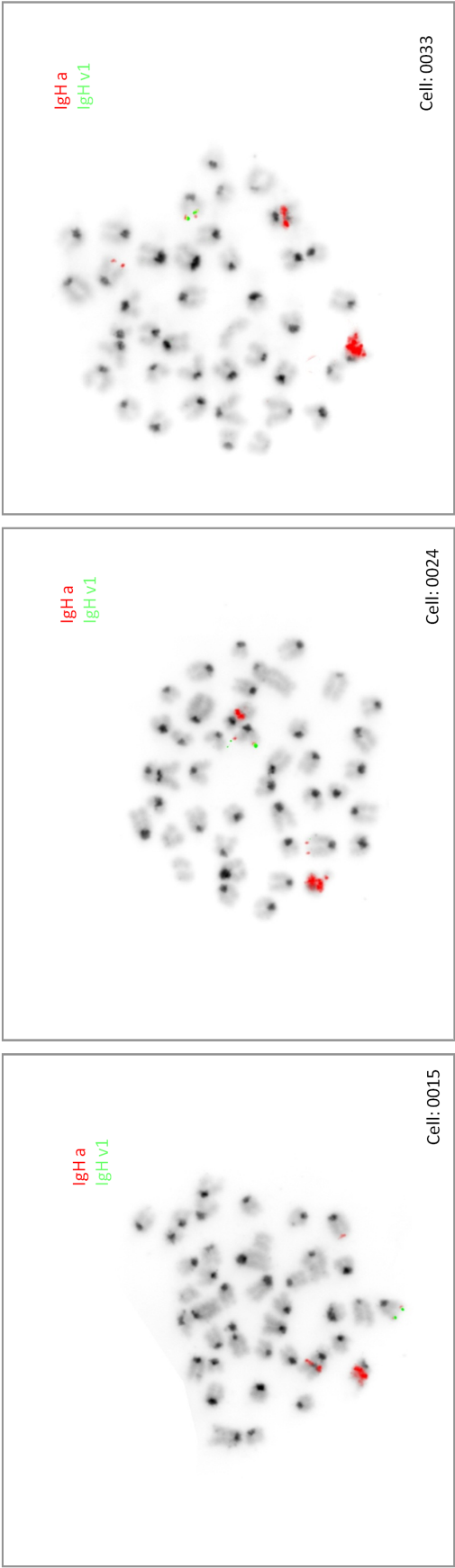

Red: IgH a probe hybridises with the alpha constant region of IgH (Proximal).

Green: IgH v1 hybridises 5' of the variable region of IgH (Distal).

F= fusion. Both red (R) and green (G) probe in close proximity to each other and represents a normal IgH gene.

* amplification of IgH a signal

CHAPTER 6

OVERALL DISCUSSION

6   OVERALL DISCUSSION

The predisposition of ataxia telangiectasia (A-T) patients to developing cancer has long been recognised (Morrell et al., 1986). Discovering the *ATM* gene mutated in the disease in 1995, and its product, ATM, a DNA damage repair protein, was the beginning of investigation into the association between ATM and cancer. As A-T is a relatively uncommon disease (it affects approximately 1 in 330,000 individuals in the UK), it is difficult to perform large scale studies of tumour development in these patients (Taylor et al., 1996, Reiman et al., 2011). However, shortly after the identification of the human *ATM* gene in 1995, the mouse Atm gene was identified and several mice models were generated in order to investigate the basis of A-T further and the relationship of loss of Atm to cancer predisposition (Savitsky et al., 1995, Pecker et al., 1996).

A-T mice that had no Atm protein expression (Barlow et al., 1996, Borghesani et al., 2000, Xu et al., 1996, Elson et al., 1996) recapitulated certain phenotypes associated with A-T such as immunodeficiency and some aspects of the neurological abnormality, but they did not develop the full range of haematological malignancies that have been diagnosed in A-T patients. Instead they almost exclusively developed thymoma, albeit at varying age and penetrance, depending on the study (See table 1.1)(Barlow et al., 1996, Borghesani et al., 2000, Xu et al., 1996, Elson et al., 1996).

The idea, here, of making the Atm-/-nu-/- mouse was to abrogate T cell tumour development in order to investigate the development of other tumour types associated with the loss of Atm. Indeed, Atm-/-nu-/- mice did not develop thymomas. Instead the Atm-/-nu-/- mice developed mostly B cell lymphoma of the spleen. To my knowledge the Atm-/-nu-/- mouse is the only mouse model of A-T that completely lacked Atm protein expression in all cells and

spontaneously developed B cell lymphoma. Therefore my study gave a unique perspective into the development of B cell lymphoma in the absence of Atm protein.

In addition to the 17 B cell lymphomas I found one T cell lymphoma in the Atm-/-nu-/- mice. This is a reversal of the predominance of thymomas in the Atm-/- single knockout animal. It is not clear whether analysis of a larger number of Atm-/-nu- tumours would reveal a consistent low proportion of T cell tumours, which would be more representative of the spectrum of tumour development in patients with A-T.

Morphological analysis of the B cell lymphoma that developed in the Atm-/-nu-/- mice suggested that they were mature B cell lymphoma; mostly diffuse large B cell lymphoma (DLBC) and Follicular lymphoma (FL), which both have a germinal centre cell origin (Khodabakhshi et al., 2012). Genetic analysis of human DLBCL and FL shows that they both have evidence of somatic hypermutation (SHM) in the variable region. In FL especially, mutation is on-going and extensive (Swerdlow, 2008). It is unknown if my Atm-/-nu-/- B cell lymphoma have SHM. Cases have been described of A-T patients developing DLBCL (Machida et al., 2013) but I am not aware of any cases of FL in A-T patients (Taylor et al., 1996, Machida et al., 2013, Sandoval and Swift, 1998).

An A-T mouse was generated by Spring and colleagues, that carried the murine equivalent of the ataxia telangiectasia mutation 7636del9, in which 44% (19 of 43) developed thymomas and in addition, 7 of 43 (16%) mice developed malignancies of non-T cell origin. Of these 7 mice Spring mice that developed non-T cell tumours, three developed B cell leukaemia after 10 months of age (Spring et al., 2001). No phenotypic or genetic information was provided about the B cell leukaemia that developed apart from that they lacked FasL up-regulation. In addition to the B cell leukaemia, ovarian granulosa cell, epithelial carcinoma, ovarian sex

cord and stromal cell tumours were also observed in the Spring mice that survived over the age of 10 months. The mutation in the Spring mouse, therefore, reduced the frequency of thymoma development from 100% - 44% in A-T mice compared to the Barlow mice. In addition, the mutation also increased the survival of the mice that did not develop thymoma, allowing the development of other tumour types to occur.

The Spring mice demonstrated that, in the absence of thymoma development, B cell leukaemia development could occur in A-T mice. The ataxia telangiectasia 7636del 9 (in frame deletion of amino acids SRI) mutation allowed expression of a very low level of ATM protein but without measurable activity (see Reiman et al., 2011) and therefore this is a null allele with respect to activity; this was also the case for the Spring mice. Another feature associated with presence of a null allele is typical increased radiosensitivity of A-T patients. This typical increased radiosensitivity is also associated with the 7636del9 allele in ataxia telangiectasia, consistent with their being no activity associated with any expressed protein from this allele.

It is not understood why the Spring mice had such a different phenotype compared with Atm null mice, but the possibility that some kinase dead Atm protein may have some effect, at least in mice, is reminiscent of the work by Yamomoto et al., (2012) and Daniel et al., (2012) who demonstrated a different effect of expression of a normal level of kinase dead Atm compared with absence of expression of any Atm protein. Another possibility in the Spring mice is that the low level of Atm protein expressed from this particular allele does have some effective activity but that is undetectable.

Approximately, 23% (16 of 71) of my Atm-/-nu-/- mice developed B cell lymphoma. Although this is a modest frequency, the Atm-/-nu-/- mouse allows the investigation into the development of B cell malignancy in the absence of Atm protein expression.

I used the Wynshaw Boris (Barlow) (Barlow et al., 1996) Atm-/- mouse to generate the Atm-/-nu-/- mouse. The Atm-/- and Atm-/-nu-/- mice were confirmed to be A-T mice as no Atm protein could be detected in tissue from either of these genotypes (Figure 3.3) and Atm-/- and Atm-/-nu-/- cells were also both unusually radiosensitive (Table 3.4 and 3.5). Despite this, introducing the nude (nu-/-) mutation into the Atm-/- mouse could have had the potential to alter the A-T phenotype in the Atm-/-nu-/- mice. Nude mice are immunocompromised due to abrogated thymic development (Pantelouris, 1968). Haematological comparison of the Atm-/-nu-/- and Atm-/- relative to wild type mice was undertaken to establish the extent to which this mutation affected the A-T phenotype in the Atm-/-nu-/- mice. Relative to wild type mice both the Atm-/- and Atm-/-nu-/- were similar. Both the Atm-/- and Atm-/-nu-/- had reduced T cell, increased granulocyte and reduced B cell proportions in the bone marrow. However a difference was detected. The proportion of transitional B cells (B220 high IgM+) was reduced in the spleen of Atm-/-nu-/- mouse compared to wild type, but the transitional (B220high IgM+) B cell population in the nude (Atm+/+nu-/-) was normal. Therefore this abnormality was unlikely to be a consequence of the nude phenotype. The Atm-/-nu-/- mice had a defect in mature B cell development in the spleen and developed mature B cell lymphoma. Therefore, the cause of the B cell developmental defect in the Atm-/-nu-/- mice could also be associated with subsequent B cell tumourigenesis.

With regard to the origin of the lymphoid tumours in A-T, cells from A-T patients have been found to be sensitive to the effects of ionising radiation, have genetic instability and an increase in the number of spontaneous translocations (Meyn, 1999) found in approximately

10% of peripheral T cells in A-T patients (Taylor et al., 1996). The translocations usually involve chromosome 7 and 14 at the locations of TCR genes. The presence of a translocation alone, apparently, could confer a selective growth advantage to the cells. However, for tumour growth additional genetic changes were observed associated with development of T cell malignancies (T-PLL) (Taylor et al., 1996). I identified translocations involving chromosomes that carried immune genes in Atm-/- thymoma cells in the control experiments I performed during this study. Liyanage and colleagues detected similar abnormalities; t(12;14) and t(12;15) translocations that were each present in 50% of the Atm-/- thymomas. In some cases both t(12;14) and t(12;15) were present in the same thymoma (Liyanage et al., 2000). Zha and colleagues showed that thymoma from A-T mice had multiple translocations, often involving breakage of the immune genes (Zha et al., 2010). Despite being frequently associated with the thymoma, it is not known if t(12;15) confers any growth advantage. However, it is known that the oncogene Myc is located on chromosome 15, and t(12;15) is likely to place the Myc gene under the regulation of the IgH promoter. Chromosome 15 abnormalities were present in almost all Atm-/- thymomas, whether in the form of t(12;15) or another type of chromosome abnormality (Liyanage et al., 2000). The requirement for increased Myc expression for tumourigenesis is questionable as abnormalities in chromosome 15 that result in Myc gene copy number have not been found to correlate with increased levels of Myc mRNA (Liyanage et al., 2000). In addition, not all Myc abnormalities involved translocations with an immune gene, so it is unlikely that this is the only mechanism that enables Atm-/- lymphoma development (Liyanage et al., 2000).

Recognising the role for Myc deregulation in the development of T cell lymphoma in Atm-/- mice and the potential for Atm-/- B cells to develop IgH-Myc complicons in vitro, Tepsuporn

and colleagues (2014) generated an A-T mouse to investigate the role of IgH- Myc translocation in the development of B cell lymphoma (Tepsuporn et al., 2014).

Very recently, Tepsuporn and colleagues generated a mouse that could test the involvement of aberrant recombination and apoptotic inactivation in the development of B cell lymphoma (Tepsuporn et al., 2014). The idea was to introduce mutations into the Atm-/- mouse that would promote DSB formation in the oncogene Myc and prevent apoptosis and promote survival in response to these abnormal DSBs, by increasing the expression of Bcl2. Compound Atm-/- mutant mice were generated that had a Myc gene that contained a RAG1/2 target sequence, DJβ; other Atm-/- mice were generated with increased Bcl2 expression due to the presence of an Eμ-Bcl2 construct. A third Atm-/- mouse was generated with both of these constructs. Both the Atm-/- mice with the DJβ sequence and the Atm-/- mice with the Eμ-Bcl2 developed B cell lymphomas; tumours occurred in approximately one third of the mice and were of peripheral B cell origin. The tumours expressed surface IgM and did not show evidence of SHM or CSR. The remaining mice developed thymoma at a similar age as Atm-/- mice. All Atm-/- mice that had both the DJβ insertion and Eμ-Bcl2 developed B cell lymphoma. B cell lymphoma in these mice had complex translocations involving chromosome 12 and 15 and had amplification of Myc. The development of B cell lymphomas in mice with both the DJβ insertion and Eμ-Bcl2 supported the idea that aberrant recombination of RAG induced breaks in mature B Cells led to lymphoma development as a result of increased Myc expression. However, even in the absence of Atm protein aberrant recombination alone was not enough to guarantee tumour development, as two thirds of mice did not develop B cell lymphoma. This was caused by apoptosis of the developing B cell tumours, since the Atm-/- with both DJβ and Eμ-Bcl2 developed B cell lymphomas. Tumourigenesis was likely due to the avoidance of apoptosis and promotion of proliferation

by Bcl2 expression from the Eμ-Bcl2 transgene. This model also reinforced the notion that tumour development is a multistep process and also suggested that the loss of Atm, alone, may not be sufficient for the development of B cell lymphoma. The suggestion was that Atm loss created an environment that enabled accumulation of unrepaired DSB but anti-apoptotic signalling was also required for B cell lymphoma development. This study also highlighted the observation that the high rate of T cell lymphoma development in Atm-/- mice and the absence of B cell lymphoma development may be because it is easier to overcome apoptotic signalling in thymic T cell than in mature B cells.

In keeping with this mechanism of tumour development, translocations involving chromosomes (12 or 14) that carry immune system genes were present in half of the Atm-/-nu-/- B cell lymphomas analysed in my study, but in only one of these tumours did the translocation involve the IgH gene. This tumour (68F2) contained der(12)t(12;15) detected by M-FISH. In addition, targeted FISH analysis of this lymphoma detected an IgH translocation, and 3 copies of the Myc gene (Table 5.8). Morphologically this tumour resembled a small cell lymphoma, which are typically of a non-germinal centre origin. The characteristics of this lymphoma matched those that were described by Tepsuporn et al, (2014). Tumour development in the Tepsuporn mice was accelerated by the genetic manipulation described above. Without engineered breaks in an oncogene and the presence of apoptotic resistant cells the likelihood of a translocation that leads to tumourigenesis may be lessened and therefore tumour development associated with IgH translocations and Myc amplification may be less common than the frequency observed in the Tepsuporn mice. In addition, tumourigenesis would be likely to take much longer. This is consistent with the tumour development observed in the Atm-/-nu-/- mouse 68F2 that was discovered at 6 months of age rather than as

early as 7 weeks in the Tepsuporn mice (Atm-/- with both DJβ and Eμ-Bcl2 mice) that developed tumours between 7 and 14 weeks of age.

Most of my Atm-/-nu-/- B cell lymphomas did not have any rearrangement of chromosomes containing immune genes. That there was a small proportion of Atm-/-nu-/- tumours with a t(12;15) translocation suggests that this was not the only or even the most common mechanism of development of B cell lymphoma in Atm-/-nu-/- mice. Myc deregulation can occur via alternative mechanisms in addition to changes to gene copy number (Sewastianik et al., 2014). It would be useful to measure the level of Myc mRNA in the Atm-/-nu-/- all B cell lymphoma to confirm that Myc protein level is in fact normal.

Atm-/-nu-/- B cell lymphoma were similar to the Atm-/- DJβ Eμ-Bcl2 B cell lymphomas in the Tepsuporn mice in that clonal chromosomal translocations were detected, although translocations rarely involved chromosome 12 and 15. Instead, abnormalities involving chromosome 17 and 18 were common in the Atm-/-nu-/- B cell lymphoma. So both the Atm-/-nu-/- and Tepsuporn mice develop B cell lymphomas associated with clonal chromosomal translocation, albeit different chromosomes and presumably different mechanisms.

Apart from both containing clonal translocations the Atm-/-nu-/- and Atm-/- DJβ Eμ-Bcl2 B cell lymphomas are largely different. Atm-/-nu-/- and Atm-/- DJβ Eμ-Bcl2 B cell lymphomas differ in their B cell origin. Like Atm-/-nu-/- B cell lymphomas, Atm-/- DJβ Eμ-Bcl2 tumours, had expression of IgM, but did not have evidence of somatic hypermutation and therefore were suggested to be Pre-GC cell origin. Atm-/-nu-/- B cell lymphoma were likely to be of a later differentiation stage. Excluding 68F2, Atm-/-nu-/- B cell lymphomas were mostly diffuse large B cell lymphomas (DLBCL) and follicular lymphomas (FL) which are of a germinal centre B cell (or post germinal centre in some cases of DLBCL) origin (Swerdlow,

2008). The Atm-/-nu-/- B cell lymphomas were not tested for evidence of SHM. If the IgH variable gene of the Atm-/-nu-/- lymphomas were mutated this would confirm their germinal centre origin (Berek and Milstein, 1987).

As discussed earlier there are few mouse models that enable investigation into B cell lymphoma in the absence of Atm. However, mice lacking the ATM interactor (ATMIN) protein specifically in B cells (ATMIN ΔB/ΔB mice), that develop B cell lymphomas (Loizou et al., 2011) have been described. ATMIM may possibly play a role in the activation of ATM, although the conditions of this activation are not thoroughly understood at this time. ATMIN ΔB/ΔB mice are phenotypically similar to Atm-/- and Atm-/-nu-/- mice in that lymphocyte development is perturbed in these mice (Loizou et al., 2011, Barlow et al., 1996). The level of CSR is also reduced in ATMIN ΔB/ΔB B cells suggesting a role for ATMIN in the repair of AID induced DSB. Immunophenotyping of the ATMIN ΔB/ΔB B cell lymphomas suggested that they range from the pre B to plasma cell stage of differentiation. Similarly, despite Atm-/-nu-/- B cell lymphoma being predominantly of germinal centre B cell origin, there is an element of phenotypic heterogeneity within the group Atm-/-nu-/- tumours analysed in this study. It would be interesting to determine the stage of differentiation of the Atm-/-nu-/- B cell lymphoma more definitively by measuring SHM. In addition, as the Atm-/-nu-/- tumours have multiple translocations and as AID has been shown to be responsible for the generation of DSB and translocations in Atm null B cells it would be interesting to measure AID expression levels in the tumours (Callén et al., 2007).

Both Atm-/- and ATMIN ΔB/ΔB mice have perturbed B cell development, reduced CSR and increased genomic instability (Loizou et al., 2011), which suggests that the roles of ATM and ATMIN are closely related, and therefore their mechanism of development of B cell lymphoma may be similar. M-FISH analysis of the ATMIN ΔB/ΔB B cell lymphoma

revealed that they have clonal translocations. These translocations involved both chromosomes that contain immune system genes and those without. In addition to this, no chromosome 15 abnormalities were detected, in the ATMIN ΔB/ΔB B cell lymphomas. If chromosome 15 was normal it is unlikely that Myc gene abnormalities were also present in the ATMIN ΔB/ΔB, B cell lymphoma. This differs to the Atm-/- T cell thymoma and Tepsuporn tumours that had chromosome 15 abnormalities in almost every tumour (Liyanage et al., 2000, Tepsuporn et al., 2014). With exception to the Atm-/-nu-/- B cell lymphoma 68F2 discussed above, and the 3 copies of Myc gene detected in Atm-/-nu-/- B cell lymphoma 5F3, chromosome 15 abnormalities and translocations involving chromosome 12 or 14 were infrequent in Atm-/-nu-/- B cell lymphoma. Thus the ATMIN ΔB/ΔB mice along with the Atm-/-nu-/- both demonstrated tumour development in B cells that was unlikely to be dependent on deregulation of Myc. Thus, there are features of B cell lymphoma development in common between these two models. It is possible that the Tepsuporn mice, requiring both DJβ and Eμ-Bcl2 constructs (induced break and resistance to apoptosis) are the exception, determined by this additional manipulation. B cell tumour development in Atm-/-nu-/- mice may represent a model close to ataxia telangiectasia; as A-T patients develop both B and T cell lymphomas.

In human lymphomas, MYC deregulation is most commonly associated with Burkitt lymphoma (BL). In more that 85% of BL IGH-MYC fusions are formed by the t(8;14) translocation. This translocation places MYC expression under the influence of the IGH promoter and consequently causes constant expression of the gene. Translocations associated with *MYC* are also found in roughly 10% of DLBCL and FL, which is similar to the Myc deregulation seen in Atm-/-nu-/- B cell lymphoma (1 in 6). In DLBCL and FL in humans *MYC* abnormalities are usually secondary to translocations involving *BCL2* or *BCL6*

(Sewastianik et al., 2014, Swerdlow, 2008). This illustrates that there are other factors to consider in addition to IGH-MYC fusions. The Atm-/-nu-/- mouse is a model that enables investigation to these other mechanisms of tumour development.

ATM mutations are frequently found in human B-CLL and MCL (Stankovic et al., 1999, Schaffner et al., 2000). Somatic loss of ATM can be caused by deletion of the part of chromosome 11 where *ATM* is located and/or mutation in the *ATM* gene (Stankovic et al., 2002). Additional genetic lesions usually accompany ATM inactivation in these tumours.

Chromosome 17 and 18 translocations were common in Atm-/-nu-/- B cell lymphomas. These chromosome breaks could be in areas that are prone to translocation such as fragile sites, but the recurrent selection for translocations in 17 and 18 suggests that genes involved in these translocations could have a role in tumour progression (Ozeri-Galai et al., 2007). Like the role of BCL2 and BCL6 in DLBCL and FL, oncogenes and/or tumour suppressor genes located on chromosome 17 and 18 could be candidates for causing tumorigenic transformation in the Atm-/-nu-/- mice. Identification of these genes would enable better understanding and treatments for B cell lymphoma both in A-T patients and ATM mutated tumours of the general population (Sandoval and Swift, 1998, Reiman et al., 2011).

CHAPTER 7

REFERENCES

7 REFERENCES

Abraham, R. T. 2001. Cell cycle checkpoint signaling through the atm and atr kinases. *Genes & development,* 15, 2177-2196.

Allen, C. D., Okada, T. & Cyster, J. G. 2007a. Germinal-centre organization and cellular dynamics. *Immunity,* 27, 190-202.

Allen, C. D., Okada, T., Tang, H. L. & Cyster, J. G. 2007b. Imaging of germinal centre selection events during affinity maturation. *Science,* 315, 528-531.

Allman, D., Li, J. & Hardy, R. R. 1999. Commitment to the b lymphoid lineage occurs before dh-jh recombination. *The Journal of experimental medicine,* 189, 735-740.

Alt, F. W., Blackwell, T. K., Depinho, R. A., Reth, M. G. & Yancopoulos, G. D. 1986. Regulation of genome rearrangement events during lymphocyte differentiation. *Immunological reviews,* 89, 5-30.

Alt, F. W., Zhang, Y., Meng, F.-L., Guo, C. & Schwer, B. 2013. Mechanisms of programmed DNA lesions and genomic instability in the immune system. *Cell,* 152, 417-429.

Ambrose, M. & Gatti, R. A. 2013. Pathogenesis of ataxia-telangiectasia: The next generation of atm functions. *Blood,* 121, 4036-4045.

Angèle, S., Laugé, A., Fernet, M., Moullan, N., Beauvais, P., Couturier, J., Stoppa-Lyonnet, D. & Hall, J. 2003. Phenotypic cellular characterization of an ataxia telangiectasia patient carrying a causal homozygous missense mutation. *Human mutation,* 21, 169-170.

Bakkenist, C. J. & Kastan, M. B. 2003. DNA damage activates atm through intermolecular autophosphorylation and dimer dissociation. *Nature,* 421, 499-506.

Barlow, C., Hirotsune, S., Paylor, R., Liyanage, M., Eckhaus, M., Collins, F., Shiloh, Y., Crawley, J. N., Ried, T., Tagle, D & Wynshaw-Boris. 1996. Atm-deficient mice: A paradigm of ataxia telangiectasia. *Cell,* 86, 159-171.

Barrans, S. L., Evans, P. A., O'connor, S. J., Kendall, S. J., Owen, R. G., Haynes, A. P., Morgan, G. J. & Jack, A. S. 2003. The t (14; 18) is associated with germinal center-derived diffuse large b-cell lymphoma and is a strong predictor of outcome. *Clinical Cancer Research,* 9, 2133-2139.

Bartkova, J., Hořejší, Z., Koed, K., Krämer, A., Tort, F., Zieger, K., Guldberg, P., Sehested, M., Nesland, J. M. & Lukas, C. 2005. DNA damage response as a candidate anti-cancer barrier in early human tumorigenesis. *Nature,* 434, 864-870.

Bastard, C., Deweindt, C., Kerckaert, J. P., Lenormand, B., Rossi, A., Pezzella, F., Fruchart, C., Duval, C., Monconduit, M. & Tilly, H. 1994. Laz3 rearrangements in non-hodgkin's lymphoma: Correlation with histology, immunophenotype, karyotype, and clinical outcome in 217 patients. *Blood,* 83, 2423-2427.

Beggs AD, Jones A, El-Bahwary M, Abulafi M, Hodgson SV, Tomlinson IP. 2012. Whole genome methylation analysis of benign and malignant colorectal tumours. *J Pathol,* 229, 697–704

Belizário, J. E. 2009. Immunodeficient mouse models: An overview. *Open Immunol J,* 2, 79-85.

Berek, C. & Milstein, C. 1987. Mutation drift and repertoire shift in the maturation of the immune response. *Immunological reviews,* 96, 23-41.

Bollum, F. 1979. Terminal deoxynucleotidyl transferase as a hematopoietic cell marker. *Blood,* 54, 1203-1215.

Borghesani, P. R., Alt, F. W., Bottaro, A., Davidson, L., Aksoy, S., Rathbun, G. A., Roberts, T. M., Swat, W., Segal, R. A. & Gu, Y. 2000. Abnormal development of purkinje cells and lymphocytes in atm mutant mice. *Proceedings of the National Academy of Sciences of the United States of America,* 97, 3336.

Bredemeyer, A. L., Sharma, G. G., Huang, C.-Y., Helmink, B. A., Walker, L. M., Khor, K. C., Nuskey, B., Sullivan, K. E., Pandita, T. K. & Bassing, C. H. 2006. Atm stabilizes DNA double-strand-break complexes during v (d) j recombination. *Nature,* 442, 466-470.

Brissette, J. L., Li, J., Kamimura, J., Lee, D. & Dotto, G. P. 1996. The product of the mouse nude locus, whn, regulates the balance between epithelial cell growth and differentiation. *Genes & development,* 10, 2212-2221.

Bross, L., Fukita, Y., Mcblane, F., Démollière, C., Rajewsky, K. & Jacobs, H. 2000. DNA double-strand breaks in immunoglobulin genes undergoing somatic hypermutation. *Immunity,* 13, 589-597.

Bryant, H. E. & Helleday, T. 2006. Inhibition of poly (adp-ribose) polymerase activates atm which is required for subsequent homologous recombination repair. *Nucleic acids research,* 34, 1685-1691.

Burma, S., Chen, B. P. & Chen, D. J. 2006. Role of non-homologous end joining (nhej) in maintaining genomic integrity. *DNA repair,* 5, 1042-1048.

Burma, S. & Chen, D. J. 2004. Role of DNA–pk in the cellular response to DNA double-strand breaks. *DNA repair,* 3, 909-918.

Callén, E., Jankovic, M., Difilippantonio, S., Daniel, J. A., Chen, H.-T., Celeste, A., Pellegrini, M., Mcbride, K., Wangsa, D. & Bredemeyer, A. L. 2007. Atm prevents the persistence and propagation of chromosome breaks in lymphocytes. *Cell,* 130, 63-75.

Camacho, S. A., Kosco-Vilbois, M. H. & Berek, C. 1998. The dynamic structure of the germinal center. *Immunology today,* 19, 511-514.

Canman, C. E., Lim, D.-S., Cimprich, K. A., Taya, Y., Tamai, K., Sakaguchi, K., Appella, E., Kastan, M. B. & Siliciano, J. D. 1998. Activation of the atm kinase by ionizing radiation and phosphorylation of p53. *Science,* 281, 1677-1679.

Cattoretti, G., Büttner, M., Shaknovich, R., Kremmer, E., Alobeid, B. & Niedobitek, G. 2006. Nuclear and cytoplasmic aid in extrafollicular and germinal center b cells. *Blood,* 107, 3967-3975.

Chaumeil, J., Micsinai, M., Ntziachristos, P., Roth, D. B., Aifantis, I., Kluger, Y., Deriano, L. & Skok, J. A. 2013. The rag2 c-terminus and atm protect genome integrity by controlling antigen receptor gene cleavage. *Nature communications,* 4.

Chen, B. P., Uematsu, N., Kobayashi, J., Lerenthal, Y., Krempler, A., Yajima, H., Löbrich, M., Shiloh, Y. & Chen, D. J. 2007. Ataxia telangiectasia mutated (atm) is essential for DNA-pkcs phosphorylations at the thr-2609 cluster upon DNA double strand break. *Journal of Biological Chemistry,* 282, 6582-6587.

Chen, G., Yuan, S. S. F., Liu, W., Xu, Y., Trujillo, K., Song, B., Cong, F., Goff, S. P., Wu, Y. & Arlinghaus, R. 1999. Radiation-induced assembly of rad51 and rad52 recombination complex requires atm and c-abl. *Journal of Biological Chemistry,* 274, 12748.

Chiarle, R., Zhang, Y., Frock, R. L., Lewis, S. M., Molinie, B., Ho, Y.-J., Myers, D. R., Choi, V. W., Compagno, M. & Malkin, D. J. 2011. Genome-wide translocation sequencing reveals mechanisms of chromosome breaks and rearrangements in b cells. *Cell,* 147, 107-119.

Chun, H. H. & Gatti, R. A. 2004. Ataxia-telangiectasia, an evolving phenotype. *DNA repair,* 3, 1187-1196.

Cooper, M. D. & Alder, M. N. 2006. The evolution of adaptive immune systems. *Cell,* 124, 815-822.

Crawford, T. O., Skolasky, R. L., Fernandez, R., Rosquist, K. J. & Lederman, H. M. 2006. Survival probability in ataxia telangiectasia. *Arch Dis Child,* 91, 610-1.

Cremona, C. A., & Behrens, A. 2014. Atm signalling and cancer. *Oncogene.* 33, 3351–3360.

Cunliffe, P., Mann, J., Cameron, A., Roberts, K. & Ward, H. 1975. Radiosensitivity in ataxia-telangiectasia. *The British journal of radiology,* 48, 374-376.

Daniel, J. A., Pellegrini, M., Lee, B.-S., Guo, Z., Filsuf, D., Belkina, N. V., You, Z., Paull, T. T., Sleckman, B. P., Feigenbaum, L. & Nussenzweig, A. 2012. Loss of atm kinase activity leads to embryonic lethality in mice. *The Journal of cell biology,* 198, 295-304.

Deriano, L., Chaumeil, J., Coussens, M., Multani, A., Chou, Y., Alekseyenko, A. V., Chang, S., Skok, J. A. & Roth, D. B. 2011. The rag2 c terminus suppresses genomic instability and lymphomagenesis. *Nature,* 471, 119-123.

Difilippantonio, M. J., Zhu, J., Chen, H. T., Meffre, E., Nussenzweig, M. C., Max, E. E., Ried, T. & Nussenzweig, A. 2000. DNA repair protein ku80 suppresses chromosomal aberrations and malignant transformation. *Nature,* 404, 510-514.

Difilippantonio, S., Celeste, A., Fernandez-Capetillo, O., Chen, H.-T., San Martin, B. R., Van Laethem, F., Yang, Y.-P., Petukhova, G. V., Eckhaus, M. & Feigenbaum, L. 2005.

Role of nbs1 in the activation of the atm kinase revealed in humanized mouse models. *Nature Cell Biology,* 7, 675-685.

Dimitrova, N., Chen, Y.-C. M., Spector, D. L. & De Lange, T. 2008. 53bp1 promotes non-homologous end joining of telomeres by increasing chromatin mobility. *Nature,* 456, 524-528.

Ehlich, A., Martin, V., Müller, W. & Rajewsky, K. 1994. Analysis of the b-cell progenitor compartment at the level of single cells. *Current Biology,* 4, 573-583.

Elson, A., Wang, Y., Daugherty, C. J., Morton, C. C., Zhou, F., Campos-Torres, J. & Leder, P. 1996. Pleiotropic defects in ataxia-telangiectasia protein-deficient mice. *Proceedings of the National Academy of Sciences,* 93, 13084.

Feldser, D., Strong, M. A. & Greider, C. W. 2006. Ataxia telangiectasia mutated (atm) is not required for telomerase-mediated elongation of short telomeres. *Proceedings of the National Academy of Sciences of the United States of America,* 103, 2249-2251.

Felix, C. A., Kolaris, C. P. & Osheroff, N. 2006. Topoisomerase ii and the etiology of chromosomal translocations. *DNA repair,* 5, 1093-1108.

Ferguson, D. O., Sekiguchi, J. M., Chang, S., Frank, K. M., Gao, Y., Depinho, R. A. & Alt, F. W. 2000. The nonhomologous end-joining pathway of DNA repair is required for genomic stability and the suppression of translocations. *Proceedings of the National Academy of Sciences,* 97, 6630-6633.

Flanagan, S. 1966. 'Nude', a new hairless gene with pleiotropic effects in the mouse. *Genetical research,* 8, 295-309.

Franco, S., Alt, F. W. & Manis, J. P. 2006. Pathways that suppress programmed DNA breaks from progressing to chromosomal breaks and translocations. *DNA repair,* 5, 1030-1041.

Gapud, E. J., Lee, B.-S., Mahowald, G. K., Bassing, C. H. & Sleckman, B. P. 2011. Repair of chromosomal rag-mediated DNA breaks by mutant rag proteins lacking phosphatidylinositol 3-like kinase consensus phosphorylation sites. *The Journal of Immunology,* 187, 1826-1834.

Gatti, R. A., Berkel, I., Boder, E., Braedt, G., Charmley, P., Concannon, P., Ersoy, F., Foroud, T., Jaspers, N. G. & Lange, K. 1988. Localization of an ataxia-telangiectasia gene to chromosome 11q22–23.

Genik, P. C., Bielefeldt-Ohmann, H., Liu, X., Story, M. D., Ding, L., Bush, J. M., Fallgren, C. M. & Weil, M. M. 2014. Strain background determines lymphoma incidence in< i> atm</i> knockout mice. *Neoplasia,* 16, 129-IN7.

Geuting, V., Reul, C. & Löbrich, M. 2013. Atm release at resected double-strand breaks provides heterochromatin reconstitution to facilitate homologous recombination. *PLoS genetics,* 9, e1003667.

Gilfillan, S., Dierich, A., Lemeur, M., Benoist, C. & Mathis, D. 1993. Mice lacking tdt: Mature animals with an immature lymphocyte repertoire. *Science,* 261, 1175-1178.

Gostissa, M., Alt, F. W. & Chiarle, R. 2011. Mechanisms that promote and suppress chromosomal translocations in lymphocytes. *Annual review of immunology,* 29, 319-350.

Grawunder, U., Wilm, M., Wu, X., Kulesza, P., Wilson, T. E., Mann, M. & Lieber, M. R. 1997. Activity of DNA ligase iv stimulated by complex formation with xrcc4 protein in mammalian cells. *Nature,* 388, 492-495.

Guo, Z., Deshpande, R. & Paull, T. T. 2010. Atm activation in the presence of oxidative stress. *Cell Cycle,* 9, 4805-4811.

Hauser, A. E., Kerfoot, S. M. & Haberman, A. M. Year. Cellular choreography in the germinal center: New visions from in vivo imaging. *In:* Seminars in immunopathology, 2010. Springer, 239-255.

He, J., Shi, L. Z., Truong, L. N., Lu, C.-S., Razavian, N., Li, Y., Negrete, A., Shiloach, J., Berns, M. W. & Wu, X. 2012. Rad50 zinc hook is important for the mre11 complex to bind chromosomal DNA double-stranded breaks and initiate various DNA damage responses. *Journal of Biological Chemistry,* 287, 31747-31756.

Hecht, F., Koler, R., Rigas, D., Dahnke, G., Case, M., Tisdale, V. & Miller, R. 1966. Leukaemia and lymphocytes in ataxia-telangiectasia. *The Lancet,* 288, 1193.

Heyer, W.-D., Ehmsen, K. T. & Liu, J. 2010. Regulation of homologous recombination in eukaryotes. *Annual review of genetics,* 44, 113-139.

Hill, M. E., Maclennan, K. A., Cunningham, D. C., Hudson, B. V., Burke, M., Clarke, P., Di Stefano, F., Anderson, L., Hudson, G. V. & Mason, D. 1996. Prognostic significance of bcl-2 expression and bcl-2 major breakpoint region rearrangement in diffuse large cell non-hodgkin's lymphoma: A british national lymphoma investigation study. *Blood,* 88, 1046-1051.

Ikehara, S., Pahwa, R. N., Fernandes, G., Hansen, C. T. & Good, R. A. 1984. Functional t cells in athymic nude mice. *Proceedings of the National Academy of Sciences of the United States of America,* 81, 886.

Isoda, T., Takagi, M., Piao, J., Nakagama, S., Sato, M., Masuda, K., Ikawa, T., Azuma, M., Morio, T. & Kawamoto, H. 2012. Process for immune defect and chromosomal translocation during early thymocyte development lacking atm. *Blood,* 120, 789-799.

Jackson, S. P. 2002. Sensing and repairing DNA double-strand breaks. *Carcinogenesis,* 23, 687-696.

Jeggo, P. & Löbrich, M. 2007. DNA double-strand breaks: Their cellular and clinical impact? *Oncogene,* 26, 7717-7719.

Johnson, N. A., Savage, K. J., Ludkovski, O., Ben-Neriah, S., Woods, R., Steidl, C., Dyer, M. J., Siebert, R., Kuruvilla, J. & Klasa, R. 2009. Lymphomas with concurrent bcl2 and myc translocations: The critical factors associated with survival. *Blood,* 114, 2273-2279.

Jungmichel, S., Clapperton, J. A., Lloyd, J., Hari, F. J., Spycher, C., Pavic, L., Li, J., Haire, L. F., Bonalli, M. & Larsen, D. H. 2012. The molecular basis of atm-dependent dimerization of the mdc1 DNA damage checkpoint mediator. *Nucleic acids research,* 40, 3913-3928.

Karlseder, J., Hoke, K., Mirzoeva, O. K., Bakkenist, C., Kastan, M. B., Petrini, J. H. & De Lange, T. 2004. The telomeric protein trf2 binds the atm kinase and can inhibit the atm-dependent DNA damage response. *PLoS biology,* 2, e240.

Kaushik, A., Kelsoe, G. & Jaton, J. C. 1995. The nude mutation results in impaired primary antibody repertoire. *European journal of immunology,* 25, 631-634.

Kepler, T. B. & Perelson, A. S. 1993. Cyclic re-entry of germinal center b cells and the efficiency of affinity maturation. *Immunology today,* 14, 412-415.

Khodabakhshi, A. H., Morin, R. D., Fejes, A. P., Mungall, A. J., Mungall, K. L., Bolger-Munro, M., Johnson, N. A., Connors, J. M., Gascoyne, R. D. & Marra, M. A. 2012. Recurrent targets of aberrant somatic hypermutation in lymphoma. *Oncotarget,* 3, 1308-1319.

Klein, I. A., Resch, W., Jankovic, M., Oliveira, T., Yamane, A., Nakahashi, H., Di Virgilio, M., Bothmer, A., Nussenzweig, A. & Robbiani, D. F. 2011. Translocation-capture sequencing reveals the extent and nature of chromosomal rearrangements in b lymphocytes. *Cell,* 147, 95-106.

Kocks, C. & Rajewsky, K. 1988. Stepwise intraclonal maturation of antibody affinity through somatic hypermutation. *Proceedings of the National Academy of Sciences,* 85, 8206-8210.

Kogan, S. C., Ward, J. M., Anver, M. R., Berman, J. J., Brayton, C., Cardiff, R. D., Carter, J. S., De Coronado, S., Downing, J. R. & Fredrickson, T. N. 2002. Bethesda proposals for classification of nonlymphoid hematopoietic neoplasms in mice. *Blood,* 100, 238-245.

Kolas, N. K., Chapman, J. R., Nakada, S., Ylanko, J., Chahwan, R., Sweeney, F. D., Panier, S., Mendez, M., Wildenhain, J. & Thomson, T. M. 2007. Orchestration of the DNA-damage response by the rnf8 ubiquitin ligase. *Science,* 318, 1637-1640.

Kondo, M., Scherer, D. C., King, A. G., Manz, M. G. & Weissman, I. L. 2001. Lymphocyte development from hematopoietic stem cells. *Current opinion in genetics & development,* 11, 520-526.

Kondo, M., Weissman, I. L. & Akashi, K. 1997. Identification of clonogenic common lymphoid progenitors in mouse bone marrow. *Cell,* 91, 661-672.

Kozlov, S. V., Graham, M. E., Jakob, B., Tobias, F., Kijas, A. W., Tanuji, M., Chen, P., Robinson, P. J., Taucher-Scholz, G. & Suzuki, K. 2011. Autophosphorylation and atm activation additional sites add to the complexity. *Journal of Biological Chemistry,* 286, 9107-9119.

Kramer, M., Hermans, J., Wijburg, E., Philippo, K., Geelen, E., Van Krieken, J., De Jong, D., Maartense, E., Schuuring, E. & Kluin, P. 1998. Clinical relevance of bcl2, bcl6, and myc rearrangements in diffuse large b-cell lymphoma. *Blood,* 92, 3152-3162.

Kühne, M., Riballo, E., Rief, N., Rothkamm, K., Jeggo, P. A. & Löbrich, M. 2004. A double-strand break repair defect in atm-deficient cells contributes to radiosensitivity. *Cancer research,* 64, 500-508.

Lakin, N. D., Weber, P., Stankovic, T., Rottinghaus, S. T., Taylor, A. & Jackson, S. P. 1996. Analysis of the atm protein in wild-type and ataxia telangiectasia cells. *Oncogene,* 13, 2707-2716.

Lavin, M. F. 2008. Ataxia-telangiectasia: From a rare disorder to a paradigm for cell signalling and cancer. *Nature Reviews Molecular Cell Biology,* 9, 759-769.

Lavin, M. F. & Kozlov, S. 2007. Atm activation and DNA damage response. *Cell Cycle (Georgetown, Tex.),* 6, 931.

Lebien, T. W. & Tedder, T. F. 2008. B lymphocytes: How they develop and function. *Blood,* 112, 1570-1580.

Lee, J.-H. & Paull, T. T. 2005. Atm activation by DNA double-strand breaks through the mre11-rad50-nbs1 complex. *Science,* 308, 551-554.

Lengauer, C., Kinzler, K. W. & Vogelstein, B. 1998. Genetic instabilities in human cancers. *Nature,* 396, 643-649.

Li, J., Chen, J., Vinters, H. V., Gatti, R. A. & Herrup, K. 2011. Stable brain atm message and residual kinase-active atm protein in ataxia-telangiectasia. *The Journal of Neuroscience,* 31, 7568-7577.

Li, X. & Heyer, W.-D. 2008. Homologous recombination in DNA repair and DNA damage tolerance. *Cell research,* 18, 99-113.

Liao, M. J. & Van Dyke, T. 1999. Critical role for atm in suppressing v (d) j recombination-driven thymic lymphoma. *Genes & development,* 13, 1246-1250.

Lieber, M. R. 2010. The mechanism of double-strand DNA break repair by the nonhomologous DNA end joining pathway. *Annual review of biochemistry,* 79, 181.

Lieber, M. R., Yu, K. & Raghavan, S. C. 2006. Roles of nonhomologous DNA end joining, v(d)j recombination, and class switch recombination in chromosomal translocations. *DNA repair,* 5, 1234-45.

Liyanage, M., Weaver, Z., Barlow, C., Coleman, A., Pankratz, D. G., Anderson, S., Wynshaw-Boris, A. & Ried, T. 2000. Abnormal rearrangement within the / t-cell receptor locus in lymphomas from atm-deficient mice. *Blood,* 96, 1940.

Loizou, J. I., Sancho, R., Kanu, N., Bolland, D. J., Yang, F., Rada, C., Corcoran, A. E. & Behrens, A. 2011. Atmin is required for maintenance of genomic stability and suppression of b cell lymphoma. *Cancer Cell,* 19, 587-600.

Lumsden, J. M., Mccarty, T., Petiniot, L. K., Shen, R., Barlow, C., Wynn, T. A., Morse, H. C., Gearhart, P. J., Wynshaw-Boris, A. & Max, E. E. 2004. Immunoglobulin class switch recombination is impaired in atm-deficient mice. *The Journal of experimental medicine,* 200, 1111.

Ma, Y. & Greider, C. W. 2009. Kinase-independent functions of tel1 in telomere maintenance. *Molecular and cellular biology,* 29, 5193-5202.

Ma, Y., Pannicke, U., Schwarz, K. & Lieber, M. R. 2002. Hairpin opening and overhang processing by an artemis/DNA-dependent protein kinase complex in nonhomologous end joining and v (d) j recombination. *Cell,* 108, 781-794.

Machida, S., Tomizawa, D., Tamaichi, H., Okawa, T., Endo, A., Imai, K., Nagasawa, M., Morio, T., Mizutani, S. & Takagi, M. 2013. Successful treatment of diffuse large b-cell lymphoma in a patient with ataxia telangiectasia using rituximab. *J Pediatr Hematol Oncol,* 35, 482-5.

Maclennan, I. 2005. Germinal centers still hold secrets. *Immunity,* 22, 656-657.

Maclennan, I. C. 1994. Germinal centers. *Annual review of immunology,* 12, 117-139.

Malu, S., Malshetty, V., Francis, D. & Cortes, P. 2012. Role of non-homologous end joining in v (d) j recombination. *Immunologic research,* 54, 233-246.

Manola, K. N., Georgakakos, V. N., Stavropoulou, C., Spyridonidis, A., Angelopoulou, M. K., Vlachadami, I., Katsigiannis, A., Roussou, P., Pantelias, G. E. & Sambani, C. 2008. Jumping translocations in hematological malignancies: A cytogenetic study of five cases. *Cancer genetics and cytogenetics,* 187, 85-94.

Marculescu, R., Le, T., Simon, P., Jaeger, U. & Nadel, B. 2002. V (d) j-mediated translocations in lymphoid neoplasms: A functional assessment of genomic instability by cryptic sites. *The Journal of experimental medicine,* 195, 85-98.

Mavrou, A., Tsangaris, G. T., Roma, E. & Kolialexi, A. 2008. The atm gene and ataxia telangiectasia. *Anticancer Res,* 28, 401-5.

Mcblane, J. F., Van Gent, D. C., Ramsden, D. A., Romeo, C., Cuomo, C. A., Gellert, M. & Oettinger, M. A. 1995. Cleavage at a v (d) j recombination signal requires only rag1 and rag2 proteins and occurs in two steps. *Cell,* 83, 387-395.

Mcheyzer-Williams, M. G. & Ahmed, R. 1999. B cell memory and the long-lived plasma cell. *Current opinion in immunology,* 11, 172-179.

Metcalfe, J. A., Parkhill, J., Campbell, L., Stacey, M., Biggs, P., Byrd, P. J. & Taylor, A. M. R. 1996. Accelerated telomere shortening in ataxia telangiectasia. *Nature genetics,* 13, 350-353.

Meyer-Hermann, M., Mohr, E., Pelletier, N., Zhang, Y., Victora, G. D. & Toellner, K.-M. 2012. A theory of germinal center b cell selection, division, and exit. *Cell reports,* 2, 162-174.

Meyn, M. S. 1999. Ataxia-telangiectasia, cancer and the pathobiology of the atm gene. *Clinical genetics,* 55, 289-304.

Micol, R., Ben Slama, L., Suarez, F., Le Mignot, L., Beaute, J., Mahlaoui, N., Dubois D'enghien, C., Lauge, A., Hall, J., Couturier, J., Vallee, L., Delobel, B., Rivier, F., Nguyen, K., Billette De Villemeur, T., Stephan, J. L., Bordigoni, P., Bertrand, Y., Aladjidi, N., Pedespan, J. M., Thomas, C., Pellier, I., Koenig, M., Hermine, O., Picard, C., Moshous, D., Neven, B., Lanternier, F., Blanche, S., Tardieu, M., Debre, M., Fischer, A. & Stoppa-Lyonnet, D. 2011. Morbidity and mortality from ataxia-telangiectasia are associated with atm genotype. *J Allergy Clin Immunol,* 128, 382-9.

Mills, K. D., Ferguson, D. O. & Alt, F. W. 2003. The role of DNA breaks in genomic instability and tumorigenesis. *Immunological reviews,* 194, 77-95.

Miosge, L. A. & Goodnow, C. C. 2005. Genes, pathways and checkpoints in lymphocyte development and homeostasis. *Immunology and cell biology,* 83, 318-335.

Misteli, T. & Soutoglou, E. 2009. The emerging role of nuclear architecture in DNA repair and genome maintenance. *Nature Reviews Molecular Cell Biology,* 10, 243-254.

Moldenhauer, G., Popov, S. W., Wotschke, B., Brüderlein, S., Riedl, P., Fissolo, N., Schirmbeck, R., Ritz, O., Möller, P. & Leithäuser, F. 2006. Aid expression identifies interfollicular large b cells as putative precursors of mature b-cell malignancies. *Blood,* 107, 2470-2473.

Moreno-Herrero, F., De Jager, M., Dekker, N. H., Kanaar, R., Wyman, C. & Dekker, C. 2005. Mesoscale conformational changes in the DNA-repair complex rad50/mre11/nbs1 upon binding DNA. *Nature,* 437, 440-443.

Morgan, J. L., Holcomb, T. M. & Morrissey, R. W. 1968. Radiation reaction in ataxia telangiectasia. *American Journal of Diseases of Children,* 116, 557-558.

Morrell, D., Cromartie, E. & Swift, M. 1986. Mortality and cancer incidence in 263 patients with ataxia-telangiectasia. *Journal of the National Cancer Institute,* 77, 89-92.

Morrison, C., Sonoda, E., Takao, N., Shinohara, A., Yamamoto, K. I. & Takeda, S. 2000. The controlling role of atm in homologous recombinational repair of DNA damage. *The EMBO journal,* 19, 463-471.

Nehls, M., Kyewski, B., Messerle, M., Waldschütz, R., Schüddekopf, K., Smith, A. J. H. & Boehm, T. 1996. Two genetically separable steps in the differentiation of thymic epithelium. *Science,* 272, 886.

Nehls, M., Pfeifer, D., Schorpp, M., Hedrich, H. & Boehm, T. 1994. New member of the winged-helix protein family disrupted in mouse and rat nude mutations. *Nature,* 372, 103-107.

Nemazee, D. 2006. Receptor editing in lymphocyte development and central tolerance. *Nature Reviews Immunology,* 6, 728-740.

Nowak-Wegrzyn, A., Crawford, T. O., Winkelstein, J. A., Carson, K. A. & Lederman, H. M. 2004. Immunodeficiency and infections in ataxia-telangiectasia. *J Pediatr,* 144, 505-11.

Nussenzweig, A. & Nussenzweig, M. C. 2010. Origin of chromosomal translocations in lymphoid cancer. *Cell,* 141, 27-38.

Offit, K., Coco, F. L., Louie, D. C., Parsa, N. Z., Leung, D., Portlock, C., Ye, B. H., Lista, F., Filippa, D. A. & Rosenbaum, A. 1994. Rearrangement of the bcl-6 gene as a prognostic marker in diffuse large-cell lymphoma. *New England Journal of Medicine,* 331, 74-80.

Ohno, H. 2004. Pathogenetic role of bcl6 translocation in b-cell non-hodgkin's lymphoma.

Orii, K. E., Lee, Y., Kondo, N. & Mckinnon, P. J. 2006. Selective utilization of nonhomologous end-joining and homologous recombination DNA repair pathways during nervous system development. *Proceedings of the National Academy of Sciences,* 103, 10017-10022.

Osmond, D. G. 1991. Proliferation kinetics and the lifespan of b cells in central and peripheral lymphoid organs. *Current opinion in immunology,* 3, 179-185.

Ozeri-Galai, E., Schwartz, M., Rahat, A. & Kerem, B. 2007. Interplay between atm and atr in the regulation of common fragile site stability. *Oncogene,* 27, 2109-2117.

Pan, Q., Petit-Frére, C., Lähdesmäki, A., Gregorek, H., Chrzanowska, K. H. & Hammarström, L. 2002. Alternative end joining during switch recombination in patients with ataxia-telangiectasia. *European journal of immunology,* 32, 1300-1308.

Pantelouris, E. 1968. Absence of thymus in a mouse mutant.

Pasqualucci, L., Neumeister, P., Goossens, T., Nanjangud, G., Chaganti, R., Küppers, R. & Dalla-Favera, R. 2001. Hypermutation of multiple proto-oncogenes in b-cell diffuse large-cell lymphomas. *Nature,* 412, 341-346.

Pecker, I., Avraham, K. B., Gilbert, D. J., Savitsky, K., Rotman, G., Harnik, R., Fukao, T., Schrock, E., Hirotsune, S. & Tagle, D. A. 1996. Identification and chromosomal localization of atm, the mouse homolog of the ataxia-telangiectasia gene. *Genomics,* 35, 39-45.

Peled, J. U., Kuang, F. L., Iglesias-Ussel, M. D., Roa, S., Kalis, S. L., Goodman, M. F. & Scharff, M. D. 2008. The biochemistry of somatic hypermutation. *Annu. Rev. Immunol.,* 26, 481-511.

Petiniot, L. K., Weaver, Z., Barlow, C., Shen, R., Eckhaus, M., Steinberg, S. M., Ried, T., Wynshaw-Boris, A. & Hodes, R. J. 2000. Recombinase-activating gene (rag) 2-mediated v(d)j recombination is not essential for tumorigenesis in atm-deficient mice. *Proceedings of the National Academy of Sciences,* 97, 6664-6669.

Petiniot, L. K., Weaver, Z., Vacchio, M., Shen, R., Wangsa, D., Barlow, C., Eckhaus, M., Steinberg, S. M., Wynshaw-Boris, A. & Ried, T. 2002. Rag-mediated v (d) j

recombination is not essential for tumorigenesis in atm-deficient mice. *Molecular and cellular biology,* 22, 3174-3177.

Rajewsky, K. 1996. Clonal selection and learning in the antibody system.

Ramiro, A. R., Jankovic, M., Callen, E., Difilippantonio, S., Chen, H.-T., Mcbride, K. M., Eisenreich, T. R., Chen, J., Dickins, R. A. & Lowe, S. W. 2006. Role of genomic instability and p53 in aid-induced c-myc–igh translocations. *Nature,* 440, 105-109.

Reiman, A., Srinivasan, V., Barone, G., Last, J., Wootton, L., Davies, E., Verhagen, M., Willemsen, M., Weemaes, C. & Byrd, P. 2011. Lymphoid tumours and breast cancer in ataxia telangiectasia; substantial protective effect of residual atm kinase activity against childhood tumours. *British journal of cancer,* 105, 586-591.

Reina-San-Martin, B., Chen, H. T., Nussenzweig, A. & Nussenzweig, M. C. 2004. Atm is required for efficient recombination between immunoglobulin switch regions. *The Journal of experimental medicine,* 200, 1103-1110.

Reliene, R. & Schiestl, R. H. 2006. Differences in animal housing facilities and diet may affect study outcomes—a plea for inclusion of such information in publications. *DNA repair,* 5, 651-653.

Robbiani, D. F. & Nussenzweig, M. C. 2013. Chromosome translocation, b cell lymphoma, and activation-induced cytidine deaminase. *Annual Review of Pathology: Mechanisms of Disease,* 8, 79-103.

Rooney, S., Chaudhuri, J. & Alt, F. W. 2004. The role of the non-homologous end-joining pathway in lymphocyte development. *Immunological reviews,* 200, 115-131.

Roukos, V. & Misteli, T. 2014. The biogenesis of chromosome translocations. *Nature Cell Biology,* 16, 293-300.

Russo, G., Isobe, M., Gatti, R., Finan, J., Batuman, O., Huebner, K., Nowell, P. C. & Croce, C. M. 1989. Molecular analysis of at (14; 14) translocation in leukemic t-cells of an ataxia telangiectasia patient. *Proceedings of the National Academy of Sciences,* 86, 602-606.

Russo, G., Isobe, M., Pegoraro, L., Finan, J., Nowell, P. C. & Croce, C. M. 1988. Molecular analysis of at (7; 14)(g35; g32) chromosome translocation in a t cell leukemia of a patient with ataxia telangiectasia. *Cell,* 53, 137-144.

Sandoval, C. & Swift, M. 1998. Treatment of lymphoid malignancies in patients with ataxia-telangiectasia. *Medical and pediatric oncology,* 31, 491-497.

Savitsky, K., Bar-Shira, A., Gilad, S., Rotman, G., Ziv, Y., Vanagaite, L., Tagle, D. A., Smith, S., Uziel, T. & Sfez, S. 1995. A single ataxia telangiectasia gene with a product similar to pi-3 kinase. *Science,* 268, 1749-1753.

Schaffner, C., Idler, I., Stilgenbauer, S., Döhner, H. & Lichter, P. 2000. Mantle cell lymphoma is characterized by inactivation of the atm gene. *Proceedings of the National Academy of Sciences,* 97, 2773-2778.

Schubert, R., Erker, L., Barlow, C., Yakushiji, H., Larson, D., Russo, A., Mitchell, J. B. & Wynshaw-Boris, A. 2004. Cancer chemoprevention by the antioxidant tempol in atm-deficient mice. *Human molecular genetics,* 13, 1793-1802.

Sedgwick, R. & Boder, E. 1991. Hereditary neuropathies and spinocerebellar atrophies. *Hereditary neuropathies and spinocerebellar atrophies. New York: Alan R Liss*, 347-423.

Sewastianik, T., Prochorec-Sobieszek, M., Chapuy, B. & Juszczyński, P. 2014. Myc deregulation in lymphoid tumors: Molecular mechanisms, clinical consequences and therapeutic implications. *Biochimica et Biophysica Acta (BBA)-Reviews on Cancer.*

Sharkey, F. E. 1978. Histopathological observations on a nude mouse colony. *The nude mouse in experimental and clinical research. Academic Press, New York*, 75-93.

Sharkey, F. E. & Fogh, J. 1979. Incidence and pathological features of spontaneous tumors in athymic nude mice. *Cancer research,* 39, 833-839.

Sharkey, F. E. & Fogh, J. 1984. Considerations in the use of nude mice for cancer research. *Cancer and Metastasis Reviews,* 3, 341-360.

Shiloh, Y. 2003. Atm and related protein kinases: Safeguarding genome integrity. *Nat Rev Cancer,* 3, 155-168.

Shiloh, Y. & Rotman, G. 1996. Ataxia-telangiectasia and the atm gene: Linking neurodegeneration, immunodeficiency, and cancer to cell cycle checkpoints. *Journal of clinical immunology,* 16, 254-260.

Shiloh, Y., Tabor, E. & Becker, Y. 1982. The response of ataxia-telangiectasia homozygous and heterozygous skin fibroblasts to neocarzinostatin. *Carcinogenesis,* 3, 815-820.

Skowronska, A., Parker, A., Ahmed, G., Oldreive, C., Davis, Z., Richards, S., ... & Stankovic, T. (2012). Biallelic ATM inactivation significantly reduces survival in patients treated on the United Kingdom Leukemia Research Fund Chronic Lymphocytic Leukemia 4 trial. *Journal of Clinical Oncology*, 30(36), 4524-32.

Sprent, J. & Kishimoto, H. 2002. The thymus and negative selection. *Immunological reviews,* 185, 126-135.

Sprent, J. & Surh, C. D. 2002. T cell memory. *Annual review of immunology,* 20, 551-579.

Spring, K., Cross, S., Li, C., Watters, D., Ben-Senior, L., Waring, P., Ahangari, F., Lu, S., Chen, P. & Misko, I. 2001. Atm knock-in mice harboring an in-frame deletion corresponding to the human atm 7636del9 common mutation exhibit a variant phenotype. *Cancer research,* 61, 4561.

Stankovic, T., Stewart, G., Byrd, P., Fegan, C., Moss, P. & Taylor, A. 2002. Atm mutations in sporadic lymphoid tumours. *Leukemia & lymphoma,* 43, 1563-1571.

Stankovic, T., Weber, P., Stewart, G., Bedenham, T., Murray, J., Byrd, P. J., Moss, P. a. H. & Taylor, A. M. R. 1999. Inactivation of ataxia telangiectasia mutated gene in b-cell chronic lymphocytic leukaemia. *The Lancet,* 353, 26-29.

Stavnezer, J., Guikema, J. E. & Schrader, C. E. 2008. Mechanism and regulation of class switch recombination. *Annual review of immunology,* 26, 261.

Stewart, G. S., Wang, B., Bignell, C. R., Taylor, A. M. R. & Elledge, S. J. 2003. Mdc1 is a mediator of the mammalian DNA damage checkpoint. *Nature,* 421, 961-966.

Stracker, T. H., Roig, I., Knobel, P. A. & Marjanović, M. 2013. The atm signaling network in development and disease. *Frontiers in genetics,* 4.

Stutman, O. 1978. Spontaneous, viral and chemically induced tumors in the nude mouse. *The nude mouse in experimental and clinical research. Academic Press, New York*, 411-415.

Summers, C., Rankin, S. M., Condliffe, A. M., Singh, N., Peters, A. M. & Chilvers, E. R. 2010. Neutrophil kinetics in health and disease. *Trends Immunol,* 31, 318-24.

Sun, Y., Jiang, X., Chen, S., Fernandes, N. & Price, B. D. 2005. A role for the tip60 histone acetyltransferase in the acetylation and activation of atm. *Proceedings of the National Academy of Sciences of the United States of America,* 102, 13182-13187.

Swerdlow, S. H. 2008. *Who classification of tumours of haematopoietic and lymphoid tissues*, World Health Organization.

Szabo, P., Shen, S. & Weksler, M. E. 1999. Age-associated defects in b lymphocyte development. *Exp Gerontol,* 34, 431-4.

Szabo, P., Zhao, K., Kirman, I., Le Maoult, J., Dyall, R., Cruikshank, W. & Weksler, M. E. 1998. Maturation of b cell precursors is impaired in thymic-deprived nude and old mice. *J Immunol,* 161, 2248-53.

Taylor, A. 1992. Ataxia telangiectasia genes and predisposition to leukaemia, lymphoma and breast cancer. *British journal of cancer,* 66, 5.

Taylor, A. M. R., Lam, Z., Last, J. I., & Byrd, P. J. 2014) Ataxia telangiectasia: more variation at clinical and cellular levels. *Clinical genetics*. epublication

Taylor, A., Metcalfe, J., Thick, J. & Mak, Y. 1996. Leukemia and lymphoma in ataxia telangiectasia. *Blood,* 87, 423.

Taylor, A. M., Flude, E., Garner, C. M., Campbell, J. B. & Edwards, M. J. 1983. Effects of the DNA strand-cleaving antitumor agent, streptonigrin, on ataxia telangiectasia cells. *Cancer research,* 43, 2700-2703.

Taylor, A. M., Harnden, D. G., Arlett, C. F., Harcourt, S. A., Lehmann, A. R., Stevens, S. & Bridges, B. A. 1975. Ataxia telangiectasia: A human mutation with abnormal radiation sensitivity. *Nature,* 258, 427-9.

Tepsuporn, S., Hu, J., Gostissa, M. & Alt, F. W. 2014. Mechanisms that can promote peripheral b-cell lymphoma in atm-deficient mice. *Cancer immunology research,* 2, 857-866.

Tonegawa, S. 1983. Somatic generation of antibody diversity. *Nature,* 302, 575-581.

Uziel, T., Savitsky, K., Platzer, M., Ziv, Y., Helbitz, T., Nehls, M., Boehm, T., Rosenthal, A., Shiloh, Y. & Rotman, G. 1996. Genomic organization of the atm gene. *Genomics,* 33, 317-320.

Vacchio, M. S., Olaru, A., Livak, F. & Hodes, R. J. 2007. Atm deficiency impairs thymocyte maturation because of defective resolution of t cell receptor α locus coding end breaks. *Proceedings of the National Academy of Sciences,* 104, 6323-6328.

Vorechovský I1, Luo L, Dyer MJ, Catovsky D, Amlot PL, Yaxley JC, Foroni L, Hammarström L, Webster AD, Yuille MA. 1997 Clustering of missense mutations in the ataxia-telangiectasia gene in a sporadic T-cell leukaemia. *Nat Genet.* 17(1), 96-9.

Vos, J., Kreeftenberg, J., Kruijt, B., Kruizinga, W. & Steerenberg, P. 1980. The athymic nude rat: Ii. Immunological characteristics. *Clinical immunology and Immunopathology,* 15, 229-237.

Wang, J. H., Alt, F. W., Gostissa, M., Datta, A., Murphy, M., Alimzhanov, M. B., Coakley, K. M., Rajewsky, K., Manis, J. P. & Yan, C. T. 2008a. Oncogenic transformation in the absence of xrcc4 targets peripheral b cells that have undergone editing and switching. *J Exp Med,* 205, 3079-90.

Wang, J. H., Alt, F. W., Gostissa, M., Datta, A., Murphy, M., Alimzhanov, M. B., Coakley, K. M., Rajewsky, K., Manis, J. P. & Yan, C. T. 2008b. Oncogenic transformation in the absence of xrcc4 targets peripheral b cells that have undergone editing and switching. *The Journal of experimental medicine,* 205, 3079-3090.

Wang, J. H., Gostissa, M., Yan, C. T., Goff, P., Hickernell, T., Hansen, E., Difilippantonio, S., Wesemann, D. R., Zarrin, A. A. & Rajewsky, K. 2009. Mechanisms promoting translocations in editing and switching peripheral b cells. *Nature,* 460, 231-236.

Weterings, E. & Chen, D. J. 2007. DNA-dependent protein kinase in nonhomologous end joining: A lock with multiple keys? *The Journal of cell biology,* 179, 183-186.

Xu, Y., Ashley, T., Brainerd, E. E., Bronson, R. T., Meyn, M. S. & Baltimore, D. 1996. Targeted disruption of atm leads to growth retardation, chromosomal fragmentation during meiosis, immune defects, and thymic lymphoma. *Genes & development,* 10, 2411.

Xu, Y. & Baltimore, D. 1996. Dual roles of atm in the cellular response to radiation and in cell growth control. *Genes & development,* 10, 2401.

Yamamoto, K., Wang, Y., Jiang, W., Liu, X., Dubois, R. L., Lin, C.-S., Ludwig, T., Bakkenist, C. J. & Zha, S. 2012. Kinase-dead atm protein causes genomic instability and early embryonic lethality in mice. *The Journal of cell biology,* 198, 305-313.

Zha, S., Bassing, C. H., Sanda, T., Brush, J. W., Patel, H., Goff, P. H., Murphy, M. M., Tepsuporn, S., Gatti, R. A. & Look, A. T. 2010. Atm-deficient thymic lymphoma is associated with aberrant tcrd rearrangement and gene amplification. *The Journal of experimental medicine,* 207, 1369.

Zhang, Y., Mccord, R. P., Ho, Y.-J., Lajoie, B. R., Hildebrand, D. G., Simon, A. C., Becker, M. S., Alt, F. W. & Dekker, J. 2012. Spatial organization of the mouse genome and its role in recurrent chromosomal translocations. *Cell,* 148, 908-921.

Zhao, J., Bacolla, A., Wang, G. & Vasquez, K. M. 2010. Non-b DNA structure-induced genetic instability and evolution. *Cellular and molecular life sciences,* 67, 43-62.

Zhu, C., Mills, K. D., Ferguson, D. O., Lee, C., Manis, J., Fleming, J., Gao, Y., Morton, C. C. & Alt, F. W. 2002. Unrepaired DNA breaks in p53-deficient cells lead to oncogenic gene amplification subsequent to translocations. *Cell,* 109, 811-821.

Zlotoff, D. A. & Bhandoola, A. 2011. Hematopoietic progenitor migration to the adult thymus. *Annals of the New York Academy of Sciences, 1217: 122-38*.